Physiologically based kinetic (PBK) models to give insight into dose-, species-, matrix- and interindividual human variation-dependent effects on bioactivation and detoxification of methyleugenol

Ala′ Al-Subeihi

Thesis committee

Promotors

Prof. dr. ir. I.M.C.M Rietjens
Professor of Toxicology

Prof. dr. P.J. van Bladeren
Professor of Toxicology

Co-promotor

Dr. ir. A. Punt
Assistant professor at the sub-department of Toxicology

Other members

Prof. dr. W.J.H. van Berkel
Wageningen University

Prof. dr. N.P.E. Vermeulen
VU University Amsterdam

Prof. dr. G.M.M. Groothuis
Groningen University

Dr. ir. A.A. de Graaf
TNO, Zeist

This research was conducted under the auspices of the Graduate School VLAG (Advanced studies in Food Technology, Agrobiotechnology, Nutrition and Health Sciences).

Physiologically based kinetic (PBK) models to give insight into dose-, species-, matrix- and interindividual human variation-dependent effects on bioactivation and detoxification of methyleugenol

Alaʹ Ali Al-Subeihi

Thesis

submitted in fulfillment of the requirements for the degree of doctor
at Wageningen University
by the authority of the Rector Magnificus
Prof. dr. M.J. Kropff,
in the presence of the
Thesis Committee appointed by the Academic Board
to be defended in public
on Monday 28 January 2013
at 11.00 a.m. in the Aula

Ala′ Al-Subeihi, 2013

Physiologically based kinetic (PBK) models to give insight into dose-, species- , matrix- and interindividual human variation-dependent effects on bioactivation and detoxification of methyleugenol

PhD Thesis, Wageningen University, Wageningen, The Netherlands
With references, with summaries in Dutch and English

ISBN 978-94-6173-429-7

Table of Contents

1

General introduction

Background

Methyleugenol (Figure 1) is an alkenylbenzene that occurs naturally in various herbs such as tarragon, basil, nutmeg and allspice (Smith *et al.*, 2002). Methyleugenol is added to food either directly as a flavoring substance or as a constituent of added essential oils (Smith *et al.*, 2002). Methyleugenol also occurs at low levels in oranges, bananas, and grapefruit juices (Nijssen *et al.*, 2008). The interest in the risk of methyleugenol as a food constituent came from its widespread use in a variety of foods and beverages as well as its structural resemblance to the known carcinogen safrole (Johnson *et al.*, 2000). In addition, methyleugenol has been reported to be DNA reactive and carcinogenic, inducing malignant tumors in multiple tissues of rats and mice as well as inducing unscheduled DNA synthesis in rat liver (Ding *et al.*, 201; NTP, 2000; Smith *et al.*, 2002). The safety of human exposure to methyleugenol at low dietary intake levels has been assessed several times. In 1965, the Expert Panel of the Flavor and Extract Manufacturers Association (FEMA) concluded that methyleugenol was GRAS (Generally Recognized As Safe) under conditions of intended use as a flavoring substance in food (Hall and Oser, 1965). In the FEMA evaluation, it was taken into account that there are experimental data suggesting a non-linear relationship between dose and profiles of metabolism and metabolic activation and that exposure due to use as a flavoring is relatively low (Smith *et al.*, 2002). In 2000, the carcinogenicity of methyleugenol was investigated in mice and rats by the National Toxicology Program (NTP) (NTP, 2000). The NTP reported that methyleugenol is

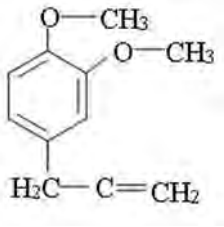

Figure 1. Structure of methyleugenol

carcinogenic in both rats and mice (NTP, 2000). In 2001, the FEMA Expert Panel reassessed the available data for methyleugenol and confirmed that there is no considerable cancer risk resulting from consumption of methyleugenol as flavoring substance and affirmed the GRAS status of methyleugenol at the use levels as a flavoring substance (Smith *et al.*, 2002). In 2001, the Scientific Committee on Food (SCF) of the European Union published a scientific opinion on methyleugenol in which it was concluded that methyleugenol is genotoxic and carcinogenic and that reductions in exposure and restrictions in use levels are indicated (SCF, 2001). Based on these findings, the use of methyleugenol as pure substance in foodstuffs has been prohibited since September 2008 within the European Union (European Commission, 2008). A recent evaluation, performed by the Joint FAO/WHO Expert Committee on Food Additives (JECFA) in 2008, has indicated that although evidence of carcinogenicity to rodents given high doses of methyleugenol exists, further research is needed to assess the potential risk to human health at relevant dietary exposure resulting from the presence of methyleugenol in foods and essential oils and its use as flavoring agent (JECFA, 2008). The occurrence of these different expert opinions in risk assessment of methyleugenol originates in part from the absence of scientific agreement to support the unequivocal translation of carcinogenicity data of rodent animal experiments obtained at high levels of exposure to the relevant human situation. Predicting the cancer risk in humans at relevant dietary intake levels requires extrapolation of the animal carcinogenicity data taking in consideration species, dose and interindividual variation. Furthermore, it implies extrapolation from rat or mouse studies with high dose levels of the pure compound to the human situation in which exposure at low dose levels occurs within the context of a complex food matrix.

The aim of the present PhD project was to obtain quantitative insight into the consequences of dose- and species-dependent effects and of interindividual differences and matrix effects for the bioactivation and detoxification of methyleugenol by using physiologically based kinetic (PBK) modeling.

Chemical and physical properties of methyleugenol

Methyleugenol (4-allyl-1,2-dimethoxybenzene) has a molecular weight of 178.2 g/mol (NTP, 2000). It is a colorless to pale yellow, oily liquid with a clove-carnation odor and a bitter taste. It is soluble in most organic solvents like ethanol, ethyl ether, and chloroform (NTP, 2000). On the other hand, it is insoluble in water, glycol, and propylene glycol (NTP, 2000). Methyleugenol evaporates readily at room temperature and darkens and thickens slowly when exposed to air (Lide, 1998; Sax′s, 1992). Methyleugenol has a boiling point of 254.7 °C, a melting point of – 4 °C, a refractive index of 1.532, and a density of 1.0396 at 20 °C (NTP, 2000).

Production, use, and human exposure to methyleugenol

Methyleugenol can be produced by methylation of eugenol (Opdyke, 1979) or by extraction from natural sources. The annual production volume of methyleugenol in the USA is 77 kg/year (Gavin *et al.*, 2007). Methyleugenol is a naturally occurring constituent of the essential oils of a number of plants (De Vincenzi *et al.*, 2000). It is present, for instance, in the essential oils from basil, pay, tea tree, citronella (Environment Canada, 2010), anise, nutmeg, mace, cinnamon leaves (Fenaroli′s, 1975), pixuri seeds (Carlini *et al*., 1983), and laurel fruits and leaves (Farm Chemical Handbook, 1992). Methyleugenol has also been detected in blackberry essence, bananas, black pepper, and bilberries (WHO, 1981). Human exposure to methyleugenol may occur through the consumption of foods flavored with these aromatic plants and/or their essential oil fractions. Methyleugenol is (or has been) used as a flavoring agent in jellies, baked goods, nonalcoholic beverages, chewing gum, candy, pudding, relish, and ice cream (NTP, 2000). Some specified groups characterized by eating fresh pesto are exposed to high levels of methyleugenol because fresh pesto is prepared from a large quantity of fresh sweet basil (Miele *et al.*, 2001). In addition some plant-based food supplements were recently shown to contain relatively high levels of methyleugenol (van den Berg *et al.*, 2011). Methyleugenol is also used as a fragrance in perfumes (0.3% to 0.8%), creams and lotions (0.01% to 0.05%), soaps and

detergents (0.02% to 0.2%) (Opdyke, 1979). One of the uses for methyleugenol is as an insect repellant (Environment Canada, 2010). In 1982, methyleugenol was used in combination with malathion to control an outbreak of oriental fruit flies in California (Hays and Laws, 1991). Methyleugenol has also been used as an anesthetic in rodents (Carlini *et al*., 1981). The average daily human intake of methyleugenol has been estimated by the SCF to be 13 mg/day, corresponding to 0.217 mg/(kg bw)/day for a 60 kg person (SCF, 2001), while the FEMA estimated the average daily intake of methyleugenol to be less than 0.01 mg/(kg bw)/day (Smith *et al.*, 2002). The estimation of the SCF was based on theoretical maximum use levels of methyleugenol in various food categories and consumption data for these food categories, whereas the intake estimation of the FEMA was based on production volume data for flavor use (SCF, 2001; Smith *et al.*, 2002).

Carcinogenicity of methyleugenol

The carcinogenicity of methyleugenol was demonstrated by Miller *et al*. (1983). In this study male B6C3F1 mice were exposed to methyleugenol prior to weaning via intraperitoneal injection. Each mouse was given 4.75 µmol methyleugenol. The outcomes of this study revealed formation of liver tumors which means that methyleugenol was carcinogenic. In another two-year carcinogenicity study (Johnson *et al.*, 2000; NTP, 2000), male and female F344/N rats and B6C3F1 mice were given by gavage methyleugenol doses of 37, 75, or 150 mg/(kg bw)/day suspended in 0.5% methylcellulose. In rats, methyleugenol induce liver neoplasms including hepatoadenoma, hepatocarcinoma and hepatocholangioma (both sexes). Also methyleugenol was observed to cause benign and malignant neuroendocrine tumors, neuroendocrine cell hyperplasia, and atrophy of the glandular stomach (both sexes). Furthermore, renal tubule hyperplasia, nephropathy and adenomacarcinoma were noticed in the kidney of male rats. Moreover, fibroadenoma in the mammary gland, fibroma and fibrosarcoma in subcutaneous tissue, malignant mesotheliomas and splenic fibrosis were observed in male rats. Squamous cell papilloma or carcinoma (combined) were noticed in the forestomach of

female rats. In mice, methyleugenol induce liver neoplasms including hepatoblastoma in both sexes and neuroendocrine tumors of the glandular stomach in male. Based on the above mentioned findings, it was concluded that methyleugenol is a multisite, multispecies carcinogen and majorly exerts its effect in the liver as demonstrated in all exposed groups (NTP, 2000).

Genotoxicity of methyleugenol

Methyleugenol has been found to induce chromosomal recombination in yeast (*Saccharomyces cerevisiae*) (Brennan *et al.*, 1996; Schiestl *et al.*, 1989) and cell transformation in Syrian hamster embryo cells (Kerckaert *et al.*, 1996; NTP, 2002). On the other hand, the results of most standard *in vitro* genotoxicity assays including the Ames test indicated that methyleugenol was not mutagenic (Brennan *et al.*, 1996; Ding *et al.*, 2011). In spite of this, methyleugenol forms DNA adducts and induces unscheduled DNA synthesis in rat liver after *in vivo* exposure (Ding *et al.*, 2011). Furthermore, methyleugenol induced DNA adducts in cultured human HepG2 hepatoma cells (Zhou *et al.*, 2007). Moreover, methyleugenol caused unscheduled DNA synthesis in primary hepatocytes obtained from mice and rats (Burkey *et al.*, 2000; Chan and Caldwell, 1992; Howes *et al.*, 1990). The unscheduled DNA synthesis due to exposure to methyleugenol required sulfotransferase mediated metabolite formation (Burkey *et al.*, 2000).

Pharmacokinetics of methyleugenol

Methyleugenol is rapidly absorbed, metabolized, and excreted after oral administration (Johnson *et al.*, 2000; Schecter *et al.*, 2004). It was reported that the time for methyleugenol to achieve the maximum concentrations in blood in rat and mice after dosing by oral gavage (37 mg/(kg bw) up to 300 mg/(kg bw)) was 5-15 min (Johnson *et al.*, 2000). Also in a study where nine volunteers were exposed to about 216 mg methyleugenol per volunteer via consumption of ginger snap cookies (3.16 mg/g), the plasma peak concentration was reached quickly at 15 min after exposure and the estimated half-life of elimination was about 90 min (Schecter *et al.*,

2004). Because the maximum blood concentration was achieved so quickly and long before the stomach could have emptied, this might give an indication that methyleugenol may be absorbed directly from the stomach and/or forestomach (Johnson *et al.*, 2000).

The important metabolic pathways of methyleugenol include *O*-demethylation of the methoxy moieties on the benzene ring, 2′,3′-epoxidation and 1′-hydroxylation of the allylic side chain (Figure 2) (NTP, 2000; Solheim and Scheline, 1976). *O*-demethylation of the *meta* or *para* methoxy substituents of methyleugenol yields the corresponding phenolic derivatives, which may be excreted as sulfate or glucuronic acid conjugate (Smith *et al.*, 2002). Epoxidation of the side chain yields a 2′,3′-epoxide. This epoxide is detoxified by epoxide hydrolase to form the dihydrodiol or via glutathione conjugation (Luo and Guenther, 1995). Hydroxylation at the 1'-position of methyleugenol is considered to represent the bioactivation pathway producing the proximate carcinogenic metabolite 1′-hydroxymethyleugenol (Drinkwater *et al.*, 1976; Miller *et al.*, 1983). In a next step 1′-hydroxymethyleugenol can be sulfonated by sulfotransferases to form the ultimate carcinogenic metabolite 1′-sulfooxymethyleugenol (Miller *et al.*, 1983).

Incubations with microsomes from 13 human liver samples showed 37-fold difference in 1′-hydroxylation of methyleugenol (Gardner *et al.*, 1997). These results suggest that the risk to humans ingesting methyleugenol is subject to marked interindividual variability. Incubations of methyleugenol either with recombinant individual human cytochromes P450 or microsomes from pooled human livers indicated that P450 1A2, 2A6, 2C9, 2C19, and 2D6 are able to bioactivate methyleugenol to the proximate metabolite 1′-hydroxymethyleugenol (Jeurissen *et al.*, 2006). Based on the data reported by Jeurissen *et al.* (2006), P450 1A2 was shown to be the most important enzyme involved in the bioactivation of methyleugenol to its proximate carcinogenic metabolite 1′-hydroxymethyleugenol. Furthermore, kinetic results revealed a 5-fold difference in the catalytic activities for 1′-hydroxylation of methyleugenol of microsomes obtained from 15 human livers (Jeurissen *et al.*, 2006). Recently, studies using *Salmonella typhimurium* TA100 strains with expression of human SULT revealed that SULT1A1 and SULT1E1 are the main liver sulfotransferase enzymes involved in activation of 1′-hydroxymethyleugenol to DNA reactive metabolites (Herrmann *et al*., 2012).

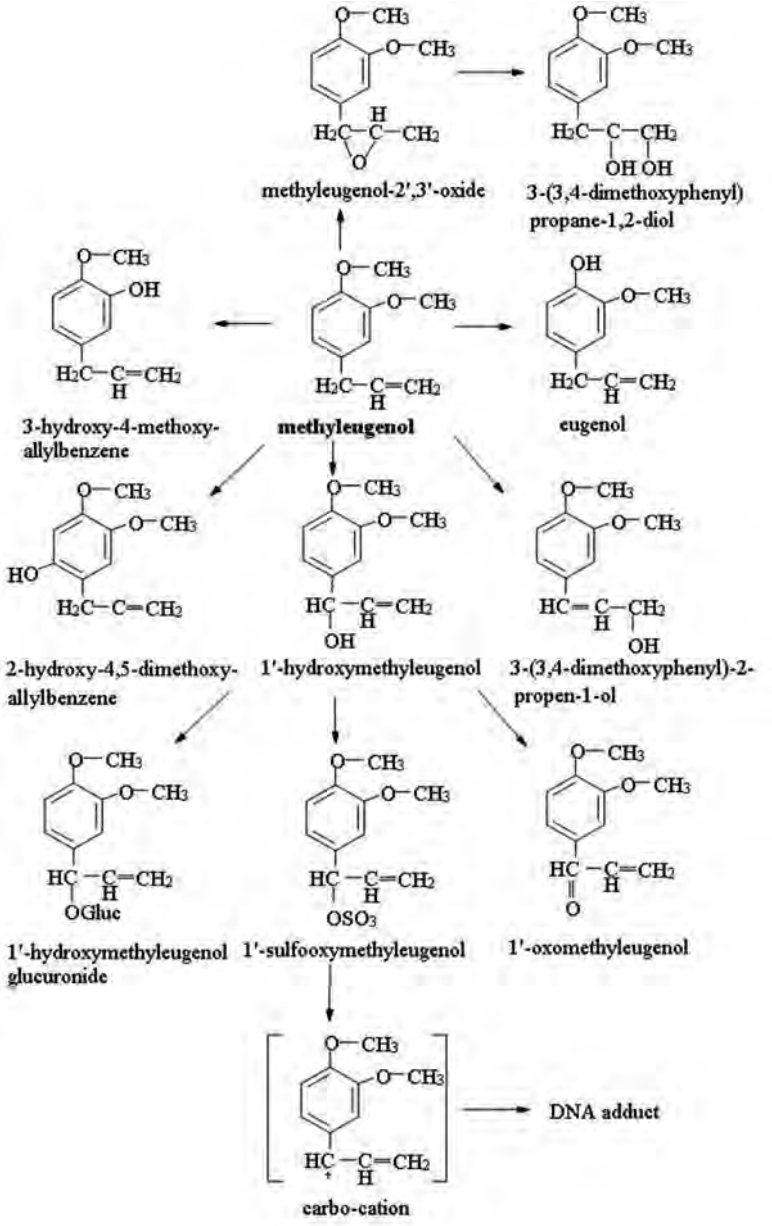

Figure 2. Suggested metabolic pathways of methyleugenol.

In addition to conversion of 1′-hydroxymethyleugenol to its DNA reactive 1′-sulfooxymethyleugenol metabolite other pathways facilitate detoxification of 1′-hydroxymethyleugenol. These include glucuronidation by UDP-glucuronosyltransferases (UGTs) and oxidation to 1′-oxomethyleugenol which may be chemically regenerating 1′-hydroxymethyleugenol, but may rather be efficiently detoxified by glutathione conjugation (Phillips *et al.*, 1981).

Approaches of cancer risk assessment

Since the occurrence of methyleugenol in botanical and botanical preparations present in food cannot readily be eliminated or avoided, estimation of the cancer risk at low dose levels will be necessary to indicate whether the presence of low concentrations of methyleugenol in the daily regular diet is of concern from a public health point of view. International agreement on how to evaluate the potential risk of genotoxic carcinogens that naturally occur in food is absent. Many different scenarios were suggested for the risk assessment of chemicals that are both genotoxic and carcinogenic. When the carcinogenicity is caused by a genotoxic mechanism, it is assumed that there is no obvious threshold and any level of exposure carries some degree of carcinogenic risk (COC, 2004). This approach, however, only identifies the hazard and does not give a quantitative estimate of the cancer risk at intake levels relevant for dietary human exposure (Dybing *et al*., 2008). EFSA reported that there are different approaches that are currently available for assessing the risk of substances that are both genotoxic and carcinogenic (EFSA, 2005). One of these approaches is linear extrapolation of animal carcinogenicity data obtained at high dose levels to low dose levels which are relevant to human intake. This approach requires definition of a point of departure to be derived from the animal data at high dose levels from which the extrapolation can be performed to zero risk at zero dose level. The point of departure may be the T25 which is the dose that increases the tumor incidence by 25% (Barlow *et al*., 2006; Dybing *et al*., 2008). It may also be the so-called Benchmark Dose 10 (BMD_{10}) (the Benchmark Dose that gives a 10% extra cancer incidence) or

its lower confidence bound ($BMDL_{10}$) determined using the Benchmark Dose approach (BMD) (EFSA, 2005; EPA, 2005). The BMD approach provides a useful tool for deriving a point of departure within the observable dose range by fitting a curve to the dose-response data from an animal bioassay and using this curve fit to estimate the intake level that corresponds to a fixed tumor incidence. The simplest way to estimate the risk associated with the average dietary human intake is to apply linear extrapolation from the BMD_{10} or T25 as the point of departure to zero dose at zero risk. Based on this extrapolation a so-called virtual safe dose (VSD) can be derived, corresponding to the dose that results in an additional cancer risk of one in a million upon lifetime exposure, which is generally considered an acceptable risk by risk managers (Rietjens *et al.*, 2010). Extrapolating from animal tumor data at high doses using mathematical modeling in order to obtain estimates of the risk to humans at low exposures has been much debated, since it is not known whether or not the model chosen actually reflects the underlying biological processes. In addition, numerical estimates may be misused or misinterpreted in further risk management and risk communication if the uncertainties and inaccuracy connected to the model may not be communicated (EFSA, 2005). Recently, EFSA considered the Margin of Exposure (MOE) approach as a useful and pragmatic option for risk assessment of substances that are both genotoxic and carcinogenic (EFSA, 2005).The MOE represents the proportion between a reference point acquired from the dose–response data obtained from experimental or epidemiological studies ($BMDL_{10}$) and the human estimated daily intake (EDI). In this approach there is no extrapolation or generation of possibly uncertain risk estimates since it takes account of intake/exposure and the available data on the dose–response relationship are used (EFSA, 2005). The magnitude of the MOE does not indicate a safe dose of a chemical but indicates whether the estimated daily intake is (or is not) close to dose levels actually causing increased tumor incidences in animal bioassays so that risk management actions might (not) be required (Dybing *et al*., 2008). EFSA considered that, when the MOE is higher than 10,000, the compound is considered to be of low priority for risk management actions (EFSA, 2005). This margin of 10,000 takes into consideration the various uncertainties in the MOE approach, such as interspecies differences and human variability in biokinetics and

biodynamics, the shape of the dose-response curve below the experimental data, and human interindividual variability in cell cycle control and DNA repair (Barlow *et al*., 2006; Dybing *et al*., 2008; EFSA, 2005).

As outlined above, the MOE approach has been defined because the classical risk assessment approaches used for assessing the risk of chemicals that are both genotoxic and carcinogenic, like the linear extrapolation of cancer incidences, have problems when cancer data obtained in animal bioassays are extrapolated to dose levels and cancer incidences orders of magnitude below the experimental data obtained in animal bioassays, in order to model the human situation. The presence of uncertainties in the shape of the dose-response curve at dose levels relevant for dietary human intake, interspecies variations in metabolism and metabolic activation and the great interindividual variability within the human population, as compared to the variability in the inbred strains used for the rodent bioassays, make it difficult to perform such extrapolations. Physiologically based kinetic (PBK) modeling can provide a method to obtain a better mechanistic basis for extrapolations from data obtained in experimental animal studies to the human situation (Andersen and Krishnan 1994; Clewell *et al*., 2001; Clewell *et al*., 2002).

PBK models

The structure of the PBK model depends primarily on the aims for which the model is developed and on the available data. The PBK models consist of many compartments which represent the tissues of interest. Each compartment has its own physiological (e.g. blood flows), physicochemical (e.g. partition coefficients) and biochemical (e.g. metabolic rates) parameters. Target tissues are generally represented as individual compartment (e.g. liver, lung, or kidney) while some non-target tissues are lumped together in one compartment (e.g. slowly perfused tissues such as muscle and skin or richly perfused tissues such as brain and spleen). Depending upon the available data, PBK models should include the target organ as a separate compartment. The PBK model consists of mathematical equations for each relevant

compartment describing absorption, distribution, metabolism and excretion (ADME) of the chemical and/or its metabolites in that respective organ of interest. In this way PBK models quantitatively describe actual physiological processes within the relevant tissues of the body (Krishnan and Andersen, 2001). Solution of the PBK equations results in outcomes that are an indication of, for example, the tissue concentration of a compound or its metabolite in any tissue over time at a certain dose, allowing analyses of effects at both high but also more realistic low dose levels (Rietjens *et al.*, 2011). Furthermore, such PBK models can be developed for different species, which facilitates interspecies extrapolation. In addition, by incorporating equations and kinetic constants for metabolic conversions by individual human samples and/or specific isoenzymes, modeling of interindividual variations and genetic polymorphisms becomes feasible (Bogaards *et al*., 2000).

In cancer risk assessment strategies, PBK models can predict internal dose levels for exposure regimens that have not been directly measured, by converting external exposure values to an internal dose metric (e.g. the predicted plasma or tissue levels of a parent compound or its reactive metabolites) in animal bioassays, as well as in human exposure scenarios (Andersen and Krishnan, 1994). Such an internal dose metric is considered to be more closely related to the toxic response than the applied external doses. Extrapolation of the cancer risk from high to low doses and from animals to humans can be performed based on the internal dose metrics rather than the applied external doses (Andersen and Krishnan, 1994).

Developing a PBK model

For the development of a PBK model for a specific compound, model parameters need to be obtained. The physiological parameters included in the developed PBK models should correspond to acceptable values for the specific species. The reference values of physiological parameters (e.g. blood flow rates and tissue volumes) for adult animals and humans are available in literature (Brown *et al.*, 1997; Chiu *et al.*, 2007 and references therein). Tissue-blood partition coefficients can be used to model the steady state concentration of a chemical in

the specific tissue compared with blood. Several methods were mentioned in the literature for obtaining tissue-blood partition coefficients (Chiu *et al.*, 2007). Tissue-blood partition coefficients for nonvolatile chemicals might be obtained *in vitro* using radioactive chemicals in ultrafiltration, equilibrium dialysis or vial equilibration procedures (Chiu *et al.*, 2007 and references therein) and can be obtained using *in silico* methods based on the octanol water partition coefficients as well. Biochemical parameters required for PBK models, including absorption rate and metabolic parameters, can be determined by fitting a model to data from *in vivo* studies (Chiu *et al.*, 2007). Alternatively, metabolic parameters might also be derived from *in vitro* experiments with tissue fractions, primary cell cultures, or tissue slices of organs involved in the metabolism of the compound. Some advantages of using *in vitro* metabolic parameters to define PBK models, include the ability to separately define and analyze individual metabolic processes, such as phase I metabolism and phase II metabolism, or bioactivation and detoxification, and to compare contributions from individual conversions to the overall metabolism across species and between individuals, when limited *in vivo* data are available as is often the case for humans (Lipscomb and Poet, 2008).

Objective and outline of this thesis

The aim of the present PhD project was to build physiologically based kinetic (PBK) models for methyleugenol for both rats and (individual) human subjects in order to obtain a quantitative insight into dose-dependent effects, species differences, and interindividual differences in bioactivation and detoxification of methyleugenol. For the development of these models, metabolic parameters were determined *in vitro* using relevant tissue fractions. The physiological parameters were obtained from the literature (Brown *et al*., 1997) and partition coefficients were estimated from the octanol-water partition coefficient based on an *in silico* method (DeJongh *et al.*, 1997). The present chapter of this thesis presents an introduction to the bioactivation, detoxification, genotoxicity and carcinogenicity of methyleugenol as well as a short introduction to PBK modeling and the aim and content of the present thesis are given.

Chapter 2 defines a PBK model for methyleugenol metabolism in male rat, elucidating dose-dependent effects in bioactivation and detoxification of methyleugenol. In **Chapter 3** a PBK model for methyleugenol bioactivation and detoxification in human is defined of which the outcomes were compared to those predicted by the PBK model for methyleugenol in male rat, described in **Chapter 2.** Comparison of the two models allows evaluation of the occurrence of species differences in metabolic activation and detoxification of methyleugenol. Whereas the PBK model for methyleugenol metabolism in human describes the relative extent of bioactivation in an average situation, interindividual differences can occur within the whole population. The activity levels of the enzymes involved in these reactions can vary in the human population due to genotype and lifestyle-based factors, which could influence the level of bioactivation of methyleugenol between different human subjects to a level that is higher than what would be observed in animal studies with inbred rodent strains. In **Chapter 4**, the influence of possible effects of the dietary matrix and its ingredients on detoxification and bioactivation of methyleugenol is investigated in some more detail. To this end the effects of the basil flavonoid nevadensin (Figure 3) on the SULT mediated bioactivation and DNA adduct formation of 1′-hydroxymethyleugenol is investigated by measuring the formation of methyleugenol-DNA adducts in the human HepG2 cell line. In order to investigate possible *in vivo* implications, the SULT inhibition by nevadensin is also integrated into the male rat and human PBK models for bioactivation and detoxification of methyleugenol. **Chapter 5** defines a PBK model for methyleugenol metabolism in individual human subjects using individual kinetic data for 1'-hydroxylation, epoxidation, and *O*-demethylation determined based on the kinetic constants for individual P450 enzymes, using individual kinetic data for glucuronidation of 1'-hydroxymethyleugenol based on kinetic constants for individual UGT enzyme, and using kinetic data for oxidation and sulfonation based on kinetic constants for individual human liver fractions. Based on the models obtained, the interindividual variation in the liver levels of 1'-sulfooxymethyleugenol due to variation in these metabolic reactions can be evaluated. In a second step, the individual models are combined with literature data on interindividual variation in activity levels of the key enzymes involved in formation, detoxification, and bioactivation of

1'-hydroxymethyleugenol, to model the maximum level of variability in the general population. **Chapter 6** presents a discussion of the results obtained in this thesis indicating on how these results can be used in the risk assessment of methyleugenol. Finally, **chapter 7** presents a summary of the results of this study.

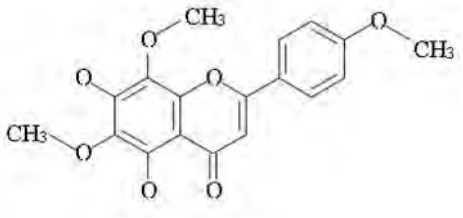

Figure 3. Structural formula of nevadensin

References

Andersen, M.E. and Krishnan, K. (1994). Physiologically based pharmacokinetics cancer risk assessment. Environ Health Persp 102, 103-108.

Barlow, S., Renwick, A.G., Kleiner, J., Bridges, J.W., Busk, L., Dybing, E., Edler, L.,Eisenbrand, G., Fink-Gremmels, J., Knaap, A., Kroes, R., Liem, D., Muller, D.J., Page, S., Rolland, V., Schlatter, J., Tritscher, A., Tueting, W., and Wurtzen, G. (2006). Risk assessment of substances that are both genotoxic and carcinogenic report of an International Conference organized by EFSA and WHO with support of ILSI Europe. Food Chem Toxicol 44, 1636-1650.

Bogaards, J.J., Hissink, E.M., Briggs, M., Weaver, R., Jochemsen, R., Jackson, P., Bertrand, M., and van Bladeren, P.J. (2000). Prediction of interindividual variation in drug plasma

levels in vivo from individual enzyme kinetic data and physiologically based pharmacokinetic modeling. Eur J Pharm Sci 12, 117-124.

Brennan, R.J., Kandikonda, S., Khrimian, A.P., DeMilo, A.B., Liquido, N.J., and Schiestl, R.H. (1996). Saturated and monofluoro analogs of the oriental fruit fly attractant methyl eugenol show reduced genotoxic activities in yeast. Mutat Res 369, 175-181.

Brown, R.P., Delp, M.D., Lindstedt, S.L., Rhomberg, L.R., and Beliles, R.P. (1997). Physiological parameter values for physiologically based pharmacokinetic models. Toxicol Ind Health 13, 407-484.

Burkey J.L., Sauer J.M., McQueen C.A., and Sipes I.G. (2000). Cytotoxicity and genotoxicity of methyleugenol and related congeners – a mechanism of activation for methyleugenol. Mutat Res 453, 25–33.

Carlini, E.A., Dallmeier, K., and Zelger, J.L. (1981). Methyleugenol as a surgical anesthetic in rodents. Experientia 37, 588-589.

Carlini, E.A., de Oliveira, A.B., and de Oliveira, G.G. (1983). Psychopharmacological effects of the essential oil fraction and of the hydrolate obtained from the seeds of Licaria puchury-major. J Ethnopharmacol 8, 225-236.

Chan, V.S., and Caldwell, J. (1992). Comparative induction of unscheduled DNA synthesis in cultured rat hepatocytes by allylbenzenes and their 1'-hydroxy metabolites. Food Chem Toxicol 30, 831-836.

Chiu, W.A., Barton, H. A., DeWoskin, R.S., Schlosser, P., Thompson, C.M., Sonawane, B., Lipscomb, J.C., and Krishnan, K. (2007). Evaluation of physiologically based pharmacokinetic models for use in risk assessment. J Appl Toxicol 27, 218–237.

Clewell, H.J. 3rd, Andersen, M.E., and Barton, H.A. (2002). A consistent approach for the application of pharmacokinetic modeling in cancer and noncancer risk assessment. Environ Health Perspect 110, 85-93.

Clewell, H.J., Gentry, P.R., Gearhart, J.M., Allen, B.C., and Andersen, M.E. (2001). Comparison of cancer risk estimates for vinyl chloride using animal and human data with a PBPK model. Sci Total Environ 274, 37-66.

(COC) (2004). Committee on Carcinogenicity of chemicals in food, consumer products and the environment. Guidance on a strategy for the risk assessment of chemical carcinogens. http://www.advisorybodies.doh.gov.uk/coc/guideline04.pdf

DeJongh, J., Verhaar, H.J. and Hermens, J.L. (1997). A quantitative property property relationship (QPPR) approach to estimate in vitro tissue-blood partition coefficients of organic chemicals in rats and humans. Arch Toxicol 72, 17-25.

De Vincenzi, D., Silano, M., Stacchini, P., and Scazzocchio, B. (2000). Constituents of aromatic plants: I. Methyleugenol. Fitoterapia 71, 216-221.

Ding, W., Levy, D.D., Bishop, M.E., Lyn-Cook Lascelles, E., Kulkarni, R., Chang, C.W., Aidoo, A., and Manjanatha, M.G. (2011). Methyleugenol genotoxicity in the Fischer 344 rat using the comet assay and pathway-focused gene expression profiling. Toxicol Sci 123,103-112.

Drinkwater, N.R., Miller, E.C., Miller, J.A., and Pitot, H.C. (1976). Hepatocarcinogenicity of estragole (1-allyl-4-methoxybenzene) and 1'-hydroxyestragole in the mouse and mutagenicity of 1'-acetoxyestragole in bacteria. J Natl Cancer Inst 57, 1323-1331.

Dybing, E., O'Brien, J., Renwick, A.G., and Sanner, T. (2008). Risk assessment of dietary exposures to compounds that are genotoxic and carcinogenic-an overview. Toxicol Lett 180, 110-117.

EFSA (2005). Opinion of the scientific committee on a request from EFSA related to a harmonised approach for risk assessment of substances which are both genotoxic and carcinogenic. EFSA J 282, 1–31. http://www.efsa.europa.eu/en/efsajournal/doc/282.pdf

Environment Canada (2010). Screening Assessment for the Challenge Benzene, 1,2-dimethoxy-4-(2-propenyl)-(Methyl eugenol). Chemical Abstracts Service Registry Number 93-15-2. Environment Canada – Health Canada. http://www.ec.gc.ca/ese-ees/0129FD3C-B0FF-41C8-8BF5-7B2CD016AD36/batch9_93-15-2_en.pdf

EPA (2005). Guidelines for carcinogen risk assessment and supplemental guidance for assessing susceptibility from early-life exposure to carcinogens. Washington, DC: U.S. Environmental Protection Agency. http://cfpub.epa.gov/ncea/raf/recordisplay

European Commission (2008). Regulation (EC) No 1334/2008 of the European Parliament and of the Council of 16 December 2008 on flavourings and certain food ingredients with flavouring properties for use in and on foods and amending Council Regulation (EEC) No 1601/91, Regulations (EC) No 2232/96 and (EC) No 110/2008 and Directive 2000/13/EC. Off J Eur Union, L354/34: http://eur-lex.europa.eu/LexUriServ/LexUriServ.do?uri =OJ:L: 2008:354:0034:0050:en:pdf

Farm Chemical Handbook (1992). Meister Publishing Co., p. C221, Willoughby, Ohio.

Fenaroli′s Handbook of Flavor Ingredients (1975). 2nd ed., Vol. 2 (T.E. Furia and N. Bellanca, Eds.), p. 200. The Chemical Rubber Co., Cleveland, Ohio.

Gardner, I., Wakazono, H., Bergin, P., de Waziers, I., Beaune, P., Kenna, J.G., and Caldwell, J. (1997). Cytochrome P450 mediated bioactivation of methyleugenol to 1′-hydroxyethyl-eugenol in Fischer rat and human liver microsomes. Carcinogenesis 18, 1775-1783.

Gavin C.L., Williams M.C., and Hallagan J.B. (2007). FEMA Poundage and Technical Effects Update Survey. Flavor and Extract Manufacturers Association, Washington, DC, USA.

Hall, R.L., and Oser, B.L. (1965). Recent progress in the consideration of flavoring ingredients under the food additives amendment III. GRAS substances. Food Technol 253, 151–197.

Hays, W.J.,and Laws, E.R., Jr., Eds. (1991). Handbook of Pesticides Toxicology, San Diego, CA: Academic Press; Vol. 2, p. 613-614.

Herrmann, K., Engst, W., Appel, K.A., Monien, B.H., and Glatt, H. (2012). Identification of human and murine sulfotransferases able to activate hydroxylated metabolites of methyleugenol to mutagens in Salmonella typhimurium and detection of associated DNA adducts using UPLC–MS/MS methods. Mutagenesis 15, 1–10.

Howes A.J., Chan V. S.W., and Caldwell J. (1990). Structure-specificity of the genotoxicity of some naturally occurring alkenylbenzenes determined by the unscheduled DNA synthesis assay in rat hepatocytes. Food Chem Toxicol 28, 537-542.

JECFA (2008). Sixty-ninth meeting Rome, Italy, 17-26 June 2008. http://www.who.int/entity /ipcs /food/jecfa/summaries/summary69.pdf

Jeurissen, S.M.F., Bogaards, J.J.P., Boersma, M.G. ter Horst, J.P.F., Awad, H.A., Fiamegos,

Y.C., van Beek, T.A., Alink G.M., Sudhölter, E.J.R., Cnubben, N.H.P., and Rietjens, I.M.C.M. (2006). Human cytochrome P450enzymes of importance for the bioactivation of methyleugenol to the proximate carcinogen 1′-hydroxymethyleugenol. Chem Res Toxicol 19, 111–116.

Johnson, J.D., Ryan, M.J., Toft, J.D., Graves, S.W., Hejtmancik, M.R., Cunningham, M.L., Herbert, R., and Abdo, K.M. (2000). Two-Year Toxicity and Carcinogenicity Study of Methyleugenol in F344/N Rats and B6C3F1 Mice. J Agr Food Chem 48, 3620-3632.

Kerckaert G.A., Brauninger R., LeBoeuf R.A., and Isfort R.J. (1996). Use of the Syrian hamster embryo cell transformation assay for carcinogenicity prediction of chemicals currently being tested by the National Toxicology Program in rodent bioassays. Environ Health Perspect 104, 1075–1084.

Krishnan, K. and Andersen, M.E. (2001). Physiologically-based pharmacokinetic modeling and toxicology. In principles and methods of toxicology (A.W. Hayes, Ed.), pp. 193-241. Raven Press, N.Y.

Lide, D.R., Ed. (1998). CRC Handbook of Chemistry and Physics, 78th ed., pp. 3-42. CRC Press, Inc., Boca Raton, FL.

Lipscomb, J.C. and Poet, T.S. (2008). In vitro measurements of metabolism for application in pharmacokinetic modeling. Pharmacol Therapeut 118, 82-103.

Luo, G. and Guenthner, T.M. (1995). Metabolism of allylbenzene 2′,3′-oxide and estragole 2′,3′-oxide in the isolated perfused rat liver. J Pharmacol Exp Ther 272, 588–596.

Miele, M., Dondero, R., Ciarallo, G., and Mazzei, M.J. (2001). Methyleugenol in Ocimum basilicum L.cv. Genovese Gigante. J Agr Food Chem 49, 517-21.

Miller, E.C., Swanson, A.B., Phillips, D.H., Fletcher, T.L., Liem, A., and Miller, J.A. (1983). Structure-activity studies of the carcinogenicities in the mouse and rat of some naturally occurring and synthetic alkenylbenzene derivatives related to safrole and estragole. Cancer Res 43, 1124-1134.

Nijssen, B., van Ingen-Visscher, K., and Donders, J. (2008). Volatile Compounds in Foods (VCF) database. TNO Nutrition and Food Research, Zeist, Netherlands. http://www.vcf-

online.nl/VcfHome.cfm; Version 10.1 accessed

NTP (2000). Toxicology and carcinogenesis studies of methyleugenol (CAS No. 93-15-12) in F344/N rats and B6C3F1 mice (Gavage studies). Natl Toxicol Program Tech Rep Ser, 491, 1-412.

Opdyke, D.L.J., Ed. (1979). Monographs on Fragrance Raw Materials, p. 555. Pergamon Press, Inc., N. Y.

Phillips, D.H., Miller, J.A., Miller, E.C., and Adams, B. (1981). Structures of the DNA adducts formed in mouse liver after administration of the proximate hepatocarcinogen 1'-hydroxy-estragole. Cancer Res 41, 176-186.

Rietjens, I.M.C.M., Louisse, J., and Punt, A. (2011). Tutorial on physiologically based kinetic modeling in molecular nutrition and food research. Mol Nutr Food Res 6, 941-956.

Rietjens, I.M.C.M., Punt, A, Schilter, B, Scholz, G., Delatour, T, and van Bladeren, P.J. (2010). *In silico* methods for physiologically based biokinetic models describing bioactivation and detoxification of coumarin and estragole: Implications for risk assessment. Mol Nutr Food Res 54, 195-207.

Sax′s Dangerous Properties of Industrial Materials (1992). 8th ed. (R.J. Lewis, Sr., Ed.), pp. 2435-2437. Van Nostrand Reinhold, N.Y.

SCF (2001). Opinion of the scientific committee on food on methyleugenol (4-allyl-1,2-dimethyxybenzene). European Commission, Scientific Committee on Food. Brussels, BE. http://ec.europa.eu/food/fs/sc/scf/out104_en.pdf

Schecter, A., Lucier, G.W., Cunningham, M.L., Abdo, K.M, Blumenthal, G., Silver, A.G., Melnick, R., Portier, C., Barr, D.B., Barr, J.R., Stanfill, S.P., Patterson Jr., D.G., Needham, L.L., Stopford, W., Masten, S., Mignogna, J., and Tung, K.C. (2004). Human consumption of methyleugenol and its elimination from serum. Environ Health Persp 112, 678-680.

Schiestl, R.H., Chan, W.S., Gietz, R.D., Mehta, R.D., and Hastings, P.J. (1989). Safrole, eugenol, and methyleugenol induce intrachromosomal recombination in yeast. Mutat Res 224, 427-436.

Smith, R.L., Adams, T.B., Doull, J., Feron, V.J., Goodman, J.I., Marnett, L.J., Portoghese, P.S.,

Waddell, W.J., Wagner, B.M., Rogers, A.E., Caldwell, J., and Sipes, I.G. (2002). Safety assessment of allylalkoxybenzene derivatives used as flavoring substances – methyl eugenol and estragole. Food Chem Toxicol 40, 851-870.

Solheim, E., and Scheline, R.R. (1976). Metabolism of alkenebenzene derivatives in the rat. II. Eugenol and isoeugenol methyl ethers. Xenobiotica 6, 137-150.

van den Berg, S.J.P.L., Restani, P., Boersma, M.G., Delmulle, L., and Rietjens, I.M.C.M. (2011). Levels of genotoxic and carcinogenic ingredients in plant food supplements and associated risk assessment. Food Nutr Sci 2, 989-1010.

WHO (1981). Evaluation of Certain Food Additives and contaminants. Twenty-sixth Report of the Joint WHO/FAO Expert Committee on Food Additives. Technical Report Series 669. Geneva, Switzerland: World Health Organization. pp. 92-94.

Zhou, G.D., Moorthy, B., Bi, J., Donnelly, K.C., and Randerath, K. (2007). DNA adducts from alkoxyallylbenzene herb and spice constituents in cultured human (HepG2) cells. Environ Mol Mutag 48, 715–721.

2

Physiologically based kinetic model of bioactivation and detoxification of the alkenylbenzene methyleugenol in rat

Based on: Al-Subeihi A.A.A., Spenkelink B., Rachmawati N., Boersma M.G., Punt A., Vervoort J., van Bladeren P.J., and Rietjens I.M.C.M. Toxicol In Vitro (2011) 25, 267-285

Abstract

The present study defines a physiologically based kinetic (PBK) model for the alkenylbenzene methyleugenol in rat based on *in vitro* metabolic parameters determined using relevant tissue fractions, *in silico* derived partition coefficients, and physiological parameters derived from the literature. The model was based on the model previously developed for the related alkenylbenzene estragole and consists of eight compartments including liver, lung, and kidney as metabolizing compartments, and separate compartments for fat, arterial blood, venous blood, richly perfused and slowly perfused tissues. Evaluation of the model was performed by comparing the PBK predicted concentration of methyleugenol in the venous compartment to methyleugenol plasma levels reported in the literature, by comparing the PBK predicted dose-dependent % of formation of 2-hydroxy-4,5-dimethoxyallylbenzene, 3-hydroxy-4-methoxy-allylbenzene, and 1′-hydroxymethyleugenol glucuronide to the corresponding % of metabolites excreted in urine reported in the literature, which were demonstrated to be in the same order of magnitude. With the model obtained, the relative extent of bioactivation and detoxification of methyleugenol at different oral doses was examined. At low doses, formation of 3-(3,4-dimethoxyphenyl)-2-propen-1-ol and methyleugenol-2′,3′-oxide leading to detoxification appears to be the major metabolic pathways, occurring in the liver. At high doses, the model reveals a relative increase in the formation of the proximate carcinogenic metabolite 1′-hydroxymethyleugenol, occurring in the liver. This relative increase in formation of 1′-hydroxymethyleugenol leads to a relative increase in formation of 1′-hydroxymethyleugenol glucuronide, 1′-oxomethyleugenol, and 1′-sulfooxymethyleugenol the latter being the ultimate carcinogenic metabolite of methyleugenol. These results indicate that the relative importance of different metabolic pathways of methyleugenol may vary in a dose-dependent way, leading to a relative increase in bioactiviation of methyleugenol at higher doses.

Introduction

Methyleugenol is a naturally occurring constituent of the essential oils of a number of plants (De Vincenzi *et al.*, 2000). It is present in, for instance, basil, nutmeg, tarragon, star anise, lemongrass, pimento and fennel (SCF, 2001). Human exposure to methyleugenol may occur through the consumption of foods flavored with these aromatic plants and/or their essential oil fractions. Miller *et al.* (1983) dosed mice with 4.75 µmol (846 µg) of methyleugenol administered by intraperitoneal injections from 1 to 22 days after birth. Hepatic tumors were found in 70% and 96% of the mice sacrificed after 13 months and between 13 and 18 months, respectively. Moreover, methyleugenol was found to cause hepatocholangiomas and hepatocholangiocarcinomas in male and female rats when administered daily at oral dose levels higher than and including 150 mg/(kg bw)/day, five days per week for two years (NTP, 2000). In 1965, the panel of the Flavor and Extract Manufacturers Association (FEMA) concluded that methyleugenol was GRAS (Generally Recognized As Safe) under conditions of intended use as a flavoring substance in food (Hall and Oser, 1965). In the FEMA evaluation it was taken into account that there are experimental data suggesting a non-linear relationship between dose and profiles of metabolism and metabolic activation and that exposure due to use as a flavoring is relatively low (Smith *et al*., 2002). In 2000, the carcinogenicity of methyleugenol was investigated in mice and rats by the National Toxicology Program (NTP) (NTP, 2000). The NTP reported that methyleugenol is carcinogenic in both rats and mice (NTP, 2000). In 2001, the FEMA Panel reassessed the available data for methyleugenol and confirmed that there is no considerable cancer risk resulting from consumption of methyleugenol as flavoring substance and affirmed the GRAS status of methyleugenol as a flavoring substance (Smith *et al.*, 2002). In 2001, the Scientific Committee on Food (SCF) of the European Union published a scientific opinion on methyleugenol in which it was concluded that methyleugenol is genotoxic and carcinogenic and that reductions in exposure and restrictions in use levels are indicated (SCF, 2001). Based on different methodologies the average daily intake of methyleugenol was

estimated by the SCF to be 13 mg/day, corresponding to 0.217 mg/(kg bw)/day for a 60 kg person (SCF, 2001), while the FEMA estimated the average daily intake of methyleugenol to be less than 0.01 mg/(kg bw)/day (Smith *et al.*, 2002). The estimation of the SCF is based on theoretical maximum use levels of methyleugenol in various food categories and consumption data for these food categories, whereas the intake estimation of the FEMA is based on production volume data for flavor use (SCF, 2001; Smith *et al.*, 2002).

Methyleugenol is unreactive by itself but undergoes metabolic activation to produce electrophilic metabolites that act as the reactive genotoxic DNA binding intermediates (Gardner *et al.*, 1997; Miele *et al.*, 2001). Figure 1 displays the different metabolic pathways of methyleugenol. Important metabolic pathways include *O*-demethylation of the methoxy moieties on the benzene ring, 2′,3′-epoxidation, and 1′-hydroxylation of the allylic side chain (NTP, 2000; Solheim and Scheline, 1976). *O*-demethylation of the *meta* or *para* methoxy substituents of methyleugenol yields the corresponding phenolic derivatives, which may be excreted as sulfate or glucuronic acid conjugate (Smith *et al.*, 2002). Epoxidation of the side chain yields a 2′,3′-epoxide. This epoxide is detoxified by epoxide hydrolase to form the dihydrodiol or via glutathione conjugation (Luo and Guenther, 1995). Hydroxylation at the 1'-position of methyleugenol is considered to represent the bioactivation pathway producing the proximate carcinogenic metabolite 1′-hydroxymethyleugenol (Drinkwater *et al.*, 1976; Miller *et al.*, 1983). In a next step 1′-hydroxymethyleugenol can be sulfonated by sulfotransferases to form the ultimate carcinogenic metabolite 1′-sulfooxymethyleugenol (Miller *et al.*, 1983).

In order to predict the degree of bioactivation and detoxification of methyleugenol at low dose intake, it is important to take non-linear effects in kinetics into account when extrapolating from high dose to low dose. The present study was undertaken to develop a physiologically based kinetic (PBK) model which will be able to give insight in possible dose-dependent differences and shifts in methyleugenol metabolism with emphasis on detoxification and bioactivation pathways. Recently, physiologically based kinetic (PBK) models for the related genotoxic and carcinogenic alkenylbenzene estragole were developed for male rat (Punt *et al.*, 2008) and human (Punt *et al.*, 2009). These models were capable of elucidating dose dependent

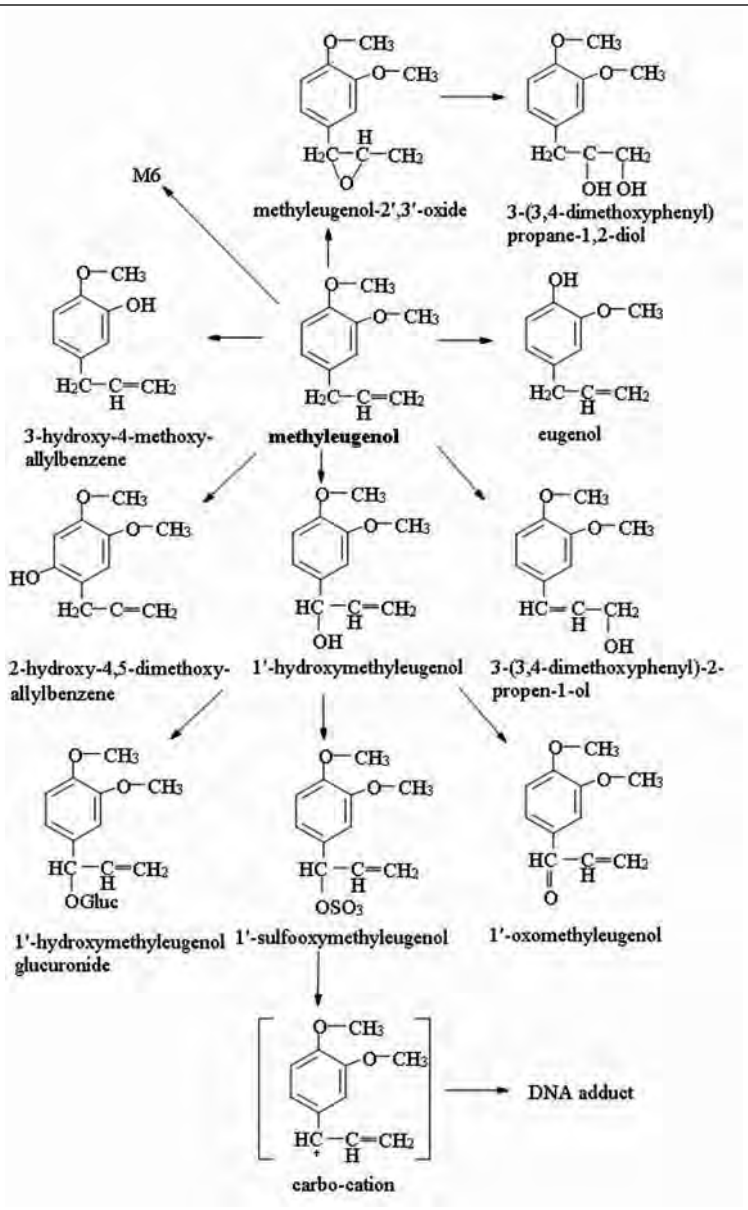

Figure 1. Suggested metabolic pathways of methyleugenol in male rat.

differences in bioactivation and detoxification of estragole, based on *in vitro* metabolic parameters. It can be expected that the PBK model thus developed for male rat (Punt *et al.*, 2008) can be used to develop a similar model for the related carcinogenic alkenylbenzenes including methyleugenol, the model compound of the present study. The objectives of the present study were to define the kinetics of relevant metabolic pathways of methyleugenol in order to define a PBK model for methyleugenol in male rat and to investigate possible dose-dependent shifts in detoxification and bioactivation of methyleugenol using the PBK model thus obtained.

Materials and Methods

Chemical and reagents

Pooled liver, kidney, lung and small intestine microsomes from male Sprague Dawley rats and pooled liver microsomes from female Sprague Dawley rats were purchased from BioPredic International (Rennes, France). Pooled liver microsomes from male Fisher 344 and female Fisher 344 rats were purchased from BD Gentest (Woburn, MA, USA). Dichloromethane, *m*-chloroperbenzoic acid, potassium fluoride, potassium carbonate, hydrochloric acid (37%), potassium dihydrogen phosphate, dipotassium hydrogen phosphate trihydrate, and acetic acid were purchased from VWR Merck (Darmstadt, Germany). β-Glucuronidase and reduced β-nicotinamide adenine dinucleotide phosphate (NADPH) were obtained from Roche Diagnostics (Mannheim, Germany). Tris(hydroxymethyl) aminomethane was obtained from Gibco BRL Life Technologies (Paisley, Scotland). Methyleugenol, eugenol, acetonitrile (chromatography grade), methanol, dimethyl-sulfoxide (DMSO), ascorbic acid, glutathione (GSH), alamethicin, and uridine 5′-diphosphoglucuronic acid (UDPGA) were purchased from Sigma-Aldrich (Steinheim, Germany). 3′-Phosphoadenosine-5′-phosphosulfate (PAPS) was obtained from Fluka (Buchs Switzerland).

Synthesis of Phase I Metabolites

Caution: 1′-Acetoxymethyleugenol, 1′-hydroxymethyleugenol, 3-(3,4-dimethoxyphen-yl)-2-propen-1-ol, methyleugenol-2′,3′-oxide, and 1′-oxomethyleugenol are carcinogenic and should be handled carefully.

1′–Hydroxymethyleugenol was synthesized as described previously for 1′-hydroxysafrole (Borchert *et al.*, 1973; Jeurissen *et al.*, 2004), using veratraldehyde as the starting material. Its identity was confirmed by comparison of its MS spectral data to literature MS data (*m/z* 179, 161, 151, 139) (Solheim and Scheline, 1976). Based on GC and HPLC analysis the purity of 1'-hydroxymethyleugenol was estimated to be more than 98 % (Jeurissen *et al.*, 2006). 3-(3,4-Dimethoxyphenyl)-2-propen-1-ol was synthesized, as described previously for 1′-hydroxyestragole (Iyer *et al.*, 2003), using 1′-acetoxymethyleugenol as the starting material. The GC-MS analysis revealed that the method described resulted in formation of 3-(3,4-dimethoxyphenyl)-2-propen-1-ol instead of 1′-hydroxymethyleugenol. Structural confirmation was obtained by comparison of its MS spectral data (*m/z* 176, 161, 151, 138) to those available from literature (Solheim and Scheline, 1976). Based on HPLC analysis, the purity of 3-(3,4-dimethoxyphenyl)-2-propen-1-ol was about 98%. 1′-Acetoxymethyleugenol was synthesized based on a method described by Iyer *et al.* (2003) for the synthesis of 1′-acetoxyestragole, using methyleugenol as the starting material. The purity of 1′-acetoxymethyleugenol was determined by HPLC as about 98%.

Methyleugenol-2′,3′-oxide was synthesized as described by Luo *et al.* (1992) using methyleugenol instead of estragole. GC-MS analysis of the product confirmed the formation of methyleugenol-2′,3′-oxide (m/z 194, 177, 165, 151, 138) (Solheim and Scheline, 1976). Further confirmation for the formation of methyleugenol-2′,3′-oxide was obtained from monitoring the hydrolysis of methyleugenol-2′,3′-oxide in incubations with male rat liver microsomes resulting in formation of 3-(3,4-dimethoxyphenyl)propane-1,2-diol.

3-(3,4-Dimethoxyphenyl)propane-1,2-diol was synthesized as described in the literature (Solheim and Scheline, 1976) and its formation was confirmed by comparing its retention time and UV spectra to those of the compound obtained from incubation of methyleugenol-2′,3′-

oxide with male rat liver microsomes.

Synthesis of 3-hydroxy-4-methoxyallylbenzene was performed according to the method described in the literature (Solheim and Scheline, 1976). Its identity was confirmed by comparing its MS spectral data (*m/z* 149, 137, 131, 121) to MS data from literature (Solheim and Scheline, 1976).

No reference compound was available for 2-hydroxy-4,5-dimethoxyallylbenzene. Its formation in the incubation mixture of methyleugenol with rat liver microsomes was confirmed comparing its MS spectral data (*m/z* 176, 151, 123, 107) to MS data from literature (Solheim and Scheline, 1976).

GC-MS analysis

GC-MS analysis was performed to identify the phase I metabolites of methyleugenol formed during the microsomal incubations. An incubation mixture of methyleugenol was extracted with CH_2Cl_2. The organic layer was transferred into a new vial and the solution was concentrated under a stream of nitrogen. Aliquots (2 µL) of the sample were injected on a HP6890 gas chromatograph, equipped with a J&W MS-5 column (30 m x 0.25 mm, 0.25 µm film) and an HP5973 mass selective detector. The GC was programmed for a 47 min run with a temperature gradient from 50 to 250 °C at 5 °C /min. The inlet temperature was 260 °C, the split ratio was 15:1 and the pressure of the helium carrier gas was 12.0 psi. The mass spectrometer was run in the electron impact mode with electron energy at 70 eV with a mass range of m/z 30 – 550 and a source temperature of 280 °C (Jeurissen *et al.*, 2006).

Phase I Metabolism

Determination of the organs which are involved in the metabolism of methyleugenol was performed as described by Punt *et al.* (2008) for estragole. The microsomal preparations of the liver, lung, kidney, and small intestine from male Sprague Dawley rats were incubated with methyleugenol in the presence of NADPH, and the formation of the metabolites was monitored over time. The incubation mixtures had a final volume of 160 µL, containing (final

concentrations) 3 mM NADPH, 1 mM ascorbic acid and 1 mg/mL microsomal protein in 0.2 M Tris-HCl (pH 7.4). After pre-incubation at 37 °C for 1 min, the reactions were started by the addition of the substrate methyleugenol added from a 100 times concentrated stock solution in DMSO. The reactions were terminated by addition of 40 µL cold acetonitrile. Initial incubations were performed at a substrate concentration of 1000 µM (final concentration) at several incubation times and microsomal protein concentrations. Blank incubations were performed without the cofactor NADPH.

The kinetic constants for the formation of different phase I metabolites of methyleugenol were determined in liver, lung, and kidney microsomes, which were found to be capable of metabolizing methyleugenol (see Results section). The incubation mixtures were as described above. Incubations with male rat liver, lung, and kidney microsomes were carried out for 10 min at a substrate concentration that ranged from 50 to 1000 µM methyleugenol. All incubations were started by addition of substrate from a 100 times concentrated stock solution in DMSO and terminated by addition of 40 µL cold acetonitrile. Under the conditions specified, the formation of the different methyleugenol metabolites was linear with time and microsomal protein concentration for all the microsomal fractions. In the blank incubations performed without NADPH low amounts of 3-(3,4-dimethoxyphenyl)-2-propen-1-ol were also formed. Therefore the formation of 3-(3,4-dimethoxyphenyl)-2-propen-1-ol was corrected for the amount of 3-(3,4-dimethoxyphenyl)-2-propen-1-ol formed in the blank incubations. In the blank incubations performed without NADPH, low amounts of eugenol were also found. The amounts of eugenol found in the blank incubations of both liver and kidney microsomes were equal or more than the amount of eugenol found in incubation mixtures. Only the formation of eugenol in lung microsomes was corrected for the amount of eugenol found in the blank incubations.

Kinetic constants for formation of phase I metabolites were also determined in incubations with liver microsomes obtained from female Sprague Dawley rats, and male and female Fisher 344 rats. As for the incubations with liver microsomes from male Sprague Dawley rats, the formation of 3-(3,4-dimethoxyphenyl)-2-propen-1-ol was corrected for the amount of 3-(3,4-

dimethoxyphenyl)-2-propen-1-ol formed in the blank incubations without cofactor.

HPLC analysis of Phase I metabolites

Before HPLC analysis of the samples, all incubations were centrifuged for 5 min at 16,000 g. Aliquots of 50 µL of the supernatant of each sample were analyzed on a Waters M600 HPLC system (Waters, Milford, MA) equipped with an Alltima C18 5-µm column, 150 x 4.6 mm (Grace Alltech, Breda, The Netherlands). Detection was performed between 200 and 350 nm using a Waters 2996 photodiode array detector (Waters, Milford, MA).

For the analysis of phase I metabolites the gradient was made with ultrapure water and acetonitrile. The flow rate was 1 mL/min and a gradient was applied from 0% to 15% acetonitrile over 5 min and then increased to 17.5 % over 20 min after which the percentage acetonitrile was increased to 35% over 15 min and kept at 35 % for 5 min. Then the percentage of acetonitrile was increased to 100% over 10 min, and kept at 100% for 5 min. Quantification of 1′-hydroxymethyleugenol was achieved by comparison of the peak areas of this metabolite in the chromatograms obtained at a wavelength of 280 nm to the calibration curve of the synthesized 1′-hydroxymethyleugenol obtained at the same wavelength. Because methyleugenol-2′,3′-oxide and 3-(3,4-dimethoxyphenyl)propane-1,2-diol have the same UV spectra as 1′-hydroxymethyleugenol, 3-(3,4-dimethoxyphenyl)-2-propen-1-ol and 2-hydroxy-4,5-dimethoxyallylbenzene have the same UV spectrum as 1′-acetoxymethyleugenol, and the unidentified metabolite eluting at a retention time of 44.9 min has almost the same UV spectra as eugenol (data not shown) it was assumed that they have the same molar extinction coefficient as 1′-hydroxymethyleugenol, 1′-acetoxymethyleugenol, and eugenol respectively.

Quantification of 3-(3,4-dimethoxyphenyl)propane-1,2-diol, reflecting formation of methyleugenol-2′,3′-oxide in liver microsomes, was therefore achieved by comparison of the peak area of 3-(3,4-dimethoxyphenyl)propane-1,2-diol in the chromatograms obtained at a wavelength of 280 nm to the calibration curve for 1′-hydroxymethyleugenol obtained at the same wavelength. In kidney microsomes, quantification of methyleugenol-2′,3′-oxide was achieved by comparison of the peak area of methyleugenol-2′,3′-oxide in the chromatograms

obtained at a wavelength of 280 nm to the calibration curve for 1′-hydroxymethyleugenol obtained at the same wavelength. While quantification of 3-(3,4-dimethoxyphenyl)-2-propen-1-ol and 2-hydroxy-4,5-dimethoxyallylbenzene was achieved by comparison of the peak area of 3-(3,4-dimethoxyphenyl)-2-propen-1-ol and 2-hydroxy-4,5-dimethoxyallylbenzene in the chromatograms obtained at a wavelength of 280 nm to the calibration curve for 1′-acetoxymethyleugenol. Quantification of the unidentified metabolite eluting at a retention time of 44.9 min was achieved by comparison of the peak area of this metabolite in the chromatograms obtained at a wavelength of 280 nm to the calibration curve for eugenol obtained at the same wavelength.

Phase II metabolism

Glucuronidation of 1′-hydroxymethyleugenol to 1′-hydroxymethyleugenol glucuronide

Incubations with male Sprague Dawley rat liver microsomes were performed as described by Punt *et al.* (2008) using 1′-hydroxymethyleugenol instead of 1′-hydroxyestragole to determine the kinetic constants for glucuronidation of 1′-hydroxymethyleugenol. The incubation mixture had a final volume of 200 μL, containing (final concentrations) 10 mM UDPGA, and 1 mg/mL microsomal protein in 0.2 M Tris-HCl (pH 7.4) containing 10 mM $MgCl_2$. The incubation mixture was pre-treated with 0.025 mg/mL of the poreforming peptide alamethicin from a 200 times concentrated stock in methanol on ice for 15 min to overcome enzyme latency and obtain maximal glucuronidation activity (Fisher *et al.*, 2000; Lin and Wong, 2002). The reactions were started by the addition of the substrate 1′-hydroxymethyleugenol from a 200 times concentrated stock solution in DMSO, after pre-incubation at 37 °C for 1 min. The reactions were carried out for 10 min and terminated by addition of 50 μL cold acetonitrile. Blank incubations were performed without the cofactor UDPGA. Additional incubations were performed in which the samples obtained were treated with β-glucuronidase to verify whether 1′-hydroxymethyleugenol glucuronide had indeed been formed. For these incubations, 90 μL of sample (reaction mixture that has not been terminated

by addition of acetonitrile) was added to 10 µL of 1 M potassium phosphate (pH 6.2). After the addition of 2 µL of β-glucuronidase solution (0.3 units), the mixture was incubated for 1 hr at 37 °C.

The kinetic constants for the formation of 1′-hydroxymethyleugenol glucuronide from 1′-hydroxymethyleugenol were determined using liver microsomes. The incubation mixtures were as described above. Incubations with male rat liver microsomes were carried out for 10 min at a substrate concentration that ranged from 50 to 2000 µM 1′-hydroxymethyleugenol. All incubations were started by addition of substrate from a 200 times concentrated stock solution in DMSO and terminated by addition of 50 µL cold acetonitrile. Under the conditions specified, the formation of 1′-hydroxymethyleugenol glucuronide was linear with time and microsomal protein concentration. In the blank incubations performed without UDPGA no 1′-hydroxymethyleugenol glucuronide was formed.

HPLC analysis of 1′-hydroxymethyleugenol glucuronide

HPLC analysis was used for quantification of 1′-hydroxymethyleugenol glucuronide using an Alltima C18 5-µm column, 150 mm x 4.6 mm (Grace Alltech, Breda, The Netherlands) coupled to Waters M600 HPLC system (Waters, Milford, MA). Elution was performed using a gradient made with ultrapure water containing 0.1% (v/v) acetic acid and acetonitrile. The flow rate was 1 mL/min and a gradient was applied from 10% to 25% acetonitrile over 30 min after which the percentage acetonitrile was increased to 100% over 2 min, and kept at 100% for 1 min. Detection was performed at 280 nm using a Waters 2996 photodiode array detector (Waters, Milford, MA). Because 1′-hydroxymethyleugenol glucuronide has the same UV spectrum as 1′-hydroxymethyleugenol (data not shown) it was assumed that it has the same molar extinction coefficient as 1′-hydroxymethyleugenol. Quantification of the 1′-hydroxymethyleugenol glucuronide was therefore achieved by comparison of the peak area of 1′-hydroxymethyleugenol glucuronide in the chromatograms obtained at a wavelength of 280 nm to the calibration curve of 1′-hydroxymethyleugenol obtained at the same wavelength.

LC-MS analysis of 1′-hydroxymethyleugenol glucuronide

The nature of 1′-hydroxymethyleugenol glucuronide was furthermore verified by LC-MS, which was performed on an Agilent 1200 HPLC system coupled to a Bruker MicroTOF mass spectrometer. Aliquots of 20 µL (injected volume) were separated on an Alltima C18 5-µm column, 150 x 2.1 mm (Grace Alltech, Breda, The Netherlands). The gradient was made with ultrapure water containing 0.1% (v/v) formic acid (eluent A) and acetonitrile with 0.1% (v/v) formic acid (eluent B) and the flow rate was set to 0.2 mL/min. A linear gradient was applied from 10% to 25% eluent B over 30 min after which the percentage of eluent B was increased to 100% over 2 min, and kept at 100% for 1 min. Mass spectrometric analysis was in the negative electrospray mode using a spray voltage of capillary voltage of 4500 V, a capillary temperature of 200 °C, and nitrogen as nebulizer gas at 8.0 L/min.

Oxidation of 1′-hydroxymethyleugenol to 1′-oxomethyleugenol

Formation of 1′-oxomethyleugenol was studied as described by Punt *et al.* (2009) for formation of 1′-oxoestragole. Incubations were performed with male rat Sprague Dawley liver microsomes, using NAD^+ as cofactor and GSH to trap the reactive 1′-oxomethyleugenol. The kinetic constants for formation of the 1′-oxomethyleugenol adduct with GSH, reflecting the formation of 1′-oxomethyleugenol, were determined with male rat liver microsomes at substrate concentrations that ranged from 10 to 1000 µM 1′-hydroxymethyleugenol. These incubation mixtures had a final volume of 160 µL, containing (final concentrations) 3 mM NAD^+, 10 mM GSH, and 1 mg/mL microsomal protein in 0.2 M Tris-HCl (pH 7.4). The reactions were terminated after 10 min by addition of 40 µL cold acetonitrile. Under these conditions the formation of the glutathione adduct, 3′-(glutathione-S-yl)-1′-oxo-2′-3′-dihydromethyleugenol (GS-1′-oxomethyleugenol), was linear with time and microsomal protein concentration.

HPLC analysis of GS-1′-oxomethyleugenol

The incubation mixture was centrifuged for 5 min at 16,000 g. HPLC analysis was used for quantification of GS-1′-oxomethyleugenol using an Alltima C18 5-µm column, 150 mm x 4.6

mm (Grace Alltech, Breda, The Netherlands) coupled to Waters M600 HPLC system. Detection was performed at 280 nm using a Waters 2996 photodiode array detector. Quantification of GS-1′-oxomethyleugenol was performed by means of a calibration curve obtained as described by Punt *et al.* (2009). To this end 1′-oxomethyleugenol was synthesized from 1′-hydroxymethyleugenol as described for 1′-oxosafrole by Fennell *et al.* (1984). A calibration curve of GS-1′-oxomethyleugenol was prepared by incubating 40 µM 1′-oxomethyleugenol with increasing concentrations of GSH, ranging from 2 to 10 µM in 0.2 M Tris-HCl (pH 7.4). The reactions were incubated for 6 hr at 37 °C resulting in full conversion of all GSH added to the incubations to GS-1′-oxomethyleugenol. The peak area of GS-1′-oxomethyleugenol in the chromatograms of these incubations were related to the quantity of GSH used in the reactions, thus providing a calibration curve for the GSH adduct of 1′-oxomethyleugenol ultimately quantifying the formation of 1′-oxomethyleugenol.

LC-MS analysis of GS-1′-oxomethyleugenol

Formation of GS-1'-oxomethyleugenol in the incubations was verified by LC-MS, which was performed on an Agilent 1200 HPLC system coupled to a Bruker MicroTOF mass spectrometer. Aliquots of 20 µL (injected volume) were separated on an Alltima C18 5-µm column, 150 x 2.1 mm (Grace Alltech, Breda, The Netherlands). The gradient was made with acetonitrile (eluent B) and ultrapure water (eluent A) both containing 0.1% (v/v) formic acid and the flow rate was set to 0.2 mL/min. A linear gradient was applied from 0 to 25% eluent B over 5 min and was kept at 25% for 5 min, after which the percentage of eluent B was increased to 100% over 2 min. Mass spectrometric analysis was performed in positive electrospray mode using a spray capillary voltage of 4500 V, a capillary temperature of 200 °C, and nitrogen as nebulizer gas at 8.0 L/min. Full scan data (m/z 125– 500) were obtained to identify the main protonated molecular ion present in the sample.

Sulfonation of 1′-hydroxymethyleugenol to 1′-sulfooxymethyleugenol

The formation of 1′-sulfooxymethyleugenol was characterized in incubations of 1′-hydroxymethyleugenol with liver S9 of male Sprague Dawley rats in the presence of GSH as scavenger of the reactive carbo-cation formed upon decomposition of the unstable 1′-sulfooxymethyleugenol. Using GSH as a scavenger of the carbo-cation of the alkenylbenzene is considered a new method since determination of the sulfo-metabolite of 1′-hydroxyestragole was performed previously based on incubation of the alkenylbenzene with 2′-deoxyguanosine as a scavenger (Punt *et al.*, 2007). The incubation mixture had a final volume of 100 µL containing the following materials (final concentration): 10 mM GSH, 2 mg/mL S9, and 0.2 mM PAPS in 0.1 M potassium phosphate (pH 8.2). The incubation was started by addition of the substrate 1′-hydroxymethyleugenol. The incubation mixture was incubated for 2 hr at 37 °C, after which 25 µL of cold acetonitrile was added. Under these conditions the formation of the glutathione adduct of the carbo-cation derived from 1′-sulfooxymethyleugenol was linear with time and S9 protein concentration. The kinetic constants for the formation of 1′-sulfooxymethyleugenol from 1′-hydroxymethyleugenol were determined using liver S9. The incubation mixtures were as described above. Incubations with male rat liver S9 were carried out for 2 hr at a substrate concentration that ranged from 50 to 1500 µM 1′-hydroxymethyleugenol. All incubations were started by addition of substrate from a 200 times concentrated stock solution in DMSO and terminated by addition of 25 µL cold acetonitrile. Under the conditions specified, the formation of 1′-sulfooxymethyleugenol was linear with time and S9 protein concentration. In the blank incubations performed without GSH formation of the GSH adduct of the carbo-cation of 1′-sulfooxymethyleugenol was not observed.

HPLC analysis of the GSH adduct of 1′-sulfooxymethyleugenol

For the HPLC analysis of the incubations in which formation of 1′-sulfooxymethyleugenol was investigated, the samples were centrifuged for 5 min at 16,000 g and 50 µL of the supernatant of each sample was analyzed on an Alltima C18 5-µm column, 150 mm x 4.6 mm (Grace Alltech, Breda, The Netherlands), coupled to a Waters 2695 alliance HPLC system. The

gradient was made with acetonitrile and ultrapure water. The flow rate was 1 mL/min and the percentage of ultrapure water was kept at 100 % for the first 5 min. Then a gradient was applied from 0 to 10 % acetonitrile over 10 min, after which the percentage of acetonitrile was increased to 30 % over 10 min and then increased to 80 % over 10 min and kept at 80 % for 2 min. Detection was performed at 270 nm using a Waters 2996 photodiode array detector (Waters). Because the GSH adduct of 1′-sulfooxymethyleugenol has the same UV spectra as 1′-acetoxymethyleugenol (data not shown) it was assumed that it has the same molar extinction coefficient as 1′-acetoxymethyleugenol. Quantification of the GSH adduct of 1′-sulfooxymethyleugenol was therefore achieved by comparison of the peak area of the GSH adduct of 1′-sulfooxymethyleugenol in the chromatograms obtained at a wavelength of 270 nm to the calibration curve of 1′-acetoxymethyleugenol obtained at the same wavelength.

LC-MS analysis of the GSH adduct of 1′-sulfooxymethyleugenol

The nature of 1′-sulfooxymethyleugenol was verified by LC-MS, which was performed on an Agilent 1200 HPLC system coupled to a Bruker MicroTOF mass spectrometer. Aliquots of 20 µL (injected volume) were separated on an Alltima C18 5-µm column, 150 x 2.1 mm (Alltech, Breda, The Netherlands). The gradient was made with ultrapure water containing 0.1% (v/v) formic acid (eluent A) and acetonitrile with 0.1% (v/v) formic acid (eluent B) and the flow rate was set to 0.2 mL/min. The percentage of eluent B was kept at 0% for 5 minutes after which a linear gradient was applied from 0% to 10% eluent B over 10 min and a subsequent increase to 30% in another 10 minutes, after which the percentage of eluent B was increased to 80% over 10 min, and kept at 80% for 2 min. Mass spectrometric analysis was in the negative electrospray mode using a spray voltage of capillary voltage of 4500 V, a capillary temperature of 200 °C, and nitrogen as nebulizer gas at 8.0 L/min.

Data analysis

The apparent maximum velocity ($V_{max(app)}$) and apparent Michaelis-Menten constant ($K_{m(app)}$) for the formation of the different phase I metabolites of methyleugenol and metabolites of 1′-

hydroxymethyleugenol were determined by fitting the data to the standard Michaelis-Menten equation $v=V_{max}/(1+(K_m/[S]))$, with [S] being the substrate concentration, using the LSW data analysis toolbox (version 1.1.1, MDL Information Systems, Inc.).

PBK model methyleugenol

The PBK model for methyleugenol was developed based on the PBK model previously defined for the detoxification and bioactivation of the related alkenylbenzene estragole (Punt *et al.*, 2008). The aim behind developing a PBK model is to estimate the formation of different methyleugenol metabolites in male rat tissues (liver, kidney, and lung) at different oral doses of methyleugenol. Figure 2 presents a schematic overview of the PBK model. The final model is composed of separate compartments for liver, lung and kidney tissues, which were found to be involved in the metabolism of methyleugenol (see Results section). Since the partition coefficient of methyleugenol in fat tissue was found to be relatively high, a separate fat compartment was included in the developed model. All other tissues such as adrenal, brain, and heart were lumped into a richly perfused tissue group, while tissues such as bone, muscle, and skin were lumped into slowly perfused tissue group (Ramsey and Anderson, 1984).

The uptake of methyleugenol from the gastrointestinal tract was modeled as a first-order process, assuming direct entry from the intestine to the liver compartment, and an absorption rate constant (Ka) value similar to that of estragole which was 1.0 hr^{-1} (Punt *et al.*, 2008).

Based on the results of phase I incubations (see Results section), it was found that methyleugenol-2′,3′-oxide, 1′-hydroxymethyleugenol, 3-(3,4-dimethoxyphenyl)-2-propen-1-ol, 2-hydroxy-4,5-dimethoxyallylbenzene, 3-hydroxy-4-methoxyallylbenzene and a relatively minor unidentified metabolite with retention time of 44.9 min (denoted M6), were formed in liver tissues, while eugenol and 3-hydroxy-4-methoxyallylbenzene were formed in lung tissues and methyleugenol-2′,3′-oxide was formed in kidney tissues (See Results section).

Based on these results the mass balance equations for methyleugenol in the metabolizing tissues are described as follows:

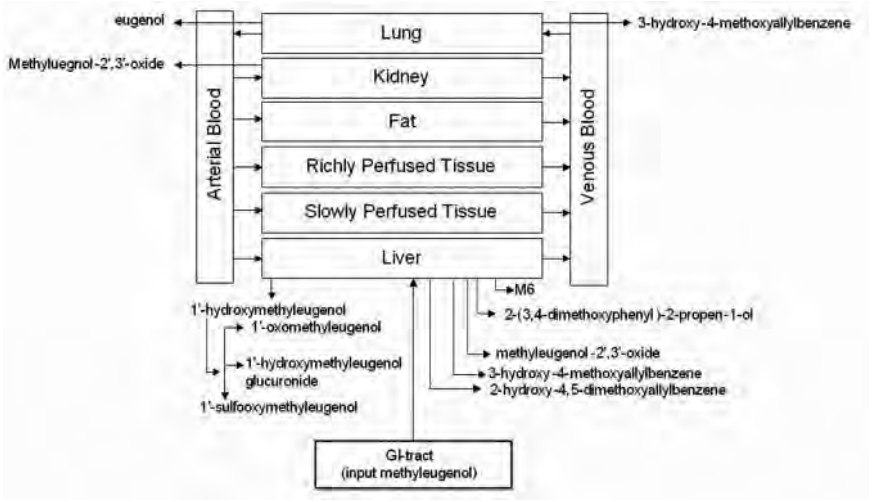

Figure 2. Representation of the conceptual model for a physiologically based pharmacokinetic model for methyleugenol.

Liver:

$$dAL_{ME}/dt = dUptake_{ME}/dt + QL*(CA_{ME} - CL_{ME}/PL_{ME}) - V_{max,L\_MEO} * CL_{ME}/PL_{ME} / (K_{m,L\_MEO} + CL_{ME}/PL_{ME}) - V_{max,L\_1'HME} * CL_{ME}/PL_{ME} / (K_{m,L\_1'HME} + CL_{ME}/PL_{ME}) - V_{max,L\_3DMPOH} * CL_{ME}/PL_{ME} / (K_{m,L\_3DMPOH} + CL_{ME}/PL_{ME}) - V_{max,L\_2HDME} * CL_{ME}/PL_{ME} / (K_{m,L\_2HDME} + CL_{ME}/PL_{ME}) - V_{max,L\_3HMA} * CL_{ME}/PL_{ME} / (K_{m,L\_3HMA} + CL_{ME}/PL_{ME}) - V_{max,L\_M6} * CL_{ME}/PL_{ME} / (K_{m,L\_M6} + CL_{ME}/PL_{ME})$$

$dUptake_{ME}/dt = - dAGI_{ME}/dt = Ka*AGI_{ME}$

AGI_{ME} (0) = Oral dose

$CL_{ME} = AL_{ME}/VL$

Lung:

$$dALu_{ME}/dt = QC*(CV_{ME}-CLu_{ME}/PLu_{ME}) - V_{max,Lu\_1EU}* CLu_{ME}/PLu_{ME} /(K_{m,Lu\_1EU}+CLu_{ME}/PLu_{ME}) - V_{max,Lu\_3HMA}* CLu_{ME}/PLu_{ME} /(K_{m,Lu\_3HMA}+ CLu_{ME}/PLu_{ME})$$

$CLu_{ME} = ALu_{ME}/VLu$

Kidney:

$$dAK_{ME}/dt = QK*(CA_{ME}-CK_{ME}/PK_{ME}) - V_{max,K\_MEO}*CVK/(K_{m,K\_MEO}+ CK_{ME}/PK_{ME})$$

$CK_{ME} = AK_{ME}/VK$

where $Uptake_{ME}$ is the amount of methyleugenol taken up from the gastrointestinal tract (µmol), AGI_{ME} (µmol) is the amount of methyleugenol remaining in the gastrointestinal tract, ATi_{ME} is the amount of methyleugenol in a tissue (Ti = L (liver), K (kidney) or Lu (lung)) (µmol), CTi_{ME} is the methyleugenol concentration in a tissue (µmol/L), CA_{ME} is the methyleugenol concentration in the arterial blood (µmol/L), CV_{ME} is the methyleugenol concentration in the venous blood (µmol/L), QTi is the blood flow rate to a tissue (L/hr), QC is the cardiac output (L/hr), VTi is the volume of a tissue, PTi_{ME} is the tissue/blood partition coefficient of methyleugenol in a tissue, and V_{max,Ti_M} and $K_{m,\ Ti\_M}$ are the maximum rate of formation and the Michaelis-Menten constant for the formation of the different phase I metabolites in a tissue:

methyleugenol-2′,3′-oxide(MEO), 1′-hydroxymethyleugenol(1′HME), 3-(3,4-dimethoxyphenyl)-2-propen-1-ol (3DMPOH), 2-hydroxy-4,5-dimethoxyallylbenzene (2HDME), eugenol (1EU), the unidentified metabolite with retention time of 44.9 min (M6) and 3-hydroxy-4-methoxyallylbenzene (3HMA). In case of methyleugenol-2′,3′-oxide, 3-(3,4-dimethoxyphenyl)-2-propen-1-ol, 2-hydroxy-4,5-dimethoxyallylbenzene, M6 (44.9 min) and 3-hydroxy-4-methoxyallylbenzene only formation of these metabolites is taken into account and no further reactions with these metabolites were modeled. Formation of 1′-hydroxymethyleugenol in the liver, but not in lung and kidney, was followed up by phase II reactions, since 1′-hydroxylation of methyleugenol was found to occur only in the liver (see Results section). To describe the disposition of 1′-hydroxymethyleugenol and its phase II metabolites a near quantitative intrahepatic conversion of 1′-hydroxymethyleugenol by phase II enzymes was assumed. This assumption was based on the findings that the overall catalytic efficiency for the phase II reaction was higher than the catalytic efficiency for the formation of 1′-hydroxymethyleugenol. For this reason only intra-organ distribution of 1′-hydroxymethyleugenol was modeled and no distribution of this metabolite over the body was taken into account. This simplification of the model reduced the number of parameters considerably, but might lead to an overestimation of the contributions of the phase II reactions (Filser *et al.*, 2001). The mass balance equation for 1′-hydroxymethyleugenol in the liver is as follows:

Liver:

$$dAL_{1'HME/dt} = + V_{max,L\_1'HME} * CL_{ME}/PL_{ME}/(K_{m,L\_1'HME}+CL_{ME}/PL_{ME}) - V_{max,L\_1'OME} * CL_{1'HME}/PL_{1'HME}/(K_{m,L\_1'OME}+CL_{1'HME}/PL_{1'HME}) - V_{max,L\_1'HMEG} * CL_{1HME}/PL_{1'HME}/(K_{m,L\_1'HMEG}+CL_{1'HME}/PL_{1'HME}) - V_{max,L\_1'HMES} * CL_{1'HME}/PL_{1'HME}/(K_{m,L\_1'HMES}+CL_{1'HME}/PL_{1'HME})$$

$$CL_{1'HME} = AL_{1'HME} / VL$$

where $AL_{1'HME}$ is the amount of 1′-hydroxymethyleugenol in the liver (µmol), $CL_{1'HME}$ is the 1′-hydroxymethyleugenol concentration in the liver (µmol/L), $PL_{1'HME}$ is the liver/blood partition coefficient of 1′-hydroxymethyleugenol, and V_{max,L_M} and K_{m,L_M} are the maximum rate of formation and the Michaelis-Menten constant for the formation of the phase II metabolites: 1′-oxomethyleugenol (1′OME), 1′-hydroxymethyleugenol glucuronide (1′HMEG), and 1′-sulfooxymethyleugenol (1′HMES) in the liver. The kinetic constants for the formation of phase I metabolites from methyleugenol and phase II metabolites from 1′-hydroxymethyleugenol were determined *in vitro* in the present study. The V_{max} values for the different phase I and phase II metabolic pathways in the liver, expressed as nmol/min/(mg microsomal protein), were scaled to the liver using a microsomal protein yield of 35 mg/(g liver) (Medinsky *et al.*, 1994). The V_{max} values for the different phase I metabolic pathways in the lung and kidney were scaled accordingly using a microsomal protein yield of 20 mg/(g lung) and 7 mg/(g kidney), respectively (Beierschmitt and Weiner, 1986; Medinsky *et al.*, 1994). The V_{max} values for sulfonation of 1′-hydroxymethyleugenol, expressed as nmol/min/ (mg S9 protein), were scaled to the liver using an S9 protein yield of 143 mg/(g liver), which corresponds to the sum of the cytosolic protein yield of 108 mg/(g liver) and the microsomal protein yield of 35 mg/(g liver) reported in the literature (Medinsky *et al.*, 1994). Furthermore this scaling factor was verified as described by Punt *et al.* (2008). The physiological parameters used in the methyleugenol model were obtained from Brown *et al.* (1997). Partition coefficients were estimated from the log K_{ow} based on a method of DeJongh *et al.* (1997) (Table 1). Log K_{ow} values were estimated with KOWWIN™ version 1.67 using the EPI Suite™ software package version 4.0 and amounted to 3.03 for methyleugenol and 1.49 for 1'-hydroxymethyleugenol. Model equations were coded and numerically integrated in Berkeley Madonna 8.0.1 (Macey and Oster, UC Berkeley, CA, USA), using the Rosenbrock's algorithm for stiff systems.

Sensitivity analysis

To identify the key parameters to which the model output is most sensitive, a sensitivity analysis was performed. Normalized sensitivity coefficients (SC) were determined according to

the following equation: SC = (C' − C) / (P' − P) *(P / C), where C is the initial value of model output, C' is the modified value of the model output resulting from an increase in parameter value, P is the initial parameter value, and P' is the modified parameter value (Evans and Andersen, 2000; Garg and Balthasar, 2007; Tardif *et al.*, 2002). Based on the literature a 5% increase in parameter values was chosen, to analyze the effect of a change in parameter on the formation of 1′-hydroxymethyleugenol, 1′-hydroxymethyleugenol glucuronide, 1′-oxomethyleugenol and 1′-sulfooxymethyleugenol expressed as % of the dose over a 24 hr period of time (Evans and Andersen, 2000). Each parameter was analyzed individually, keeping the other parameters to their initial values.

Table 1. Parameters used in the physiologically based kinetic model for methyleugenol in rat.

Physiological parameters[a]		**Tissue: blood partition coefficients**[b]	
body weight (kg)	0.25		
percentage of body weight		methyleugenol	
liver	3.4	liver	2.3
lungs	0.5	lung	2.3
kidney	0.7	kidney	2.3
fat	7.0	fat	69.5
rapidly perfused	4.4	rapidly perfused	2.3
slowly perfused	67.6	slowly perfused	0.8
arterial blood	1.85	1′-hydroxymethyleugenol	
venous blood	5.55	liver	1.1
cardiac output (L/hr)	5.4		
percentage of cardiac output			
liver	25.0		
kidney	14.1		
fat	7.0		
rapidly perfused	36.9		
slowly perfused	17.0		

[a] Brown et al. (1997)

[b] DeJongh et al.(1997)

Results

Formation of Phase I metabolites

Figure 3 presents the HPLC chromatograms of incubations of methyleugenol with male rat liver, lung, and kidney microsomes in the presence of NADPH as cofactor. The results obtained reveal that liver, lung, and kidney microsomes were all capable of metabolizing methyleugenol to different types of metabolites at varying rates. The HPLC chromatogram of incubations of methyleugenol with liver microsomes (Figure 3A) reveals formation of six metabolites of methyleugenol which were identified as 3-(3,4-dimethoxyphenyl)propane-1,2-diol (RT = 15.9 min), 1′-hydroxymethyleugenol (RT = 32.1 min), 3-(3,4-dimethoxyphenyl)-2-propen-1-ol (RT = 34.2 min), 2-hydroxy-4,5-dimethoxyallylbenzene (RT = 35.1 min), methyleugenol-2′,3′-oxide (RT = 40.8 min), an unidentified metabolite eluting at a retention time of 44.9 min denoted M6, and 3-hydroxy-4-methoxyallylbenzene (RT = 52.7 min). 3-(3,4-Dimethoxyphenyl)propane-1,2-diol, 1′-hydroxymethyleugenol, 3-(3,4-dimethoxyphenyl)-2-propen-1-ol, and methyleugenol-2′,3′-oxide were identified based on the similarities of their retention times and UV spectra to those of chemically synthesized reference compounds. Further identification of 1′-hydroxymethyleugenol, 3-(3,4-dimethoxyphenyl)-2-propen-1-ol, and methyleugenol-2′,3′-oxide was performed by GC-MS providing mass spectral characteristics identical to those reported in the literature (Solheim and Scheline, 1976) (Table 2). No reference compound was available for 2-hydroxy-4,5-dimethoxyallylbenzene but this metabolite was identified by analyzing a dichloromethane extract of a microsomal incubation by GC-MS. The mass spectral data of the metabolite were found to match those described for 2-hydroxy-4,5-dimethoxyallylbenzene in the literature (Solheim and Scheline, 1976) (Table 2).

Incubating methyleugenol-2′,3′-oxide with male rat liver microsomes in the absence of any cofactor revealed that in these incubations methyleugenol-2′,3′-oxide is completely hydrolyzed to 3-(3,4-dimethoxyphenyl)propane-1,2-diol within the time frame of the incubation. Hydrolysis is not observed in the blank incubations without microsomes, which indicates that the conversion

A.

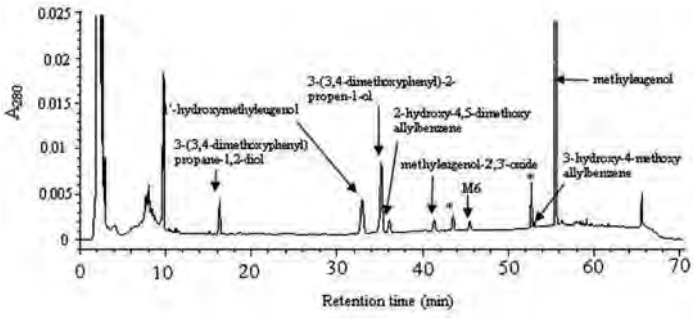

B.

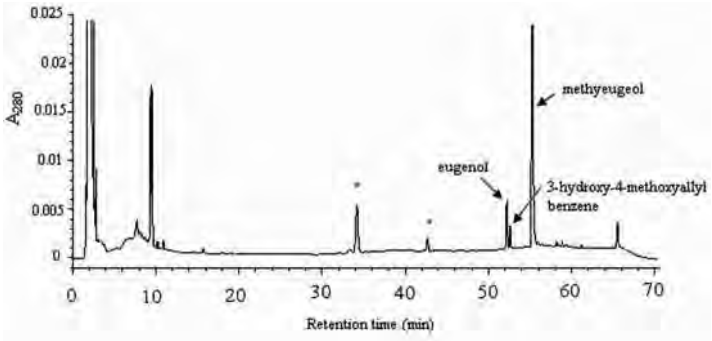

C.

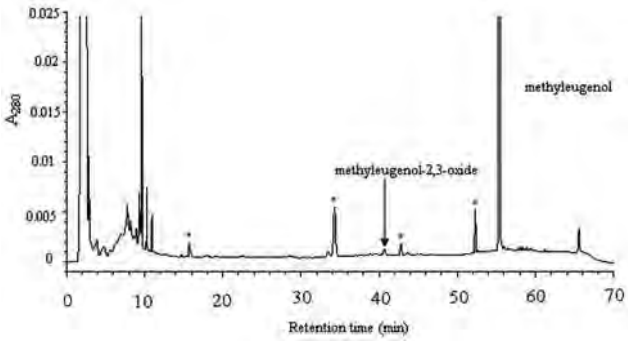

Figure 3. HPLC chromatograms of incubations of methyleugenol (1 mM) with: A. Sprague Dawley male rat liver microsomes (1 mg/mL), B. Sprague Dawley male rat lung microsomes (1 mg/mL), C. Sprague Dawley male rat kidney microsomes, in the presence of NADPH (3 mM) as cofactor, and vitamin C (1 mM) as antioxidant.

Table 2. Retention times and relative abundance of M^+ and prominent fragments of methyleugenol and its metabolites.

Compound name	Retention time (min)	M^+	Prominent fragments (m/e) Relative abundance
methyleugenol	17.7	178	163 151 147 107
3-hydroxy-4-methoxyallylbenzene	16.6	164	149 137 131 121
1′-hydroxymethyleugenol	22.6	194	176 161 151 139
3-(3,4-dimethoxyphenyl)-2-propen-1-ol	25.3	194	176 161 151 138
2-hydroxy-4,5-dimethoxyallylbenzene	23.1	194	179 151 123 107
methyleugenol-2′,3′-oxide	26.6	194	177 165 151 138

is most likely catalyzed by epoxide hydrolases present in the microsomal preparation (Guenthner and Luo, 2001; Luo *et al.*, 1992; Luo and Guenthner, 1995,). Because the peak area of 3-(3,4-dimethoxyphenyl)propane-1,2-diol resulting from hydrolyzing methyleugenol-2′,3′-oxide with liver microsomes was equal to the peak area of methyleugenol-2′,3′-oxide present at the start of the incubation (i.e. equal to the amount of methyleugenol-2′,3′-oxide in the blank incubation without microsomes), the peak area of 3-(3,4-dimethoxyphenyl)propane-1,2-diol was used for quantification of methyleugenol-2′,3′-oxide formation with liver microsomes. Small amounts of methyleugenol-2′,3′-oxide, formed in the liver microsomal preparation, were not converted to 3-(3,4-dimethoxyphenyl)propane-1,2-diol (<10% of 3-(3,4-dimethoxyphenyl)-propane-1,2-diol) and they were neglected. We found that the synthesis of 3-hydroxy-4-methoxyallylbenzene was accompanied with formation of eugenol, its isomer. HPLC analysis of the product resulting from chemical synthesis indicated that two monodemethylated isomers were formed in equal amounts and it was not possible to separate them by distillation as reported by Solheim and Scheline (1976). The HPLC chromatogram of commercially available eugenol revealed that eugenol had a retention time of 52.1 min. A hexane extract of the synthesized isomer mixture was injected onto the HPLC and the chromatogram obtained revealed two peaks, one with a RT of 52.1 min and the other with a RT of 52.7 min. From this it can be concluded that the isomer at RT 52.7 min was 3-hydroxy-4-methoxyallylbenzene and

that in the incubation of rat liver microsomes with methyleugenol, eugenol was not formed as a major metabolite. Additional evidence for the formation of 3-hydroxy-4-methoxyallylbenzene was obtained by analyzing a dichloromethane extract of the microsomal incubations by GC-MS. The mass spectra obtained revealed the same mass spectrum that had been found by Solheim and Scheline, (1976) for 3-hydroxy-4-methoxyallylbenzene (Table 2). The metabolite denoted M6 eluting at 44.9 min was only a minor metabolite and therefore has not been identified in the present work.

In the chromatogram of incubations with male rat lung microsomes two metabolites of methyleugenol were identified, corresponding to eugenol and 3-hydroxy-4-methoxyallylbenzene, both resulting from *O*-demethylation (Figure 3B). In the chromatogram of incubations with male rat kidney microsomes one metabolite of methyleugenol was identified, corresponding to methyleugenol-2′,3′-oxide which did not convert to 3-(3,4-dimethoxyphenyl)propane-1,2-diol as observed in incubations with liver microsomes (Figure 3C). A peak corresponding to 3-(3,4-dimethoxyphenyl)-2-propen-1-ol was observed in the incubations with both lung and kidney microsomes. However, because the area of this peak was equal to the area of the same peak in the blank incubations without NADPH, it was concluded that 3-(3,4-dimethoxyphenyl)-2-propen-1-ol is not formed in incubations with both lung and kidney microsomes. Also a peak corresponding to eugenol was observed in the incubations with both lung and kidney microsomes. In kidney microsomal incubations, this peak was equal to the same peak in the blank without NADPH. On the other hand, in lung microsomal incubation, there was a formation for eugenol and it was corrected to the amount found in the blank incubation without NADPH.

The presence of eugenol in blank incubations can be justified by noting that methyleugenol used in the current study was synthesized from eugenol; the HPLC chromatogram of DMSO methyleugenol standard showed that traces amounts of eugenol were present with methyleugenol. In every addition of methyleugenol to the incubation mixture, eugenol was added in minor traces.

Kinetics of formation of Phase I Metabolites

Male rat liver, lung and kidney microsomes were incubated with increasing methyleugenol concentrations to determine the kinetic parameters for the formation of the various phase I metabolites of methyleugenol. Figures 4A-F show the rate of formation of 1′-hydroxymethyleugenol, methyleugenol-2′,3′-oxide measured as 3-(3,4-dimethoxyphenyl)-propane-1,2-diol**,** 3-hydroxy-4-methoxyallylbenzene, M6, 3-(3,4-dimethoxyphenyl)-2-propen-1-ol, and 2-hydroxy-4,5-dimethoxyallylbenzene, respectively, all in incubations with male rat liver microsomes with increasing methyleugenol concentrations. Table 3 summarizes the apparent K_m and V_{max} values obtained from these plots. The results obtained with male rat liver microsomes reveal that 1′-hydroxymethyleugenol is the most abundant metabolite formed, followed by methyleugenol-2′,3′-oxide measured as 3-(3,4-dimethoxyphenyl)propane-1,2-diol, 3-(3,4-dimethoxyphenyl)-2-propen-1-ol, M6, and 2-hydroxy-4,5-dimethoxyallylbenzene. *O*-demethylation was shown to be the least important metabolic route in these incubations. The apparent V_{max} for *O*-demethylation was about 25 times lower than the apparent V_{max} for formation of 1′-hydroxymethyleugenol, whereas the apparent K_m was about 1.7 times lower. Overall, the catalytic efficiency for the formation of the 3-hydroxy-4-methoxyallylbenzene (the *O*-demethylated metabolite) by male rat liver microsomes, calculated as the apparent V_{max}/K_m, was about 14.4 times lower than the catalytic efficiency for the formation of 1′-hydroxymethyleugenol.

The results obtained with male rat lung microsomes reveal that 3-hydroxy-4-methoxyallylbenzene and eugenol were formed, the two metabolites resulting from *O*-demethylation, with 3-hydroxy-4-methoxyallylbenzene being the major metabolite (Figure 5A and 5B). Table 3 summarizes the apparent K_m and V_{max} values obtained from these plots. The apparent V_{max} for 3-hydroxy-4-methoxyallylbenzene was about 3.2 times higher than the apparent V_{max} for formation of eugenol, whereas the apparent K_m was about 1.7 times higher. Overall, the catalytic efficiency for the formation of the 3-hydroxy-4-methoxyallylbenzene by male rat lung microsomes, calculated as the apparent V_{max}/K_m, was about 2 times higher than the catalytic efficiency for the formation of eugenol. Comparing the catalytic efficiencies for

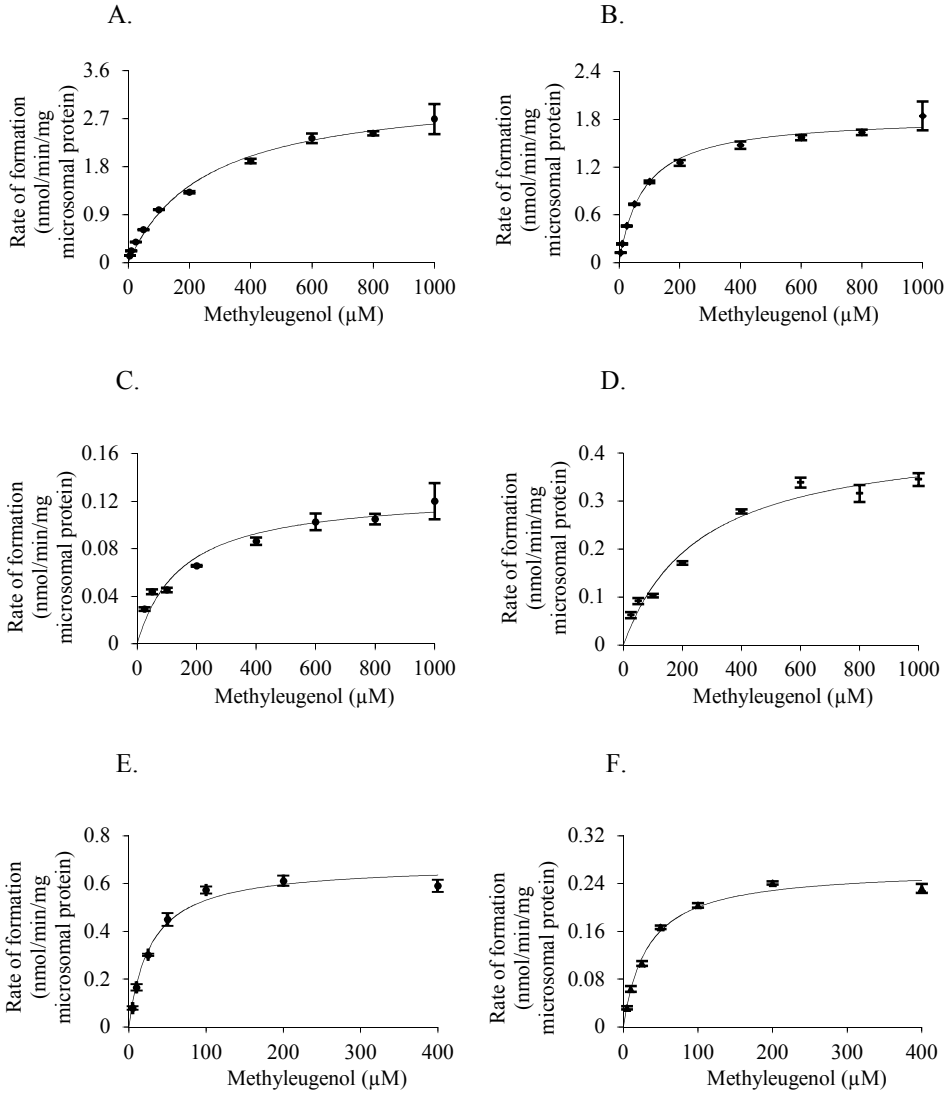

Figure 4. Formation rate of phase I metabolites in incubations with liver microsomes of male Sprague Dawley rats at increasing concentrations (5 – 1000 µM) of methyleugenol indicating formation of A. 1′-hydroxymethyleugenol, B. methyleugenol-2′,3′-oxide, C. 3-hydroxy-4-methoxyallylbenzene and D. M6 and at increasing concentrations (5 – 400 µM) of methyleugenol indicating formation of E. 3-(3,4-dimethoxyphenyl)-2-propen-1-ol and F. 2-hydroxy-4,5-dimethoxyallylbenzene.

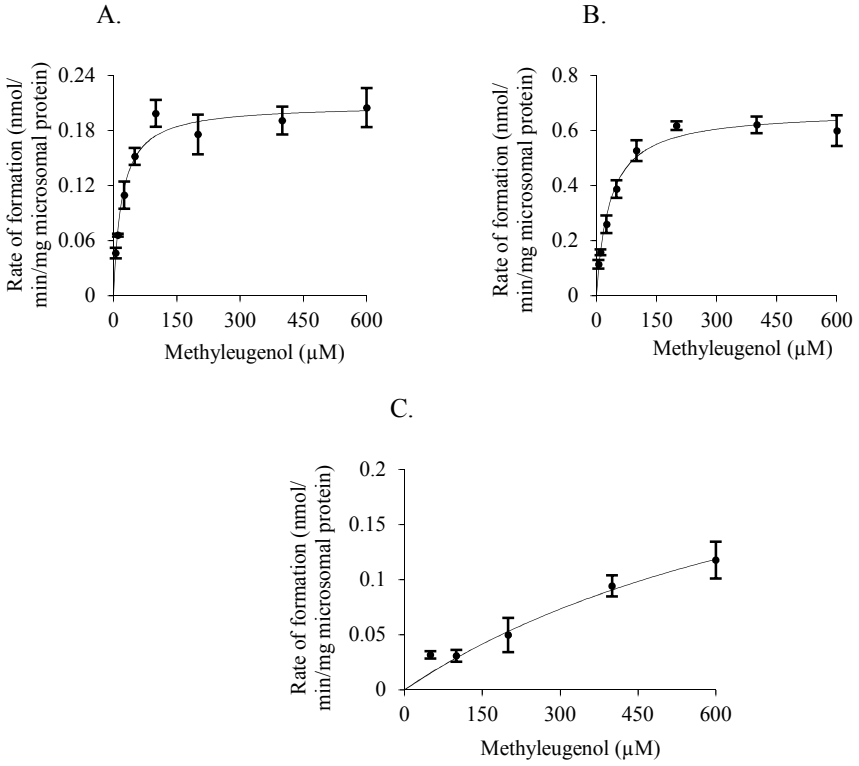

Figure 5. Formation rate of the Phase I metabolites in incubations with lung microsomes of male Sprague Dawley rats at increasing concentrations (5–600 μM) of methyleugenol indicating formation of A. eugenol and B. 3-hydroxy-4-methoxyallylbenzene, and C. formation rate of methyleugenol-2′,3′-oxide in incubations with kidney microsomes of male Sprague Dawley at increasing concentrations of methyleugenol (5 – 600 μM).

the formation of phase I metabolites in the different organs that were scaled to the *in vivo* situation (Table 3) reveals that in male rat conversion of methyleugenol to 3-hydroxy-4-methoxyallylbenzene is most efficiently catalyzed in the lung compared to the liver. On the other hand, formation of 1′-hydroxymethyleugenol, methyleugenol-2′,3′-oxide measured as 3-(3,4-dimethoxyphenyl)propane-1,2-diol, 3-(3,4-dimethoxyphenyl)-2-propen-1-ol, 2-hydroxy-4,5-dimethoxyallylbenzene, and M6 is most efficiently catalyzed in the liver.

Table 3. Kinetic parameters for phase I metabolism of methyleugenol in incubations with live microsomes from male Sprague Dawley rat.

organ	metabolite	k_m(app)[a,b]	V_{max}(app)[a,c]	*in vitro* catalytic efficiency[d] (V_{max}(app)/K_m(app))	scaled V_{max}, *in vivo*[e]	*in vivo* catalytic efficiency[f] (scaled V_{max}, *in vivo*/K_m(app)
liver	methyleugenol-2′,3′-oxide	81 ± 15.5	1.84 ± 0.08	23	32.8[g]	0.4
	1′-hydroxymethyleugenol	253 ± 90	3.26 ± 0.45	13	58.2[g]	0.23
	3-(3,4-dimethoxyphenyl)-2-propen-1-ol	28 ± 2.3	0.68 ± 0.025	24	12.1[g]	0.43
	2-hydroxy-4,5-dimethoxyallylbenzene	32 ± 1.1	0.27 ± 0.006	8.4	4.8[g]	0.15
	3-hydroxy-4-methoxyallylbenzene	150 ± 55.5	0.13 ± 0.018	0.9	2.3[g]	0.015
	M6	259 ± 16.4	0.44 ± 0.004	1.7	7.9[g]	0.03
lung	eugenol	19 ± 3	0.21± 0.03	11	0.32[h]	0.02
	3-hydroxy-4-methoxyallylbenzene	33 ± 18.7	0.67 ± 0.077	20	1.01[h]	0.03
kidney	methyleugenol-2′,3′-oxide	968 ± 230	0.31± 0.05	0.32	0.23[i]	0.00024

[a]mean ± SD
[b](μM)
[c](nmol/min/mg microsomal protein)
[d](μL/min/mg microsomal protein)
[e](μmol/hr)
[f](L/hr)
[g] $V_{max\ (app)}$ /(1000 nmol/μmol) * (60 min/hr) * (35 mg microsomal protein/ g liver) * (34 g liver/kg bw)* (0.25 kg bw)
[h] $V_{max\ (app\ )}$ /(1000 nmol/μmol) * (60 min/hr) * (20 mg microsomal protein/ g lung) * (5 g lung/kg bw)* (0.25 kg bw)
[i] $V_{max\ (app)}$ /(1000 nmol/μmol) * (60 min/hr) * (7 mg microsomal protein/ g kidney) * (7 g kidney/kg bw)* (0.25 kg bw)

Formation of Phase II Metabolites

1′-Hydroxymethyleugenol glucuronide

HPLC analysis of an incubation of 1′-hydroxymethyleugenol with male rat liver microsomes in the presence of UDPGA as a cofactor, conditions previously shown to result in glucuronidation of 1′-hydroxyestragole to 1′-hydroxyestragole glucuronide (Punt *et al.*, 2008), revealed formation of one metabolite with RT of 19.3 min (chromatogram not shown). Treatment of the sample with β-glucuronidase, resulted in complete disappearance of the peak at 19.3 min accompanied by a comparable increase of the peak representing 1′-hydroxymethyleugenol. This confirms that the metabolite corresponds to the glucuronosyl

conjugate of 1′-hydroxymethyleugenol. Furthermore the spectrum of the metabolite, obtained by LC-MS, reveals a deprotonated molecule at *m/z 369*, which corresponds to the theoretically expected mass and confirms that the metabolite corresponds to 1′-hydroxymethyleugenol glucuronide.

1′-Oxomethyleugenol

HPLC analysis of an incubation of 1′-hydroxymethyleugenol with male rat liver microsomes using NAD^+ as a cofactor, conditions previously shown to result in oxidation of 1′-hydroxyestragole to 1′-oxoestragole (Punt *et al.*, 2009), revealed formation of a metabolite with RT of 11.4 min (chromatogram not shown). HPLC analysis of control incubations of 1′-hydroxymethyleugenol in the absence of NAD^+ revealed no appearance of the peak at RT of 11.4 min (chromatogram not shown). This argument was used as a confirmation for the formation of the GSH adduct of 1'-oxomethyleugenol and thus of 1'-oxomethyleugenol in the incubation with NAD^+. Furthermore the spectrum of the metabolite, obtained by LC-MS, reveals a deprotonated molecule at *m/z 500*, which corresponds to the theoretically expected mass for the GSH adduct of 1′-oxomethyleugenol.

1′-Sulfooxymethyleugenol

HPLC analysis of an incubation of 1′-hydroxymethyleugenol with male rat liver S9 using PAPS as a cofactor and GSH as a scavenger for the reactive carbo-cation derived from the unstable 1′-sulfooxymethyleugenol metabolite revealed formation of a metabolite with RT of 12.9 min (chromatogram not shown). HPLC analysis of incubations of 1′-hydroxymethyleugenol in the absence of GSH and in the presence of PAPS and liver S9 protein revealed no appearance of the peak at 12.9 min (chromatogram not shown). This argument was used as a confirmation for the formation of the GSH adduct of the carbo-cation of 1′-sulfooxymethyleugenol, and thus an indirect detection of formation of 1′-sulfooxymethyleugenol in the complete incubation. Furthermore the spectrum of the metabolite, obtained by LC-MS, reveals a deprotonated molecule at *m/z 484*, which corresponds to the theoretically expected mass and confirms that

the metabolite corresponds to the GSH adduct of the carbo-cation formed from 1'-sulfooxymethyleugenol.

Kinetics of phase II metabolite formation

Figure 6A and 6B present the formation of 1′-hydroxymethyleugenol glucuronide and 1′-oxomethyleugenol respectively, in incubations with microsomal preparations with male rat liver and either UDPGA or NAD^+ at increasing 1′-hydroxymethyleugenol concentrations. In addition, Figure 6C presents the formation of the GSH conjugate of the carbo-cation of 1′-sulfooxymethyleugenol in incubations with a rat liver S9 preparation, PAPS and increasing 1′-hydroxymethyleugenol concentrations. The kinetic parameters (V_{max} and K_m), obtained by fitting the data to the standard Michaelis-Menten equation, are presented in Table 4. Comparing the kinetic constants for glucuronidation to sulfonation and oxidation reveals that the apparent V_{max} for 1′-sulfooxymethyleugenol formation was about 12773 times lower than the apparent V_{max} for formation of 1′-hydroxymethyleugenol glucuronide, whereas the apparent K_m was about 8 times lower. Overall, the catalytic efficiency for the formation of the 1′-sulfooxymethyleugenol by male rat liver proteins, calculated as the apparent V_{max}/K_m, was about 1750 times lower than the catalytic efficiency for the formation of 1′-hydroxymethyleugenol glucuronide by male rat liver proteins. The apparent V_{max} for 1′-oxomethyleugenol was about 10 times lower than the apparent V_{max} for formation of 1′-hydroxymethyleugenol glucuronide, whereas the apparent K_m was about 4.4 times higher. The catalytic efficiency for the formation of the 1′-oxomethyleugenol by male rat liver microsomes was about 44 times lower than the catalytic efficiency for the formation of 1′-hydroxymethyleugenol glucuronide by male rat liver microsomes. Thus, based on these kinetic data it can be concluded that in male rat liver glucuronidation may be the preferential pathway for conversion of 1′-hydroxymethyleugenol, followed by oxidation to 1′-oxomethyleugenol and to a much lower extent by sulfonation to 1′-sulfooxymethyleugenol.

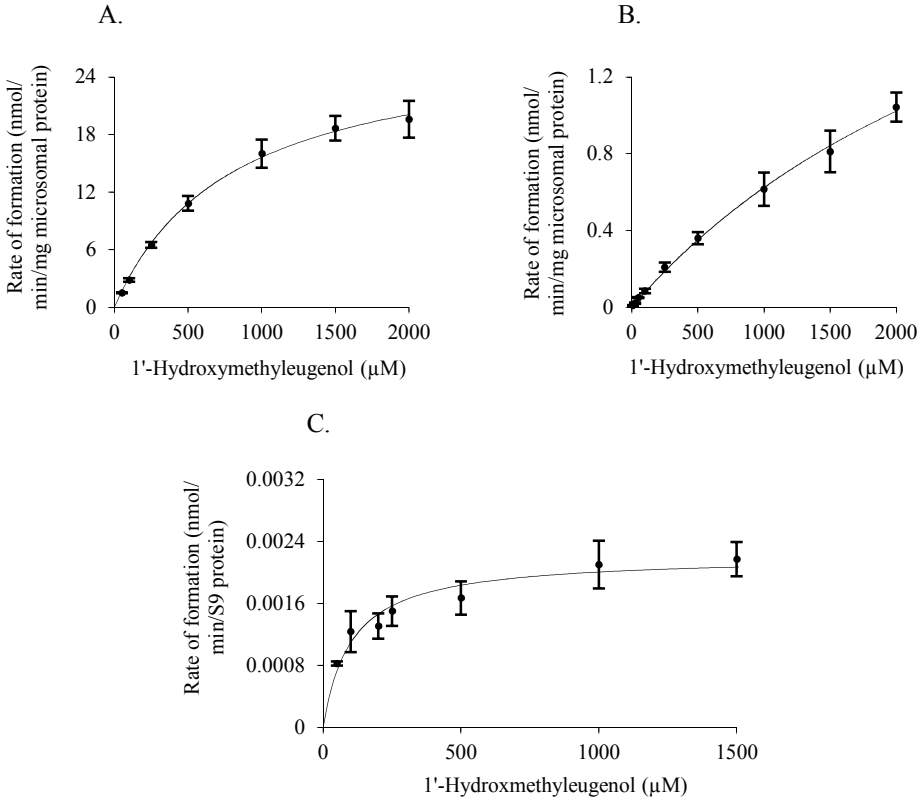

Figure 6. Formation rate of A. 1′-hydroxymethyleugenol glucuronide in incubations with liver microsomes of male Sprague Dawley rat at increasing concentration of 1′-hydroxymethyleugenol (50 – 2000 μM), B. 1′-oxomethyleugenol in incubations with liver microsomes of male Sprague Dawley rat at increasing concentration of 1′-hydroxymethyleugenol (50 – 2000 μM), and C. 1′-sulfooxymethyleugenol in incubations with liver S9 of male Sprague Dawley rat at increasing concentration of 1′-hydroxymethyleugenol (50 – 1500 μM).

Performance of the PBK model

With the kinetic constants obtained, all parameters of the PBK model were defined (Table 3 and Table 4) and the model as described in the Material and Method section was used for model predictions. In a first step, predictions were made that allow investigating the performance of the PBK model obtained. In an *in vivo* study performed by Solheim and Scheline (1976), rats

Table 4. Kinetic parameters for the phase II metabolites of methyleugenol in incubations with liver microsomes from male Sprague Dawley rat.

organ	metabolite	k_m(app)[a,b]	V_{max}(app)[a,c]	*in vitro* catalytic efficiency[d] (Vmax(app)/Km(app))	scaled V_{max} *in vivo*[e]	*in vivo* catalytic efficiency[f] (scaled Vmax, in vivo/Km(app)
liver	1′-hydroxymethyleugenol glucuronide	799 ± 192	28.1 ± 6.1	35	502[g]	0.63
	1′-oxomethyleugenol	3534 ± 3038	2.83 ± 0.92	0.8	51[g]	0.014
	1′-sulfooxymethyleugenol	102 ± 29.5	0.0022 ± 0.0054	0.02	0.16[h]	0.0016

[a] mean ± SD
[b] (μM)
[c] (nmol/min/(mg microsomal protein)
[d] (μl/min/(mg microsomal protein)
[e] (μmol/hr)
[f] (L/ hr)
[g] $V_{max\ (app)}$ /(1000 nmol/μmol) * (60 min/hr) * (35 mg microsomal protein/ g liver) * (34 g liver/kg bw)* (0.25 kg bw)
[h] $V_{max\ (app)}$ /(1000 nmol/μmol) * (60 min/hr) * (143 mg S9 protein/ g liver) * (34 g liver/kg bw)* (0.25 kg bw)

were given 200 mg/(kg bw) of methyleugenol. The results showed that 95% of the dose was recovered in urine. In another study performed by NTP (NTP, 2000), male rats were given 118 mg/(kg bw) of methyleugenol, and the results showed that 100% of the dose was excreted in urine collected over 24 hr. These data illustrate that the principal excretion pathway is through urine and that biliary excretion is insignificant. Therefore evaluation of performance of the PBK model could be done by comparison of plasma concentrations of methyleugenol and urinary metabolite formation observed *in vivo* and predicted by the PBK model. The PBK model-based predictions for concentrations of methyleugenol in venous blood at different time points after dosing were compared to the reported plasma levels of methyleugenol in male Fisher 344 rats exposed to a single oral gavage dose of 150 mg/(kg bw) (NTP, 2000). Figure 7 presents the results obtained and reveals that the PBK model predicted plasma concentrations of methyleugenol are generally only 2-4 fold to up to at most one order of magnitude at the early time points, higher than the actually measured ones. Also, the PBK model predicted accurately

the percentage of methyleugenol converted to the 1′-hydroxymethyleugenol glucuronide metabolite, after oral administration of 118 mg/kg of methyleugenol to male Fisher 344 rat. The observed excreted amount of the 1′-hydroxymethyleugenol glucuronide metabolite in urine collected over 24 hr was 20 % of the dose (NTP, 2000), while the PBK-based predicted amount was 26 %. In another *in vivo* study, male rats received a dose of 200 mg/(kg bw) of methyleugenol, the PBK model-based predictions for concentrations of 2-hydroxy-4,5-dimethoxyallylbenzene and 3-hydroxy-4-methoxyallylbenzene were compared to the corresponding metabolites in urine samples (collected over 24 hr). The PBK model predicted accurately the percentage of methyleugenol converted to 3-hydroxy-4-methoxyallylbenzene to amount to 3.6% of the dose whereas the actual measured level amounted to 4.0% of the dose. The predicted formation of 2-hydroxy-4,5-dimethoxyallylbenezene is about 2.6-fold higher (predicted to be 7.8% of the dose) than the actual measured level of formation (amounting to 3.0% of the dose) but remains within the same order of magnitude (Solheim and Scheline, 1976).

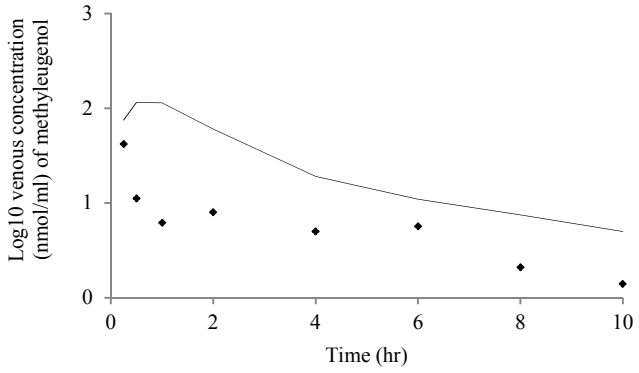

Figure 7. PBK predicted $\log_{10}$ concentrations of methyleugenol (nmol/ml) in venous blood of male Sprague Dawley rat (—) compared to the reported $\log_{10}$ concentrations in (nmol/ ml) plasma blood of male Fisher 344 rat (•), both obtained at an oral dose of 150 mg/(kg bw) (NTP, 2000).

Model predictions

The PBK model developed was used to predict the liver concentrations of methyleugenol and 1′-hydroxymethyleugenol and conversion of 1′-hydroxymethyleugenol to 1′-hydroxymethyleugenol glucuronide, 1′-oxomethyleugenol, and 1′-sulfooxymethyleugenol in the liver of male rat. Figure 8A presents the predicted time dependent concentration (μM) of methyleugenol and 1′-hydroxymethyleugenol, the time dependent predicted levels (nmol/(g liver)) of 1′-hydroxymethyleugenol glucuronide, 1′-oxomethyleugenol, and 1′-sulfooxymethyleugenol at a dose of 0.05 mg/(kg bw). This dose of 0.05 mg/(kg bw) was selected to allow comparison with the outcomes obtained previously for the model of 1′-estragole (Punt *et al.*, 2008) and represents an exposure level in the range of estimated daily exposure to these alkenylbenzenes (SCF, 2001). Since the model does not contain further reactions for the phase II metabolites of 1′-hydroxymethyleugenol, the PBK model estimates the total accumulated amounts of these 1′-hydroxymethyleugenol metabolites in liver over time but not the actual time dependent concentrations present in the liver. For this reason the estimated formation of 1′-sulfoxymethyleugenol does not represent the actual concentration of this metabolite that would occur in the liver, but the total quantities that would theoretically be formed in the liver over time. The model outcomes predict that 15 hr after dosing, methyleugenol and 1′-hydroxymethyleugenol are completely metabolized and indicate a total overall formation of 1.4 nmol/(g liver) of 1′-hydroxymethyleugenol glucuronide, 0.032 nmol/(g liver) of 1′-oxomethyleugenol, and 0.0035 nmol/(g liver) of 1′-sulfooxymethyleugenol, corresponding to 17.0%, 0.39%, and 0.042% of the dose respectively. Figure 8B presents the predicted time-dependent concentration of methyleugenol and 1′-hydroxymethyleugenol, the formation of 1′-hydroxymethyleugenol glucuronide, 1′-oxomethyleugenol, and 1′-sulfooxymethyleugenol after administration of 300 mg/(kg bw) methyleugenol, a dose which was also selected to allow comparison with the outcomes of the estragole model (Punt *et al.*, 2008), and which represents a high level exposure in a range reported to result in induction of hepatomas when administered on a daily basis (Abdo *et al.*, 2001; NTP, 2000). At this dose, the total conversion of methyleugenol and 1′-hydroxymethyleugenol was predicted to take

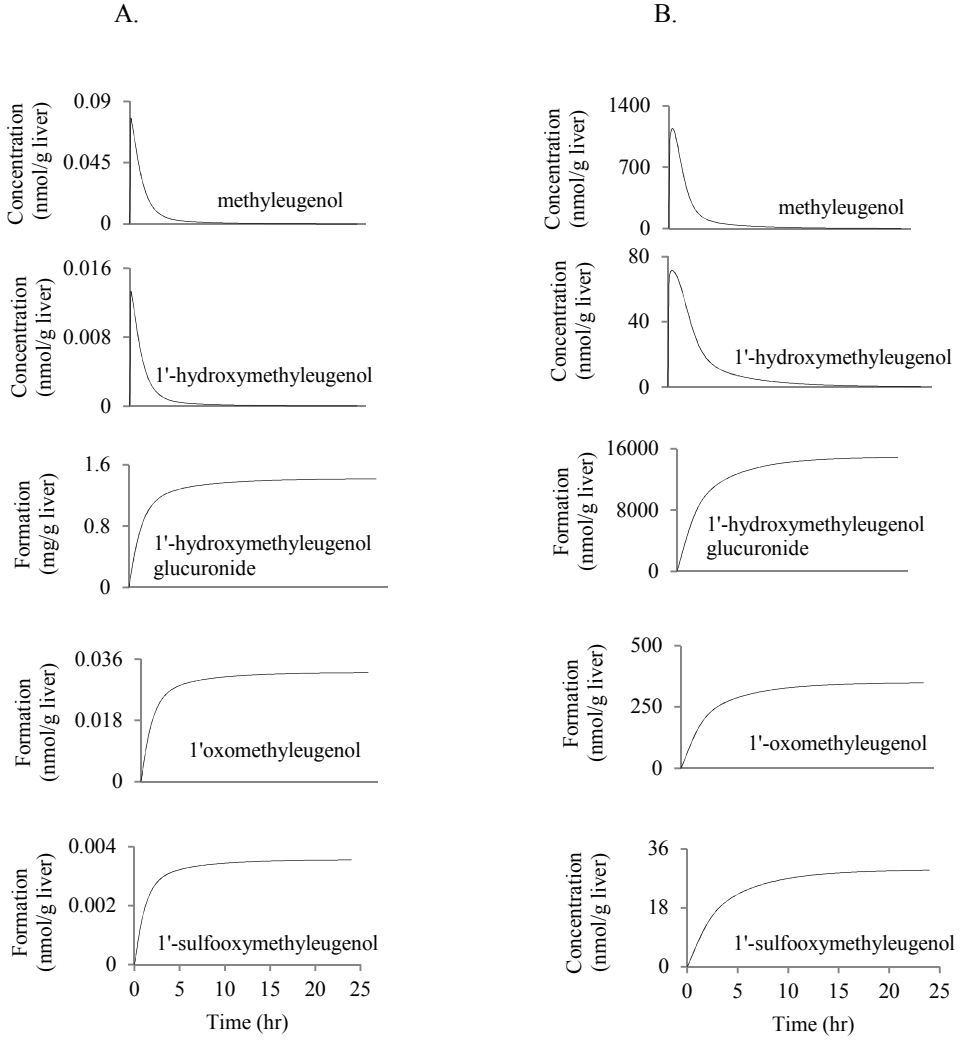

Figure 8. PBK model-predicted time dependent concentration (nmol/(g liver)) of methyleugenol, 1′-hydroxymethyleugenol, and formation of 1′-hydroxymethyleugenol glucuronide, 1′-oxomethyleugenol, and 1′-sulfooxymethyleugenol following exposure to A. 0.05 mg/(kg bw), and B. 300 mg/(kg bw).

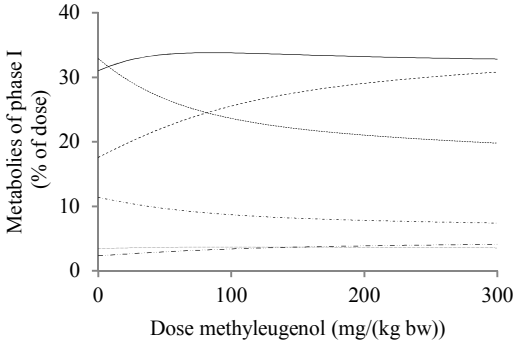

Figure 9. The PBK model-predicted dose-dependent percentage of formation of phase I metabolites in Sprague Dawley rat: methyleugenol 2′,3′-oxide (—), 1′-hydroxymethyleugenol (– – –), 3-(3,4-dimethoxyphenyl)-2-propen-1-ol (---), 2-hydroxy-4,5-dimethoxyallylbenzene (–·–·–), M6 (–··–··–), and 3-hydroxy-4-methoxyallylbenzene (····).

longer than at a low dose of 0.05 mg/(kg bw), with methyleugenol and 1′-hydroxymethyleugenol being almost completely metabolized after 20 hr. At a dose of 300 mg/(kg bw) the percentage of the dose that is ultimately converted into 1′-hydroxymethyleugenol glucuronide, 1′-oxomethyleugenol, and 1′-sulfooxymethyleugenol is relatively higher than what is predicted at a dose of 0.05 mg/(kg bw). At this dose 14796 nmol/(g liver) of 1′-hydroxymethyleugenol glucuronide is formed, corresponding to 29.9% of the dose. In the case of 1′-oxomethyleugenol and 1′-sulfooxymethyleugenol 346 and 29.3 nmol/(g liver) are formed, which correspond to 0.70 % and 0.06% of the dose respectively. The results obtained also reveal that the observed relative increase in the percentage of the dose that is ultimately converted into 1′-hydroxymethyleugenol glucuronide, 1′-oxomethyleugenol, and 1′-sulfooxymethyleugenol can be justified by a change in phase I metabolism of methyleugenol.

Figure 9 presents a plot of the percentage of the methyleugenol dose that is converted into the different phase I metabolites at different oral dose levels of methyleugenol. At low dose levels of methyleugenol (0.05 mg/(kg bw)), approximately 31.0%, 17.6%, 11.4%, 32.9%, 2.3% and 3.4% of the dose is metabolized to methyleugenol-2′,3′-oxide, 1′-hydroxymethyleugenol, 2-hydroxy-4,5-dimethoxyallylbenzene, 3-(3,4-dimethoxyphenyl)-2-propen-1-ol, M6, and 3-

hydroxy-4-methoxyallylbenzene respectively, which makes epoxidation and 3′-hydroxylation the major metabolic routes. As the dose increases to 300 mg/kg bw, approximately 32.8%, 30.8%, 7.4%, 19.8%, 4.1% and 3.5% of the dose is metabolized to methyleugenol-2′,3′-oxide, 1′-hydroxymethyleugenol, 2-hydroxy-4,5-dimethoxyallylbenzene, 3-(3,4-dimethoxyphenyl)-2-propen-1-ol, M6, and 3-hydroxy-4-methoxyallylbenzene respectively. This relative decrease in formation of 2-hydroxy-4,5-dimethoxyallylbenzene and 3-(3,4-dimethoxyphenyl)-2-propen-1-ol, accompanied by an increase in the relative formation of the proximate carcinogen 1′-hydroxymethyleugenol, M6, and 3-hydroxy-4-methoxyallylbenzene is a result of saturation of both the 3′-hydroxylation on the allyl group and the hydroxylation at C2 of the benzene ring.

Figure 9 shows that an increase in the dose of methyleugenol is accompanied by a relative increase of the amount of methyleugenol which is metabolized to the proximate carcinogenic metabolite 1′-hydroxymethyleugenol. This increase in 1′-hydroxymethyleugenol lead to a relative increase in the formation of phase II metabolites of 1′-hydroxymethyleugenol, including the proximate carcinogen 1′-sulfooxymethyleugenol with the dose (Figure 10A, 10B, and 10C). Under linear conditions for phase I metabolism (0.05-10 mg methyleugenol/(kg bw)) the PBK based predicted formation of phase I metabolites as % of the dose amounted to 31.0%, 17.6%, 2.3%, 32.9%, and 3.4% at a dose of 0.05 mg/(kg bw) and to 31.8%, 18.6%, 11.0%, 31.3%, 2.5%, and 3.5% at a dose of 10 mg/(kg bw) for methyleugenol-2′,3′-oxide, 1′-hydroxymethyleugenol, 2-hydroxy-4,5-dimethoxyallylbenzene, 3-(3,4-dimethoxyphenyl)-2-propen-1-ol, M6, and 3-hydroxy-4-methoxyallylbenzene respectively. Under saturating conditions (300-4300 mg methyleugenol/(kg bw)) the PBK based predicted formation of phase I metabolites, as % of the dose, amounted to 32.8%, 30.8%, 7.4%, 19.8%, 4.1%, and 3.5% at a dose of 300 mg/(kg bw) and to 12.8%, 21.4%, 1.9%, 4.8%, 2.9%, and 1.3% at a dose of 4300 mg/(kg bw) for methyleugenol-2′,3′-oxide, 1′-hydroxymethyleugenol, 2-hydroxy-4,5-dimethoxyallylbenzene, 3-(3,4-dimethoxyphenyl)-2-propen-1-ol, M6, and 3-hydroxy-4-methoxyallylbenzene respectively.

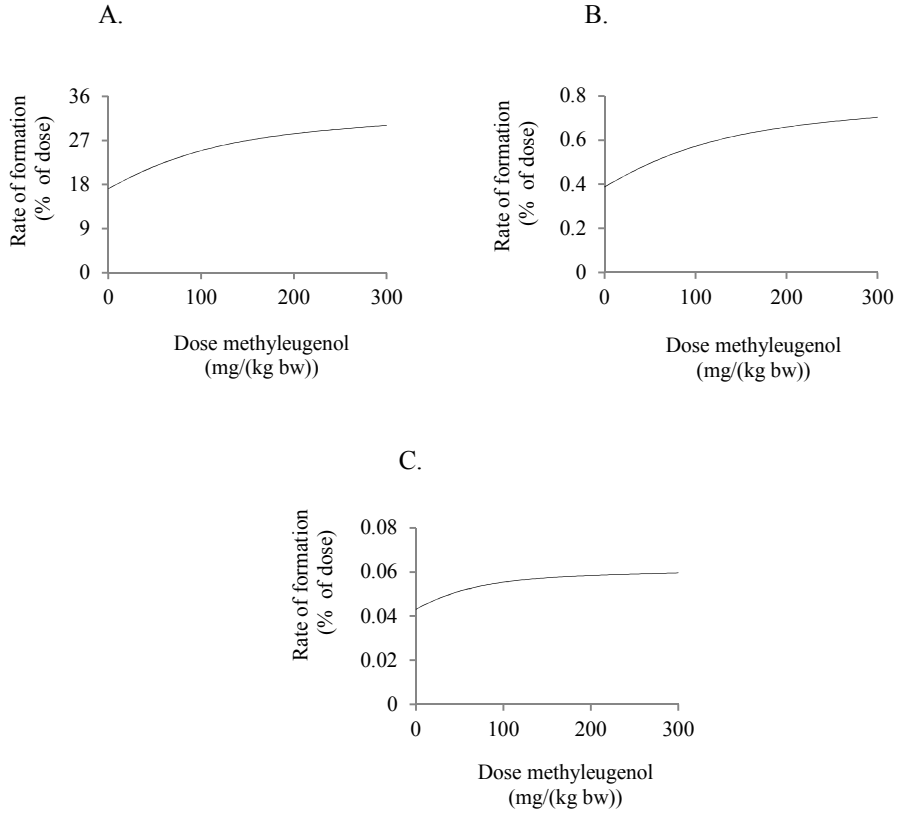

Figure 10. The PBK model-predicted dose-dependent percentage of formation of phase II metabolites in the liver of Sprague Dawley rat: A. 1′-hydroxymethyleugenol glucuronide, B. 1′-oxomethyleugenol, and C. 1′-sulfooxymethyleugenol.

Sensitivity analysis

A sensitivity analysis was performed to determine the model parameters which affect the formation of 1′-hydroxymethyleugenol, 1′-hydroxymethyleugenol glucuronide, 1′-oxomethyeugenol, and 1′-sulfooxymethyleugenol as model outputs. These metabolites are only formed in the liver. Figure 11A presents the parameters which have an effect on the formation

of 1′-hydroxymethyleugenol. Formation of 1′-hydroxymethyleugenol primarily depends on the kinetic constants for its formation ($V_{max,L\_1'HME}$, $K_{m,L\_1'HME}$) at both doses of 0.05 and 300 mg/(kg bw). To a small extent, the formation of 1′-hydroxymethyleugenol depends on the kinetic constants of the other competing phase I metabolites formed in the liver. Figure 11B presents the kinetic parameters which influence the formation of 1′-hydroxymethyleugenol glucuronide. Glucuronidation of 1′-hydroxymethyleugenol primarily depends on the kinetic constants for formation of 1′-hydroxymethyleugenol ($V_{max,L\_1'HME}$, $K_{m,L\_1'HME}$) and to a minor extent on the kinetic constants for the formation of 3-(3,4-dimethoxyphenyl)-2-propen-1-ol (V_{max,L_3DMPOH}, K_{m,L_3DMPOH}), methyleugenol-2′,3′-oxide (V_{max,L_MEO}, K_{m,L_MEO}), and 2-hydroxy-4,5-dimethoxyallylbenzene (V_{max,L_2HDME}, K_{m,L_2HDME}). Figure 11C reveals that the formation of 1′-oxomethyleugenol depends on the formation constants of 1′-hydroxymethyleugenol ($V_{max,L\_1'HME}$, $K_{m,L\_1'HME}$), but also on the kinetic constants for the formation of 1′-hydroxymethyleugenol glucuronide (V_{max,L_1HMEG}, $K_{m,L\_1'HMEG}$) and on the kinetic constants ($V_{max,L\_1'OME}$, $K_{m,L\_1'OME}$) for the formation of 1′-oxomethyleugenol itself. Figure 11D reveals that the formation of the ultimate carcinogen 1′-sulfooxymethyleugenol not only depends on the kinetic constants for the formation of the proximate carcinogen 1′-hydroxymethyleugenol ($V_{max,L\_1'HME}$, $K_{m,L\_1'HME}$), but also on the kinetic constants for formation of 1′-hydroxymethyleugenol glucuronide ($V_{max,L\_1'HMEG}$, $K_{m,L\_1'HMG}$) and on the kinetic constant for formation of 1′-sulfooxymethyleugenol itself ($V_{max,L\_1'HMES}$, $K_{m,L\_1'HMES}$). This indicates that glucuronidation of 1′-hydroxymethyleugenol is an important competing metabolic pathway to sulfonation due to its higher catalytic efficiency. Moreover the formation of 1′-sulfooxymethyleugenol also depends on the liver microsomal protein yield (MPL) and liver S9 protein yield (S9PL).

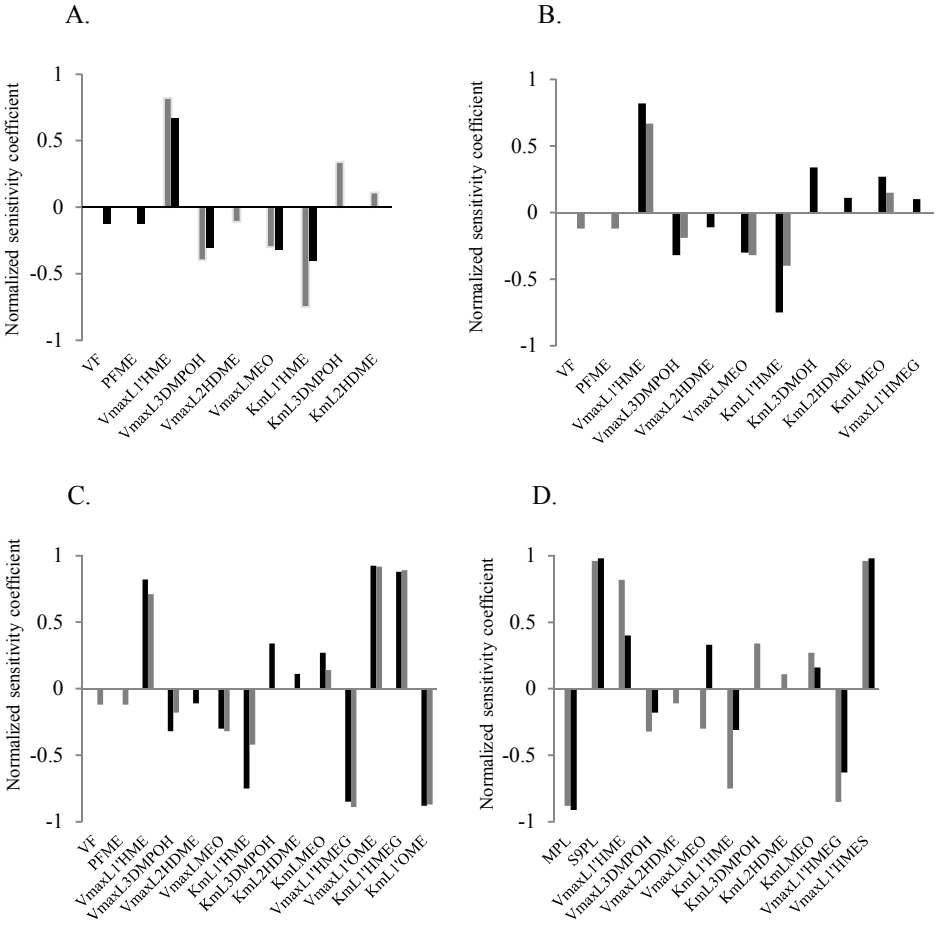

Figure 11. Sensitivity of the predicted formation of A. 1′-hydroxymethyleugenol, B. 1′-hydroxymethyleugenol glucuronide, C. 1′-oxomethyleugenol, and D. 1′-sulfooxymethyleugenol to different model parameters. Gray bars correspond to the normalized sensitivity coefficients at a dose of 0.05 mg/(kg bw) and black bars at a dose of 300 mg/(kg bw). VF = volume of fat tissue, PFME = fat/blood partition coefficient of methyleugenol, MPL = Liver microsomal protein yield, S9PL = Liver S9 protein yield, *V*max and *K*m are the maximum rate of formation and the Michaelis-Menten constant for the formation of the different metabolites (M) in liver: methyleugenol-2′,3′-oxide (MEO), 1′-hydroxymethyleugenol (1′HME), 3-(3,4-dimethoxyphenyl)-2-propen-1-ol (3DMPOH), 2-hydroxy-4,5-dimethoxyallylbenzene (2HDME), M6, 3-hydroxy-4-methoxyallylbenzene (3HMA), 1′-hydroxymethyleugenol glucuronide (1′HMEG), 1′-oxomethyleugenol (1′OME), and 1′-sulfooxymethyleugenol (1′HMES) in liver tissue.

Factors that could affect the PBK model outcome

Strain and gender differences

Strain and gender differences have been shown to affect the kinetics and metabolism of drugs (Campbell, 1995). Since the PBK model was developed using data obtained from male Sprague Dawley rat samples, the metabolic parameters were also determined using tissue samples from female Sprague Dawley, and female and male Fisher 344 rats, in order to study the impact of strain and gender differences on the PBK model outcomes. The kinetic parameters of different strains and genders are presented in Table 5. Comparison of these kinetic parameters reveals that there are no strain or gender differences in the formation of 1′-hydroxymethyleugenol, 2-hydroxy-4,5-dimethoxyallylbenzene, 3-(3,4-dimethoxyphenyl)-2-propen-1-ol, and 3-hydroxy-4-methoxyallylbenzene between male and female Sprague Dawley rats and male and female Fisher 344 rats. Although some variation in K_m and V_{max} values for these metabolic routes occurs, the overall catalytic efficiencies are about the same for the different strains and genders. Only gender differences do occur in the formation of methyleugenol-2′,3′-oxide. Methyleugenol-2′,3′-oxide formation was found to be more efficient when measured for liver microsomes from male Sprague Dawley and Fisher 344 rats while it is less efficient with female Sprague Dawley and Fisher 344 rat liver microsomes. The effect of the differences in kinetic parameters on the outcome of the PBK model was studied by determining the changes in the predicted formation of 1′-hydroxymethyleugenol**.** Figure 12 presents the PBK predicted formation of 1′-hydroxymethyleugenol as a percentage of the dose over a 24 hr time-frame when kinetic constants of phase I metabolism by liver microsomes of male or female Sprague Dawley rats, or male or female Fisher 344 rats, were applied, and all other parameters were kept the same. It is observed that the formation of 1′-hydroxymethyleugenol in female Sprague Dawley rats is 1.5 fold higher than in male Sprague Dawley rats while no difference in the formation of 1′-hydroxymethyleugenol was found between the different strains of the same sex. These results indicate that sex dependent differences in phase I kinetics may influence the model outcome although they influence the

Table 5. The kinetic parameters for liver metabolites ($V_{max(app)}$, $K_{m(app)}$, and catalytic efficiency (V_{max}(app)/K_m(app))) of male Sprague Dawley, female Sprague Dawley, male Fisher 344 and female Fisher 344 rats).

metabolite	strain	$V_{max(app)}$[a]	$K_{m(app)}$[b]	catalytic efficiency[c] (V_{max}(app)/K_m(app))
methyleugenol-2′,3′-oxide	Male Sprague Dawley	1.84	81	22.7
	Female Sprague Dawley	1.69	2184	0.77
	Male Fisher 344	2.0	100	20.0
	Female Fisher 344	0.96	1496	0.64
1'-hydroxymethyleugenol	Male Sprague Dawley	3.26	253	12.9
	Female Sprague Dawley	1.39	90	15.4
	Male Fisher 344	3.6	181	19.9
	Female Fisher 344	1.79	69	25.9
2-hydroxy-4,5dimethoxyallyl-benzene	Male Sprague Dawley	0.26	32	8.1
	Female Sprague Dawley	0.18	22.3	8.1
	Male Fisher 344	0.28	31.2	9.0
	Female Fisher 344	0.17	31.4	5.4
3-(3,4-dimethoxyphenyl)-2-propen-1-ol	Male Sprague Dawley	0.68	28	24.3
	Female Sprague Dawley	0.44	17	25.9
	Male Fisher 344	0.75	27.2	27.6
	Female Fisher 344	0.48	23	20.9
M6	Male Sprague Dawley	0.44	259	1.7
	Female Sprague Dawley	0.033	607	0.054
	Male Fisher 344	0.30	86	3.5
	Female Fisher 344	0.22	37	6.0
3-hydroxy-4-methoxyallylbenzene	Male Sprague Dawley	0.13	150	0.87
	Female Sprague Dawley	0.11	261	0.42
	Male Fisher 344	0.25	361	0.69
	Female Fisher 344	0.12	216	0.56

[a](nmol/min/(mg microsomal protein)
[b](μM)
[c](μL/ min/(mg microsomal protein)

formation of 1′-hydroxymethyleugenol and consequently its phase II metabolites to only a small extent (2 fold at most). On the other hand, the strain dependent differences do not influence the formation of 1′-hydroxymethyleugenol and its phase II metabolites.

Scaling factor of *in vitro* metabolic parameters to the *in vivo* situation

Scaling of *in vitro* metabolic parameters to the *in vivo* situation can also influence the model outcome since the microsomal protein yield from different tissues used to scale the V_{max} values

to the *in vivo* situation were based on the values taken from the literature (Beierschmitt and Weiner, 1986; Medinsky *et al.*, 1994). The effect of changing microsomal protein yield on the outcome of the PBK model was examined through monitoring the formation of 1′-hydroxymethyleugenol. At doses of 0.05 mg/(kg bw), it was noted that decreasing the liver microsomal protein yield by 4-times led to a decrease in the formation of 1′-hydroxymethyleugenol from approximately 17.6% to 15.6%, while at 300 mg/(kg bw) the decrease was approximately from 30.8% to 26.6%. Lowering the lung microsomal protein yield 4-times led to a small increase in the predicted formation of 1'-hydroxymethyleugenol from 17.6% to 18.0% and from 30.8% to 31.3% at 0.05 and 300 mg/(kg bw) doses, respectively. In case of kidney, no influence was observed on the predicted formation of 1'-hydroxymethyleugenol following changing the kidney microsomal protein yield at both 0.05 and 300 mg/kg bw doses. Also some uncertainty may exist in the *in vitro* derived apparent K_m values, which have been used for the *in vivo* apparent K_m values. No indication can be given on the level of uncertainty in these K_m values (Punt *et al.*, 2008). Based on the model, a 4-fold increase in K_m values for phase I metabolism in liver has however the same effects on the estimated formation of the different phase I metabolites at a different oral dose as a 4-fold decrease in scaling of V_{max} values.

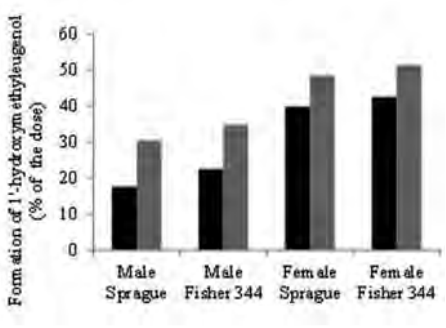

Figure 12. PBK model-predicted relative formation of 1′-hydroxymethyleugenol when using kinetic constants for phase I metabolism by liver microsomes of male or female Sprague Dawley rats, or male or female Fisher 344 rats keeping all other parameters the same. Gray bars correspond to the predicted formation of 1′-hydroxymethyleugenol as % of the dose at a dose of 0.05 mg/(kg bw) and black bars at a dose of 300 mg/(kg bw).

Discussion

The objective of the present study was to define a PBK model for methyleugenol in male rat, based on *in vitro* metabolic parameters, which would allow evaluation of the dose-dependent differences in bioactivation and detoxification at different oral doses of methyleugenol. The PBK modeling approach has the advantage of giving insight in the organs involved in metabolism of methyleugenol and how that affects the ultimate chances on conversion to the ultimate carcinogenic metabolite 1′-sulfooxymethyleugenol in the liver. Through the model, the formation of the proximate carcinogenic metabolite (1′-hydroxymethyleugenol) and the ultimate carcinogenic metabolite (1′-sulfooxymethyleugenol) of methyleugenol in the liver of male rat can be predicted.

The developed model was evaluated by comparing the PBK model predicted concentration of methyleugenol in venous blood to literature data on methyleugenol concentrations in plasma of male Fisher 344 rats at different time points (NTP, 2000). At 0.25, 4, 6, 8, and 10 hr, the outcomes of the PBK model were in the same order of magnitude as these literature results. At time points of 1 and 2 hr, the PBK predicted venous blood concentration of methyleugenol was somewhat overestimated. For instance at 2 hr, it was found that the predicted venous blood concentration of methyleugenol was about 18 times higher than what is observed in the literature. We should bear in mind that the present *in vitro* study was undertaken using tissue fractions obtained from male Sprague Dawley rats while the *in vivo* study was performed using male Fisher 344 rats (NTP, 2000). Also, differences in predicted and observed blood concentrations of methyleugenol could be partly due to the fact that the model predicts whole blood concentrations whereas the *in vivo* study covers plasma concentrations. This comparison between whole blood and plasma concentrations can only be made based on the assumption that the whole blood and plasma concentrations are equal. Furthermore, protein binding may provide another explanation for the fact that the PBK predicted venous blood concentrations of methyleugenol are somewhat higher than the observed blood concentrations. An additional

evaluation of the model was performed by comparing the PBK predicted % of formation of both 2-hydroxy-4,5-dimethoxyallylbenzene and 3-hydroxy-4-methoxyallylbenzene to the literature date of urine samples (collected over 24 hr) of a male Wister rat given a single oral dose of 200 mg/(kg bw) of methyleugenol. The PBK model predicted accurately the formation of 3-hydroxy-4-methoxyallylbenzene while the PBK model based predicted formation of 2-hydroxy-4,5-dimethoxyallylbenzene was only 2.6-fold higher than the reported literature value and thus within the same order of magnitude (Solheim and Scheline, 1976). Additional evaluation was performed by comparing the PBK model based predicted % of formation of 1′-hydroxymethyleugenol glucuronide in urine (collected over 24 hr) of a male Fisher rat given a single oral dose of 118 mg/(kg bw) of methyleugenol. The PBK model accurately predicted the level of formation of the 1'-hydroxymethyleugenol glucuronide metabolite which was only 1.3-fold higher than the observed *in vivo* value (NTP, 2000). The difference between the experimental data and the literature data could be to some extent due to the strain dependent differences in kinetics and scaling of *in vitro* metabolic data, although additional results of the present study revealed that influences of species differences in especially phase I kinetics were limited. The sensitivity analysis revealed that the influence of uncertainties in metabolic parameters and scaling of *in vitro* metabolic parameters to the *in vivo* situation could affect the outcomes of the PBK model. Overall it is important to stress that deviations within one order of magnitude are generally considered acceptable within the present state-of-the-art of integrating *in vitro* data and PBK modeling (Hissink *et al.*, 1997; Lupfert and Reichel, 2005; Punt *et al.*, 2008; Quick and Shuler, 1999). This implies that conclusions derived from the present model should preferably not be based on absolute outcomes but rather on comparison of different conditions in a relative way as done in the present study. The PBK model developed in the present study can be used to study dose-dependent bioactivation.

We have observed that increasing the dose is accompanied with increasing formation of the reactive metabolite 1′-sulfooxymethyleugenol for methyleugenol. At a low dose of 0.05 mg/(kg bw), which is relevant for dietary human intake, formation of methyleugenol-2′,3′-oxide and 3-(3,4-dimethoxyphenyl)-2-propen-1-ol are the major metabolic routes amounting to 31.0 % and

32.9% of the dose respectively. These metabolites are formed in the liver. Due to saturation of these metabolic routes at higher doses, a relative increase in formation of the proximate carcinogenic metabolite 1′-hydroxymethyleugenol occurs, resulting in a relative increase in formation of 1′-sulfooxymethyleugenol as well. Formation of 1′-sulfooxymethyleugenol increased from 0.042% of the dose at a dose of 0.05 mg/(kg bw) to 0.06% of the dose at a dose of 300 mg/(kg bw).

Similar dose-dependent effects in bioactivation have previously been observed with the PBK model developed for the related alkenylbenzene estragole (Punt *et al.*, 2008). In case of estragole, the formation of the ultimate carcinogenic metabolite 1′-sulfooxyestragole increased from 0.08% of the dose at a dose of 0.05 mg/(kg bw) to 0.16% at a dose of 300 mg/(kg bw). The underlying mechanism resulting in these dose-dependent effects on bioactivation of estragole were, however, different than currently observed for methyleugenol. For estragole, the dose-dependent effects in bioactivation were a result from a shift in phase I metabolism from *O*-demethylation to 1′-hydroxylation with increasing doses of estragole. *O*-demethylation of estragole is the major metabolic route at low doses, occurring mainly in the lung and kidney of male rat. Due to saturation of the *O*-demethylation pathway in lung and kidney at higher doses, formation of the proximate carcinogenic metabolite 1′-hydroxyestragole, occurring mainly in the liver, becomes relatively more important leading to a relative increase in formation of 1′-sulfooxyestragole as well. In case of methyleugenol, the dose-dependent effects in bioactivation were a result from a shift in phase I metabolism from 3′-hydroxylation and hydroxylation of the benzene ring to 1′-hydroxylation with increasing doses of methyleugenol. Due to saturation of the 3′-hydroxylation and the hydroxylation of benzene ring pathways in liver at higher doses, formation of the proximate carcinogenic metabolite 1′-hydroxymethyleugenol, occurring in the liver, becomes relatively more important leading to a relative increase in formation of 1′-sulfooxymethyleugenol.

Although the metabolic pathways of methyleugenol and the importance of different metabolic routes have, so far, been considered to be similar to those for estragole (Smith *et al.*, 2010; Smith *et al.*, 2002), the present study reveals some major differences in the metabolic

conversion of these related compounds. An important difference is that the *O*-demethylation route is not the major detoxification route of methyleugenol at low doses (predicted to account for 3.4% of the dose at a dose of 0.05 mg/(kg bw)), whereas this has been observed to be the major detoxification route at low doses for estragole (predicted to account for 56% of the dose at a dose of 0.05 mg/kg bw) (Punt *et al.*, 2008). With the previously developed PBK model for estragole in male rat we observed that formation of this metabolite of estragole mainly occurred in the lung tissue. Such a high level of extrahepatic metabolism of estragole in male rat is possibly due to a relatively high systemic bioavailability (57%) of estragole and the capacity of the lung to catalyze *O*-demethylation with a high affinity. In case of methyleugenol, the efficiency by which lung tissue fractions catalyze *O*-demethylation was much lower than observed for estragole (20 µL/min/(mg microsomal protein) for methyleugenol versus 1360 µL/min/(mg microsomal protein) for estragole (Punt *et al.*, 2008)). This can explain the lower level of conversion of methyleugenol via this metabolic pathway. The relative low level of *O*-demethylation of methyleugenol is supported by *in vivo* data revealing that only 3.0% of the dose is excreted via this metabolic route in male Wistar rats exposed to 200 mg/(kg bw), whereas in case of estragole this metabolic route has been reported to account for 29-50% of the dose in female Wistar rats exposed to a comparable oral dose of 500 mg/(kg bw) (Anthony *et al.*, 1987; Solheim and Scheline 1976). Altogether, the observed differences in metabolic conversion between estragole and methyleugenol indicate the importance of evaluating the metabolic fate of methyleugenol and consequences of dose-dependent effects in bioactivation versus detoxification for the risk assessment of methyleugenol separate from estragole.

The relative increase in the formation of the proximate carcinogenic metabolite 1′-hydroxymethyleugenol and the ultimate carcinogenic metabolite 1′-sulfooxymethyleugenol in the liver of male rat with increasing dose of methyleugenol implies a relative increase in bioactivation of methyleugenol with the dose. This indicates that when extrapolating from high dose animal experiments to low doses relevant for dietary human intake, it is important to take into account non-linear effects in kinetics. In addition to dose-dependent effects, species differences in metabolism and metabolic activation should also be taken into account in the

extrapolation of animal carcinogenicity data to the human situation. To determine the overall differences between humans and male rats in bioactivation of methyleugenol, it is of importance to compare the relative extent of different metabolic pathways between these species. To this end, now a similar PBK model for the human situation is being constructed. Comparison of the results predicted by such a PBK model for the human to those predicted by the rat model of the present study can provide further insight in species differences in metabolism and metabolic activation of the alkenylbenzene methyleugenol.

Acknowledgement

For the LC-MS analysis we thank Hilde Wolvers. We thank Dr. Yiannis Fiamegos for the synthesis of 1′-hydroxymethyleugenol. This work was supported by a grant from sandwich PhD fellowship program / Wageningen University, the Netherlands.

References

Abdo, K.M., Cunningham M.L., Snell M.L., Herbert R.A., Travlos G.S., and Eldridge S.R. (2001). 14-week toxicity and cell proliferation of methyleugenol administered by gavage to F344 rats and B6C3F1 mice. Food Chem Toxicol 39, 303-316.

Anthony, A., Caldwell, J., Hutt, A.J., and Smith, R.L. (1987). Metabolism of estragole in rat and mouse and influence of dose size on excretion of the proximate carcinogen 1′-hydroxyestragole. Food Chem Toxicol 25, 799-806.

Beierschmitt, W.P., and Weiner, M. (1986). Age-related changes in renal metabolism of acetaminophen in male Fischer 344 rats. Age 9, 7-13.

Borchert, P., Wislocki, P.G., Miller, J.A., and Miller, E.C. (1973). The metabolism of the naturally occurring hepatocarcinogen safrole to 1'-hydroxysafrole and the electrophilic reactivity of 1'-acetoxysafrole. Cancer Res 33, 575-589.

Brown, R.P., Delp, M.D., Lindstedt, S.L., Rhomberg, L.R., and Beliles, R.P. (1997). Physiological parameter values for physiologically based pharmacokinetic models. Toxicol Ind Health 13, 407-484.

Campbell, D.B. (1995). The use of toxicokinetics for the safety assessment of drugs acting in the brain. Mol Neurobiol 11, 193-216.

DeJongh, J., Verhaar, H.J., and Hermens, J.L. (1997). A quantitative property-property relationship (QPPR) approach to estimate in vitro tissue-blood partition coefficients of organic chemicals in rats and humans. Arc Toxicol 72, 17-25.

De Vincenzi, D., Silano, M., Stacchini, P., and Scazzocchio, B. (2000). Constituents of aromatic plants: I. Methyleugenol. Fitoterapia 71, 216-221.

Drinkwater, N.R., Miller, E.C., Miller, J.A., and Pitot, H.C. (1976). Hepatocarcinogenicity of estragole (1-allyl-4-methoxybenzene) and 1′-hydroxyestragole in the mouse and mutagenicity of 1'-acetoxyestragole in bacteria. J of Nat Cancer Instit 57, 1323-1331.

Evans, M.V., and Andersen, M.E. (2000). Sensitivity analysis of a physiological model for 2,3,7,8-tetrachlorodibenzo-p-dioxin (TCDD): assessing the impact of specific model parameters on sequestration in liver and fat in the rat. Toxicol Sci 54, 71-80.

Fennell, T.R., Miller, J.A., and Miller, E.C. (1984). Characterization of the biliary and urinary glutathione and N-acetylcysteine metabolism of hepatic carcinogen 1′-hydroxysafrole and its 1′-oxometabolites in rat and mice. Cancer Res 44, 3231-3240.

Filser, J.G., Faller, T.H., Bhowmik, S., Schuster, A., Kessler, W., Putz, C., and Csanady, G.A. (2001). First-pass metabolism of 1,3-butadiene in once through perfused livers of rats and mice. Chem Biol Interact 135-136, 249-265.

Fisher, M.B., Campanale, K., Ackermann, B.L., Vanden Branden, M., and Wrighton, S.A. (2000). In vitro glucuronidation using human liver microsomes and the pore-forming peptide alamethicin. Drug Metab Dispos 28, 560-566.

Gardner, I., Wakazono, H., Bergin, P., Waziers, I., Beaune, P., Kenna, J.G., and Caldwell, J. (1997). Cytochrome P450 mediated bioactivation of methyleugenol to 1′-hydroxy-

methyleugenol in Fischer 344 rat and human liver microsomes. Carcinogenesis 18, 1775-1783.

Garg, A., and Balthasar, J.P. (2007). Physiologically-based pharmacokinetic (PBPK) model to predict IgG tissue kinetics in wild-type and FcRn-knockout mice. J of Pharmacokinet Phar 34, 687-709.

Guenthner, T.M., and Luo, G. (2001). Investigation of the role of the 2′,3′-epoxidation pathway in the bioactivation and genotoxicity of dietary allylbenzene analogs. Toxicology 160, 47-58.

Hall, R.L., and Oser, B.L. (1965). Recent progress in the consideration of flavoring ingredients under the food additives amendment III. GRAS substances. Food Technol 253, 151-197.

Hissink, A.M., van Ommen, B., Kruse, J., and van Bladeren, P.J. (1997). A physiologically based pharmacokinetic (PB-PK) model for 1,2-dichlorobenzene linked to two possible parameters of toxicity. Toxicol Appl Pharmacol 145, 301-310.

Iyer, L.V., Ho, M.N., Shinn, W.M., Bradford, W.W., Tanga, M.J., Nath, S.S., and Green, C.E. (2003). Glucuronidation of 1′-Hydroxyestragole (1′-HE) by human UDP-Glucuronosyl-transferases UGT2B7 and UGT1A9. Toxicol Sci 73, 36-43.

Jeurissen, S.M.F., Bogaards, J.J.P, Awad, H.M., Boersma, M.G., Brand, W., Fiamegos, Y.C.,van Beek T.A., Alink, G.M., Sudhölter E.J.R , Cnubben N.H.P, and Rietjens I.M.C.M. (2004). Human cytochrome P450 enzyme specificity for bioactivation of safrole to the proximate carcinogen 1′-hydroxysafrole. Chem Res Toxicol 17, 1245-1250.

Jeurissen, S.M.F, Bogaards, J.J.P, Boersma, M.G., ter Horst J.P.F, Awad, H.M., Fiamegos, Y.C., van Beek T.A., Alink, G.M, Sudhölter E.J.R, Cnubben N.H.P, and Rietjens I.M.C.M. (2006). Human cytochrome P450 enzyme specificity for bioactivation of methyleugenol to the proximate carcinogen 1′-hydroxymethyleugenol. Chem Res Toxicol 19, 111-116.

Lin, J.H., and Wong, B.K. (2002). Complexities of glucuronidation affecting in vitro in vivo extrapolation. Curr Drug Metab 3, 623-646.

Luo, G., and Guenthner, T.M. (1995). Metabolism of allylbenzene 2′,3′-oxide and estragole 2′,3′-oxide in the isolated perfused rat liver. J Pharmacol Exp Ther 272, 588-596.

Luo, G., Qato, M.K., and Guenthner, T.M. (1992). Hydrolysis of the 2′,3′-allylic epoxides of allylbenzene, estragole, eugenol, and safrole by both microsomal and cytosolic epoxide hydrolases. Drug Metab Dispos 20, 440-445.

Lupfert, C., and Reichel, A. (2005). Development and application of physiologically based pharmacokinetic-modeling tools to support drug discovery. Chem Biodivers 2, 1462-1486.

Medinsky, M.A., Leavens, T.L., Csanady, G.A., Gargas, M.L., and Bond, J.A. (1994). In vivo metabolism of butadiene by mice and rats: a comparison of physiological model predictions and experimental data. Carcinogenesis 15, 1329-1340.

Miele, M., Dondero, R., Ciarallo, G., and Mazzei, M.J. (2001). Methyleugenol in Ocimum basilicum L.cv. Genovese Gigante. J Agr Food Chem 49, 517-521.

Miller, E.C., Swanson, A.B., Phillips, D.H., Fletcher, T.L., Liem, A., and Miller, J. (1983). Structure-activity studies of the carcinogenicities in the mouse and rat of some naturally occurring and synthetic alkenylbenzene derivatives related to safrole and estragole. Cancer Res, 43, 1124-1134.

NTP (2000). Toxicology and carcinogenesis studies of methyleugenol (CAS No. 93-15-12) in F344/N rats and B6C3F1 mice (Gavage studies). Natl Toxicol Program Tech Rep Ser, 491, 1-412.

Punt, A., Delatour, T., Scholz, G., Schilter, B., Bladeren, P.J., and Rietjens, I.M.C.M. (2007). Tandem mass spectrometry analysis of N^2-(*trans*-Isoestragol-3′-yl)-2′-deoxyguanosine as a strategy to study species differences in sulfotransferase conversion of the proximate carcinogen 1′-hydroxyestragole. Chem Res Toxicol 20, 991-998.

Punt, A., Freidig, A.P, Delatour, T., Scholz, G., Boersma, M.G., Schilter, B., van Bladeren, P.J., and Rietjens, I.M.C.M.. (2008). A physiologically based biokinetic (PBBK) model for estragole bioactivation and detoxification in rat. Toxicol Appl Pharmacol 231, 248-259.

Punt, A., Paini, A., Boersma, M.G., Freidig, A.P., Delatour, T., Scholz, G., Schilter, B., van Bladeren, P.J., and Rietjens I.M.C.M. (2009). Use of physiologically based biokinetic (PBBK) modeling to study estragole bioactivation and detoxification in humans as compared to male rats. Toxicol Sci 110, 255–269.

Quick, D.J., and Shuler, M.L. (1999). Use of in vitro data for construction of a physiologically based pharmacokinetic model for naphthalene in rats and mice to probe species differences. Biotechnol Prog 15, 540-555.

Ramsey, J.C., and Andersen, M.E. (1984). A physiologically based description of the inhalation pharmacokinetics of styrene in rats and humans. Toxicol Appl Pharmacol 73, 159-175.

SCF (2001). Opinion of the scientific committee on food on methyleugenol (4-allyl-1,2-dimethyxybenzene). European Commission, Scientific Committee on Food. Brussels, BE. http://ec.europa.eu/food/fs/sc/scf/out104_en.pdf

Smith, B., Cadby, P., Leblanc, J., and Setzer, R. (2010). Application of the margin of exposure (MoE) approach to substances in food that are genotoxic and carcinogenic. Example: Methyleugenol, CASRN: 93-15-2. Food Chem Toxicol 48, S89-S97.

Smith, R.L., Adams, T.B., Doull, J., Feron, V., Goodman, J.I., Marnett, L.J., Portoghese, P.S., Waddell, W.J., Wagner, B.M., Rogers, A.E., Caldwell, J., and Sipes, I.G. (2002). Safety assessment of allylalkoxybenzene derivatives used as flavoring substances – methyl eugenol and estragole. Food Chem Toxicol 40, 851-870.

Solheim, E., and Scheline, R. (1976). Metabolism of alkenebenzene derivatives in the rat. II. eugenol and isoeugenol methyl ethers. Xenobiotica 6, 137-150.

Tardif, R., Droz, P.O., Charest-Tardif, G., Pierrehumbert, G., and Truchon, G. (2002). Impact of human variability on the biological monitoring of exposure to toluene: I. Physiology based toxicokinetics modeling. Toxicol Lett 134, 155-163.

3

Physiologically based kinetic modeling of bioactivation and detoxification of the alkenylbenzene methyleugenol in human as compared with rat

Based on: Al-Subeihi A.A.A., Spenkelink B., Punt A., Boersma M.G., van Bladeren P.J., and Rietjens I.M.C.M. Toxicol Appl Pharm (2012) 260, 271-284

Abstract

This study defines a physiologically based kinetic (PBK) model for methyleugenol in human based on *in vitro* and *in silico* derived parameters. With the model obtained, bioactivation and detoxification of methyleugenol at different doses levels could be investigated. The outcomes of the current model were compared with those of a previously developed PBK model for methyleugenol in male rat. The results obtained reveal that formation of 1′-hydroxymethyleugenol glucuronide, a major metabolic pathway in male rat liver, appears to represent a minor metabolic pathway in human liver whereas in human liver a significantly higher formation of 1′-oxomethyleugenol compared with male rat liver is observed. Furthermore, formation of 1′-sulfooxymethyleugenol, which readily undergoes desulfonation to a reactive carbo-cation that can form DNA or protein adducts, is predicted to be the same in the liver of both human and male rat at oral doses of 0.0034 and 300 mg/(kg bw). Altogether despite a significant difference in especially the metabolic pathways of the proximate carcinogenic metabolite 1′-hydroxymethyleugenol between human and male rat, the influence of species differences on the ultimate overall bioactivation of methyleugenol to 1′-sulfooxymethyleugenol appears to be negligible. Moreover, the PBK model predicted the formation of 1′-sulfooxymethyleugenol in the liver of human and rat to be linear from doses as high as the benchmark dose (BMD_{10}) down to as low as the virtual safe dose (VSD). This study shows that kinetic data do not provide a reason to argue against linear extrapolation from the rat tumor data to the human situation.

Introduction

Methyleugenol is a natural constituent of the essential oils of a number of plants (De Vincenzi *et al.*, 2000). It occurs in clove oil, allspice, cinnamon bark, walnuts, basil, nutmeg, tarragon, star anise, lemongrass, pimento and fennel (SCF, 2001). Methyleugenol is commonly used as a flavoring agent, either natural or synthetic, in many food stuffs, for instance, candy, cookies such as gingersnaps, ice cream, tomato ketchup and relish (Burdock, 1995; Leung, 1980). The use of methyleugenol as pure substance in food is momentarily limited to the US since the European Union recently decided to prohibit the use of the compound (European Commission, 2008). Botanical extracts containing methyleugenol are however still allowed and in use. Methyleugenol was found to account for 2.6 %, 3.7 %, 13 % and 0.8 % of the volatile oil of basil, bay (leaves), pimento (berry), and nutmeg, respectively (Smith *et al.*, 2002). Moreover, methyleugenol is used as a fragrance in some perfumes and toiletries at concentrations of 0.002-0.3% (SRI International, 1990). Though the International Fragrance Research Association (IFRA) has recently restricted the use of methyleugenol and established a limit of 2.5 µg/(kg bw)/day (IFRA, 2009). In 1965, the Expert Panel of the Flavor and Extract Manufacturers Association (FEMA) concluded that methyleugenol was GRAS (Generally Recognized As Safe) under conditions of intended use as a flavoring substance in food (Hall and Oser, 1965). In the FEMA evaluation, it was taken into account that there are experimental data suggesting a non-linear relationship between dose and profiles of metabolism and metabolic activation and that exposure due to use as a flavoring is relatively low (Smith *et al.*, 2002). Methyleugenol was nominated for toxicological characterization and testing by the National Toxicology Program (NTP) because it is widely used and it structurally resembles the known carcinogens safrole and estragole (Miller *et al.*, 1983; NTP, 1998). In 2000, the carcinogenicity of methyleugenol was investigated in mice and rats by the National Toxicology Program (NTP) (NTP, 2000). The NTP reported that methyleugenol is carcinogenic in both rats and mice (NTP, 2000). It was also shown that methyleugenol possesses a cytotoxic and genotoxic activity in rat hepatocytes

(Burkey *et al.*, 2000). In 2001, the FEMA Panel reassessed the available data for methyleugenol and confirmed that there is no considerable cancer risk resulting from consumption of methyleugenol as flavoring substance and affirmed the GRAS status of methyleugenol as a flavoring substance given the low levels of exposure (Smith *et al.*, 2002). In 2001, the Scientific Committee on Food (SCF) of the European Union published a scientific opinion on methyleugenol in which it was concluded that methyleugenol is genotoxic and carcinogenic and that reductions in exposure and restrictions in use levels are indicated (SCF, 2001). On the other hand, it is of interest to note that although methyleugenol forms DNA adducts (Gardner *et al.*, 1997; Phillips *et al.*, 1984) and induces unscheduled DNA synthesis in rat liver (Chan and Caldwell, 1992), it is negative in many *in vitro* genotoxicity assays and also did not induce DNA damage in liver, bone marrow, and bladder in a regular *in vivo* Comet assay in the Fischer 344 rat following exposure to methyleugenol at dose level up to 2000 mg/(kg bw)/day (Ding *et al.*, 2011). The average daily intake of methyleugenol was estimated by the SCF to be 13 mg/day, corresponding to 0.217 mg/(kg bw)/day for a 60 kg person (SCF, 2001), while the FEMA, using a different methodology, estimated the average daily intake of methyleugenol to be less than 0.01 mg/(kg bw)/day (Smith *et al.*, 2002). The estimation of the SCF was based on theoretical maximum use levels of methyleugenol in various food categories and consumption data for these food categories, whereas the intake estimation of the FEMA was based on production volume data for flavor use (SCF, 2001; Smith *et al.*, 2002).

Methyleugenol is unreactive by itself but undergoes metabolic activation to produce an electrophilic metabolite that acts as the reactive genotoxic DNA binding intermediate (Gardner *et al.*, 1997; Miele *et al.*, 2001). Figure 1 displays the different metabolic pathways of methyleugenol. Important metabolic pathways include *O*-demethylation of the methoxy moieties on the benzene ring, 2′,3′-epoxidation, and 1′-hydroxylation of the allylic side chain (NTP, 2000; Solheim and Scheline, 1976). *O*-demethylation of the methoxy substituents of methyleugenol yields the corresponding phenolic derivatives (3-hydroxy-4-methoxyallylbenzene and eugenol), which may be excreted as sulfate or glucuronic acid conjugate (Smith *et al.*, 2002). Epoxidation of the side chain yields a 2′,3′-epoxide (methyleugenol-2′,3′-oxide). This

epoxide (methyleugenol-2′,3′-oxide) is detoxified by epoxide hydrolase to form the dihydrodiol (3-(3,4-dimethoxyphenyl)propane-1,2-diol) or via glutathione conjugation (Luo and Guenther, 1995). Hydroxylation at the 1'-position of methyleugenol is considered to represent the bioactivation pathway producing the proximate carcinogenic metabolite 1′-hydroxymethyleugenol (Drinkwater *et al.*, 1976; Miller *et al.*, 1983). In a next step 1′-hydroxymethyleugenol can be sulfonated by sulfotransferases to form 1′-sulfooxymethyleugenol which readily undergoes desulfonation to carbo-cation that can form DNA adduct (Miller *et al.*, 1983).

Recently, physiologically based kinetic (PBK) models were developed for methyleugenol in male rat (Al-Subeihi *et al.*, 2011) and for the related genotoxic and carcinogenic alkenylbenzene estragole in male rat (Punt *et al.*, 2008) and in human (Punt *et al.*, 2009). These models were capable of elucidating dose-dependent effects in bioactivation and detoxification of methyleugenol and estragole, based on *in vitro* metabolic parameters. In addition to dose-dependent effects, species differences in metabolism and metabolic activation can also occur. For instance, Punt *et al.* (2007) previously demonstrated that male rats are more efficient in sulfonation of 1′-hydroxyestragole than humans, and that male rats are far more efficient in glucuronidation of 1′-hydroxyestragole than humans, whereas humans preferentially oxidize 1′-hydroxyestragole to 1′-oxoestragole, a reaction hardly observed in male rats.

The objective of the present study was to develop a PBK model for methyleugenol in human to determine the overall differences between humans and male rats in bioactivation and detoxification of methyleugenol. To this end, the present study investigated the kinetics of possible metabolic reactions of methyleugenol and 1′-hydroxymethyleugenol in incubations with relevant human tissue fractions. The kinetic data obtained were used to build a PBK model for methyleugenol metabolism in human to predict the relative extent of bioactivation and detoxification of methyleugenol at dose levels relevant for dietary human intake. An evaluation of the model defined was performed by comparing the predicted concentrations of methyleugenol in whole blood to the levels of methyleugenol in serum blood of human volunteers exposed to methyleugenol reported in the literature (Schecter *et al.*, 2004). The

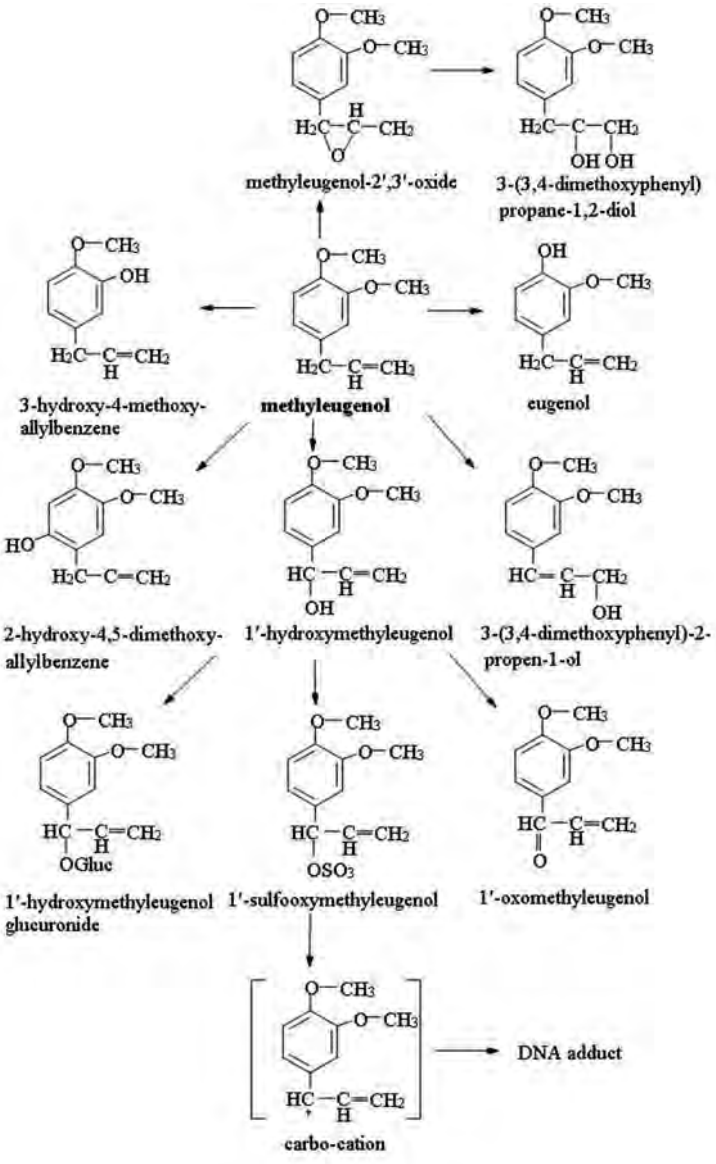

Figure 1. Suggested metabolic pathways of methyleugenol in human.

outcomes of the model were subsequently compared with those of the previously defined PBK model for methyleugenol in male rat to evaluate the occurrence of species differences in metabolic activation and detoxification of methyleugenol.

Materials and Methods

Chemical and reagents

Pooled mixed gender human liver microsomes, cytosol and S9 were purchased from BD Gentest (Woburn, MA, USA). Pooled mixed gender kidney, lung and small intestine microsomes were purchased from BioPredic International (Rennes, France). Hydrochloric acid (37%), potassium dihydrogen phosphate, dipotassium hydrogen phosphate trihydrate, and acetic acid were purchased from VWR International (Darmstadt, Germany). NADPH, $NADP^+$, NADH and NAD^+ were obtained from Roche Diagnostics (Mannheim, Germany). Methyleugenol, eugenol, methanol, dimethylsulfoxide (DMSO), ascorbic acid, alamethicin, glutathione (GSH), and uridine 5′-diphosphoglucuronic acid (UDPGA) were purchased from Sigma-Aldrich (Steinheim, Germany). Acetonitrile (UPLC/MS grade) was obtained from Biosolve (Valkenswaard, Netherlands). 3′-Phosphoadenosine-5′-phosphosulfate (PAPS) was obtained from Sigma Aldrich (Steinheim, Germany). 1′-Acetoxymethyleugenol, 1′-hydroxymethyleugenol, 3-(3,4-dimethoxyphenyl)-2-propen-1-ol, methyleugenol-2′,3′-oxide, 3-(3,4-dimethoxyphenyl)propane-1,2-diol, 3-hydroxy-4-methoxyallylbenzene, and 1′-oxomethyleugenol were synthesized and characterized as described previously (Al-Subeihi *et al.,* 2011).

Caution: 1′-acetoxymethyleugenol, 1′-hydroxymethyleugenol, 3-(3,4-dimethoxyphenyl)-2-propen-1-ol, methyleugenol-2′,3′-oxide, and 1′-oxomethyleugenol are carcinogenic and should be handled carefully.

In vitro incubations

Phase I Metabolism

Determination of the organs in human which are involved in the metabolism of methyleugenol was performed as described for male rat (Al-Subeihi *et al.*, 2011). In short, the microsomal preparations of the liver, lung, kidney, and small intestine from human were incubated with methyleugenol in the presence of NADPH, and the formation of the metabolites was monitored over time. The incubation mixtures had a final volume of 160 µL, containing (final concentrations) 3 mM NADPH, 1 mM ascorbic acid and 1 mg/mL microsomal protein in 0.2 M Tris-HCl (pH 7.4). After pre-incubation at 37 °C for 1 min, the reactions were started by the addition of the substrate methyleugenol added from a 100 times concentrated stock solution in DMSO. The reactions were terminated by addition of 40 µL cold acetonitrile. Initial incubations were performed at a substrate concentration of 1000 µM (final concentration) at several incubation times and microsomal protein concentrations. Blank incubations were performed without the cofactor NADPH.

The kinetic constants for the formation of different phase I metabolites of methyleugenol were determined in liver microsomes, which were found to be capable of metabolizing methyleugenol (see Results section). The incubation mixtures were as described above. Incubations with human microsomes were carried out for 10 min at a substrate concentration that ranged from 25 to 800 µM methyleugenol. Under the conditions specified, the formation of the different methyleugenol metabolites was linear with time and microsomal protein concentration. In the blank incubations performed without NADPH low amounts of 3-(3,4-dimethoxyphenyl)-2-propen-1-ol and eugenol were formed. Therefore the formation of 3-(3,4-dimethoxyphenyl)-2-propen-1-ol and eugenol was corrected for the amount of these metabolites already formed in the blank incubations.

HPLC analysis of Phase I metabolites

Before HPLC analysis of the samples, all incubations were centrifuged for 5 min at 16,000 g. Aliquots of 50 μL of the supernatant of each sample were analyzed as previously described (Al-Subeihi *et al.*, 2011).

Quantification of 1′-hydroxymethyleugenol was achieved by comparison of the peak area of this metabolite in the chromatograms obtained at a wavelength of 280 nm to the calibration curve of the synthesized 1′-hydroxymethyleugenol obtained at the same wavelength. Because 3-(3,4-dimethoxyphenyl)propane-1,2-diol has the same UV spectrum as 1′-hydroxymethyleugenol, 2-hydroxy-4,5-dimethoxyallylbenzene, and 3-(3,4-dimethoxyphenyl)-2-propen-1-ol have the same UV spectrum as 1′-acetoxymethyleugenol (data not shown), it was assumed that they have the same molar extinction coefficient as 1′-hydroxymethyleugenol, and 1′-acetoxymethyleugenol, respectively. Quantification of 3-(3,4-dimethoxyphenyl)-propane1,2-diol, reflecting formation of methyleugenol-2′,3′-oxide in liver microsomes, was therefore achieved by comparison of the peak area of the metabolite in the chromatograms obtained at a wavelength of 280 nm to the calibration curve for 1′-hydroxymethyleugenol obtained at the same wavelength. The quantification of 3-(3,4-dimethoxyphenyl)-2-propen-1-ol and 2-hydroxy-4,5-dimethoxyallyl-benzene was achieved by comparison of their peak areas in the chromatograms obtained at a wavelength of 280 nm to the calibration curve for 1′-acetoxymethyleugenol. Quantification of eugenol in liver microsomes was achieved by comparison of the peak area of eugenol obtained in the chromatograms to the calibration curve of eugenol (commercially available) obtained at the same wavelength.

Phase II metabolism

Glucuronidation of 1′-hydroxymethyleugenol to 1′-hydroxymethyleugenol glucuronide

Incubations with pooled mixed gender human liver microsomes were performed as described by Al-Subeihi *et al.* (2011). The incubation mixture had a final volume of 200 μL, containing (final concentrations) 10 mM UDPGA, and 1 mg/mL microsomal protein in 0.2 M

Tris-HCl (pH 7.4) containing 10 mM $MgCl_2$. The incubation mixture was pre-treated with 0.025 mg/mL of the poreforming peptide alamethicin from a 200 times concentrated stock in methanol on ice for 15 min to overcome enzyme latency and obtain maximal glucuronidation activity (Fisher *et al.*, 2000; Lin and Wong, 2002). The reactions were started by the addition of the substrate 1′-hydroxymethyleugenol from a 200 times concentrated stock solution in DMSO, after pre-incubation at 37 °C for 1 min. The reactions were carried out for 6 hr and terminated by addition of 50 µL cold acetonitrile. Blank incubations were performed without the cofactor UDPGA. Verification of the formation of 1′-hydroxymethyleugenol glucuronide was performed by treatment of incubations with β-glucuronidase and analysis of samples by LC-MS as described previously (Al-Subeihi *et al.*, 2011).

The kinetic constants for the formation of 1′-hydroxymethyleugenol glucuronide from 1′-hydroxymethyleugenol were determined using pooled mixed gender human liver microsomes. The incubation mixtures were as described above. Incubations with human liver microsomes were carried out for 6 hr at a substrate concentration that ranged from 50 to 2000 µM 1′-hydroxymethyleugenol. Under the conditions specified the formation of 1′-hydroxymethyleugenol glucuronide was linear with time and microsomal protein concentration. In the blank incubations performed without UDPGA no 1′-hydroxymethyleugenol glucuronide was formed.

HPLC analysis was used for quantification of 1′-hydroxymethyleugenol glucuronide as described previously (Al-Subeihi *et al.*, 2011). Because 1′-hydroxymethyleugenol glucuronide has the same UV spectrum as 1′-hydroxymethyleugenol (data not shown) it was assumed that it has the same molar extinction coefficient as 1′-hydroxymethyleugenol. Quantification of 1′-hydroxymethyleugenol glucuronide was therefore achieved by comparison of the peak area of 1′-hydroxymethyleugenol glucuronide in the chromatograms obtained at a wavelength of 280 nm to the calibration curve of 1′-hydroxymethyleugenol obtained at the same wavelength.

Oxidation of 1′-hydroxymethyleugenol to 1′-oxomethyleugenol

Formation of 1′-oxomethyleugenol was studied as described by Al-Subeihi *et al.* (2011). Incubations were performed with pooled mixed gender human liver microsomes or cytosol, using NAD^+, NADP, $NADPH^+$ or NADPH as cofactor and GSH to trap the reactive 1′-oxomethyleugenol. The kinetic constants for formation of the 1′-oxomethyleugenol adduct with glutathione, reflecting the formation of 1′-oxomethyleugenol, were determined with human liver microsomes or cytosol at substrate concentrations that ranged from 10 to 2000 μM or 50 to 2000 μM 1′-hydroxymethyleugenol, respectively. The incubation mixtures with microsomes had a final volume of 160 μL, containing (final concentrations) 3 mM NAD^+, 2 mM GSH, and 1 mg/mL microsomal protein in 0.2 M Tris-HCl (pH 7.4). The reactions were terminated after 10 min by addition of 40 μL cold acetonitrile. For cytosolic preparations, the incubation mixtures had a final volume of 200 μL, containing (final concentrations) 3 mM $NADP^+$, 2 mM GSH, and 1 mg/mL cytosolic protein in 0.2 M Tris-HCl (pH 7.4). The reactions were terminated after 10 min by addition of 50 μL cold acetonitrile. Under these conditions the formation of the glutathione adduct, 3′-(glutathione-S-yl)-1′-oxo-2′-3′-dihydromethyleugenol (GS-1′-oxomethyleugenol), was linear with time and either microsomal or cytosolic protein concentration.

The incubation mixtures with either microsomal or cytosolic preparations were centrifuged for 5 min at 16,000 g. HPLC analysis used for quantification of GS-1′-oxomethyleugenol formed in microsomes was performed as described previously (Al-Subeihi *et al.*, 2011). For the HPLC analysis of the incubations in which formation of 1′-oxomethyleugenol in cytosol was investigated a different HPLC method was used. For these samples 50 μL of the supernatants were analyzed on an Alltima C18 5-μm column, 150 mm × 4.6 mm (Grace Alltech, Breda, The Netherlands), coupled to a Waters 2695 Alliance HPLC system. The gradient was made with acetonitrile and ultrapure water containing 0.1% acetic acid. The flow rate was 1 mL/min and the gradient was applied from 0 to 10% acetonitrile over 10 min, after which the percentage of acetonitrile was increased to 25% over 10 min and then increased to 100% over 5 min and kept at 100% for 1 min. Detection was performed at 280 nm using a Waters 2996 photodiode array

detector. Quantification of GS-1′-oxomethyleugenol formed in incubations with either microsomes or cytosol was performed by means of a calibration curve obtained as described by Al-Subeihi *et al.* (2011) and Punt *et al.* (2009).

Sulfonation of 1′-hydroxymethyleugenol to 1′-sulfooxymethyleugenol

The formation of 1′-sulfooxymethyleugenol was characterized in incubations of 1′-hydroxymethyleugenol with human liver S9 in the presence of GSH as scavenger, as described previously by Al-Subeihi *et al.* (2011). The incubation mixture had a final volume of 100 µL containing the following materials (final concentration): 5 mM GSH, 2 mg/mL S9, and 0.2 mM PAPS in 0.1 M potassium phosphate (pH 8.2). The incubation was started by addition of the substrate 1′-hydroxymethyleugenol. The incubation mixture was incubated for 2 hr at 37 °C, after which 25 µL of cold acetonitrile was added. Under these conditions the formation of the glutathione adduct of carbo-cation derived from 1′-sulfooxymethyleugenol was linear with time and S9 protein concentration. The kinetic constants for the formation of 1′-sulfooxymethyleugenol from 1′-hydroxymethyleugenol were determined using human liver S9. The incubation mixtures were as described above. Incubations with human liver S9 were carried out for 2 hr at a substrate concentration that ranged from 50 to 1500 µM 1′-hydroxymethyleugenol. All incubations were started by addition of substrate from a 200 times concentrated stock solution in DMSO and terminated by addition of 25 µL cold acetonitrile. In the blank incubations performed without GSH formation of the GSH adduct of the carbo-cation of 1′-sulfooxymethyleugenol was not observed. Before HPLC analysis of the samples, all incubations were centrifuged for 5 min at 16,000 g. Aliquots of 50 µL of the supernatant of each sample were analyzed and quantified as previously described (Al-Subeihi *et al.*, 2011).

PBK model methyleugenol

The PBK model for methyleugenol was developed based on the PBK models previously defined for the detoxification and bioactivation of methyleugenol in rat (Al-Subeihi *et al.*, 2011), and for the related alkenylbenzene estragole in rat (Punt *et al.*, 2008) and in human (Punt

et al., 2009). Figure 2 presents a schematic overview of the PBK model. The final model is composed of separate compartments including liver which was the only organ found to be involved in the metabolism of methyleugenol (see Results section). Since the partition coefficient of methyleugenol in fat tissue was predicted to be relatively high (Table 1), a separate fat compartment was included in the developed model. All other tissues such as adrenal, brain, heart, kidney and lungs were lumped into a richly perfused tissue group, while tissues such as bone, muscle, and skin were lumped into a slowly perfused tissue group (Ramsey and Anderson, 1984). The uptake of methyleugenol from the gastrointestinal tract was modeled as a first-order process, assuming direct entry from the intestine to the liver compartment, and an absorption rate constant (k_a) value similar to that of estragole, which was 1.0 hr^{-1} (Punt *et al.*, 2008). Based on the results of phase I incubations (see Results section), it

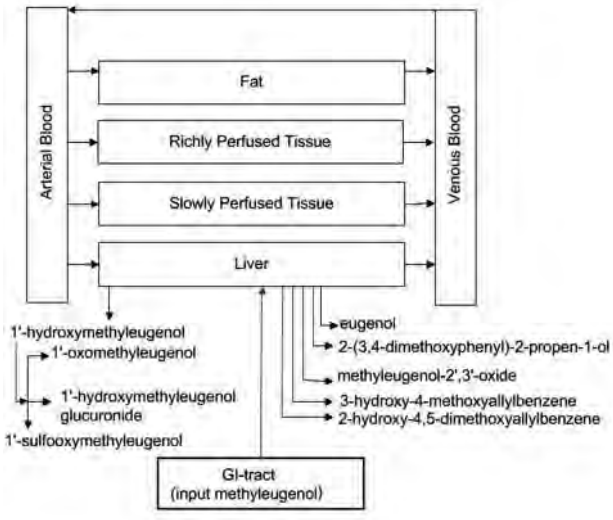

Figure 2. Representation of the conceptual model for a physiologically based kinetic model for methyleugenol in human.

Table 1. Parameters used in the physiologically based kinetic model for methyleugenol in human.

Physiological parameters[a]		**Tissue:blood partition coefficients**[b]	
body weight (kg)	63.8	methyleugenol	
percentage of body weight			
liver	2.6	liver	6.2
fat	21.4	fat	103
rapidly perfused	5	rapidly perfused	6.2
slowly perfused	51.7	slowly perfused	3.9
blood	7.9		
cardiac output (L/hr)	323	1'-hydroxymethyleugenol	
percentage of cardiac output		liver	1.4
liver	22.7		
fat	5.2		
rapidly perfused	47.3		
slowly perfused	24.8		

[a] Brown et al. (1997)
[b] DeJongh et al.(1997)

was found that metabolites of methyleugenol to be taken into account are methyleugenol-2′,3′-oxide, 1′-hydroxymethyleugenol, 3-(3,4-dimethoxyphenyl)-2-propen-1-ol, 2-hydroxy-4,5-dimethoxyallylbenzene, eugenol and 3-hydroxy-4-methoxyallylbenzene. Based on these results the mass balance equations for methyleugenol in the metabolizing tissues are described as follows:

Liver:

$$dAL_{ME}/dt = dUptake_{ME}/dt + QL*(CA_{ME} - CL_{ME}/PL_{ME}) - V_{max,L\_MEO}* CL_{ME}/PL_{ME} / (K_{m,L\_MEO} + CL_{ME}/PL_{ME}) - V_{max,L\_1'HME}* CL_{ME}/PL_{ME} / (K_{m,L\_1'HME}+CL_{ME}/PL_{ME}) - V_{max,L\_3DMPOH}* CL_{ME}/PL_{ME} / (K_{m,L\_3DMPOH}+ CL_{ME}/PL_{ME}) - V_{max,L\_2HDME}* CL_{ME}/PL_{ME} / (K_{m,L\_2HDME}+ CL_{ME}/PL_{ME}) - V_{max,L\_3HMA}* CL_{ME}/PL_{ME} / (K_{m,L\_3HMA}+ CL_{ME}/PL_{ME}) - V_{max,L\_1EU}* CL_{ME}/PL_{ME} / (K_{m,L\_1EU} + CL_{ME}/PL_{ME})$$

$dUptake_{ME}/dt = - dAGI_{ME}/dt = k_a * AGI_{ME}$,

AGI_{ME} (0) = Oral dose

$CL_{ME} = AL_{ME}/VL$

where $Uptake_{ME}$ is the amount of methyleugenol taken up from the gastrointestinal tract (µmol), AGI_{ME} (µmol) is the amount of methyleugenol remaining in the gastrointestinal tract, AL_{ME} is the amount of methyleugenol in the liver (µmol) and CL_{ME} is the methyleugenol concentration in the liver (µmol/L). CA_{ME} is the methyleugenol concentration in the arterial blood (µmol/L) which is considered to be equal to the methyleugenol concentration in the mixed venous blood compartment. QL is the blood flow rate to the liver (L/hr), QC is the cardiac output (L/hr), VL is the volume of the liver, PL_{ME} is the tissue/blood partition coefficient of methyleugenol in the liver, and V_{max,L_M} and K_{m,L_M} are the maximum rate of formation and the Michaelis-Menten constant for the formation of the different phase I metabolites in the liver: methyleugenol-2′,3′-oxide, 1′-hydroxymethyleugenol, 3-(3,4-dimethoxyphenyl)-2-propen-1-ol, 2-hydroxy-4,5-dimethoxyallylbenzene, eugenol, and 3-hydroxy-4-methoxyallylbenzene. In case of methyleugenol-2′,3′-oxide, 2-hydroxy-4,5-dimethoxyallylbenzene, 3-(3,4-dimethoxyphenyl)-2-propen-1-ol, eugenol and 3-hydroxy-4-methoxyallylbenzene, only formation of these metabolites is taken into account and no further reactions with these metabolites were modeled. Formation of 1′-hydroxymethyleugenol in the liver, but not in any other compartment, was followed up by phase II reactions, since 1′-hydroxylation of methyleugenol was found to occur only in the liver (see Results section). To describe the disposition of 1′-hydroxymethyleugenol and its phase II metabolites a near quantitative intrahepatic conversion of 1′-hydroxymethyleugenol by phase II enzymes was assumed. This assumption was based on the finding that the overall catalytic efficiency for the phase II reactions was higher than the catalytic efficiency for the formation of 1′-hydroxymethyleugenol. For this reason only intra-organ distribution of 1′-hydroxymethyleugenol was modeled and no distribution of this metabolite over the body was taken into account. This simplification of the model reduced the number of parameters

considerably, but might lead to an overestimation of the contributions of the phase II reactions (Filser *et al.*, 2001). The mass balance equation for 1′-hydroxymethyleugenol in the liver is as follows:

Liver:

$$dAL_1'_{HME/dt} = + V_{max,L\_1'HME} * CL_{ME}/PL_{ME}/(K_{m,L\_1'HME} + CL_{ME}/PL_{ME})$$
$$- V_{max,L\_1'OME\_mic} * CL_1'_{HME}/PL_1'_{HME}/(Km,L\_1'_{OME\_mic} + CL_1'_{HME}/PL_1'_{HME})$$
$$- V_{max,L\_1'OME\_cyt} * CL_1'_{HME}/PL_1'_{HME}/(Km,L\_1'_{OME\_cyt} + CL_1'_{HME}/PL_1'_{HME})$$
$$- V_{max,L\_1'HMEG} * CL_1'_{HME}/\ PL_1'_{HME}/(Km,L\_1'_{HMEG} + CL_1'_{HME}/PL_1'_{HME})$$
$$- V_{max,L\_1'HMES} * CL_1'_{HME}/\ PL_1'_{HME}/(K_{m,L\_1'HMES} + CL_1'_{HME}/PL_1'_{HME})$$

$$CL_1'_{HME} = AL_1'_{HME} / VL$$

where $AL_1'_{HME}$ is the amount of 1′-hydroxymethyleugenol in the liver (µmol), $CL_1'_{HME}$ is the 1′-hydroxymethyleugenol concentration in the liver (µmol/L), $PL_1'_{HME}$ is the liver/blood partition coefficient of 1′HME, and V_{max,L_M} and K_{m,L_M} are the maximum rate of formation and the Michaelis-Menten constant for the formation of phase II metabolites: 1′-oxomethyleugenol formed by microsomal enzymes (1′OME_mic), 1′-oxomethyleugenol formed by cytosolic enzymes (1′OME_cyt), 1′-hydroxymethyleugenol glucuronide, and 1′-sulfooxymethyleugenol in the liver. The kinetic constants for the formation of phase I metabolites from methyleugenol and the metabolites formed from 1′-hydroxymethyleugenol were determined *in vitro* in the present study. The V_{max} values for the different phase I and phase II metabolic reactions, in the liver, expressed as nmol/min/(mg microsomal protein), were scaled to the liver using a microsomal protein yield of 32 mg/(g liver) (Barter *et al.*, 2007). The V_{max} values for cytosolic oxidation of 1′-hydroxymethyleugenol expressed as nmol/min/(mg cytosolic protein) was scaled to the liver using a cytosolic protein yield of 80.7 mg/(g liver) (Cubitt *et al.*, 2011). The V_{max} values for sulfonation of 1′-hydroxymethyleugenol, expressed as nmol/min/(mg S9

protein) was scaled to the liver using an S9 protein yield of 143 mg/(g liver) as previously inferred by Punt *et al.* (2008, 2009). This scaling factor was verified by determining the difference in various cytochrome P450 marker substrate activities between pooled human liver S9 and pooled human liver microsomes as specified by the supplier. On average these P450 marker substrate activities where 4.7±2.5-fold lower in pooled human liver S9 compared with pooled human liver microsomes. This indicates that the scaling factor from liver S9 to the liver needs to be on average 4.7 times higher than the scaling factor from human liver microsomes to the liver. This is in line with the 4.5-fold higher scaling factor for human liver S9 used in the present study. On the whole, the different scaling factors were in line with what we have used in our previous study for the human model for bioactivation and detoxification of the related alkenylbenzene estragole (Punt *et al.*, 2009), thus facilitating comparison.

The physiological parameters used in the methyleugenol model were obtained from Brown *et al.* (1997). Partition coefficients were estimated from the log K_{ow} based on a method of DeJongh *et al.* (1997) (Table 1). Log K_{ow} values were estimated with KOWWIN™ version 1.67 using the EPISuite™ software package version 4.0 and amounted to 3.03 for methyleugenol and 1.49 for 1′-hydroxymethyleugenol. Model equations were coded and numerically integrated in Berkeley Madonna 8.0.1 (Macey and Oster, UC Berkeley, CA, USA), using the Rosenbrock's algorithm for stiff systems.

Sensitivity analysis

To identify the key parameters to which the model output is most sensitive, a sensitivity analysis was performed at a methyleugenol dose of 0.0034 mg/(kg bw). In this sensitivity analysis all model parameters were tested including physiological parameters, tissue blood partitions coefficients, and kinetics parameters for formation of the different metabolites. Normalized sensitivity coefficients (SC) were determined according to the following equation: SC = (C' − C)/(P' − P) *(P/C), where C is the initial value of model output, C' is the modified value of the model output resulting from an increase in parameter value, P is the initial parameter value, and P' is the modified parameter value (Rietjens *et al.*, 2011). Based on the

literature a 5% increase in parameter values was chosen, to analyze the effect of a change in parameter on the formation of 1′-hydroxymethyleugenol and 1′-sulfooxymethyleugenol expressed as % of the dose over a 24 hr period of time (Evans and Andersen, 2000). Each parameter was analyzed individually, keeping the other parameters to their initial values.

Results

Formation of Phase I metabolites

The results obtained from HPLC analysis of incubations of methyleugenol with mixed gender human liver, lung, kidney, and intestine microsomes in the presence of NADPH as cofactor reveal that only the liver microsomes were capable of metabolizing methyleugenol to different types of metabolites at varying rates. The HPLC chromatogram of incubations of methyleugenol with liver microsomes (Figure 3) reveals formation of six metabolites of methyleugenol which were identified as 3-(3,4-dimethoxyphenyl)propane-1,2-diol (RT = 15.9 min), 1′-hydroxymethyleugenol (RT = 32.1 min), 3-(3,4-dimethoxyphenyl)-2-propen-1-ol (RT = 34.2 min), 2-hydroxy-4,5-dimethoxyallylbenzene (RT = 35.1 min), eugenol (RT = 52.1 min), and 3-hydroxy-4-methoxyallylbenzene (RT = 52.7 min). 3-(3,4-dimethoxyphenyl)propane-1,2-diol, 1′-hydroxymethyleugenol and 3-(3,4-dimethoxyphenyl)-2-propen-1-ol were identified based on the similarities of their retention times and UV spectra to those of chemically synthesized reference compounds. Eugenol was identified based on the similarities of its retention time and UV spectra to that of commercially obtained eugenol. Further identification of 1′-hydroxymethyleugenol, 3-(3,4-dimethoxyphenyl)-2-propen-1-ol, and methyleugenol-2′,3′-oxide was previously performed by GC-MS as described by Al-Subeihi *et al.* (2011). No reference compound was available for 2-hydroxy-4,5-dimethoxyallylbenzene but this metabolite was identified as previously described by Al-Subeihi *et al.* (2011).

Incubating methyleugenol-2′,3′-oxide with liver microsomes in the absence of any cofactor revealed that methyleugenol-2′,3′-oxide is completely hydrolyzed to 3-(3,4-dimethoxyphenyl)-

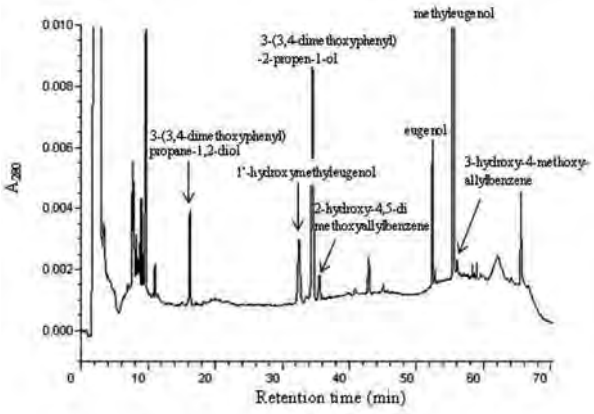

Figure 3. HPLC chromatogram of an incubation of methyleugenol (1 mM) with human liver microsomes (1 mg/ml) in the presence of NADPH (3 mM) as cofactor, and vitamin C (1 mM) as antioxidant.

propane-1,2-diol (Al-Subeihi *et al.*, 2011), which is formed upon hydrolysis of methyleugenol-2′,3′-oxide by epoxide hydrolases present in the microsomal preparation (Guenthner and Luo, 2001; Luo *et al.*, 1992; Luo and Guenthner, 1995).

3-hydroxy-4-methoxyallylbenzene was identified as previously described by Al-Subeihi *et al.*, (2011).

Kinetics of formation of Phase I Metabolites

Human liver microsomes were incubated with increasing methyleugenol concentrations to determine the kinetic parameters for the formation of the various phase I metabolites of methyleugenol. Figure 4 (A-F) shows the rate of formation of 1′-hydroxymethyleugenol, methyleugenol-2′,3′-oxide measured as 3-(3,4-dimethoxyphenyl)propane-1,2-diol**,** 3-hydroxy-4-methoxyallylbenzene, 2-hydroxy-4,5-dimethoxyallylbenzene, 3-(3,4-dimethoxyphenyl)-2-propen-1-ol, and eugenol, respectively. Table 2 summarizes the apparent K_m and V_{max} values

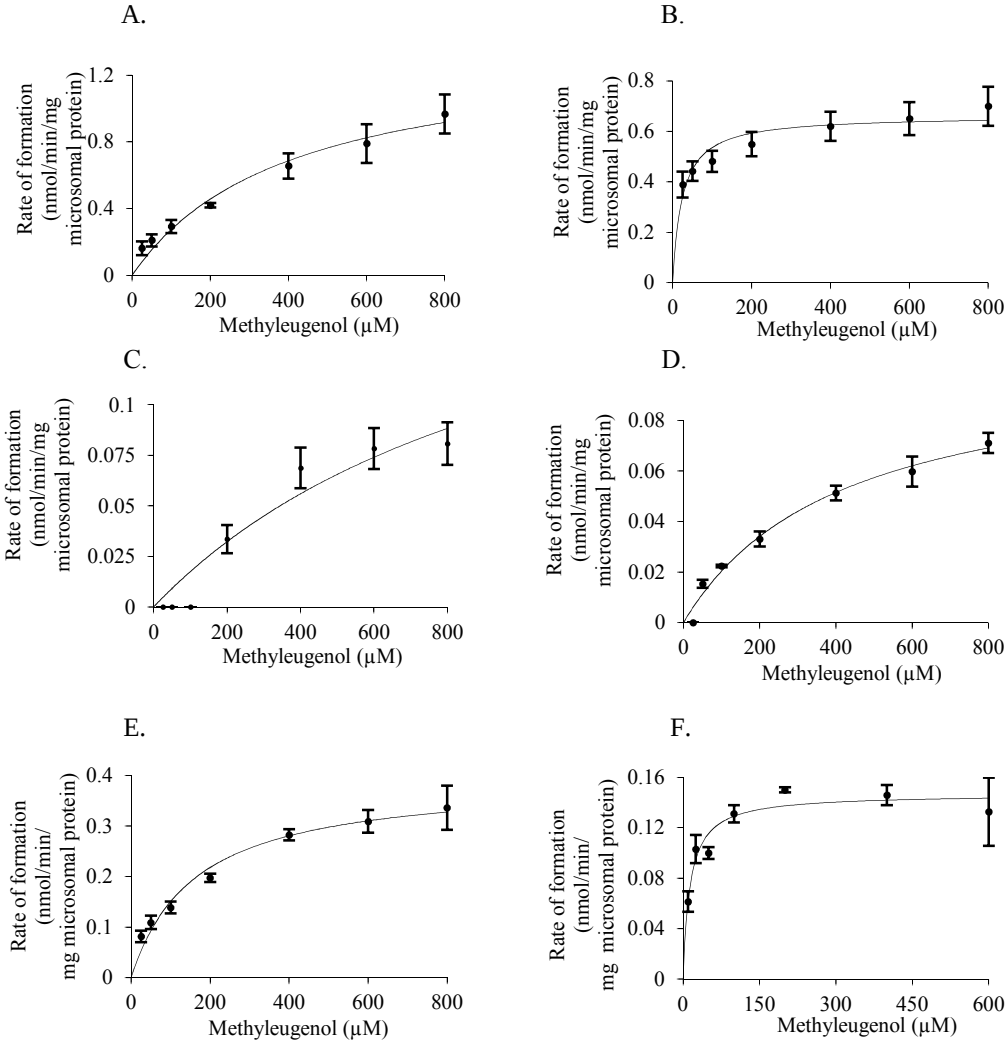

Figure 4. Formation rate of phase I metabolites in incubations with human liver microsomes at increasing concentrations (25 – 800 µM) of methyleugenol indicating formation of A. 1′-hydroxymethyleugenol, B. methyleugenol-2′,3′-oxide, C. 3-hydroxy-4-methoxyallylbenzene, D. 2-hydroxy-4,5-dimethoxyallylbenzene, E. 3-(3,4-dimethoxyphenyl)-2-propen-1-ol, and F. at increasing concentrations (25 – 600 µM) of methyleugenol indicating formation of eugenol.

Table 2. Kinetic parameters for phase I metabolism of methyleugenol in incubations with human liver microsomes.

metabolite	K_m(app)[a,b]	V_{max}(app)[a,c]	*in vitro* catalytic efficiency[d] (V_{max}(app)/K_m(app)	Scaled V_{max}(app), *in vivo*[e]	*in vivo* catalytic efficiency[f] (scaled V_{max}(app), *in vivo*/$K_{m(app)}$)
methyleugenol-2′,3′-oxide	23.7 ± 5	0.66 ± 0.11	27.8	1.27	54
1′-hydroxymethyleugenol	404 ± 195	1.38 ± 0.38	3.4	2.65	6.6
3-(3,4-dimethoxyphenyl)-2-propen-1-ol	161 ± 90	0.39 ± 0.08	2.4	0.75	4.7
2-hydroxy-4,5-dimethoxyallylbenzene	415 ± 84	0.10 ± 0.02	0.24	0.19	0.46
eugenol	13.6 ± 12.3	0.15 ± 0.02	11.0	0.29	21.3
3-hydroxy-4-methoxyallylbenzene	1097 ± 142	0.21 ± 0.02	0.2	0.40	0.36

[a] mean ± SD
[b] μM
[c] nmol/min/(mg microsomal protein)
[d] (μL/min/(mg microsomal protein)
[e] μmol/(hr(g liver)), calculated from the *in vitro* $V_{max(app)}$ based on a microsomal protein yield of 32 mg/(g liver)
[f] L/(hr(g liver))

obtained from these plots. The results reveal that 1′-hydroxymethyleugenol is the most abundant metabolite formed, followed by methyleugenol-2′,3′-oxide measured as 3-(3,4-dimethoxyphenyl)propane-1,2-diol, 3-(3,4-dimethoxyphenyl)-2-propen-1-ol, 3-hydroxy-4-methoxyallylbenzene and eugenol. Formation of 2-hydroxy-4,5-dimethoxyallylbenzene was shown to be the least important metabolic route in these incubations. The apparent V_{max} for 2-hydroxy-4,5-dimethoxyallylbenzene was about 14 times lower than the apparent V_{max} for formation of 1′-hydroxymethyleugenol, whereas the apparent K_m was equal. Overall, the catalytic efficiency for the formation of the 2-hydroxy-4,5-dimethoxyallylbenzene by human liver microsomes, calculated as the apparent V_{max}/K_m, was about 14 times lower than the catalytic efficiency for the formation of 1′-hydroxymethyleugenol.

Formation of 1′-hydroxymethyleugenol metabolites

1′-Hydroxymethyleugenol glucuronide

HPLC analysis of an incubation of 1′-hydroxymethyleugenol with human liver microsomes in the presence of UDPGA as a cofactor, revealed formation of one metabolite with RT of 19.3

min (chromatogram not shown). Treatment of the sample with β-glucuronidase, resulted in complete disappearance of the peak at 19.3 min accompanied by a comparable increase of the peak representing 1′-hydroxymethyleugenol. This confirms that the metabolite corresponds to the glucuronosyl conjugate of 1′-hydroxymethyleugenol. Furthermore the spectrum of the metabolite, obtained by LC-MS, reveals a deprotonated molecule at *m/z 369*, which corresponds to the theoretically expected mass and confirms that the metabolite corresponds to 1′-hydroxymethyleugenol glucuronide (Al-Subeihi *et al.*, 2011).

1′-Oxomethyleugenol

HPLC analysis of an incubation of 1′-hydroxymethyleugenol with human liver microsomes using NAD^+ as a cofactor and GSH as a trapping agent for the reactive 1′-oxomethyleugenol, revealed the formation of a metabolite with RT of 11.4 min (chromatogram not shown). HPLC analysis of control incubations of 1′-hydroxymethyleugenol in the absence of NAD^+ revealed no appearance of the peak at RT of 11.4 min (chromatogram not shown). This argument was used as a confirmation for the formation of the GSH adduct of 1′-oxomethyleugenol and thus of 1′-oxomethyleugenol in the incubation with NAD^+. Previously the nature of this metabolite was confirmed by LC-MS revealing a deprotonated molecule at *m/z* 500 (Al-Subeihi *et al.*, 2011). Incubations with human liver microsomes in the presence of other cofactors, including NADH, $NADP^+$, or NADPH and GSH also revealed some formation of the glutathione adduct with 1′-oxomethyleugenol, but at a much smaller extent than the incubations with NAD^+. These reactions were therefore not considered to significantly contribute to the overall reaction rate (chromatograms not shown).

HPLC analysis of the incubations of 1′-hydroxymethyleugenol with human liver cytosol using $NADP^+$ as cofactor and GSH as a trapping agent for the reactive 1′-oxomethyleugenol also revealed formation of the glutathione conjugate of 1′-oxomethyleugenol. Using a different HPLC method than for the analysis of the incubations with human liver microsomes for the same reaction the RT of this metabolite was observed to be 18.2 min (chromatogram not shown). HPLC analysis of control incubations of 1′-hydroxymethyleugenol in the absence of

$NADP^+$ revealed no peak at this retention time (chromatogram not shown). Incubations with human liver cytosol in the presence of other cofactors, including NAD^+ or NADH and GSH also revealed formation of the glutathione adduct with 1′-oxomethyleugenol, but to a much smaller extent than the incubations with $NADP^+$. These reactions were therefore not considered to significantly contribute to the overall reaction rate. The same incubations with NADPH as cofactor, revealed no formation of the glutathione adduct with 1′-oxomethyleugenol (chromatograms not shown).

1′-Sulfooxymethyleugenol

HPLC analysis of an incubation of 1′-hydroxymethyleugenol with human liver S9 using PAPS as a cofactor and GSH as a scavenger for the reactive carbo-cation derived from the unstable 1′-sulfooxymethyleugenol metabolite, revealed formation of a metabolite with RT of 12.9 min (chromatogram not shown). HPLC analysis of incubations of 1′-hydroxymethyleugenol in the absence of GSH and in the presence of PAPS and liver S9 protein revealed no appearance of the peak at 12.9 min (chromatogram not shown). This argument was used as a confirmation for the formation of the GSH adduct of the carbo-cation of 1′-sulfooxymethyleugenol, and thus an indirect detection of formation of 1′-sulfooxymethyleugenol in the complete incubation. Furthermore the spectrum of the metabolite, obtained by LC-MS, reveals a protonated molecule at *m/z 484*, which corresponds to the theoretically expected mass and confirms that the metabolite corresponds to the GSH adduct of the carbo-cation formed from 1′-sulfooxymethyleugenol (Al-Subeihi *et al.*, 2011).

Kinetics of phase II metabolite formation

Figure 5A presents the formation of 1′-hydroxymethyleugenol glucuronide in incubations with microsomal preparations from human liver and UDPGA at increasing 1′-hydroxymethyleugenol concentrations. Figure 5B and Figure 5C present the formation of 1′-oxomethyleugenol in incubations with microsomal or cytosolic preparations from human liver and either NAD^+ or $NADP^+$ plus GSH at increasing 1′-hydroxymethyleugenol concentrations.

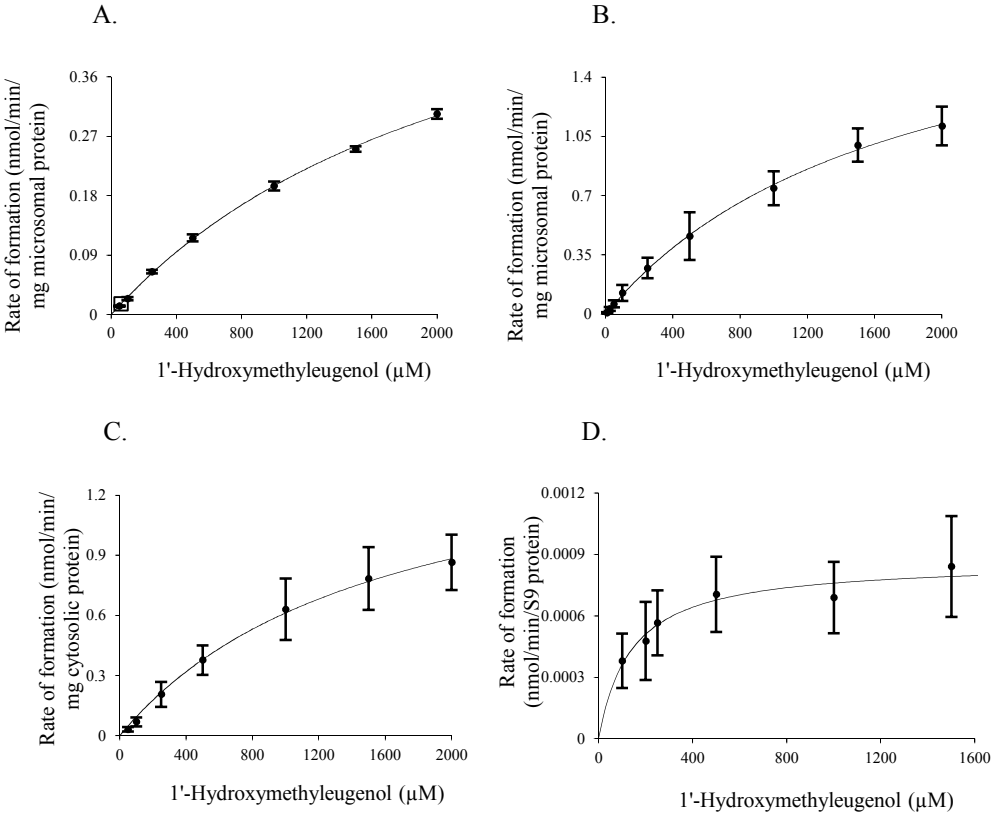

Figure 5. Formation rate of 1′-hydroxymethyleugenol metabolites including A. 1′-hydroxymethyleugenol glucuronide (1′HMEG) in incubations with human liver microsomes at increasing concentration of 1′-hydroxymethyleugenol (50 – 2000 μM), B. 1′-oxomethyleugenol (1′OME) in incubations with human liver microsomes at increasing concentration of 1′-hydroxymethyleugenol (50 – 2000 μM), C. 1′-oxomethyleugenol (1′OME) in incubations with human liver cytosol at increasing concentration of 1′-hydroxymethyleugenol (50 – 2000 μM), and D. 1′-sulfooxymethyleugenol (1′HMES) in incubations with human liver S9 at increasing concentration of 1′-hydroxymethyleugenol (50 – 1500 μM).

In addition, Figure 5D presents the formation of the GSH conjugate of the carbo-cation of 1′-sulfooxymethyleugenol in incubations with a human liver S9 preparation, PAPS, GSH and increasing 1′-hydroxymethyleugenol concentrations. The kinetic parameters (V_{max} and K_m), obtained by fitting the data to the standard Michaelis-Menten equation, are presented in Table3.

Table 3. Kinetic parameters for the metabolites of 1'-hydroxymethyleugenol in incubations with human liver preparations.

metabolite	k_m**(app)**[a,b]	V_{max}**(app)**[a]	***in vitro*** **catalytic efficiency** (V_{max}**(app)**/K_m**(app)**	**Scaled** V_{max}**,** ***in vivo***[h]	***in vivo*** **catalytic efficiency** [i] **(scaled** V_{max}**,** ***in vivo***/$K_{m(app)}$**)**
1'-hydroxymethyleugenol glucuronide	2393 ± 486	0.66 ± 0.087[c]	0.28 [e]	1.27	0.53
1'-oxomethyleugenol in liver microsomes	1744 ± 2997	2.1 ± 1.83[c]	1.2 [e]	4.03	2.31
1'-oxomethyleugenol in liver cytosol	1580 ± 538	1.58 ± 0.206[c]	1[f]	7.65	4.84
1'-sulfooxymethyleugenol	139 ± 82	0.0009 ± 0.0002[d]	0.0065[g]	0.0077	0.056

[a] mean ± SD
[b] μM
[c] nmol/min/(mg microsomal protein)
[d] nmol/min/(mg S9 protein)
[e] (μL/min/(mg microsomal protein)
[f] (μL /min/(mg cytosolic protein)
[g] (μL/min/(mg S9 protein)
[h] μmol/(hr(g liver)), calculated from the in vitro $V_{max(app)}$ based on a microsomal protein yield of 32 mg/(g liver), cytosolic protein yield of 80.7 mg/(g liver) and a S9 protein yield of 143 mg/(g liver)
[i] L/(hr (g liver))

Comparing the scaled kinetic constants for glucuronidation to sulfonation and oxidation reveals that the scaled $V_{max(app)}$ for 1′-sulfooxymethyleugenol formation was about 165 times lower than the scaled $V_{max(app)}$ for formation of 1′-hydroxymethyleugenol glucuronide. Overall, the scaled catalytic efficiency for the formation of the 1′-sulfooxymethyleugenol by human liver proteins, calculated as the scaled $V_{max(app)}/K_{m(app)}$, was about 9.5 times lower than the catalytic efficiency for the formation of 1′-hydroxymethyleugenol glucuronide by human liver proteins. The scaled $V_{max(app)}$ for 1′-oxomethyleugenol by human liver cytosolic proteins was about 6 times higher than the scaled $V_{max(app)}$ for formation of 1′-hydroxymethyleugenol glucuronide by human liver proteins, whereas the $K_{m(app)}$ was about 1.5 times lower. The catalytic efficiency for the formation of the 1′-oxomethyleugenol by human liver cytosolic proteins (scaled $V_{max(app)}/K_{m(app)}$)

was about 9 times higher than the catalytic efficiency for the formation of 1′-hydroxymethyleugenol glucuronide (scaled $V_{max(app)}/K_{m(app)}$) by human liver proteins. Thus, based on these kinetic data it can be concluded that in human liver oxidation may be the preferential pathway for conversion of 1′-hydroxymethyleugenol, followed by conjugation to1′-hydroxymethyleugenol glucuronide and to a much lower extent by sulfonation to 1′-sulfooxymethyleugenol.

Performance of the PBK model

With the kinetic constants obtained, all parameters of the PBK model were defined (Table 2 and Table 3) and the model as described in the Materials and Methods section was used for model predictions. In a first step, predictions were made that allow investigating the performance of the PBK model obtained. To this end, the PBK model-based predictions for concentrations of reported serum blood levels of methyleugenol reported for nine human volunteers after consumption of a meal consisting of 12 gingersnaps, containing approximately 0.216 mg methyleugenol (0.0034 mg/(kg bw)), considering an average body weight of 63.8 kg)

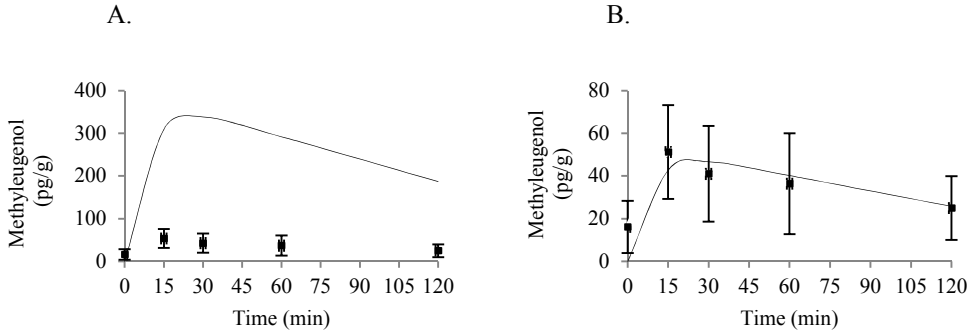

Figure 6. PBK predicted $\log_{10}$ concentrations of methyleugenol (expressed in ppt (pg/ml))in whole blood of human (—) compared with the reported $\log_{10}$ concentrations (ppt) in serum blood of human (.), at an oral dose of 0.0034 mg/(kg bw) (Schecter *et al.*, 2004), assuming A. 100% and B. 15% bioavailability.

(Schecter *et al.*, 2004). Figure 6 A presents the results obtained and reveals that the PBK model predicted blood concentrations of methyleugenol are higher than the actually measured ones. In these original calculations by the PBK model 100% bioavailability of methyleugenol was assumed. However, in the human intervention study bioavailability may have been significantly lower, because volunteers were given methyleugenol in the form of gingersnaps containing methyleugenol together with an orange juice beverage. Additional PBK modeling revealed that when the bioavailability of methyleugenol from the gingersnaps and orange juice food matrix would be 13.8%, the experimental value would match the PBK predicted values (Figure 6B).

Model predictions

The PBK model developed was used to predict the liver concentrations of methyleugenol and 1′-hydroxymethyleugenol and conversion of 1′-hydroxymethyleugenol to 1′-hydroxymethyleugenol glucuronide, 1′-oxomethyleugenol, and 1′-sulfooxymethyleugenol in the liver of human. Figure 7 presents the time dependent predicted concentration (nmol/(g liver)) of methyleugenol and 1′-hydroxymethyleugenol, and the time dependent predicted formation (nmol/(g liver)) of 1′-hydroxymethyleugenol glucuronide, 1′-oxomethyleugenol, and 1′-sulfooxymethyleugenol at a dose of 0.0034 mg/(kg bw). This dose of 0.0034 mg/(kg bw) represents the dose of methyleugenol used in the study of Schecter *et al.* (2004). Since the model does not contain further reactions for the phase II metabolites of 1′-hydroxymethyleugenol, the PBK model estimates the total formed amounts of 1′-hydroxymethyleugenol metabolites in liver over time but not the actual time dependent concentrations present in the liver. The model outcomes predict that 24 hr after dosing, methyleugenol and 1′-hydroxymethyleugenol are completely metabolized and indicate a total overall formation of 0.0035 nmol/(g liver) of 1′-hydroxymethyleugenol glucuronide, 0.015 nmol/(g liver) of 1′-oxomethyleugenol, and 0.00037 nmol/(g liver) of 1′-sulfooxymethyleugenol, corresponding to 0.48%, 6.5%, and 0.05% of the dose respectively.

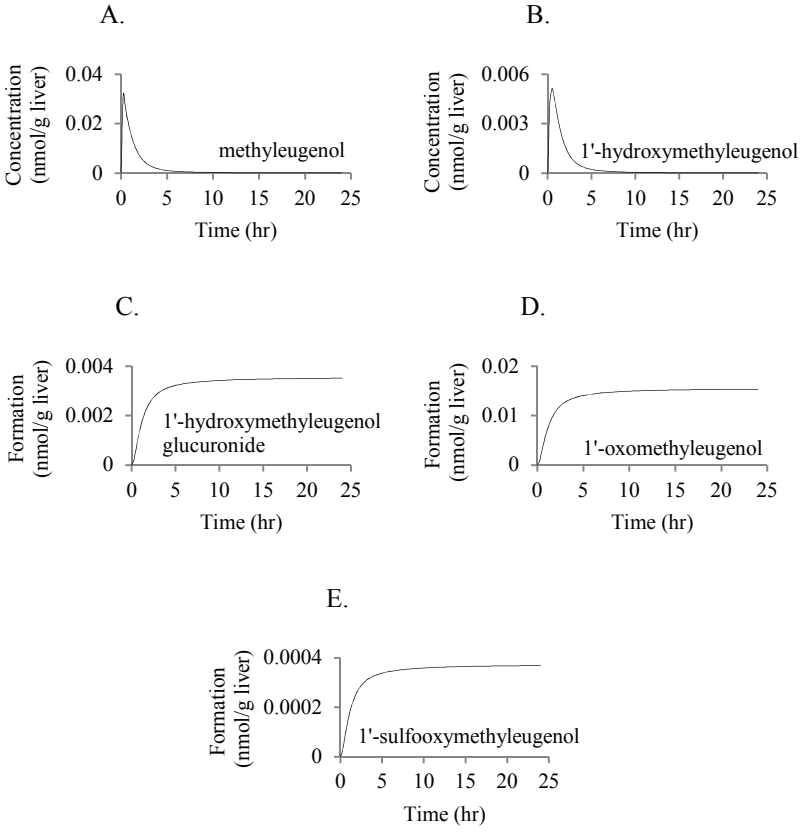

Figure 7. PBK model-predicted time dependent concentration (nmol/(g liver)) of (A) methyleugenol, (B) 1′-hydroxymethyleugenol, and formation of (C) 1′-hydroxymethyleugenol glucuronide, (D) 1′-oxomethyleugenol, and (E) 1′-sulfooxymethyleugenol following an oral dose of 0.0034 mg/(kg bw).

Sensitivity analysis

A sensitivity analysis was performed to determine the model parameters which affect the formation of 1′-hydroxymethyleugenol and 1′-sulfooxymethyleugenol in the liver as model outputs. Figure 8 presents the parameters which have an effect on the formation of 1′-hydroxymethyleugenol and the formation of 1′-sulfooxymethyleugenol at methyleugenol dose

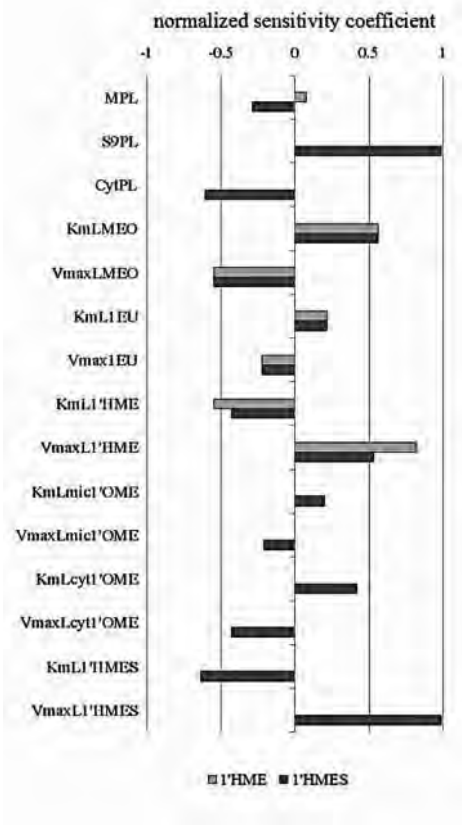

Figure 8. Sensitivity of the predicted formation of 1′-hydroxymethyleugenol and 1′-sulfooxymethyleugenol to different model parameters at a dose 0.0034 mg/(kg bw). Black bars correspond to the normalized sensitivity coefficients for formation of 1′-hydroxymethyleugenol and grey bars correspond to the normalized sensitivity coefficients for formation of 1′-sulfooxymethyleugenol. MPL = Liver microsomal protein yield, S9PL = Liver S9 protein yield, CytPL = Liver cytosolic protein yield, V_{max} and K_m are the maximum rate of formation and the Michaelis-Menten constant for the formation of the different metabolites (M) in liver: methyleugenol-2′,3′-oxide (MEO), 1′-hydroxymethyleugenol (1′HME), 3-(3,4-dimethoxyphenyl)-2-propen-1-ol (3DMPOH), 2-hydroxy-4,5-dimethoxyallylbenzene (2HDME), eugenol (1EU), 3-hydroxy-4-methoxyallylbenzene (3HMA), 1′-hydroxymethyleugenol glucuronide (1′HMEG), 1′-oxomethyleugenol formed by microsomal enzyme (1′OMEmic), 1′-oxomethyleugenol formed by cytosolic enzyme (1′OMEcyt) and 1′-sulfooxymethyleugenol (1′HMES) in liver tissue.

of 0.0034 mg/(kg bw). Formation of 1′-hydroxymethyleugenol primarily depends on the kinetic constant for its formation ($V_{max,L\_1'HME,}$ $K_{m,L\_1'HME}$) and the kinetic constants for formation of methyleugenol-2′,3′-oxide (V_{max,L_MEO}, K_{m,L_MEO}). To a small extent, the formation of 1′-hydroxymethyleugenol depends on the kinetic constants for formation of eugenol (V_{max,L_1EU}, K_{m,L_1EU}). On the other hand, the formation of 1′-sulfooxymethyleugenol primarily depends on the kinetic constants for formation of 1′-hydroxymethyleugenol ($V_{max,L\_1'HME}$, $K_{m,L\_1'HME}$), the kinetic constants (V_{max,L_MEO}, K_{m,L_MEO}) for the formation of methyleugenol-2′,3′-oxide, and the kinetic constants for the formation of 1′-oxomethyleugenol ($V_{max,L\_1'OME}$, $K_{m,L\_1'OME}$) from the microsomal metabolism and the cytosolic metabolism as well. The formation of 1′-sulfooxymethyleugenol also depends on the kinetic constants for formation of this metabolite itself ($V_{max,L\_1'HMES}$, $K_{m,L\_1'HMES}$) and on the kinetic constants for the formation of eugenol (V_{max,L_1EU}, K_{m,L_1EU}). Moreover the formation of 1′-sulfooxymethyleugenol also depends on the liver microsomal protein yield (MPL), the liver cytosolic protein (CytPL), and the liver S9 protein yield (S9PL).

Impact of species differences on the bioactivation and detoxification of methyleugenol

Species differences have been shown to affect the metabolism of estragole into some metabolites (Punt *et al.*, 2009). Also, the outcomes of the rat PBK model (Al-Subeihi *et al.*, 2011) and the outcomes of human PBK model, developed in the present study, reveal some species differences in phase I and phase II metabolism. Figure 9 shows an overview of the PBK-based predictions for the dose-dependent formation of methyleugenol-2′,3′-oxide, eugenol (only in the liver of human), 1′-hydroxymethyleugenol, the proximate carcinogenic metabolite, 1′-hydroxymethyleugenol glucuronide, 1′-oxomethyleugenol, and 1′-sulfooxymetheugenol which readily undergoes desulfonation to a reactive carbo-cation that can form DNA adduct in the liver of rat and human at dose levels up to 300 mg(kg bw). The results obtained clearly reflect significant species-dependent differences in the relative importance of *O*-demethylation, being an important metabolic pathway only in human (Figure 9B), while the detoxification of 1′-hydroxymethyleugenol to 1′-hydroxymethyleugenol glucuronide is an important pathway

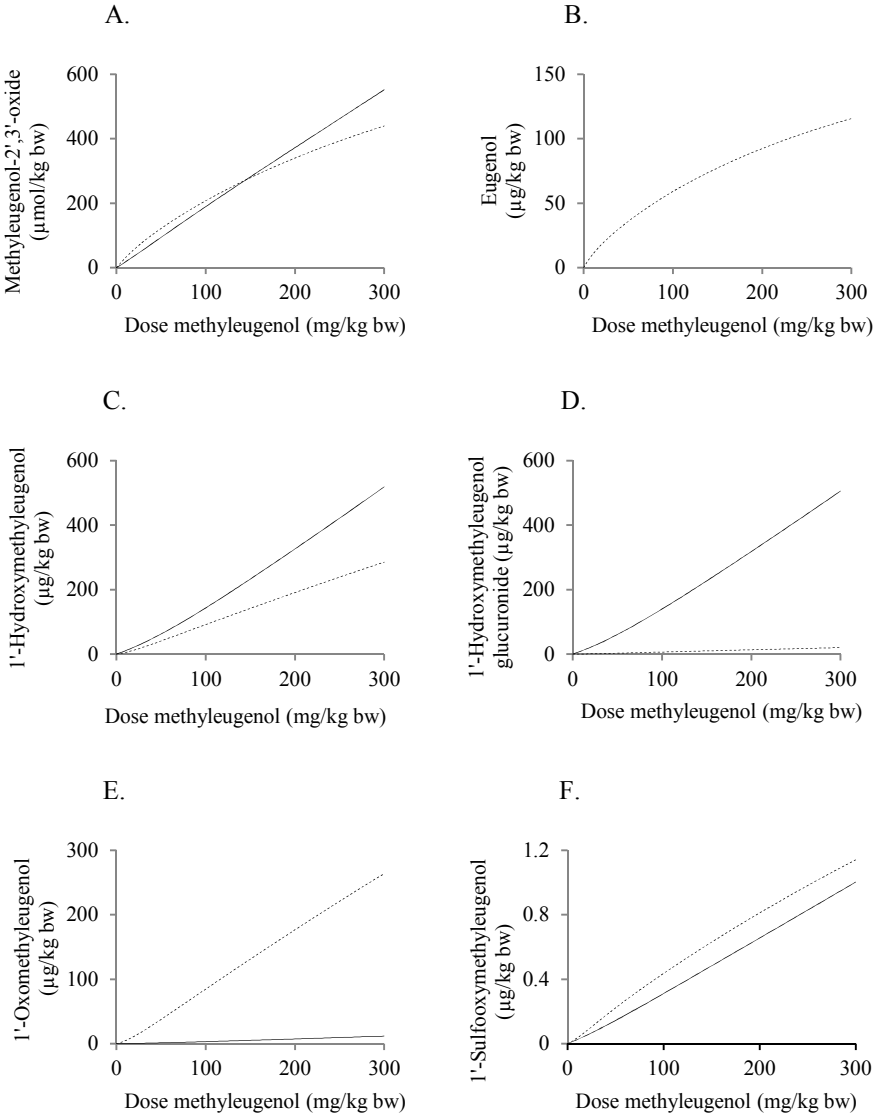

Figure 9. PBK model-based predictions for the dose-dependent formation of (A) methyleugenol-2',3'-oxide, (B) eugenol, (C) 1'-hydroxymethyleugenol, (D) 1'-hydroxymethyleugenol glucuronide, (E) 1'-oxomethyleugenol, and (F) 1'-sulfooxymethyleugenol of rat (solid line) and human (dotted line) at dose levels up to 300 mg/(kg bw).

in male rat (Figure 9D) and its detoxification to 1′-oxomethyleugenol is an important pathway in human (Figure 9E). These results also indicate that lower levels of urinary excretion of 1′-hydroxymethyleugenol glucuronide in human than in male rat do not necessarily reflect lower levels of formation of the proximate carcinogenic metabolite 1′-hydroxymethyleugenol and 1′-sulfooxymethyleugenol which readily undergoes desulfonation to a reactive carbo-cation that can form DNA adduct. The PBK results obtained indicate that in spite of marked species differences in glucuronidation and oxidation of 1′-hydroxymethyleugenol, the resulting species differences in formation of 1′-sulfooxymethyleugenol in human and male rat seems to be negligible at a dose of 0.0034 mg/(kg bw) and 300 mg/(kg bw) respectively. Formation of 1′-oxomethyleugenol has not been considered to be an important metabolic route of 1′-hydroxymethyleugenol before because in rat relatively small amounts of this metabolite are formed (Al-Subeihi *et al.*, 2011). Based on the approach of identifying principal metabolic pathways of methyleugenol in incubations with tissue fractions of relevant organs, it could be revealed that in human oxidation of 1′-hydroxymethyleugenol is a substantial metabolic pathway, and it was predicted by the PBK model to account for 6.6% to 15.9% at the dose of 0.0034 to 300 mg/(kg bw).

Implications of the PBK data for risk assessment

Figure 10 shows the PBK predicted dose dependent formation of 1′-sulfooxymethyleugenol in the liver of human and male rat as a function of dose, also presenting the value of the BMD_{10} and the so-called virtual safe dose (VSD). The BMD_{10} is the dose at which 10% extra tumor incidence above background level is observed in rodent bioassays. This value was previously calculated to amount to 27-47 mg/(kg bw)/day when using data for the induction of hepatomas in male rats (Rietjens *et al.*, 2008) or to 12 to 27 mg/(kg bw)/day when using data for induction of liver adenomas or carcinomas (combined) for male rats (Smith *et al.*, 2010). The latter study also reported a model average value of 22 mg/(kg bw)/day. From the lowest BMD_{10} value for the induction of the malignant hepatomas the value for the so-called virtual safe dose (VSD), the dose that would result in an estimated additional cancer risk of one in a million upon life

time exposure, can be calculated using linear extrapolation. The VSD thus obtained amounts to 0.27 µg/(kg bw)/day. The results thus obtained and depicted in Figure 10 indicate that the PBK predicted formation of 1′-sulfooxymethyleugenol which readily undergoes desulfonation to a reactive carbo-cation that can form DNA adduct, in the liver of both male rat and human appears to be linear from a dose as high as the BMD_{10} down to a dose as low as the VSD when plotted on a log-log scale as done in Figure 10 as well as on a linear scale (Figure not shown). Since the BMD_{10} appears to be within the linear part of the curve and since the rat and human curves do not differ substantially as the absolute difference between the rat and human curve is 0.49 to 1.06 fold over the whole dose, the PBK results of the present study support that possible nonlinear kinetics and species differences in kinetics should not be used as arguments against using a linear low dose cancer risk extrapolation from high dose animal data to the low dose human situation.

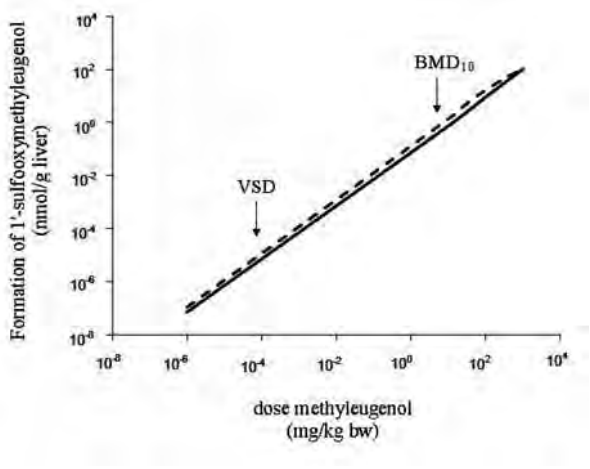

Figure 10. PBK model predicted dose-dependent formation of 1'-sulfooxymethyleugenol in the liver of rat (solid line) and human (dotted line).
Model predictions were made assuming 100% bioavailability of methyleugenol.

Discussion

The objective of the present study was to define a PBK model for methyleugenol in human, based on *in vitro* metabolic parameters. With this model, the formation of 1′-hydroxymethyleugenol (the proximate carcinogenic metabolite) and of 1′-sulfooxymethyleugenol (which readily undergoes desulfonation to a reactive carbo-cation that can form DNA adduct) in the liver of human could be predicted at different oral doses of methyleugenol. The model therefore allows evaluation of possible dose-dependent effects in bioactivation and detoxification at different oral doses of methyleugenol as well as evaluation of the overall differences between humans and male rats in bioactivation and detoxification of methyleugenol. The outcome of the human PBK model shows a linear increase up to a dose of 500 mg/(kg bw) in formation of the proximate carcinogenic metabolite, 1′-hydroxymethyleugenol, leading to a linear increase in the formation of 1′-sulfooxymethyleugenol which readily undergoes desulfonation to a reactive carbo-cation that can form DNA adduct. The result that increased formation of 1′-hydroxymethyleugenol results in increased possibilities for formation of 1′-sulfooxymethyleugenol and, as a result increased DNA adduct formation, is in line with the results of Gardner *et al.* (1996) who reported that rats treated with different oral doses of methyleugenol show a linear increase in the protein adduct formation in the liver.

The PBK model defined was evaluated by comparing the PBK model predicted concentration of methyleugenol in blood to literature data on methyleugenol concentrations in serum blood of human volunteers at different time points upon intake of methyleugenol (Schecter *et al.*, 2004). These experimental data reveal the occurrence of methyleugenol already in serum blood of humans, even after prolonged fasting. This observation has been taken to suggest that some methyleugenol may be stored in distribution matrices like adipose tissue that are at equilibrium with the blood (Robison and Barr, 2006). The fasting, from midnight to 07.30 hr as applied in the study by Schecter *et* al. (2004), might not be enough to get rid of all

methyleugenol from the body of the volunteers, explaining their relatively high background levels. At 15, 30, 60, and 120 min, the outcomes of the PBK model were 5.7 to 7.9-fold higher when compared with the literature results. This deviation of the PBK model predictions from the experimental data might be due to several reasons. First, the bioavailability of methyleugenol in blood when given orally in a pure form is likely to be higher than when it is given as a part of the food matrix. The human experimental data were based on a study in which volunteers were served a breakfast known to contain methyleugenol, consisting of a brand of gingersnaps found on initial analysis to contain approximately 3.3 μg methyleugenol per gram, or 18 μg/cookie. The gingersnaps were purchased locally from a large supermarket. Orange juice was provided as a beverage. Each subject's meal consisted of 12 gingersnaps, containing approximately 216 μg methyleugenol. From this it becomes clear that the dose of methyleugenol was only known approximately and, even more important, that it was not given as a pure compound but as part of gingersnaps and also consumed together with an orange juice beverage. This provides an additional uncertainty about the dose level in the *in vivo* study because of the unknown bioavailability of methyleugenol form the gingersnaps when consumed within a complex food matrix. In the original calculations by the PBK model 100% bioavailability was assumed. However, bioavailability in this available human study may be significantly lower. Additional PBK modeling revealed that when the bioavailability of methyleugenol from the gingersnaps and orange juice food matrix would be 13.8%, the experimental value would accurately match the PBK predicted values (Figure 6B). Furthermore, an analysis of other model adjustments including parameters that appeared to be of influence on the model outcome based on a sensitivity analysis (blood flow, cardiac output, volume of the liver, maximum rate of formation and Michaelis-Menten constants for formation of phase I and phase II metabolites, and absorbance rate constant) was performed. None of these model adjustments resulted in improvement of the fit to a level comparable to that achieved by the adjustment of the bioavailability (data not shown). The occurrence of such a difference in the bioavailability of a compound when ingested within a food matrix or as a pure compound has been reported for other compounds as well. Manach *et al.* (2004) for example

reported that the level of ferulic acid metabolites recovered in the urine of rats amounts to only 3% of the ingested dose when ferulic acid is provided as wheat bran, whereas the metabolites represent 50% of the dose when ferulic acid is dosed as a pure compound. Also the bioavailability of ß-carotene is one order of magnitude higher when provided as a pure compound added to foods than when it is present naturally in foods (van het Hof *et al.*, 2000). Another reason contributing to the difference in predicted and observed blood concentrations of methyleugenol could be the fact that the model predicts whole blood concentrations whereas the *in vivo* study covers serum concentrations. This comparison between whole blood and serum concentrations can only be made based on the assumption that the whole blood and serum concentrations are equal. Furthermore, protein binding may provide another explanation for the fact that the PBK predicted blood concentrations of methyleugenol are higher than the observed serum blood concentrations. Finally it is important to stress that outcomes of PBK models should be used preferably in a relative way as done when making the dose- and species-dependent predictions of the present study.

The present study focused on the species differences between male rat and human at different dose levels including those relevant dietary human intakes. The PBK-based predictions for the formation of metabolites at different oral doses show significant species differences as reflected in a 1.8 to 2.5-fold lower formation of the proximate metabolite 1′-hydroxymethyleugenol accompanied by a higher formation of eugenol resulting from *O*-demethylation in the liver of human (eugenol was not formed in the liver of rat) compared with male rat at dose levels up to 300 mg/(kg bw). In spite of the lower formation of the proximate carcinogenic metabolite 1′-hydroxymethyleugenol in humans, this does not necessarily reflect lower levels of formation of the 1′-sulfooxymethyleugenol metabolite which readily undergoes desulfonation to a reactive carbo-cation that can form DNA adduct. The PBK-model results obtained indicate that there are no substantial species differences in formation of 1′-sulfooxymethyleugenol up to dose levels of 300 mg/(kg bw). The PBK model predicted formation of 1′-sulfooxymethyleugenol was 1.14 to 1.57-fold higher in human than in male rat over the whole dose. This indicates that the species-dependent differences in bioactivation of

methyleugenol to 1′-sulfooxymethyleugenol are smaller than the default factor of 4 generally assumed to reflect interspecies variation in kinetics (assuming that the default factor of 10 can be divided into a factor of 4 for kinetics and 2.5 for dynamics) (WHO, 1999). This can be taken into account when extrapolating the carcinogenicity data obtained in animals at high doses to the human situation.

It is also of interest to note that Zhou *et al.* (2007) reported the formation of DNA adducts in human HepG2 cells following treatment with methyleugenol at concentrations in the range of about 50-450 μM. The PBK model now developed predicts that such concentrations of methyleugenol in human liver are reached at dose levels of 4.6 to 26.7 mg/(kg bw). These are dose levels at which in animal bioassays tumor formation is observed (NTP, 2000).

Worldwide different approaches exist to assess the risk of compounds that are both genotoxic and carcinogenic. Numerical estimates of the risk associated with human exposure might be derived by extrapolation of carcinogenicity data obtained in animals at high dose levels to low dose levels relevant for the human situation. Many mathematical models have been proposed by which such an extrapolation below the available experimental data can be performed, of which linear extrapolation is the simplest and most conservative form (COC, 2004). Extrapolating from animal tumor data at high doses using mathematical modeling in order to obtain estimates of the risk to humans at low dose exposure levels has been much debated, since it is not known whether or not the model chosen actually reflects the underlying biological processes. In addition, it is argued that species differences are not taken into account. Furthermore obtaining numerical estimates may be misused or misinterpreted in further risk management and risk communication, where the uncertainties and inaccuracy connected to the model may not be communicated (EFSA, 2005).

The results of the PBK models for male rat (Al-Subeihi *et al.*, 2011) and human, the latter obtained in the present study, indicate that kinetic data do not provide a reason to argue against a linear extrapolation from the rat tumor data to the human situation. This is illustrated in Figure 10, in which the PBK-model predicted dose-dependent formation of 1′-sulfooxymethyleugenol in the liver of rat and human is displayed. Both curves are observed to be linear from doses as

high as the BMD_{10} down to dose levels as low as the VSD, when plotted on a log-log scale as done in Figure 10 and almost linear when plotted on a linear scale (Figure not shown). Deviations from linearity in formation of 1′-sulfooxymethyleugenol are only observed for both rats and human at dose levels above 60 mg/(kg bw)/day, which is higher than the BMD_{10}. Since the BMD_{10} appears to be located within the linear part of the curves and since the rat and human curves do not differ substantially, the PBK results of the present study support that possible non-linear kinetics and species differences in kinetics should not be used as an argument against using a linear low dose cancer risk extrapolation from animal data to the low dose human situation. This illustrates that PBK models provide a useful tool in risk assessment of food-borne chemicals when evaluating human risks.

Acknowledgement

This work was supported by a grant from sandwich PhD fellowship program / Wageningen University, the Netherlands.

References

Al-Subeihi, A.A.A., Spenkelink, B., Rachmawati, N., Boersma, M.G., Punt, A., Vervoort, J., van Bladeren, P.J., and Rietjens, I.M.C.M. (2011). Physiologically based biokinetic model of bioactivation and detoxification of the alkenylbenzene methyleugenol in rat. Toxicol In Vitro 25, 267-285.

Barter, Z.E., Bayliss, M.K., Beaune, P.H., Boobis, A.R., Carlile, D.J., Edwards, R.J., Houston J.B., Lake, B.G., Lipscomb, J.C., Pelkonen, O.R., Tucker, G.T., and Rostami-Hodjegan, A. (2007). Scaling factors for the extrapolation of in vivo metabolic drug clearance from in vitro data: Reaching a consensus on values of human microsomal protein and hepatocellularity per gram of Liver. Curr Drug Metab 8, 33-45.

Brown, R.P., Delp, M.D., Lindstedt, S.L., Rhomberg, L.R., and Beliles, R.P. (1997). Physiological parameter values for physiologically based pharmacokinetic models. Toxicol Ind Health 13, 407-484.

Burdock, G.A., ed. (1995). Fenaroli′s Handbook of Flavor Ingredients, Vol. II, 3rd Edition, CRC Press, Boca Raton, FL.

Burkey, J.L., Sauer, J.M., McQueen, CA., and Sipes, I.G. (2000). Cytotoxicity and genotoxicity of methyleugenol and related congeners—a mechanism of activation for methyleugenol. Mutat Res 453, 25–33.

Chan, V.S., and Caldwell, J. (1992). Comparative induction of unscheduled DNA synthesis in cultured rat hepatocytes by allylbenzenes and their 1′-hydroxy metabolites. Food Chem Toxicol 30, 831–836.

COC (2004). (Committee on Carcinogenicity of Chemicals in Food, consumer products and the environment). Guidance on a strategy for the risk assessment of chemical carcinogens. http://www.iacoc.org.uk/publications/documents/guideline04.pdf

Cubitt, H.E., Houston, J.B., and Galetin, A. (2011). Prediction of Human Drug Clearance by Multiple Metabolic Pathways: Integration of hepatic and intestinal microsomal and cytosolic data. Drug Metab Dispos 39, 864-873.

DeJongh, J.,Verhaar, H.J., and Hermens, J.L. (1997). A quantitative property-property relationship (QPPR) approach to estimate in vitro tissue-blood partition coefficients of organic chemicals in rats and humans. Arch Toxicol. 72, 17-25.

De Vincenzi, D., Silano, M., Stacchini, P., and Scazzocchio, B. (2000). Constituents of aromatic plants: I. Methyleugenol. Fitoterapia 71, 216-221.

Ding, W., Levy, D.D., Bishop, M. E., Lyn-Cook Lascelles, E., Kulkarni, R., Chang, C.W., Aidoo, A., and Manjanatha, M.G. (2011). Methyleugenol genotoxicity in the Fischer 344 rat using the comet assay and pathway-focused gene expression profiling. Toxicol Sci 123,103-112.

Drinkwater, N.R., Miller, E.C., Miller, J.A., and Pitot, H.C. (1976). Hepatocarcinogenicity of

estragole (1-allyl-4-methoxybenzene) and 1′-hydroxyestragole in the mouse and mutagenicity of 1'-acetoxyestragole in bacteria. J Natl Cancer Inst 57, 1323-1331.

EFSA (2005). Opinion of the scientific committee on a request from EFSA related to a harmonised approach for risk assessment of substances which are both genotoxic and carcinogenic. EFSA J 282, 1–31. http://www.efsa.europa.eu/en/efsajournal/ pub/ 282.htm

Evans, M.V. and Anderson, M.E. (2000). Sensitivity analysis of a physiological model for 2,3,7,8-tetrachlorodibrnzo-p-dioxin (TCDDD): Assessing the impact of specific model parameters on sequestration in liver and fat in rat. Toxicol Sci 54, 71-80.

European Commission (2008). Regulation (EC) No 1334/2008 of the European Parliament and of the Council of 16 December 2008 on flavourings and certain food ingredients with flavouring properties for use in and on foods and amending Council Regulation (EEC) No 1601/91, Regulations (EC) No 2232/96 and (EC) No 110/2008 and Directive 2000/13/EC. Off J Eur Union, L354/34: http://eur-lex.europa.eu/LexUriServ/LexUriServ.do?uri=OJ:L:2008:354:0034:0050:en:pdf

Filser, J.G., Faller, T.H., Bhowmik, S., Schuster, A., Kessler, W., Putz, C., and Csanady, G.A. (2001). First-pass metabolism of 1,3-butadiene in once through perfused livers of rats and mice. Chem Biol Interact 135-136, 249-265.

Fisher, M.B., Campanale, K., Ackermann, B.L., Vanden Branden, M., and Wrighton, S.A. (2000). In vitro glucuronidation using human liver microsomes and the pore-forming peptide alamethicin. Drug Metab Dispos 28, 560-66.

Gardner, I., Bergin, P., Stening, P., Kenna, J.G., and Caldwell, J. (1996). Immunochemical detection of covalently modified protein adducts in livers of rats treated with methyleugenol. Chem Res Toxicol 9, 713–721.

Gardner, I., Wakazono, H., Bergin, P., Waziers, I., Beaune, P., Kenna, J.G., and Caldwell, J. (1997). Cytochrome P450 mediated bioactivation of methyleugenol to 1′-hydroxymethyleugenol in Fischer 344 rat and human liver microsomes. Carcinogenesis 18, 1775-1783.

Guenthner, T.M., and Luo, G. (2001). Investigation of the role of the 2′,3′-epoxidation pathway

in the bioactivation and genotoxicity of dietary allylbenzene analogs. Toxicology 160, 47-58.

Hall, R.L., and Oser, B.L. (1965). Recent progress in the consideration of flavoring ingredients under the food additives amendment III. GRAS substances. Food Technol 253, 151-197.

IFRA (2009). International Fragrance Research Association, October 14. www.ifraorg.org

Leung, A.Y. (1980). Encyclopedia of Common Natural Ingredient used in Food, Drugs and Cosmetics. John Wiley and Sons, New York.

Lin, J.H., and Wong, B.K. (2002). Complexities of glucuronidation affecting in vitro in vivo extrapolation. Curr Drug Metab 3, 623-646.

Luo, G., and Guenthner, T.M. (1995). Metabolism of allylbenzene 2′,3′-oxide and estragole 2′,3′-oxide in the isolated perfused rat liver. J Pharmacol Exp Ther 272, 588-596.

Luo, G., Qato, M.K., and Guenthner, T.M. (1992). Hydrolysis of the 2′,3′-allylic epoxides of allylbenzene, estragole, eugenol, and safrole by both microsomal and cytosolic epoxide hydrolases. Drug Metab Dispos 20, 440-445.

Manach, C., Scalbert, A., Morand, C., Remesy, C., and Jimenez, L. (2004). Polyphenols: Food sources and bioavailability. Am J Clin Nut 79, 727-742.

Miele, M., Dondero, R., Ciarallo, G., and Mazzei, M.J. (2001). Methyleugenol in Ocimum basilicum L.cv. Genovese Gigante. J Agr Food Chem 49, 517-521.

Miller, E.C., Swanson, A.B., Phillips, D.H., Fletcher, T.L., Liem, A., and Miller, J. (1983). Structure-activity studies of the carcinogenicities in the mouse and rat of some naturally occurring and synthetic alkenylbenzene derivatives related to safrole and estragole. Cancer Res 43, 1124-1134.

NTP (1998). Toxicology and carcinogenesis studies of methyleugenol (CAS No. 93-15-12) in F344/N Rats and B6C3F1 Mice (Gavage Studies). Natl Toxicol Program Tech Rep Ser 491. NIH Publication No. 98-3950.

NTP (2000). Toxicology and carcinogenesis studies of methyleugenol (CAS No. 93-15-12) in F344/N rats and B6C3F1 mice (Gavage studies). Natl Toxicol Program Tech Rep Ser, 491, 1-412.

Phillips, D.H., Reddy, M.V., and Randerath, K. (1984). ^{32}P-post-labelling analysis of DNA adducts formed in the livers of animals treated with safrole, estragole and other naturally-occurring alkenylbenzenes. II. Newborn male B6C3F1 mice. Carcinogenesis 5, 1623–1628.

Punt, A., Delatour, T., Scholz, G., Schilter, B., Bladeren, P.J., and Rietjens, I.M.C.M. (2007). Tandem mass spectrometry analysis of N^2-(*trans*-Isoestragol-3′-yl)-2′-deoxyguanosine as a strategy to study species differences in sulfotransferase conversion of the proximate carcinogen 1′-hydroxyestragole. Chem Res Toxicol 20, 991-998.

Punt, A, Freidig, A.P., Delatour, T., Scholz, G., Boersma, M.G., Schilter, B., van Bladeren, P.J., and Rietjens, I.M.C.M. (2008). A physiologically based biokinetic (PBBK) model for estragole bioactivation and detoxification in rat. Toxicol Appl Pharm 231, 248-259.

Punt, A., Paini, A., Boersma, M.G., Freidig, A.P., Delatour,T., Scholz**,** G., Schilter, B., van Bladeren, P.J., and Rietjens I.M.C.M. (2009). Use of physiologically based biokinetic (PBBK) modeling to study estragole bioactivation and detoxification in humans as compared with male rats. Toxicol Sci 110, 255–269.

Ramsey, J.C., and Andersen, M.E. (1984). A physiologically based description of the inhalation pharmacokinetics of styrene in rats and humans. Toxicol Appl Pharm 73, 159-175.

Rietjens, I.M.C.M., Louisse, J., and Pun, A. (2011). Tutorial on physiologically based kinetic modeling in molecular nutrition and food research. Mol Nutr Food Res 55, 941–956.

Rietjens, I.M.C.M., Slob, W., Galli, C., and Silano, V. (2008). Risk assessment of botanicals and botanical preparations intended for use in food and food supplements: Emerging issues. Toxicol Lett 180,131–136.

Robison S.H., and Barr D.B. (2006). Use of biomonitoring data to evaluate methyl eugenol exposure. Environ Health Perspect 114, 1797–1801.

SCF (2001). Opinion of the Scientific Committee on Food on Methyleugenol (4-allyl-1,2-dimethoxybenzene). European Commission, Scientific Committee on Food. Brussels, BE. http://ec.europa.eu/food/fs/sc/scf/out102_en.pdf

Schecter, A., Lucier, G.W., Cunningham, M.L., Abdo, K.M, Blumenthal, G., Silver, A.G., Melnick, R., Portier, C., Barr, D.B., Barr, J.R., Stanfill, S.P., Patterson Jr., D.G., Needham, L.L., Stopford, W., Masten, S., Mignogna, J., and Tung, K.C. (2004). Human consumption of methyleugenol and its elimination from serum. environ health persp 112, 678-680.

Smith, B., Cadby, P., Leblanc, J., and Setzer, R. (2010). Application of the margin of exposure (MoE) approach to substances in food that are genotoxic and carcinogenic. Example: Methyleugenol, CASRN: 93-15-2. Food Chem Toxicol 48, S89-S97.

Smith, R.L., Adams, T.B., Doull, J., Feron, V., Goodman, J.I., Marnett, L.J., Portoghese, P.S., Waddell, W.J., Wagner, B.M., Rogers, A.E., Caldwell, J., and Sipes, I.G. (2002). Safety assessment of allylalkoxybenzene derivatives used as flavoring substances - methyl eugenol and estragole. Food Chem Toxicol 40, 851-870.

Solheim, E., and Scheline, R. (1976). Metabolism of alkenebenzene derivatives in the rat. II. Eugenol and isoeugenol methyl ethers. Xenobiotica 6, 137-150.

SRI International (1990). Directory of Chemical Producers, United States of America. Menlo Park, CA: Stanford Research Institute International.

van het Hof, K.H., West, C.E., Weststrate, J.A., and Hautvast, J.G. (2000). Dietary factors that affect the bioavailability of carotenoids. J Nutr 130, 503-506.

WHO (1999). International Programme on Chemical Safety (IPCS): Assessing human health risks of chemicals: principles for the assessment of risk to human health from exposure to chemicals, Environmental Health Criteria 210, World Health Organisation, Geneva, Switzerland. http://www.inchem.org/documents/ehc/ehc/ehc210.htm

Zhou, G.D., Moorthy, B., Bi, J., Donnelly, K.C., and Randerath, K. (2007). DNA adducts from alkoxyallylbenzene herb and spice constituents in cultured human (HepG2) cells. Environ Mol Mutag 48, 715– 721.

4

Inhibition of methyleugenol bioactivation by the herb-based constituent nevadensin and prediction of possible *in vivo* consequences using physiologically based kinetic modeling

Based on: Al-Subeihi A.A.A., Paini A., Punt A., Vervoort J., van Bladeren P.J., and Rietjens I.M.C.M.
Submitted

Abstract

Methyleugenol occurs naturally in a variety of spices, herbs, including basil, and their essential oils. Methyleugenol induces hepatomas in rodent bioassays following its conversion to a DNA reactive metabolite. In the present study, the basil constituent nevadensin was shown to be able to inhibit DNA adduct formation in HepG2 cells exposed to the proximate carcinogen 1′-hydroxymethyleugenol in the presence of this flavonoid. This inhibition occurs at the level of sulfotransferase (SULT)-mediated bioactivation of 1′-hydroxymethyleugenol. In order to investigate possible *in vivo* implications the SULT inhibition by nevadensin was integrated into the male rat and human PBK models for bioactivation and detoxification of methyleugenol. The results thus obtained reveal that co-administration of methyleugenol with nevadensin may reduce the levels of bioactivation of 1′-hydroxymethyleugenol to the DNA reactive metabolite, without reducing its detoxification via glucuronidation or oxidation. This effect may be significant even at realistic low dose human exposure levels. The results obtained point at a potential reduction of the cancer risk when methyleugenol exposure occurs by oral intake within a relevant food matrix containing SULT inhibitors compared to what is observed in rodent bioassays upon exposure to pure methyleugenol dosed by gavage.

Introduction

Methyleugenol is a compound naturally occurring in a variety of spices and herbs, including clove, allspice, cinnamon leaves, walnuts, basil, nutmeg, anise, pimento, citronella, laurel fruits leaves and others, as well as in their essential oils (Smith *et al.*, 2010). The general population is primarily exposed to methyleugenol via ingestion of food stuffs flavored with methyleugenol containing essential oils (Smith *et al.*, 2010), including for instance, candy, cookies such as gingersnaps, ice cream, tomato ketchup and relish (Burdock, 1995; Leung, 1980). The average daily intake of methyleugenol was estimated by the Scientific Committee on Food (SCF) to be 13 mg/day, corresponding to 0.217 mg/(kg bw)/day for a 60 kg person (SCF, 2001), while the Flavor and Extract Manufacturers Association (FEMA), using a different methodology, estimated the average daily intake of methyleugenol resulting from flavor use to be less than 0.01 mg/(kg bw)/day (Smith *et al.*, 2002). The estimation of the SCF was based on theoretical maximum use levels of methyleugenol in various food categories and consumption data for these food categories, whereas the intake estimation of the FEMA was based on production volume data for flavor use (SCF, 2001; Smith *et al.*, 2002). In the European Union, but not in the US, the usage of pure methyleugenol in food has been banned (European Commission, 2008). It was reported that methyleugenol displays cytotoxic and genotoxic activity in rat hepatocytes (Burkey *et al.*, 2000).

Methyleugenol was shown to induce tumours in various tissues of rats and mice at high dose levels (Miller *et al.*, 1983; NTP, 2000). In particular, the compound was shown to be a hepatocarcinogen in both species. Methyleugenol was nominated for toxicological characterization and testing by the National Toxicology Program (NTP) because it is widely used in a variety of foods, beverages, and cosmetics, as well as because of its structural resemblance to the known carcinogens safrole and estragole (Miller *et al.*, 1983; NTP, 1998).

In 2000, the carcinogenicity of methyleugenol was investigated in mice and rats (NTP, 2000). The NTP reported that methyleugenol is carcinogenic in both rats and mice when dosed

at high dose levels as pure compound suspended in methylcellulose 0.5 % (NTP, 2000). Methyleugenol was shown to form DNA adducts in liver and other tissues of rodent models, suggesting that the compound is a DNA reactive carcinogen (Boberg *et al.*, 1983; Phillips *et al.*, 1981). However, methyleugenol tested negative in the Ames test and other standard *in vitro* genotoxicity assays (Ding *et al.*, 2011; NTP, 2000).

Methyleugenol is unreactive by itself but undergoes metabolic activation to produce an electrophilic metabolite that acts as the DNA reactive intermediate (Gardner *et al.*, 1997; Miele *et al.*, 2001). Figure 1 displays the bioactivation pathway of methyleugenol which starts with hydroxylation of the 1'-position of methyleugenol to produce the proximate carcinogenic metabolite 1′-hydroxymethyleugenol (Drinkwater *et al.*, 1976; Miller *et al.*, 1983). In a next step 1′-hydroxymethyleugenol can be sulfonated by SULT to form 1′-sulfoxymethyleugenol which readily undergoes desulfonation to a carbo-cation that can form DNA adducts (Miller *et al.*, 1983). Recently, studies using *Salmonella typhimurium* TA100 strains with expression of human SULT revealed that SULT1A1 and SULT1E1 are the main liver sulfotransferease enzymes involved in activation of 1′-hydroxymethyleugenol to DNA reactive metabolites (Herrmann *et al*., 2012).

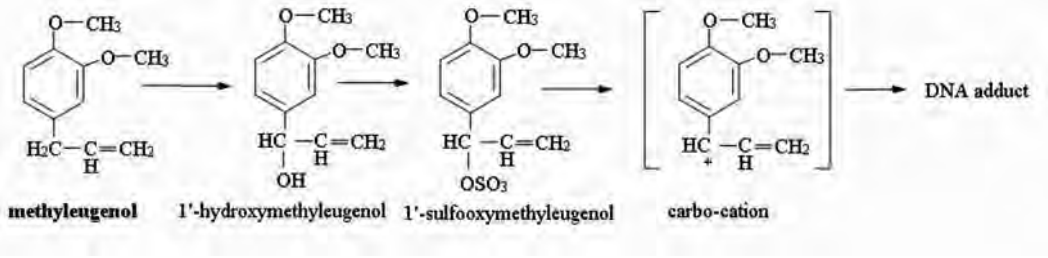

Figure 1. Structural representation of the pathway for bioactivation of methyleugenol.

However, it is important to note that the carcinogenicity observed in studies in which animals are exposed to high dose levels of the pure compound by gavage may not be representative for the situation where humans are exposed to methyleugenol at low levels via dietary intake with a food matrix being present. For the related alkenylbenzene estragole it was actually demonstrated that other ingredients present in an alkenylbenzene containing herb or food item may inhibit the SULT mediated bioactivation of estragole to its ultimate DNA reactive 1′-sulfooxy metabolite (Alhusainy *et al.*, 2010; Jeurissen *et al.*, 2008). For instance a methanolic basil extract was shown to cause a dose dependent inhibition of DNA adduct formation in 1′-hydroxyestragole exposed human HepG2 cells (Jeurissen *et al.*, 2008). In a subsequent study, the flavonoid nevadensin (Figure 2) was identified as the potent SULT inhibitor present in these methanolic basil extracts (Alhusainy *et al.*, 2010). So far, the existence of such matrix dependent interactions with the bioactivation of alkenylbenzenes was only demonstrated for estragole (Alhusainy *et al.*, 2010). Therefore the objective of the present study was to study the potential of nevadensin to inhibit the SULT mediated bioactivation and subsequent DNA adduct formation of methyleugenol. By incorporating the nevadensin mediated SULT inhibition in the recently developed physiologically based models for bioactivation and detoxification of methyleugenol in rat (Al-Subeihi *et al.*, 2011) and human (Al-Subeihi *et al.*, 2012), the possible effects of SULT inhibition by nevadensin expected to occur in the *in vivo* situation at realistic low dose exposure scenario′s was also investigated.

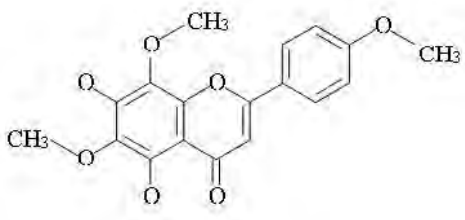

Figure 2. Structural formula of nevadensin

Materials and Method

Materials

2′-Deoxyguanosine was purchased from Sigma (Basel, Switzerland), and 1,2,3,7,9-$^{15}N_5$-2′-deoxyguanosine was obtained from Cambridge Isotope Laboratories (Cambridge, MA). Fetal bovine serum (FBS), DMEM/F12 (L-glutamine, 15 mM HEPES) medium and phosphate buffered saline (PBS) (pH 7.4) were purchased from Gibco (UK). Dimethyl sulfoxide (DMSO), methanol, zinc sulphate (heptahydrate), phosphodiesterase I from *Crotalus adamanteus* (venom phosphodiesterase), phosphodiesterase II from bovine spleen (spleen phosphodiesterase), nuclease P1 and alkaline phosphatase were purchased from Sigma (Schnelldorf, Germany). Acetonitrile was purchased from Biosolve BV (Valkenswaard, The Netherlands). Formic acid and ethanol were obtained from VWR Merck (Darmstadt, Germany). Nevadensin was purchased from Apin Chemicals (Milton, UK). Pentachlorophenol (PCP, 98%) was obtained from Sigma-Riedel de Haen (Seelze, Germany). 1′-hydroxymethyleugenol and 1′-acetoxymethyleugenol were synthesized as described previously (Al-Subeihi *et al.*, 2011). Human HepG2 cells were purchased from the American type culture collection (Manassas, Virginia).

Synthesis of N^2-(*trans*-isomethyleugenol-3′-yl)-2′-deoxyguanosine (ME-3'-N^2-dG) and $^{15}N_5$-labelled N^2-(*trans*-isomethyleugenol-3′-yl)-2′-deoxyguanosine ($(^{15}N_5)$ ME-3'-N^2-dG)

ME-3'-N^2-dG was synthesized via a reaction between 1′-acetoxymethyleugenol and 2′-deoxyguanosine based on the protocol of Punt *et al.*, (2007). In brief, 250 µL of a 0.01 g/mL solution of 1′-acetoxymethyleugenol in DMSO was added to 2250 µL of 2.5 mM 2′-deoxyguanosine in 2.5 mM ammonium carbonate (pH 7.4). The same reaction was performed for the synthesis of $(^{15}N_5)$ ME-3'-N^2-dG in which 1′-acetoxymethyleugenol was allowed to react with $^{15}N_5$- labeled 2′-deoxyguanosine. The incubations were stirred for 48 hr at 37 °C. Both ME-3'-N^2-dG and $(^{15}N_5)$ ME-3'-N^2-dG were purified by HPLC-UV on a M600 liquid

chromatography system (Waters, Milford, MA) equipped with an Alltima C18 5 µm column, 150 x 4.6 mm (Alltech, Breda, The Netherlands). The gradient was made with ultrapure water and acetonitrile. The flow rate was 1 mL/min. A linear gradient was applied from 10% to 15% acetonitrile over 30 min after which the percentage of acetonitrile was increased to 100% over 2 min, kept at 100% for 1 min, lowered to 10% in 2 min, and kept at these initial conditions for 10 min for equilibration of the system. Detection was carried out using a Waters 966 photodiode array detector (Waters, Milford, MA) at 260 nm. Both ME-3'-N^2-dG and *($^{15}N_5$)* ME-3'-N^2-dG were collected at a retention time of 11.4 min. The purity of both ME-3'-N^2-dG and *($^{15}N_5$)* ME-3'-N^2-dG was more than 98%, according to LC-MS/MS and HPLC analyses.

Cytotoxicity test

The cytotoxicity of nevadensin, 1′-hydroxymethyleugenol, PCP, and DMSO was evaluated using the MTT test (Hussain *et al.*, 1993; Mosmann, 1983). HepG2 cells were plated in a 96-well plate at a density of 2 x10^4 cells per well 24 hr prior to exposure. Just before exposure the medium was removed and cells were washed with 100 µL HBSS. Cells were exposed to 0.5% DMSO (control) or the test compounds in exposure medium (DMEM/F12 + glutamax + 50 µg/mL gentamicin) at concentrations of nevadensin, 1′-hydroxymethyleugenol, and/or PCP as indicated and added from respectively 5000, 1000, and 400 times concentrated stock solutions in DMSO for 4 hr in a humidified atmosphere at 37 °C. Then, 5 µL of a 5 mg/mL MTT solution in PBS were added and the cells were incubated for another 1 hr. Thereafter, the medium was removed and 100 µL of DMSO were added to all wells to dissolve the formazan crystals. The absorbance was measured at 562 nm and cell viability was defined as the ratio between the absorbance measured for nevadensin, 1′-hydroxymethyleugenol, PCP or DMSO treated cell samples and the absorption measured for untreated cell samples.

Incubation of HepG2 cells with 1′-hydroxymethyleugenol

Human HepG2 cells were cultured in a 75cm^2 flask (Corning, NY, USA) with DMEM/F12 medium containing glutamax, 10% FBS and incubated in a humidified incubator under 5% CO_2

and 95% air at 37 °C. Once reaching 80-90% confluence the cells were incubated overnight (~14 hr) in the presence of 1′-hydroxymethyleugenol at a final concentration of 100 μM (added from a 1000 times concentrated stock solution in DMSO) and nevadensin at a final concentration of 0, 0.002, 0.02, 0.2, or 2 μM (added from 5000 times concentrated stock solutions in DMSO) or PCP at a final concentration of 12.5 μM (added from a 400 times concentrated stock solution in DMSO). The final DMSO concentration was 0.35%. After overnight incubation, cells were washed twice with phosphate–buffered saline (PBS), scraped, collected into an eppendorf tube, and pelleted at 211 g (1500 rpm, Eppendorf Centrifuge 5424) for 5 min. DNA was extracted and digested as reported in the next section.

DNA extraction and digestion

DNA was extracted from human HepG2 cells as previously described (Alhusainy *et al.,* 2010; Jeurissen *et al.* 2008; Paini *et al.,* 2010). Briefly, DNA was extracted using the Get pure DNA Kit-Cell protocol (Dojindo Molecular Technology Inc., Kumamoto, Japan) and 3 to 10 $*10^6$ cells per sample (following the manufacturer's instructions). The yield and purity of the extracted DNA was determined using the NanoDrop technique measuring the absorbance ratio A260 nm/A280 nm. DNA samples with an absorbance ratio of 1.8-2 were considered sufficiently pure. The quantity of DNA per sample was calculated from the NanoDrop output in ng/mL using a molar extinction coefficient for double stranded DNA of 50 L/(mol*cm) at a wavelength of 260 nm. Digestion of isolated DNA was done as reported previously (Paini *et al.*, 2010). In short, to 50 μg DNA in 80 μL water, 20 μL buffer P1 (300 mM sodium acetate, 1 mM $ZnSO_4$, pH 5.3), 11 μL SPDE (spleen phosphodiesterase) solution (0.0004 U/μL in water), and 10 μL nuclease P1 (0.5 μg/μL in water) were added and the resulting solution was incubated for 4 hr at 37 °C. Following incubation, 20 μL buffer (500 mM Tris-HCl, 1 mM EDTA, pH 8.0), 12 μL VPDE (venom phosphodiesterase) solution (0.00026 U/μL in water), and 6 μL alkaline phosphatase (0.764 U/μL in water) were added and the mixture was incubated for 3 hr at 37 °C (Paini *et al.*, 2010). Following these incubations samples were filtered using eppendorf tubes with a cut off membrane of 5,000 nominal molecular weight limit

(NMWL) (Millipore). The hydrolyzed filtered sample was evaporated to dryness and reconstituted in 50 µL water and stored at -20 °C until LC-MS/MS analysis.

LC-MS/MS method for detection and quantification of ME-3'-N^2-dG

LC-MS/MS analysis was performed on a Perkin Elmer 200 Series HPLC System (Perkin Elmer, Waltham, Massachusetts) coupled to an API 3000 system (Applied Biosystem, Foster City, California). Samples were injected on an Agilent Zorbax Extend-C18 column, 2.1*50 mm, 3.5 Micron 80 Å (Basel, Switzerland), with a Zorbax guard column. The gradient was made with ultrapure water containing 0.1% (v/v) formic acid and 100% acetonitrile. The flow rate was set at 0.3 mL/min. A linear gradient was applied from 10% to 50% acetonitrile over 3 min, after which the percentage of acetonitrile was brought to 100% in 1 min, and kept at 100% acetonitrile over 2 min. The amount of acetonitrile was lowered to 10% over 1 min, and the column was equilibrated at these initial conditions for 8 min. ME-3'-N^2-dG eluted at 2.58 minutes. The mass spectrometric analysis was performed with the following settings: nebulizer gas (air) was set at 15 psi, curtain gas (nitrogen, which is used to keep the analyser region clean) was set at 10 psi, the ion spray voltage at 4700 V, the collision gas (CAD) was 5 eV, the ion source temperature was set at 300 °C, the declustering potential was set at 37 V, the focusing potential was set at 200 V, the entrance potential at 9 V, and the collision cell exit was set at 15 V. Nitrogen was used as sheath gas turbo, ion spray, with a pressure of 7000 L/h. The dwell time per transition was 0.05 sec. A divert valve was used in order to discard the gradient after elution of the peak. Quantification of the DNA adduct was carried out using selected-ion detection in the multiple reaction-monitoring mode (MRM), the characteristic transitions for the ME-3′-N^2-dG and for the *($^{15}N_5$)* ME-3'-N^2-dG are displayed in Table 1.

Inhibition constant (K_i)

In the present study a K_i of 4 nM for nevadensin was used. This value was obtained from a previous study (Alhusainy *et al.*, 2010) and represents the K_i for inhibition of SULT mediated conversion of 7-hydroxycoumarin to 7-hydroxycoumarin sulphate by the identified inhibitor

Table 1. Transition reaction (m/z) and the collision energy used to obtain the daughter fragments by LC-MS/MS.

	Transition(m/z) (used for quantification)	Collision energy (eV)	Transition (m/z) (used for confirmation)	Collision energy (eV)
ME-3′-N^2-dG	444→328	18	444→177 444→164	37 40
($^{15}N_5$) ME-3′-N^2-dG	449→333	18	449→169	40

nevadensin. This K_i was used in the model of methyleugenol assuming equal K_i values for the two substrates (1′-hydroxymethyleugenol and 7-hydroxycoumarin) and this was based on the fact that the type of inhibition was found to be non-competitive and, thus, not occurring at the substrate binding site of SULT.

Methyleugenol PBK model

The rat and human PBK models developed in our previous work to describe the dose-dependent bioactivation and detoxification of methyleugenol in male rat liver (Al-Subeihi *et al.*, 2011) and human liver (Al-Subeihi *et al.*, 2012) were used in the present study to model the possible consequences of SULT inhibition for bioactivation and detoxification of methyleugenol. Figure 3 (A-B) and Table 2 present the schematic overview of the model as well as an overview of the parameters used. Differential equations used to describe metabolite formation and conversion in the various organs can be found in our previous work (Al-Subeihi *et al.*, 2011, 2012). The models include separate compartments for liver, lung and kidney, which were found to be involved in the metabolism of methyleugenol. Furthermore, a separate compartment for fat tissue was included in order to take into account the relatively higher partition coefficient of methyleugenol in fat tissue. All other tissues were lumped into a rapidly perfused tissue group or a slowly perfused tissue group. The kinetic constants for phase I metabolism of methyleugenol as well as for metabolism of 1′-hydroxymethyleugenol are summarized in Table 3 and were according to our previous studies (Al-Subeihi *et al.*, 2011,

A.

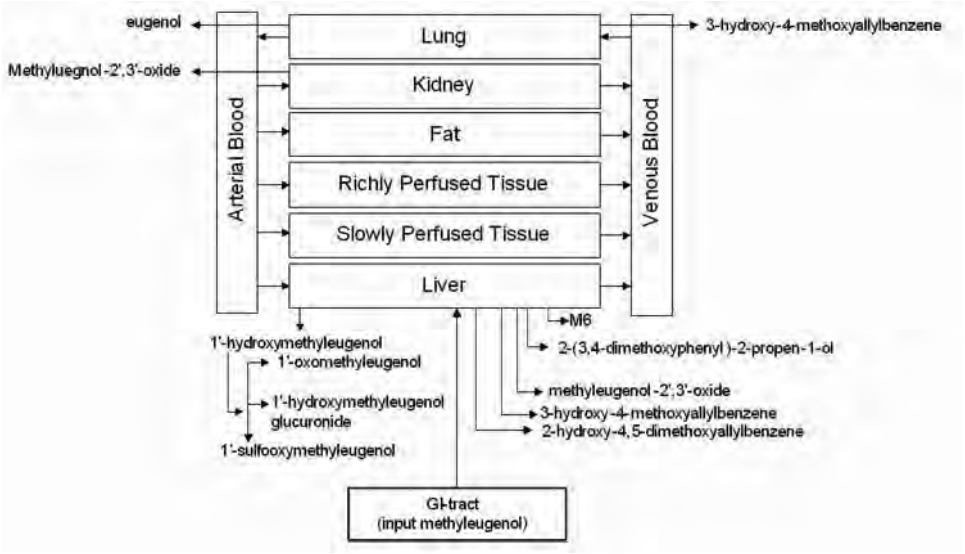

B.

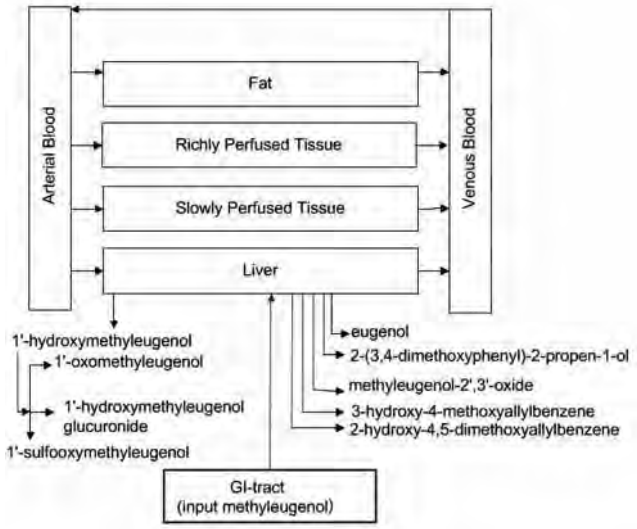

Figure 3. Representation of the conceptual model for the physiologically based kinetic model for methyleugenol in (A) male rat and (B) human.

Table 2. Parameters used in the physiologically based kinetic model for methyleugenol in both male rat and human.

Physiological parameters[a]	Rat	Human	**Tissue: blood partition coefficients**[b]	Rat	Human
body weight (kg)	0.3	63.8	methyleugenol		
percentage of body weight					
liver	3.4	2.6	liver	2.3	6.2
lungs	0.5		lungs	2.3	
kidney	0.7		kidney	2.3	
fat	7	21.4	fat	70	103
rapidly perfused	4.4	5	rapidly perfused	2.3	6.2
slowly perfused	68	51.7	slowly perfused	0.8	3.9
blood		7.9			
arterial blood	1.9				
venous blood	5.6				
cardiac output (L/hr)	5.4	323	1'-hydroxymethyleugenol		
			liver	1.1	1.4
percentage of cardiac output					
liver	25	22.7			
kidney	14				
fat	7	5.2			
rapidly perfused	37	47.3			
slowly perfused	17	24.8			

[a] Brown et al. (1997)

[b] Calculated based on DeJongh et al.(1997)

2012). In the present study the inhibition of SULT-mediated conversion by the identified inhibitor nevadensin (Alhusainy *et al.*, 2010) was integrated in the model. Since the inhibitor nevadensin was shown to inhibit the SULT catalyzed conversion of 7-hydroxycoumarin to 7-hydroxycoumarin sulphate in a non-competitive way, reducing V_{max} and not affecting K_m, a modulation factor $(1+([I]/K_i)$ for the apparent V_{max} value was included in the Michaelis–Menten equation representing the sulfonation pathway as follows:

$AM_{1'HMES}=V_{max,L\_1'HMES}/(1+([I]/K_i))*CL_{1'HME}/PL_{1'HME}/(K_{m,L\_1'HMES}+CL_{1'HME}/PL_{1'HME})$

where $AM_{1'HMES}$ is the amount of 1′-sulfooxymethyleugenol (µmol), $V_{max,L\_1'HMES}$ is the maximum rate of formation of 1′-sulfooxymethyleugenol, [I] is the concentration of the identified SULT inhibitor nevadensin in the liver (µmol/L), K_i is the inhibition constant for inhibition of the sulfonation by the identified SULT inhibitor (µmol/L), $CL_{1'HME}$ is the concentration of 1′-hydroxymethyleugenol in the liver (µmol/L), $PL_{1'HME}$ is the liver/blood

Table 3. Kinetic parameters for phase I metabolism of methyleugenol in incubations with human liver microsomes.

organ	phase I metabolite	***Km*(app)[a,b]**		**V*max*(app)[a,c]**	
		rat	*human*	*rat*	*human*
liver	methyleugenol-2′,3′-oxide	81 ± 15.5	23.7 ± 5	1.84 ± 0.08	0.66 ± 0.11
	1′-hydroxymethyleugenol	253 ± 90	404 ± 195	3.26 ± 0.45	1.38 ± 0.38
	3-(3,4-dimethoxyphenyl)-2-propen-1-ol	28 ± 2.3	161 ± 90	0.68 ± 0.025	0.39 ± 0.08
	2-hydroxy-4,5-dimethoxyallylbenzene	32 ± 1.1	415 ± 84	0.27 ± 0.006	0.10 ± 0.02
	eugenol	-	13.6 ± 12.3	-	0.15 ± 0.02
	3-hydroxy-4-methoxyallylbenzene	150 ± 55.5	1097 ± 142	0.13 ± 0.018	0.21 ± 0.02
	M6 (unidentified metabolite)	259 ± 16.4	-	0.44 ± 0.004	-
lung	eugenol	19 ± 3	-	0.21± 0.03	-
	3-hydroxy-4-methoxyallylbenzene	33 ± 18.7	-	0.67 ± .077	-
kidney	methyleugenol-2′,3′-oxide	968 ± 230	-	0.31± 0.05	-
	1′-hydroxymethyleugenol (1'HME) metabolite				
liver	1'-hydroxymethyleugenol glucuronide	799 ± 192	2393 ± 486	28.1 ± 6.1	0.66 ± 0.087[c]
	1'-oxomethyleugenol in liver microsomes	3534 ± 3038	1744 ± 2997	2.83 ± 0.92	2.1 ± 1.83[c]
	1'-oxomethyleugenol in liver cytosol	-	1580 ± 538	-	1.58 ± 0.206[d]
	1'-sulfooxymethyleugenol	102 ± 29.5	139 ± 82	0.0022 ± 0.0054	0.0009 ± 0.0002[e]

[a]mean±SD
[b]µM
[c]nmol/ min/mg microsomal protein
[d]nmol/ min/ mg cytosolic protein
[e]nmol/min/mg S9 protein

partition coefficient of 1′-hydroxymethyleugenol, and K_m,L is the Michaelis–Menten constant for the formation of 1′-sulfooxymethyleugenol (μmol/L) in the liver. Using our PBK models for methyleugenol bioactivation and detoxification (Al-Subeihi *et al.*, 2011, 2012), the time dependent concentration of methyleugenol (CL_{ME}) in the liver of male rat and human following an exposure to different doses of methyleugenol in the presence of varying amounts of nevadensin can be predicted. As a first approximation, the molar ratio (f) between methyleugenol and nevadensin was kept at a constant value during the modeling time. To this end, nevadensin was assumed to follow a similar time dependent concentration curve in the liver as methyleugenol and this was represented in the model by using the following equation: $[I] = CL_{ME} * f$ where CL_{ME} is the concentration of methyleugenol in the liver (μmol/L) and f represents the molar ratio between the nevadensin and methyleugenol concentrations. To obtain some insight into the effects resulting from possible differences in kinetics and bioavailability of the two compounds, the modeling was performed at different molar ratios (f). Thus the molar ratio (f) was varied from 0 (no nevadensin) to 2 (representing a nevadensin concentration that is twice as high as methyleugenol). Accordingly, the effect of varying doses of nevadensin on the formation of 1′-sulfooxymethyleugenol, 1′-hydroxymethyleugenol glucuronide, and 1′-oxomethyleugenol after 24 hr could be predicted at different methyleugenol doses. The doses of methyleugenol chosen for the modeling were 0.217 mg/(kg bw), the dose level considered relevant for human dietary exposure from all food sources (SCF, 2001) and 50 mg/(kg bw) representing a dose level higher than the dose at which methyleugenol was demonstrated to produce a single 44 kDa microsomal protein adduct in rats (Smith *et al.*, 2002) and in the range of dose levels that induce liver tumor formation (NTP, 2000).

Statistical analysis

To test whether the effects were significant, a two sample *t*-test (one-sided, equal variances) was performed, after an F test for equal variances was done, using Excel (Microsoft Office 2000).

Results

Synthesis and characterization of ME-3'-N^2-dG and ($^{15}N_5$) ME-3'-N^2-dG

Incubation of 1′-acetoxymethyleugenol with 2′-deoxyguanosine resulted in the formation of several adducts with 2′-deoxyguanosine as detected by HPLC-UV (Figure 4). Our chromatographic profile was comparable to that reported in the literature for the same reaction between the structurally related 1′-acetoxyestragole and 2′-deoxyguanosine (Punt *et al.*, 2007). Based on analogy to outcomes of the synthesis of E-3'-N^2-dG from 1′-acetoxyestragole by the same procedure it was expected that the most abundant peak at 11.4 min (Figure 4) corresponds to the adduct of interest ME-3'-N^2-dG. Figure 5 presents the structures of the various adducts detected based on this analogy to previous adducts identified for N^2-*(trans*-isoestragole-3′-yl)-2′-deoxyguanosine (ES-3'-N^2-dG*)*. This nature of the major adduct is also in line with results reported by Phillips *et al.* (1981), Punt *et al.*, (2007), and Wiseman *et al.* (1985) for the nature of the major DNA adduct of estragole; E-3′-N^2-dG. ME-3'-N^2-dG thus obtained was collected at 11.4 min and subsequently used as a standard to confirm the formation of the adduct of interest and to develop the quantitative LC-MS/MS method for detecting and quantifying DNA nucleotide adducts of methyleugenol. A similar chromatographic profile was obtained when the

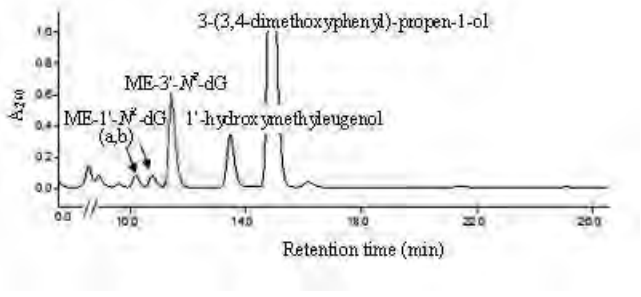

Figure 4. HPLC-UV chromatogram of methyleugenol adducts with 2′-deoxyguanosine formed in a reaction between 1′-acetoxymethyleugenol and 2′-deoxyguanosine. On the basis of previous identification by Phillips *et al.* (1981), Punt *et al.* (2007), and Wiseman *et al.* (1985) for the 2′-deoxyguanosine adduct of estragole, peaks were characterized as two diastereomers of ME-1′-N^2-dG and ME-3′-N^2-dG.

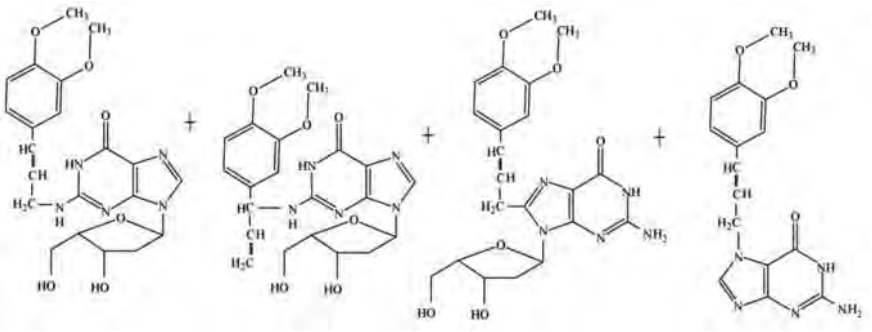

major adduct ME-3'-N^2-dG | minor adduct ME-1'-N^2-dG | minor adduct ME-3'-8-dG | minor adduct ME-3'-7-dG

Figure 5. Expected structure of adducts of methyleugenol reactive metabolite with 2′-deoxyguanosine based on the analogy of reaction of estragole with 2′-deoxyguanosine as identified by Phillips *et al.* (1981) and Wiseman *et al.* (1985). ME-3'-N^2-dG = N^2-(*trans*-isomethyleugenol-3'-yl)-2'-deoxyguanosine, ME-3'-8-dG = 8-(*trans*-isomethyl-eugenol-3'yl)-2'-deoxyguanosine, ME-1'-N^2-dG = N^2-(methyleugenol-1'-yl)-2'-deoxyguanosine, and ME-3'-7-dG = 7-(*trans*-methyleugenol-3'-yl)-2'-guanine.

reaction was performed using *($^{15}N_5$)* ME-3'-N^2-dG, and the isolation of the labeled adduct was undertaken in the same way as described for the non-labeled analogue.

The characterizations of ME-3'-N^2-dG and *($^{15}N_5$)* ME-3'-N^2-dG were carried out on the basis of the LC-MS/MS results depicted in Figure 6. In Figure 6A, the transitions used for the MS/MS spectrum of ME-3'-N^2-dG provided a molecular ion at *m*/*z* 444 corresponding to the protonated molecule $[M + H]^+$. The 5 Da upmass shift observed in the MS/MS spectrum of *($^{15}N_5$)* ME-3'-N^2-dG (*m*/*z* 449) (Figure 6B) was consistent with the *penta*-^{15}N labeling of the guanine moiety. When fragmented by collision, the ion of ME-3'-N^2-dG at *m*/*z* 444 gave rise to three major fragment ions at *m*/*z* 328, 177, and 164 (insert Figure 6A). The fragment ions at *m*/*z* 328, m/*z* 177, and *m*/*z* 164 were rationalized in terms of a loss of the deoxyribose group, loss of the 2′-deoxyguanosine group, and loss of deoxyribose and phenylethyl groups, respectively. The same MS/MS spectrum of ME-3'-N^2-dG was obtained in the study of Herrmann *et al.* (2012). Identification of ME-3'-N^2-dG was further supported by the observation of the mass

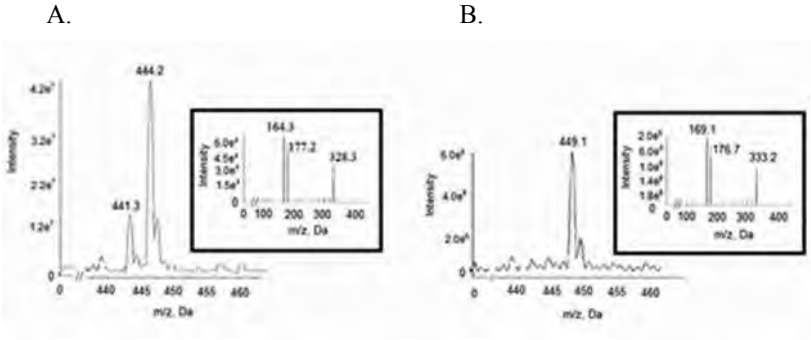

Figure 6. API 3000 Q1 spectrum of the parent ion representing: (A) the non-labelled synthesised ME-3′-N^2-dG (444 m/z, Da). The insert represents the daughter ions (328, 177, 164 m/z, Da) formed from the parent ion (444 m/z, Da) and (B) the labelled synthesised ($^{15}N_5$) ME-3'-N^2-dG (449 m/z, Da). The insert represents the daughter ions (338, 169 m/z, Da) formed from the parent ion (449 m/z, Da).

loss of the deoxyribose group and the phenylethyl group in the transition *m/z* 449 → 333 and *m/z* 449 → 169, respectively obtained in the case of *($^{15}N_5$)* ME-3'-N^2-dG (insert Figure 6B).

Inhibition of ME-3'-N^2-dG formation in the human hepatoma cell line HepG2

Figure 7A shows the LC-MS/MS chromatogram for the 444 → 328 transition of hydrolysed DNA isolated from human HepG2 incubated with 100 µM 1′-hydroxymethyleugenol. The peak of ME-3'-N^2-dG appears at 2.7 min in the chromatogram. Figure 7B presents the ME-3'-N^2-dG formation detected in HepG2 cells exposed to 100 µM 1′-hydroxymethyleugenol (1′HME) for ~14 hr in the absence and presence of increasing concentrations of nevadensin or 12.5 µM PCP added as a positive control for SULT inhibition. At the concentrations tested the compounds were not toxic to the HepG2 cells according to the results of the MTT test (data not shown). The results of Figure 7B reveal that ME-3'-N^2-dG formation in HepG2 cells exposed to 1′-hydroxymethyleugenol was almost completely blocked by co-exposure to the model SULT inhibitor PCP. For nevadensin, a dose dependent inhibition was observed with 0.2 and 2 µM inhibiting ME-3'-N^2-dG formation in HepG2 cells exposed to 1′-hydroxymethyleugenol by 80 and 88 % respectively.

A.

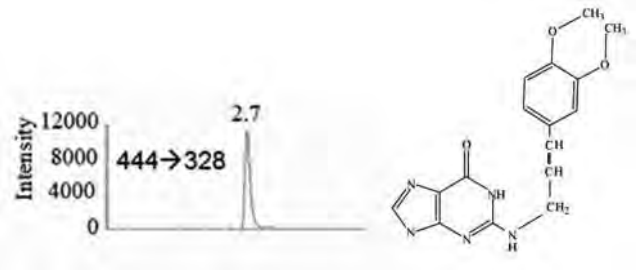

B.

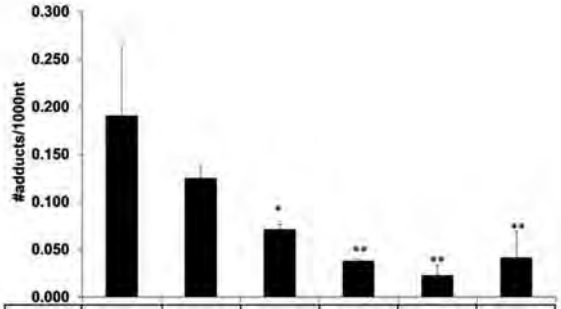

1'HME µM	100	100	100	100	100	100
NEV µM	0	0.002	0.02	0.2	2	0
PCP µM	0	0	0	0	0	12.5

Figure 7. LC-MS/MS chromatogram of the adduct (444→328) formed in human HepG2 cells exposed to 100 µM 1′-hydroxymethyleugenol (A) and DNA adduct levels detected in human HepG2 cells treated with 100 µM 1′-hydroxymethyleugenol (1′HME) and increasing concentration of nevadensin (NEV) or 12.5 µM pentachlorophenol (PCP) as positive control (B). Data points represent mean (± SD) of triplicate measurements obtained in independent experiments. An asterisk (*) indicates a significant inhibition compared to the incubation without inhibitor, * $p < 0.05$; ** $p \leq 0.01$.

PBK-based predictions for methyleugenol phase II metabolism in the presence of nevadensin

Figure 8 illustrates the PBK predicted effect of an increasing dose of nevadensin (expressed as molar ratio to the dose of methyleugenol, which was kept at a constant value of 0.217 mg/(kg

bw) or 50 mg/(kg bw) respectively in Figure 8A and 8B) on the formation of 1′-sulfooxymethyleugenol in male rat and human liver. The data calculated for varying molar ratios of nevadensin to methyleugenol also reflect what would happen if the bioavailability of nevadensin would be lower than 100%, which is not unlikely given the value of 20% reported in literature (Han *et al.*, 1981). As predicted by the PBK model, the co-administration of a dose of methyleugenol of 0.217 mg/(kg bw) (SCF, 2001) together with an increasing dose of nevadensin will lead to a dose dependent decrease in the formation of the ultimate DNA reactive metabolite 1′-sulfooxymethyleugenol (Figure 8A), whereas the levels of 1′-hydroxymethyleugenol glucuronide and 1′-oxomethyleugenol formation were predicted to remain unaffected (data not shown). Assuming 100% uptake of nevadensin and hepatic clearance similar to that of methyleugenol, the PBK model predicts that at a molar ratio between methyleugenol and nevadensin of 1, a 92.2% and 97.7% inhibition of the formation of 1′-sulfooxymethyleugenol in the liver of male rat and human can be expected (Figure 8A). Assuming 1% instead of 100% uptake of nevadensin (equivalent to a nevadensin to methyleugenol molar ratio of 0.01), the model still predict about 27.5 % and 60.4 % inhibition of 1′-sulfooxymethyleugenol formation as compared to control in male rat and human respectively (Figure 8A).

Figure 8B presents the results obtained when the same PBK modeling was performed at a dose of methyleugenol of 50 mg/(kg bw) (Smith *et al.*, 2002). At a molar ratio of nevadensin to methyleugenol of 0.06 (assuming the same ratio at which the nevadensin and the related alkenylbenzene estragole are expected to be present in dried basil (Alhusainy *et al.*, 2010)) the model predicts an almost complete inhibition of 1′-sulfooxymethyleugenol formation in the liver of male rat and human when assuming 100% uptake of nevadensin (Figure 8B). At the same molar ratio of 0.06 but assuming 1% uptake of nevadensin (theoretically equivalent to a nevadensin to methyleugenol molar ratio of 6×10^{-4}), the PBK model still predicts 85% and 93% inhibition of 1′-sulfooxymethyleugenol formation in the two species respectively (Figure 8B).

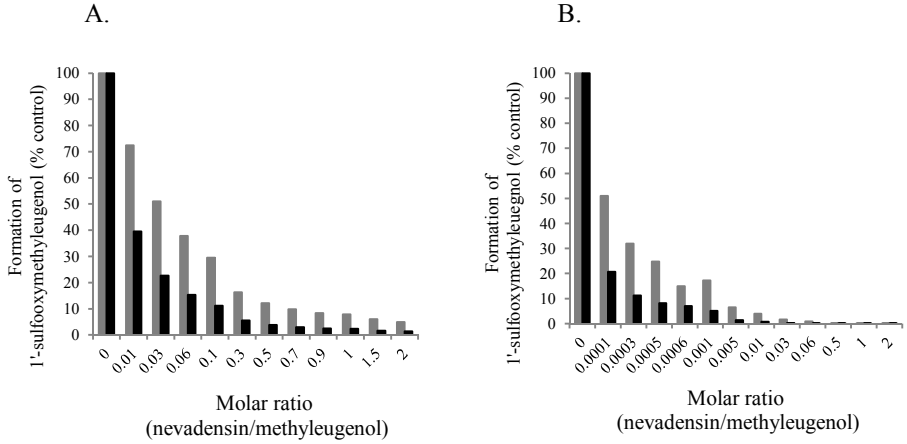

Figure 8. PBK-based predictions for the dose-dependent effect of nevadensin on 1′-sulfooxymethyleugenol formation in the liver of male rat (grey bar) and human (black bar) at (A) 0.217 mg/(kg bw) and (B) 50 mg/(kg bw) of methyleugenol.

Discussion

Methyleugenol is an alkenylbenzene that occurs in many herbs and spices. The compound is carcinogenic in various livers of mice and rats when administered at high dose levels but negative in standard *in vitro* genotoxicity tests (Ding *et al.*, 2011). It has been indicated that hydroxylation followed by sulfonation is an important bioactivation pathway leading to DNA adduct formation and eventually tumor formation by methyleugenol in animal models (Smith *et al.*, 2002).

In a previous study, it was demonstrated that the flavonoid nevadensin, which is an important constituent of herbs like basil (Grayer *et al.*, 1996), is able to inhibit the bioactivation of the related alkenylbenzene estragole to its DNA reactive metabolite at the level of the SULT mediated conversion of 1′-hydroxyestragole to 1′-sulfoxyestragole (Alhusainy *et al.*, 2010; Jeurissen *et al.*, 2008). The objective of the present study was to examine whether the herb

based constituent nevadensin would also be able to inhibit the SULT mediated bioactivation of methyleugenol and its subsequent formation of DNA adducts, and to investigate the possible *in vivo* consequences of such an inhibition using PBK modeling. The effect of nevadensin on the SULT mediated DNA adduct formation by 1′-hydroxymethyleugenol was investigated in the human hepatoma cell line HepG2. HepG2 cells contain different enzymes involved in the metabolism of 1′-hydroxymethyleugenol such as SULT and UDP-glucuronosyltransferases (Brandon *et al.*, 2003, 2006; Knasmuller *et al.*, 1998). A method for the quantification of ME-3′-N^2-dG was developed based on a recently developed LC-MS/MS method also suitable to quantify the corresponding adducts from estragole (Punt *et al.*, 2007). Incubations with human HepG2 cells exposed to 1′-hydroxymethyleugenol in the presence of increasing concentrations of nevadensin revealed a dose-dependent inhibition of ME-3′-N^2-dG formation by nevadensin at concentrations ranging from 0.002 to 2 μM. At 2 μM ME-3′-N^2-dG formation was inhibited by 88%.

In subsequent investigations of the present study the inhibition of SULT by nevadensin was incorporated into our PBK models for methyleugenol bioactivation and detoxification in male rat and human (Al-Subeihi *et al.*, 2011, 2012). These modified PBK models allow evaluation of the bioactivation and detoxification of methyleugenol in the liver of male rat and human when exposure to methyleugenol is combined with exposure to nevadensin. This approach illustrates the conclusions reported before that PBK modeling facilitates the extrapolation of the occurrence and magnitude of interactions of binary mixtures from the *in vitro* to the *in vivo* situation (Krishnan *et al.*, 2002). The modified PBK models described in the present study allowed prediction of the dose-dependent inhibition of the formation of the ultimate DNA reactive metabolite 1′-sulfooxymethyleugenol in the liver of male rat and human administered methyleugenol in the presence of nevadensin. The models also predict the nevadensin-mediated changes in the overall formation of the metabolites that reflect detoxification by glucuronidation and oxidation of 1′-sulfooxymethyleugenol. The present PBK models do not contain a sub-model for nevadensin since that would be a study in itself. We defined the *Ki* for inhibition of SULT activity by nevadensin and included this inhibition kinetics in the model. As

a first approximation for the ADME (absorption, distribution, metabolism and excretion) characteristics of nevadensin we assumed these characteristics to be similar to those of methyleugenol, resulting in a fixed ratio between the concentration of methyleugenol and that of nevadensin at any point in time. Possible differences in the uptake and kinetics of nevadensin compared to that of methyleugenol were investigated by modeling several ratio′s between nevadensin and methyleugenol with a ratio of 1 assuming similar uptake, but a ratio of 0.01 assuming only 1 % uptake of nevadensin as compared to 100% methyleugenol uptake. In this way the effect of nevadensin ADME characteristics on the inhibition of methyleugenol bioactivation could be evaluated without the need for parameterization and individual nevadensin sub-model. Different molar ratios of the two compounds were modeled to provide some insight in the effects of possible differences in kinetics and bioavailability of the two compounds. The PBK models developed predict that at a methyleugenol dose level of 50 mg/(kg bw) and a nevadensin to methyleugenol ratio of 0.06, the estimated ratio between the nevadensin and the related alkenylbenzene estragole in basil, nevadensin would inhibit 1′-sulfooxymethyleugenol formation in male rat and human liver by respectively 98% and 99% or 85% and 93% assuming 100 or 1% nevadensin uptake respectively. Thus formation of 1′-sulfooxymethyleugenol is expected to be significantly, though not completely, blocked. Other flavonoids that are part of the human diet, including quercetin, possess a potent SULT inhibitory activity as well (De Santi *et al.*, 2002; Gibb *et al.*, 1987; Marchetti *et al.*, 2001; Morimitsu *et al.*, 2004) implying that the formation of 1′-sulfooxymethyleugenol could be even lower due to the combination of methyleugenol exposure with other food borne SULT inhibitors together with nevadensin from basil (Alhusainy *et al.*, 2012). Moreover, not only can the bioactivation of allylalkoxybenzenes be affected by the food matrix but also their bioavailability might be reduced (Schilter *et al.*, 2003) due to reduced absorption from the gastrointestinal tract which can be attributed to slow or inadequate release of allylalkoxybenzenes from the complex food matrix. Support for this possible limited release of methyleugenol from a food matrix can be found in our previous work where PBK model based predictions for methyleugenol blood levels were compared to data from a study in which nine

volunteers consumed a meal consisting of gingersnaps containing approximately 0.216 mg methyleugenol (0.0034 mg/(kg bw), considering an average body weight of 63.8 kg) (Schecter *et al.*, 2004). The serum blood levels of the volunteers were measured at different time points and compared to the venous blood levels of PBK model-based predictions for blood levels of methyleugenol (Al-Subeihi *et al.*, 2012). The results obtained revealed that the PBK model predicted blood concentrations of methyleugenol were higher than the actually measured ones (Al-Subeihi *et al.*, 2012); a discrepancy that may be due to limited bioavailability of methyleugenol from the ginger snap food matrix as compared to the 100% bioavailability of methyleugenol assumed in the PBK modeling. At 13.8 % bioavailability of methyleugenol from the ginger snaps predicted and observed venous blood levels of methyleugenol were similar. Another point of interest is that the modeling also reveals that the effect of a given ratio of nevadensin to methyleugenol on 1′-sulfooxymethyleugenol formation varies with the dose of methyleugenol. Thus at a molar ratio of nevadensin to methyleugenol of 0.06, the percentage of inhibition decreases going from 98% and 99 % at a methyleugenol dose of 50 mg/(kg bw) to 62.2% and 84.7% at a methyleugenol dose of 0.217 mg/(kg bw) in male rat and human liver, respectively. This can be explained by the fact that the concentration of the inhibitor nevadensin is higher in the former situation (at 50 mg/(kg bw)) than in the latter situation (at 0.217 mg/(kg bw)) resulting in more efficient inhibition given the K_i of 4 nM. This is a well-known characteristic of non-competitive inhibition (Simmons, 1996). Altogether, the PBK modeling reveals that the inhibition of SULT mediated bioactivation to 1′-sulfooxymethyleugenol upon combined exposure to methyleugenol and nevadensin may be significant even at realistic low dose human exposure levels and even when the uptake of nevadensin would be significantly lower than 100%. The efficiency of nevadensin in inhibiting the sulfonation of 1′-hydroxymethyleugenol and thus its potential protective effect against bioactivation of methyleugenol to the proximate DNA reactive metabolite still needs to be established in *in vivo* experiments where factors such as its bioavailability and metabolic stability will play a crucial role. Recent studies in which estragole was dosed to rats in either the absence or presence of nevadensin revealed significant reduction in the amount of estragole DNA adducts formed in

the liver upon co-administration of estragole with the flavonoid SULT inhibitor nevadensin (Alhusainy *et al.*, 2012), suggesting that the effects observed in the present study for methyleugenol may in future also appear relevant for the *in vivo* situation. Of interest in this respect is as well that methylated flavones such as nevadensin have been demonstrated to be much more metabolically stable than their non-methylated analogues which is reflected by their resistance to hepatic metabolism and stability in the intestinal epithelial cell layer (Walle, 2007; Wen and Walle, 2006). Furthermore, they also have higher intestinal absorption through Caco-2 cell monolayers (Walle, 2007; Wen and Walle, 2006). Both factors should increase their oral bioavailability as compared to the bioavailability of non-methylated flavones.

In conclusion, the present study points at an important matrix effect of combined exposure to methyleugenol and nevadensin. SULT inhibition was shown to lead to the inhibition of the formation of the ultimate DNA reactive metabolite. If, like for estragole, the PBK predicted data can be validated *in vivo*, which is an important issue for future research, this would imply that the consumption of methyleugenol within a matrix of sweet basil or other food items containing SULT inhibitors would pose a risk that is lower than what would be estimated based on results from rodent bioassays in which methyleugenol is dosed as a pure compound by gavage without the relevant food matrix being present.

Acknowledgement

The authors would like to thank the Nestlé Research Centre for providing the LC-MS/MS API 3000 instrument. This work was supported by a grant from sandwich PhD fellowship program / Wageningen University, the Netherlands.

References

Alhusainy, W., Paini, A., Punt, A., Louisse, J., Spenkelink, B., Vervoort, J., Delatour, T.,Scholz, G., Schilter, B., Adams, T., van Bladeren, P.J., and Rietjens, I.M.C.M. (2010). Identification of Nevadensin as an Important Herb-Based Constituent Inhibiting Estragole bioactivation and Physiology-Based Biokinetic Modeling of Its Possible in vivo Effect, Toxicol Appl Pharm 245, 179-190.

Alhusainy, W., van den Berg, S. J.P.L., Paini, A., Campana, A., Asselman, M., Spenkelink, A., Punt, A., Scholz, G., Schilter, B., Adams, T.B., van Bladeren, P.J., and Rietjens, I.M.C.M. (2012). Matrix modulation of the bioactivation of estragole by constituents of different alkenylbenzene-containing herbs and spices and physiologically based biokinetic modeling of possible in vivo Effects. Toxicol Sic 129, 174-187.

Al-Subeihi, A.A.A., Spenkelink, B., Boersma, M. G., Punt, A.,van Bladeren, P.J., and Rietjens, I.M.C.M. (2012). Physiologically based kinetic modeling of bioactivation and detoxification of the alkenylbenzene methyleugenol in human as compared with rat. Toxicol Appl Pharm 260, 271-284.

Al-Subeihi, A.A.A., Spenkelink, B., Rachmawati, N., Boersma, M.G., Punt, A., Vervoort, J.,van Bladeren, P.J., and Rietjens, I.M.C.M. (2011). Physiologically based biokinetic model of bioactivation and detoxification of the alkenylbenzene methyleugenol in rat. Toxicol In Vitro 25, 267-285.

Boberg, E.W., Miller, E.C., Miller, J.A., Poland, A. and Liem, A. (1983). Strong evidence from studies with brachymorphic mice and pentachlorophenol that 1′-sulfooxysafrole is the major ultimate electrophilic and carcinogenic metabolite of 1′-hydroxysafrole in mouse liver. Cancer Res 43, 5163–5173.

Brandon, E.F.A., Bosch, T.M., Deenen, M.J., Levink, R., van der Wal, E., van Meerveld, J.B., Bijl, M., Beijnen, J.H., Schellens, J.H.M., and Meijerman, I. (2006). Validation of in vitro cell models used in drug metabolism and transport studies; genotyping of cytochrome P450,

phase II enzymes and drug transporter polymorphisms in the human hepatoma (HepG2), ovarian carcinoma (IGROV-1) and colon carcinoma (CaCo-2, LS180) cell lines. Toxicol Appl Pharmacol 211, 1–10.

Brandon, E.F., Raap, C.D., Meijerman, I., Beijnen, J.H., and Schellens, J.H. (2003). An update on in vitro test methods in human hepatic drug biotransformation research: Pros and cons. Toxicol Appl Pharmacol 189, 233-246.

Brown, R.P., Delp, M.D., Lindstedt, S.L., Rhomberg, L.R., and Beliles, R.P. (1997). Physiological parameter values for physiologically based pharmacokinetic models. Toxicol Ind Health 13, 407-484.

Burdock, G.A., ed. (1995). Fenaroli′s Handbook of Flavor Ingredients, Vol. II, 3rd Edition, CRC Press, Boca Raton, FL.

Burkey J.L., Sauer J.M., McQueen C.A., and Sipes I.G. (2000). Cytotoxicity and genotoxicity of methyleugenol and related congeners – a mechanism of activation for methyleugenol. Mutat Res 453, 25-33.

DeJongh, J.,Verhaar, H.J., and Hermens, J.L. (1997). A quantitative property-property relationship (QPPR) approach to estimate in vitro tissue-blood partition coefficients of organic chemicals in rats and humans. Arc Toxicol. 72, 17-25.

De Santi, C., Pietrabissa, A., Mosca, F., Rane, A., and Pacifici, G.M. (2002). Inhibition of phenol sulfotransferase (SULT1A1) by quercetin in human adult and foetal livers. Xenobiotica 32, 363–368.

Ding, W., Levy, D.D., Bishop, M.E., Lyn-Cook Lascelles, E., Kulkarni, R., Chang, C.W., Aidoo, A., and Manjanatha, M.G. (2011). Methyleugenol genotoxicity in the Fischer 344 rat using the comet assay and pathway-focused gene expression profiling. Toxicol Sci 123,103-112.

Drinkwater, N.R., Miller, E.C., Miller, J.A., and Pitot, H.C. (1976). Hepatocarcinogenicity of estragole (1-allyl-4-methoxybenzene) and 1′-hydroxyestragole in the mouse and mutagenicity of 1'-acetoxyestragole in bacteria. J Natl Cancer Inst 57, 1323-1331.

European Commission (2008). Regulation (EC) No 1334/2008 of the European Parliament and

of the Council of 16 December 2008 on flavourings and certain food ingredients with flavouring properties for use in and on foods and amending Council Regulation (EEC) No 1601/91, Regulations (EC) No 2232/96 and (EC) No 110/2008 and Directive 2000/13/EC. Off J Eur Union, L354/34: http://eur-lex.europa.eu/LexUriServ/LexUriServ.do?uri=OJ:L:2008:354:0034:0050:en:pdf

Gardner, I., Wakazono, H., Bergin, P., Waziers, I., Beaune, P., Kenna, J.G., and Caldwell, J. (1997). Cytochrome P450 mediated bioactivation of methyleugenol to 1′-hydroxymethyl-eugenol in Fischer 344 rat and human liver microsomes. Carcinogenesis 18, 1775-1783.

Gibb, C., Glover, V., and Sandler, M. (1987). In vitro inhibition of phenolsulphotransferase by food and drink constituents. Biochem Pharmacol 36, 2325–2330.

Grayer, R.J., Bryan, S.E., Veitch, N.C., Goldstone, F.J., Paton, A., and Wollenweber, E. (1996). External flavones in sweet basil, Ocimum basilicum, and related taxa. Phytochemistry 43, 1041–1047.

Han, G.Z., Su, C.Y., and Zhang, Y. (1981). Determination of nevadensin in biological specimens and its pharmacokinetic study. Acta Pharmacol Sin 2, 182–185.

Herrmann, K., Engst, W., Appel, K.A., Monien, B.H., and Glatt, H. (2012). Identification of human and murine sulfotransferases able to activate hydroxylated metabolites of methyleugenol to mutagens in Salmonella typhimurium and detection of associated DNA adducts using UPLC–MS/MS methods. Mutagenesis 15, 1–10.

Hussain, R.F., Nouri, A.M., and Oliver, R.T. (1993). A new approach for measurement of cytotoxicity using colorimetric assay. J Immunol Methods 160, 89.

Jeurissen, S.M.F., Punt, A., Delatour, T., and Rietjens, I.M.C.M. (2008). Basil extract inhibits the sulfotransferase mediated formation of DNA adducts of the procarcinogen 1′-hydroxyestragole by rat and human liver S9 homogenates and in HepG2 human hepatoma cells. Food Chem Toxicol 46, 2296–2302.

Knasmuller, S., Parzefall, W., Sanyal, R., Ecker, S., Schwab, C., Uhl, M., Mersch-Sunermann, V., Williamsen, G., Hietsch, G., Langer, T., Darroudi, F., and Natarajan, A.T. (1998). Use of metabolically competent human hepatoma cells for the detection of mutagens and

antimutagens. Mutat Res 402, 185–202.

Krishnan, K., Haddad, S., Béliveau, M., and Tardif, R. (2002). Physiological modeling and extrapolation of pharmacokinetic interactions from binary to more complex chemical mixtures. Environ Health Perspect. 110, 989–994.

Leung A.Y., ed. (1980). Encyclopedia of Common Natural Ingredients. John Wiley and Sons, New York.

Marchetti, F., De Santi, C., Vietri, M., Pietrabissa, A., Spisni, R., Mosca, F., and Pacifici, G.M. (2001). Differential inhibition of human liver and duodenum sulphotransferase activities by quercetin, a flavonoid present in vegetables, fruit and wine. Xenobiotica 31, 841–847.

Miele, M., Dondero, R., Ciarallo, G., and Mazzei, M.J. (2001). Methyleugenol in Ocimum basilicum L.cv. Genovese Gigante. J Agr Food Chem 49, 517-21.

Miller, E.C., Swanson, A.B., Phillips, D.H., Fletcher, T.L., Liem, A., and Miller, J. (1983). Structure-activity studies of the carcinogenicities in the mouse and rat of some naturally occurring and synthetic alkenylbenzene derivatives related to safrole and estragole. Cancer Res 1983, 1124-1134.

Morimitsu, Y., Sugihara, N., and Furuno, K. (2004). Inhibitory effect of flavonoids on sulfo and glucurono-conjugation of acetaminophen in rat cultured hepatocytes and liver subcellular preparations. Biol Pharm Bull 27, 714–717.

Mosmann, T. (1983). Rapid colorimetric assay for cellular growth and survival: Application to proliferation and cytotoxicity assays. J Immunol Methods 65, 55-63.

NTP (1998). Toxicology and carcinogenesis studies of methyleugenol (CAS No. 93-15-12) in F344/N Rats and B6C3F1 Mice (Gavage Studies). Natl Toxicol Program Tech Rep Ser 491. NIH Publication No. 98-3950.

NTP (2000). Toxicology and carcinogenesis studies of methyleugenol (CAS No. 93-15-12) in F344/N rats and B6C3F1 mice (Gavage studies). Natl Toxicol Program Tech Rep Ser, 491, 1-412.

Paini, A., Punt, A., Viton, F., Scholz, G., Delatour, T., Marin-Kuan, M., Schilter, B., van Bladeren, P.J., and Rietjens, I.M.C.M. (2010). A physiologically based biodynamic (PBBD)

model for estragole DNA binding in rat liver in vivo based on in vitro kinetic data and estragole DNA adduct formation in rat primary hepatocytes. Toxicol Appl Pharmacol 245, 57-66.

Phillips, D.H., Miller, J.A., Miller, E.C., and Adams, B. (1981). Structures of the DNA adducts formed in mouse liver after administration of the proximate hepatocarcinogen 1′-hydroxyestragole. Cancer Res 41, 176-186.

Punt, A., Delatour, T., Scholz, G., Schilter, B., Bladeren, P.J., and Rietjens, I.M.C.M. (2007). Tandem Mass spectrometry analysis of N^2-(*trans*-Isoestragol-3′-yl)-2′-deoxyguanosine as a strategy to study species differences in sulfotransferase Conversion of the Proximate Carcinogen 1′-Hydroxyestragole. Chem Res Toxicol 20, 991-998.

SCF (2001). Opinion of the Scientific Committee on Food on Methyleugenol (4-allyl-1,2-dimethoxybenzene). European Commission, Scientific Committee on Food. Brussels, BE. http://ec.europa.eu/food/fs/sc/scf/out102_en.pdf

Schecter, A., Lucier, G.W., Cunningham, M.L., Abdo, K.M, Blumenthal, G., Silver, A.G., Melnick, R., Portier, C., Barr, D.B., Barr, J.R., Stanfill, S.P., Patterson Jr., D.G., Needham, L.L., Stopford, W., Masten, S., Mignogna, J., and Tung, K.C. (2004). Human consumption of methyleugenol and its elimination from serum. Environ Health Persp 112, 678-680.

Schilter, B., Andersson, C., Anton, R., Constable, A., Kleiner, J., O'Brien, J., Renwick, A.G., Korver, O., Smit, F., and Walker, R. (2003). Guidance for the safety assessment of botanicals and botanical preparations for use in food and food supplements. Food Chem Toxicol 41, 1625–1649.

Simmons, J.E. (1996). Application of physiologically based pharmacokinetic modeling to combination toxicology. Food Chem Toxicol 34, 1067–1073.

Smith, R.L., Adams, T.B., Doull, J., Feron, V., Goodman, J.I., Marnett, L.J., Portoghese, P.S., Waddell, W.J., Wagner, B.M., Rogers, A.E., Caldwell, J., and Sipes, I.G. (2002). Safety assessment of allylalkoxybenzene derivatives used as flavoring substances methyleugenol and estragole. Food Chem Toxicol 40, 851-870.

Smith, B., Cadby, P., Leblanc, J., and Setzer, R. (2010). Application of the margin of exposure

(MoE) approach to substances in food that are genotoxic and carcinogenic. Example: Methyleugenol, CASRN: 93-15-2. Food Chem. Toxicol 48, S89-S97.

Walle, T. (2007). Methylation of dietary flavones greatly improves their hepatic metabolic stability and intestinal absorption. Mol Pharm 4, 826–832.

Wen, X., and Walle, T. (2006). Methylated flavonoids have greatly improved intestinal absorption and metabolic stability. Drug Metab Dispos 34, 1786–1792.

Wiseman, R.W., Fennell, T.R., Miller, J.A., and Miller, E.C. (1985). Further characterization of the DNA adducts formed by electrophilic esters of the hepatocarcinogens 1′-hydroxysafrole and 1′-hydroxyestragole in vitro and in mouse liver in vivo, including new adducts at C-8 and N-7 of guanine residues. Cancer Res 45, 3096-3105.

5

Evaluation of the interindividual human variation in bioactivation of methyleugenol using physiologically based kinetic modeling and Monte Carlo simulation

Based on: Al-Subeihi, A. A. A., Kiwamoto, R., Spenkelink, B., van Bladeren, P.J., Rietjens, I. M.C.M., and Punt, A.
In preparation

Abstract

The present study aims at predicting the level of formation of the ultimate carcinogenic metabolite of methyleugenol 1′-sulfooxymethyleugenol in the human population by taking the variability in key bioactivation and detoxification reactions into account using Monte Carlo simulations. Insight in the variation in relevant metabolic routes was obtained by determining kinetic constants for the metabolic reactions by specific isoenzymes or by measuring the kinetic constants in incubations with a range of individual human liver fractions. The results of the study indicate that formation of 1′-sulfooxymethyleugenol is predominantly affected by i) P450 1A2 catalyzed bioactivation of methyleugenol to 1′-hydroxymethyleugenol ii) P450 2B6 catalyzed epoxidation of methyleugenol and iii) the apparent kinetic constants for detoxification of 1′-hydroxymethyleugenol via oxidation and iv) the apparent kinetic constants for bioactivation of 1′-hydroxymethyleugenol to 1′-sulfooxymethyleugenol. Based on the Monte Carlo simulation a chemical-specific adjustment factor (CSAF) for intraspecies variation could be derived which is defined as the 95th or 99th percentile divided by the 50th percentile of the predicted distribution of the formation of 1′-sulfooxymethyleugenol in the liver. The obtained CSAF value at the 95th percentile was 3.7 indicating that the default uncertainty factor of 3.16 for human variability in kinetics may adequately protect 95% of the population. Protecting 99% of the population requires a larger uncertainty factor of 5.8.

Introduction

Methyleugenol (3,4-dimethoxyallylbenzene) is a member of a family of chemicals known as alkoxy allylbenzenes which includes also compounds such as safrole and estragole (Robison and Barr, 2006). Methyleugenol enters the diet via different food sources like herbs and spices (e.g. basil, sweet bay, cloves and lemon grass) which are consumed at low levels in the human diet (Gardner *et al.*, 1997). Methyleugenol was selected to be studied by the National Toxicology Program (NTP) because of its broad use and its structural resemblance to the other carcinogenic alkoxy allylbenzenes including safrole and estragole. Based on the results of the National Toxicology Program (NTP) study, methyleugenol revealed a carcinogenic effect in both F344 rat and B6C3F1 mice (NTP, 2000). The Expert Panel of the Flavor and Extracts Manufacturers Association (FEMA) classified methyleugenol as GRAS (generally recognized as safe) at the proposed levels of flavor use in 1965 (Hall and Oser, 1965). In 2001, the FEMA Panel reassessed the available data for methyleugenol and confirmed that there is no considerable cancer risk resulting from consumption of methyleugenol as flavouring substance and affirmed the GRAS status of methyleugenol as a flavoring substance given the low levels of exposure (Smith *et al.*, 2002). In 2001, the Scientific Committee on Food (SCF) of the European Union published a scientific opinion on methyleugenol in which it was concluded that methyleugenol is genotoxic and carcinogenic and that reductions in exposure and restrictions in use levels are indicated (SCF, 2001). The average daily intake of methyleugenol was estimated by the SCF to be 13 mg/day, corresponding to 0.217 mg/(kg bw)/day for a 60 kg person (SCF, 2001). The FEMA, using a different methodology, estimated the average daily intake of methyleugenol to be less than 0.01 mg/(kg bw)/day (Smith *et al.*, 2002). The estimation of the SCF was based on theoretical maximum use levels of methyleugenol in various food categories and consumption data for these food categories, whereas the intake estimation of the FEMA was based on production volume data for flavor use (SCF, 2001; Smith *et al.*, 2002).

Methyleugenol is unreactive by itself and requires metabolic activation to produce electrophilic metabolites that act as the DNA reactive intermediates (Gardner et al., 1997; Miele *et al.*, 2001). Figure 1 displays the metabolic pathways of methyleugenol. Important metabolic pathways include *O*-demethylation of the methoxy moieties on the benzene ring, and 2′,3′-epoxidation and 1′-hydroxylation of the allylic side chain (NTP, 2000; Solheim and Scheline, 1976). *O*-demethylation of the methoxy substituents of methyleugenol yields the corresponding phenolic derivatives, which may be excreted as sulfate or glucuronic acid conjugate (Smith *et al.*, 2002). Epoxidation of the side chain yields a 2′,3′-epoxide. This epoxide is detoxified by epoxide hydrolase to form the dihydrodiol or via glutathione conjugation (Luo and Guenther, 1995). Hydroxylation at the 1'-position of methyleugenol is considered to represent the bioactivation pathway producing the proximate carcinogenic metabolite 1′-hydroxymethyleugenol (Drinkwater *et al.*, 1976; Miller *et al.*, 1983). In a next step 1′-hydroxymethyleugenol can be sulfonated by sulfotransferases to form 1'-sulfooxymethyleugenol which readily undergoes desulfonation to a reactive carbo-cation that can form DNA or protein adducts (Miller *et al.*, 1983).

Genotype- and lifestyle-based factors can influence the activity of the enzymes involved in the bioactivation and detoxification of methyleugenol which could in theory lead to large variability in the level of formation of the ultimate carcinogenic metabolite 1′-sulfooxymethyleugenol. Results from previously published physiologically based kinetic (PBK) models for methyleugenol in rat and human (Al-Subeihi *et al.*, 2011, 2012), and sensitivity analyses for these models, revealed that formation of 1′-sulfooxymethyleugenol is mainly affected by the kinetic constants for 1′-hydroxylation, *O*-demethylation, and epoxidation of methyleugenol as well as kinetic constants for oxidation and sulfonation of 1′-hydroxymethyleugenol. For male rat the formation of 1′-sulfooxymethyleugenol was furthermore significantly affected by the extent of glucuronidation of 1′-hydroxymethyleugenol (Al-Subeihi *et al.*, 2011). The present study aims at predicting the level of formation of 1′-sulfooxymethyleugenol in the human population by taking the variability in these metabolic reactions into account using Monte Carlo simulations. Insight in the variation in the key metabolic

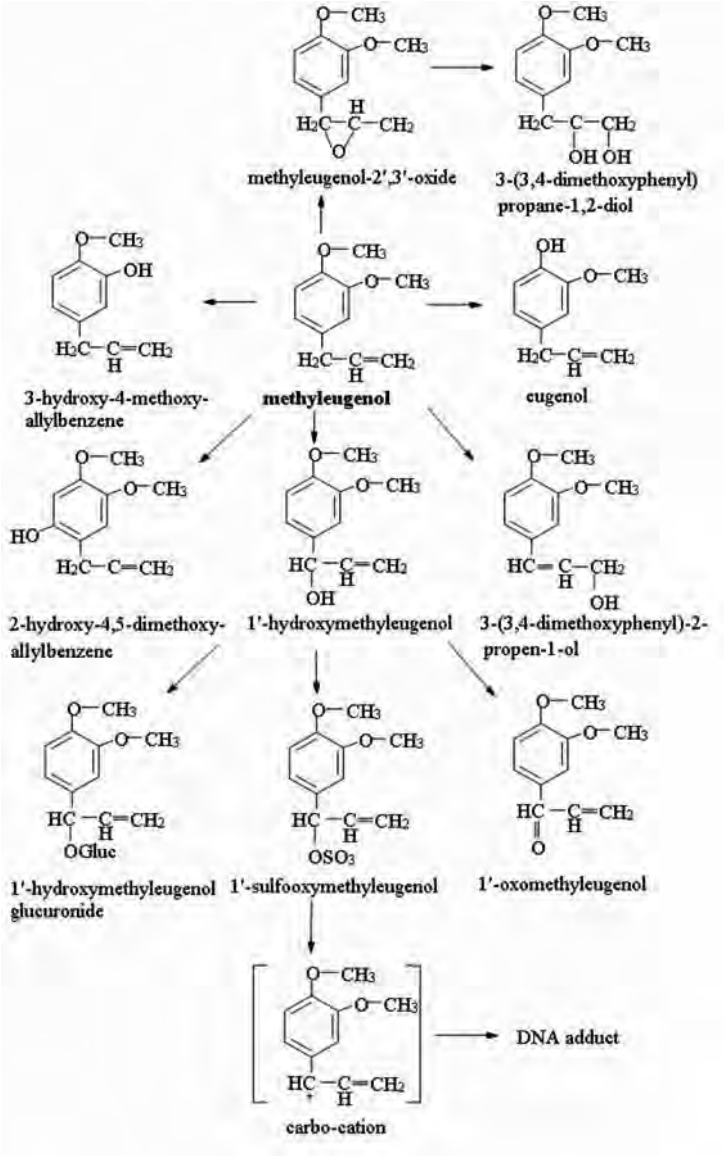

Figure 1. Suggested metabolic pathways of methyleugenol.

routes was obtained by determining kinetic constants for the metabolic reactions by specific isoenzymes and taking the literature reported level of variation in activity of these enzymes in the population into account or, when specific isoenzymes were not commercially available, by measuring the kinetic constants in incubations with a range of individual human liver fractions. Altogether the results of the present study allow evaluation of human interindividual variation in the formation of the ultimate carcinogenic metabolite 1′-sulfooxymethyleugenol within the population as a whole.

Materials and Methods

Chemicals and reagents

Supersomes expressing the human P450 enzymes 1A2, 2A6, 2B6, 2C8, 2C9*1, 2C19, 2D6*1, 2E1, or 3A4, supersomes expressing the human UGT enzymes UGT1A1, 1A3, 1A4, 1A6, 1A7, 1A8, 1A9, 1A10, 2B4, 2B7, 2B15, or 2B17 and pooled human liver microsomes were obtained from BD Gentest (Woburn, MA, USA). Twenty individual human liver S9 homogenates were purchased from Xenotech (Lenexa, Kansas, USA). Two individual human liver S9 homogenates were purchased from Celsis (Brussels, Belgium). Hydrochloric acid (37%), potassium dihydrogen phosphate, dipotassium hydrogen phosphate trihydrate, and acetic acid were purchased from VWR International (Darmstadt, Germany). NADPH, $NADP^+$, NADH and NAD^+ were obtained from Roche Diagnostics (Mannheim, Germany). Methyleugenol, eugenol, methanol, ascorbic acid, dimethylsulfoxide (DMSO), alamethicin and uridine 5′-diphosphoglucuronic acid (UDPGA) were purchased from Sigma-Aldrich (Steinheim, Germany). Acetonitrile (UPLC/MS grade) was obtained from Biosolve (Valkenswaard, Netherlands). Glutathione (GSH) and 3′-phosphoadenosine-5′-phosphosulfate (PAPS) were obtained from Sigma Aldrich (Schnelldorf, Germany). 1′-Hydroxymethyleugenol, methyleugenol-2′,3′-oxide, 3-(3,4-dimethoxyphenyl)propane-1,2-diol, and 1′-oxomethyleugenol were synthesized and characterized as described previously (Al-Subeihi *et al.*, 2011).

Caution: 1′-hydroxymethyleugenol, methyleugenol-2′,3′-oxide, and 1′-oxomethyleugenol are carcinogenic and should be handled carefully.

Methods

1′-Hydroxylation, epoxidation, and *O*-demethylation of methyleugenol by cDNA recombinant P450 enzymes

Methyleugenol was incubated with supersomes expressing P450 1A2, 2A6, 2B6, 2C8, 2C9*1, 2C19, 2D6*1, 2E1, or 3A4 to determine the human cytochrome P450 enzymes involved in the 1′-hydroxylation, epoxidation, and *O*-demethylation of methyleugenol and the kinetic constants for these reactions. The incubations were performed in 160 μL incubation mixtures that contained (final concentrations) 3mM NADPH and 0.05 nmol P450/mL supersomes in 0.2 M Tris-HCl (pH 7.4). The reactions were started after 1 min preincubation at 37 °C by adding the substrate methyleugenol (ranging from 5 to 1000 μM final concentrations varying depending on the P450 enzyme studied and added from a 100 times concentrated stock solution in DMSO). The reactions were terminated after 10 min by adding 40 μL of ice-cold acetonitrile. All incubations were performed in triplicate, and control incubations were performed without NADPH. Samples were centrifuged for 5 min at 16,000 g and stored at −20 °C until HPLC analysis. Formation of phase I metabolites was quantified using the same HPLC conditions for analysis of phase I metabolites as previously described (Al-Subeihi *et al.*, 2012).

Glucuronidation of 1′-hydroxymethyleugenol by recombinant UGT enzymes

1′-Hydroxymethyleugenol was incubated with supersomes expressing UGT1A1, 1A3, 1A4, 1A6, 1A7, 1A8, 1A9, 1A10, 2B4, 2B7, 2B15, or 2B17 to determine the human UGT enzymes involved in glucuronidation of 1′-hydroxymethyleugenol. The incubation mixtures had a final volume of 200 μL, containing (final concentrations) 10 mM UDPGA, and 1 mg/mL protein in 0.2 M Tris-HCl (pH 7.4) containing 10 mM $MgCl_2$. To overcome enzyme latency, the

incubation mixtures were pre-treated on ice for 15 min with 0.025 mg/mL of the poreforming peptide alamethicin added from a 200 times concentrated stock in methanol (Fisher *et al.*, 2000; Lin and Wong, 2002). The reactions were started by the addition of 2000 μM of the substrate 1′-hydroxymethyleugenol from a 200 times concentrated stock solution in DMSO after pre-incubation of the incubation mixture at 37 °C for 1 min. The reactions were carried out for 6 hr and terminated by addition of 50 μL cold acetonitrile. Blank incubations were performed without the cofactor UDPGA. Samples were centrifuged for 5 min at 16,000 g and stored at −20 °C until HPLC analysis. The kinetic constants for glucuronidation of 1′-hydroxymethyleugenol by UGT1A9 and 2B7, which were observed to catalyse this reaction (see Results section), were determined using similar incubation conditions as described above but at different protein and substrate concentrations. In case of UGT1A9 incubations were performed at a protein concentration of 0.5 mg/mL and a substrate concentration ranging from 100 to 4000 μM and in case of UGT2B7 at a protein concentration of 1 mg/mL and a substrate concentration ranging from 250 to 4000 μM. Formation of 1′-hydroxymethyleugenol glucuronide by UGTs was quantified using the same HPLC conditions as previously described for detection of 1′-hydroxymethyleugenol glucuronide formed in incubations with pooled mixed human microsomes (Al-Subeihi *et al.*, 2012).

Oxidation of 1′-hydroxymethyleugenol by individual human liver S9 samples

The kinetics for oxidation of 1′-hydroxymethyleugenol by twenty two individual human liver S9 samples were determined as previously described by Al-Subeihi *et al.* (2012) for determining oxidation by pooled human liver fractions. Incubations were performed using NAD^+ and $NADP^+$ as cofactor and GSH to trap the reactive 1′-oxomethyleugenol at substrate concentrations that ranged from 100 to 3000 μM 1′-hydroxymethyleugenol. The incubation mixtures had a final volume of 200 μl, containing (final concentrations) 3 mM NAD^+, 3 mM $NADP^+$, 2 mM GSH, and 1 mg/mL S9 protein in 0.2 M Tris-HCl (pH 7.4). The reactions were terminated after 10 min by addition of 50 μL cold acetonitrile and the incubation mixtures were centrifuged for 5 min at 16,000 g and the supernatant was collected and stored at −20 °C until

UPLC analysis. To this end 3.5 µL of the samples were injected into an Acquity column BEH C18 1.7 µm 2.1*50 mm, with a guard column filter (Acquity, Waters). The runs were performed on an Acquity (Waters) UPLC system coupled to a PDA detector. The flow was 0.6 mL/min and the gradient started with 100% of 0.1% acetic acid in nanopure water and 0% of acetonitrile. After 0.57 min the amount of acetonitrile was increased to 25% and kept at 25% for 0.2 min, after which the acetonitrile amount was increased to 100% and kept at 100% for 30 s, after which starting conditions were reset. At these conditions the glutathione conjugate of 1'-oxomethyleugenol (GS-1′-oxomethyleugenol) eluted at 0.97 min. Blank incubations without the addition of NAD^+ and $NADP^+$ were performed for each individual human liver S9 fraction. The amount of 1'-oxomethyleugenol formed in the different samples was corrected for the amount formed in blank incubations. Quantification of GS-1′-oxomethyleugenol formed in these incubations with S9 was performed as described by Al-Subeihi *et al.* (2012).

Sulfonation of 1′-hydroxymethyleugenol by individual human liver S9 samples

To characterize the kinetics for sulfonation of 1'-hydroxymethyleugenol incubations with 5 individual human liver S9 homogenates (2 mg protein/mL final concentration) were performed as previously described by Al-Subeihi *et al.* (2012) in 0.1 M potassium phosphate (pH 8.2). Incubations contained different concentrations of the substrate 1'-hydroxymethyleugenol, at final concentrations ranging from 25 to 1000 µM (added from 100 times concentrated stock solutions in DMSO), PAPS (0.2 mM final concentration) as cofactor, and GSH (5 mM final concentration) as trapping agent of the transient 1'-sulfooxymethyleugenol. The final volume of the incubation was 100 µL. The reactions were started after 1 min preincubation at 37 °C by adding PAPS, and all incubations were carried out for 3 hr at 37 °C. The reactions were terminated by adding 25 µL acetonitrile, after which incubations were centrifuged for 5 min at 16,000 g and the supernatant was collected and stored at −80 °C until LC-MS/MS analysis. Blanks were made without the addition of PAPS and the amount of 1′-sulfooxymethyleugenol formed in the samples was corrected for the amount formed in these blank incubations. Formation of the glutathione conjugate with 1′-sulfooxymethyleugenol was quantified by LC-

MS/MS as described by Paini *et al.* (2012) for quantification of the guanosine conjugate of 1′-sulfooxyestragole.

PBK modeling and Monte Carlo simulation

The PBK model previously developed for methyleugenol in human (Al-Subeihi *et al.*, 2012) was used in the present study to integrate the kinetic data obtained. The model was adjusted by replacing the kinetic constants for 1′-hydroxylation, epoxidation, and *O*-demethylation of methyleugenol and the kinetic constants for glucuronidation, oxidation, and sulfonation of 1′-hydroxymethyleugenol, that were previously defined based on incubations with pooled human liver samples, with the kinetic constants obtained in the present study from incubations with recombinant enzymes or individual human liver S9 factions. All other model parameters as well as the differential equations were kept as they were previously defined (Al-Subeihi *et al.*, 2012). As a first step, the kinetic data obtained were used to simulate 1′-sulfooxymethyleugenol formation in an average individual human subject by taking average relative activity factors for recombinant enzymes into account and the average K_m and V_{max} values for sulfonation and oxidation of 1′-hydroxymethyleugenol as obtained in the present study with incubations of individual human liver S9 fractions. In case of 1′-hydroxyalation, epoxidation, and *O*-demethylation of methyleugenol by recombinant cytochrome P450 enzymes and glucuronidation of 1′-hydroxymethyleugenol by recombinant UGT enzymes the V_{max} values, expressed as nmol/min/(mg recombinant enzyme), were scaled to the liver according to the following equation:

$$V_{maxP450/UGT} * RAF_{P450/UGT} * MMPL * \text{Liver weight. (µmol/hr)},$$

in which the relative activity factor (RAF) represents relative activity of the different P450 enzymes or UGT enzymes in supersomes compared to pooled human liver microsomes as reported by Patten *et al.* (2009) and Stresser *et al.* (2009) for different P450 enzymes and as determined in the present study for the different UGT enzymes. MMPL represents the

microsomal protein yield of 32 mg/(g liver) (Barter *et al.*, 2007) and the liver weight represents an average weight of the liver corresponding to 1659 g in the present model. The RAFs for UGT1A9 and UGT2B7 were obtained by incubating both pooled human liver microsomes (1 mg/mL) and the supersomes expressing the UGT enzymes (1 mg/mL) with propofol (600 μM final concentration) as selective probe substrate for UGT1A9 and 3'-azido-3'-deoxythymidine (AZT) (5 mM final concentration) as selective probe substrate for UGT2B7. Incubations with these probe substrates were carried out using the same incubation conditions of glucuronidation of 1′-hydroxymethyleugenol with pooled human liver microsomes but the reaction was terminated after 1 hr for propofol and 30 min for AZT.

In case of oxidation and sulfonation, the average V_{max} values, expressed as nmol/min/(mg S9 protein) obtained from the incubations with different individual human tissue fractions were scaled to the liver according to the following equation:

$$V_{maxS9} * \text{S9PL} * \text{Liver weight. (μmol/hr)},$$

in which S9PL represents the S9 protein yield of 143 mg/(g liver) (Punt *et al.*, 2009) and the liver weight represents an average weight of the liver corresponding to 1659 g .

With this model, representing an average individual human subject, a sensitivity analysis was performed to analyze the relative effect of changes in activity levels of the recombinant P450 enzymes involved in 1′-hydroxylation, epoxidation, and *O*-demethylation of methyleugenol and the recombinant UGTs enzymes involved in glucuronidation of 1′-hydroxymethyleugenol as well as the relative effect of changes in activity levels of oxidation of 1′-hydroxymethyleugenol and other metabolic parameters on the formation of 1′-sulfooxymethyleugenol in human liver. Normalized sensitivity coefficients (SC) were determined according to the following equation: $SC = (C' - C)/(P' - P) * (P/C)$, where C is the initial value of model output, C' is the modified value of the model output resulting from an increase in parameter value, P is the initial parameter value, and P' is the modified parameter value (Rietjens *et al.*, 2011). Based on the literature a 5% increase in parameter values was

chosen, to analyze the effect of a change in parameter on the formation of 1′-sulfooxymethyleugenol expressed nmol/(g liver) over a 24 hr period of time (Evans and Andersen, 2000). Each parameter was analyzed individually, keeping the other parameters to their initial values.

In a second step, Monte Carlo simulations were performed to simulate the level of variation in the formation of 1′-sulfooxymethyleugenol that could occur in the population as a whole. For this analysis, a total of 10,000 simulations were performed, where in each simulation, the V_{max} values for 1′-hydroxylation, epoxidation and *O*-demethylation of methyleugenol by different P450 enzymes, the V_{max} values for glucuronidation of 1′-hydroxymethyleugenol by different UGT enzymes and the apparent V_{max} and K_m values for oxidation and sulfoantion of 1′-hydroxymethyleugenol were randomly taken from a log-normal distribution. The kinetic constants for the different metabolic reactions were assumed to vary independently. For this simulation, the mean μ_W and standard deviation σ_W describing the log-normal distribution of each V_{max} or K_m value were derived using the following equation (Zhang *et al.*, 2007):

$$\mu_W = \ln (\mu_X/\sqrt{(1+CV^2_X)}) \text{ and } \sigma_W^2 = \ln (1+ CV^2_X),$$

where μ_X is the average V_{max} or K_m and CV_X is the coefficient of variation for each of the reactions representing the extent of variability in the reaction. For P450 enzymes and UGT enzymes the coefficients of variation were obtained from the literature (Girard *et al.*, 2004; Holthe *et al.*, 2003; Rostami-Hodjegan and Tucker, 2007). The coefficients of variation in the V_{max} and K_m values for sulfonation and oxidation were obtained in the present study based on the incubations with individual human liver S9. The outputs were then analyzed statistically to calculate the different percentiles of the distribution of the predicted formation of 1′-sulfooxymethyleugenol using SPSS (IBM SPSS Version 19, IBM, NY, USA).

Results

Formation of 1′-hydroxymethyleugenol, methyleugenol-2′,3′-oxide and eugenol by cDNA recombinant expressed enzymes

Incubations with cDNA recombinant expressed P450 enzymes were performed to define the human P450 enzymes involved in the formation of 1′-hydroxymethyleugenol, methyleugenol-2′,3′-oxide, and eugenol. Among the different P450 enzymes P450 1A2, 2C9*1, 2C19, 2D6*1 and 3A4 were observed to be able to catalyse 1′-hydroxylation of methyleugenol. Epoxidation of methyleugenol to methyleugenol-2′,3′-oxide was observed to be catalysed by P450 2B6 and 2E1, whereas *O*-demethylation to eugenol was only catalysed by P450 1A2. The kinetic constants for each of these reactions were determined. Figure 2, Figure 3 and Figure 4, show the rate of formation of respectively 1′-hydroxymethyleugenol, methyleugenol-2′,3′-oxide and eugenol by the different cytochrome P450 enzymes, and Table 1 presents the kinetic constants derived from these data. In addition, Table 1 presents the V_{max} values that are scaled to the *in vivo* situation, as well as the *in vivo* catalytic efficiency of each enzyme. The results obtained show that although various enzymes are intrinsically capable of catalysing 1′-hydroxylation and epoxidation of methyleugenol, correcting for the *in vivo* relative activity of each of these enzymes shows that *in vivo* P450 1A2 is the main enzyme involved in 1′-hydroxylation of methyleugenol and P450 2B6 appears to be predominantly responsible for epoxidation of 1′-hydroxymethyleugenol. The highest overall *in vivo* catalytic efficiency was predicted for epoxidation (amounting to 159 L/hr), which was 1.6-fold higher than the sum of the catalytic efficiencies for 1′-hydroxylation by the different P450 enzymes (amounting to 98.7 L/hr), and 16.7-fold higher than the catalytic efficiency for *O*-demethylation to eugenol (amounting to 9.5 L/hr).

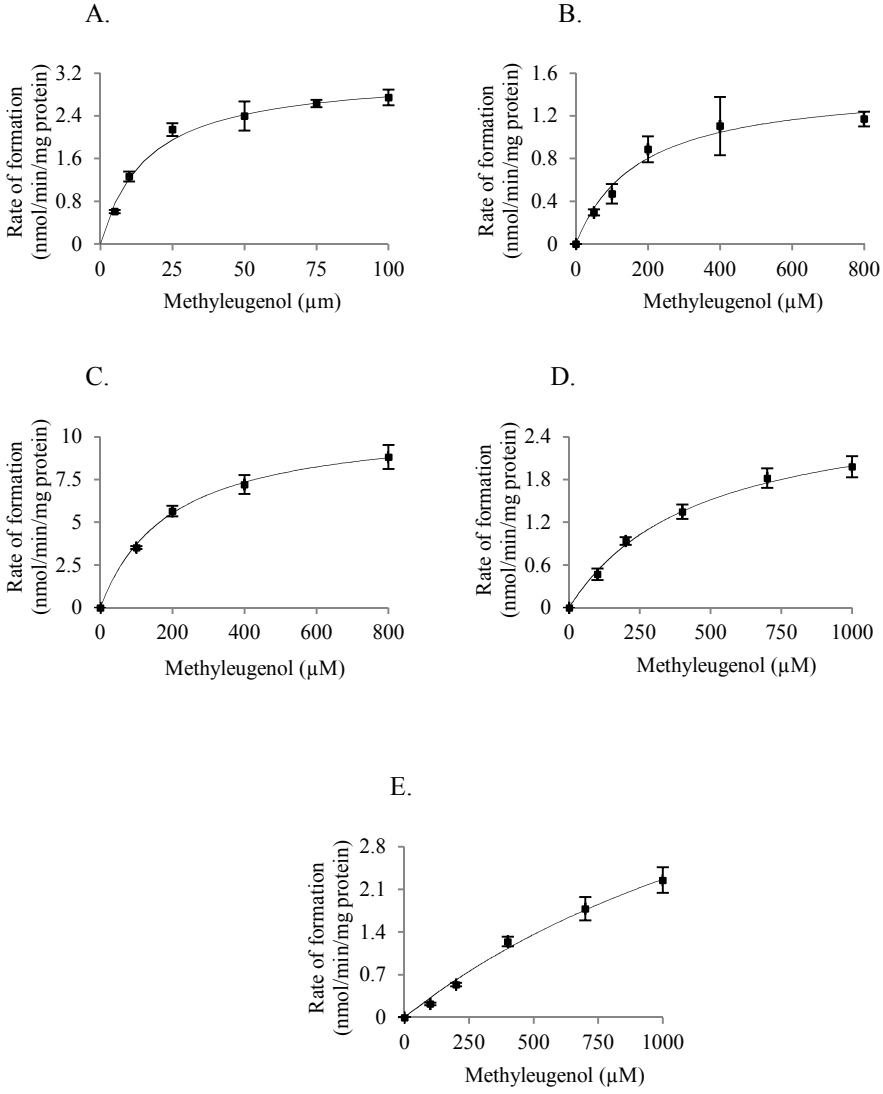

Figure 2. Formation rate of 1′-hydroxymethyleugenol in incubations of methyleugenol at varying concentrations (50 – 1000 μM) with different cDNA recombinant P450 enzymes: A. P450 1A2, B. P450 2C9*1, C. P450 2C19, D. P450 2D6*1, and E. P450 3A4.

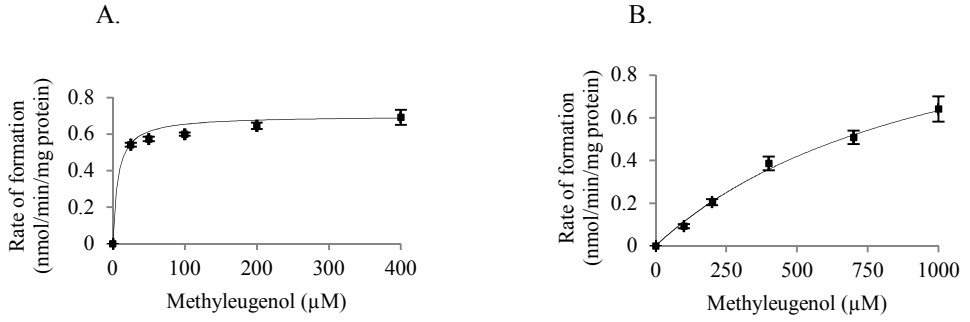

Figure 3. Formation rate of methyleugenol-2′,3′-oxid in incubations of methyleugenol at varying concentrations (50 – 1000 μM) with cDNA recombinant P450 enzymes: A. P450 2B6, and B. P450 2E1.

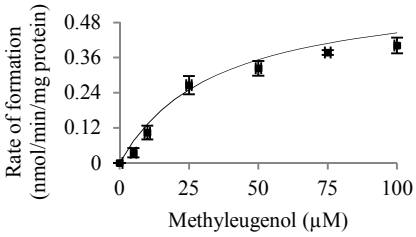

Figure 4. Formation rate of eugenol in incubations of methyleugenol at varying concentrations (5 – 100 μM) with cDNA recombinant P450 1A2.

Formation of 1′-hydroxymethyleugenol glucuronide by cDNA recombinant expressed enzymes

Incubations with cDNA recombinant expressed UGT enzymes were performed to define the human UGT enzymes involved in the formation of 1′-hydroxymethyleugenol glucuronide. Among the different UGT enzymes tested, only UGT1A9 and UGT2B7 were observed to be able to catalyse glucuronidation of 1′-hydroxymethyleugenol. Figure 5 shows the rate of

Table 1. Kinetic parameters for methyleugenol 1′-hydroxylation, epoxidation, and demethylation by cDNA expressed cytochrome P450 enzymes.

Metabolic pathway	Enzyme	V_{max}[a] (nmol/min/mg protein)	K_m[a] (µM)	*In vitro* catalytic efficiency (V_{max}/K_m) (µL/min/mg protein)	RAF[b]	[c]Scaled $V_{max,\ in\ vivo}$ (µmol/hr)	*In vivo* catalytic efficiency ($V_{max,\ in\ vivo}/K_m$) (L/hr)
1'-hydroxylation	P450 1A2	3.2 ± 0.2	16 ±2	200	0.14	1366	85
	P450 2C9*1	1.5 ± 0.3	174 ± 33	10	0.42	2007	12
	P450 2C19	10.9 ± 1.2	194 ±19	56	0.01	42	0.2
	P450 2D6*1	2.9 ± 0.3	457 ±60	6	0.01	128	0.3
	P450 3A4	6.8 ± 2.3	2003 ± 650	3	0.16	2407	1.2
Epoxidation	P450 2B6	0.7 ± 0.03	7 ±1	100	0.50	1115	159
	P450 2E1	1.3 ± 0.5	1050 ± 201	1	0.13	538	0.5
Demethylation	P450 1A2	0.6 ± 0.05	26 ± 6	23	0.14	256	9.5

[a]mean ± SD

[b]Relative Activity Factor (RAF), representing the relative activity of the enzyme in pooled (n=150) human liver microsomes compared with BD Supersomes™ as reported by BD Biosciences (Patten et al., 2009; Stresser et al., 2009) based on the measured activity of selective probe substrates.

[c]$V_{max,P450}$/(1000 nmol/µmol)*(60 min/hr)*RAF_{P450}*(32 mg microsomal protein/g liver)*(1659 g liver)

glucuronidation of 1′-hydroxymethyleugenol by these UGT enzymes, and Table 2 presents the kinetic constants derived from these data. Table 2 also presents the V_{max} values that are scaled to the *in vivo* situation based on which the *in vivo* catalytic efficiencies(V_{max}, *in vivo*/K_m) of these enzymes were calculated. Taking the *in vivo* catalytic efficiencies of UGT1A9 and 2B7 into account, both enzymes are predicted to contribute significantly to the glucuronidation reaction of 1′-hydroxymethyleugenol *in vivo*. The overall *in vivo* catalytic efficiency was predicted to amount to 0.95 L/hr corresponding to the sum of the individual catalytic efficiencies.

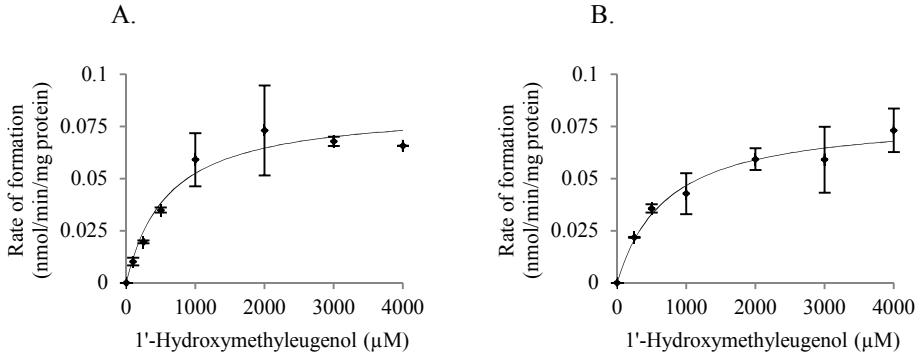

Figure 5. Formation rate of 1′-hydroxymethyleugenol glucuronide in incubations of 1′-hydroxymethyleugenol at varying concentrations (100 – 4000 µM) with recombinant UGT enzymes: A. UGT1A9 and B. UGT2B7.

Table 2. Kinetic parameters for glucuronidation of 1′-hydroxymethyleugenol by cDNA expressed UGT enzymes.

enzyme	[a] V_{max} **(nmol/min/mg protein)**	[a] K_m **(µM)**	***in vitro* catalytic effeciency (V_{max}/K_m) (µL/min/mg protein)**	[b] **RAF**	[c] **Scaled V_{max}, *in vivo* (µmol/hr)**	***in vivo* catalytic efficiency (V_{max}, *in vivo*/K_m) (L/h)**
UGT 1A9	0.084± 0.006	601 ± 113	0.14	0.64	171	0.28
UGT 2B7	0.08± 0.02	715 ± 270	0.11	1.88	479	0.67

[a] mean ± SD

[b] Relative Activity Factor (RAF), representing the relative activity of the enzyme in pooled (n=20) human liver microsomes compared with BD Supersomes™ as determined in the present study by measuring the activity of selective probe substrates.

[c] $V_{max,UGT}$/(1000 nmol/µmol)*(60 min/hr)*RAF_{UGT}*(32 mg microsomal protein/g liver)*(1659 g liver)

Oxidation and sulfonation of 1′-hydroxymethyleugenol by human individual liver S9 fractions

Table 3 shows the kinetic constants, V_{max} and K_m, for oxidation of 1′-hydroxymethyleugenol for 22 human individuals while Table 4 shows the kinetic constants, V_{max} and K_m, for sulfonation of 1′-hydroxymethyleugenol for 5 human individuals. These kinetic constants were derived experimentally by incubating liver S9 homogenates with the relevant cofactors and increasing concentrations of 1′-hydroxymethyleugenol. The V_{max} values that are scaled to the *in vivo* situation are also presented in Table 3 and Table 4 based on which the *in vivo* catalytic efficiencies (V_{max}, *in vivo*/K_m) were calculated. The range between the highest and lowest catalytic efficiency for oxidation of 1′-hydroxymethyleugenol was observed to be 8.3-fold. The average *in vivo* catalytic efficiency for oxidation was 58 L/hr. In case of sulfonation, the range between the highest and lowest catalytic efficiency was observed to be 4-fold and the average catalytic efficiency was observed to be 3 L/hr.

PBK modeling and sensitivity analysis

The kinetic data obtained for 1′-hydroxylation, epoxidation, and *O*-demethylation of methyleugenol by specific cytochrome P450 enzymes, the kinetic data for glucuronidation of 1′-hydroxymethyleugenol by specific UGT enzymes and the kinetic data for oxidation and sulfonation by individual human liver S9 were integrated in the previously developed PBK model for methyleugenol in human. With the developed model, a sensitivity analysis was performed to identify the metabolic parameters that have the most influence on the predicted formation of 1′-sulfooxymethyleugenol. Normalized SCs were calculated for different metabolic parameters at a dose of 0.217 mg/(kg bw) methyleugenol by increasing parameter values with 5%. Only metabolic parameters that had a normalized SC higher than 0.1 (in absolute value) are displayed in Figure 6. The predicted formation of 1′-sulfooxymethyleugenol in the liver was observed to be most sensitive to changes in the kinetic constants for 1′-hydroxylation of methyleugenol by P450 1A2, epoxidation of methyleugenol by P450 2B6, and

Table 3. Kinetics parameters for oxidation of 1′-hydroxymethyleugenol by human individual liver S9.

Code	V_{max} (nmol/min/mg S9 protein)	K_m (μM)	*in vitro* catalytic effeciency (V_{max}/K_m) (μL/min/mg S9 protein)	scaled V_{max}, *in vivo*[a] (μmol/hr)	*in vivo* catalytic efficiency (V_{max}, *in vivo*/K_m) (L/h)
HLS9_420	3.01	1230	2.45	42845	34.8
HLS9_438	3.71	1520	2.44	52809	34.7
HLS9_422	3.72	1180	3.15	52951	44.9
HLS9_280	3.8	954	3.98	54090	56.7
HLS9_441	3.85	2350	1.64	54802	23.3
HLS9_133	3.96	864	4.58	56368	65.2
HLS9_120	4.49	1380	3.25	63912	46.3
HLS9_M962	4.51	1720	2.62	64196	37.3
HLS9_428	4.59	1140	4.03	65335	57.3
HLS9_251	4.66	2670	1.75	66331	24.8
HLS9_354	4.73	2230	2.12	67328	30.2
HLS9_236	4.79	3730	1.28	68182	18.3
HLS9_291	4.79	1830	2.62	68182	37.3
HLS9_432	5.21	1520	3.43	74160	48.8
HLS9_F962	5.44	2070	2.63	77434	37.4
HLS9_270	6.21	610	10.28	88395	144.9
HLS9_311	6.45	1430	4.51	91811	64.2
HLS9_393	6.45	1230	5.24	91811	74.6
HLS9_322	6.87	1040	6.61	97789	94.0
HLS9_296	7.22	1300	5.55	102771	79.1
HLS9_422	7.23	677	10.68	102913	152.0
HLS9_346	8.26	1790	4.61	117575	65.7

[a] V_{max}/(1000 nmol/μmol)*(60 min/hr)*(143 mg S9 protein /g liver)*(1659 g liver)

Table 4. Kinetics parameters for sulfonation of 1′-hydroxymethyleugenol by human individual liver S9.

Code	V_{max} (nmol/min/mg S9 protein)	K_m (µM)	*In vitro* catalytic effeciency (V_{max}/K_m) (µL/min/mg S9 protein)	Scaled V_{max}, *in vivo*[a] (µmol/hr)	*In vivo* catalytic efficiency (V_{max}, *in vivo*/K_m) (L/hr)
HLS9_133	0.02	90	0.22	285	3.2
HLS9_120	0.014	71	0.20	199	2.8
HLS9_251	0.013	172	0.08	185	1.1
HLS9_236	0.031	102	0.30	441	4.3
HLS9_270	0.027	110	0.25	384	3.5

[a] V_{max}/(1000 nmol/µmol)*(60 min/hr)*(143 mg S9 protein /g liver)*(1659 g liver)

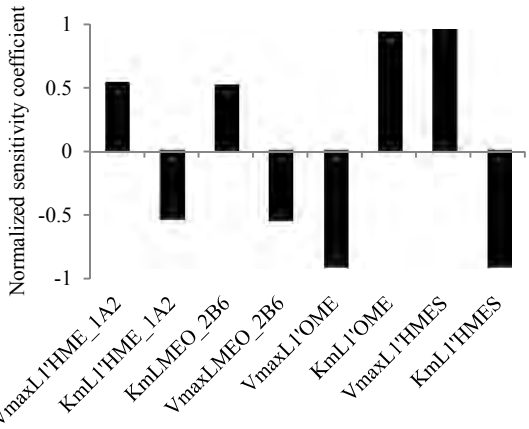

Figure 6. Sensitivity of the predicted formation of 1′-sulfooxymethyleugenol to metabolic parameters at a dose of 0.217 mg/(kg bw). V_{max} and K_m values are the Michaelis-Menten constants for the formation of 1′-hydroxymethyleugenol (1′HME) and methyleugenol-2′,3′-oxide (MEO) by recombinant P450 enzymes that are scaled to the average *in vivo* situation, and the average Michaelis-Menten constants for oxidation of 1′-hydroxymethyleugenol (1′OME) and sulfonation of 1′-hydroxymethyleugenol (1′HMES) as determined in incubations with individual human liver S9 fractions.

the apparent kinetic constants for oxidation and sulfonation of 1′-hydroxymethyleugenol. This sensitivity analysis shows that the formation of 1′-sulfooxymethyleugenol in the liver is not affected by the kinetic constants for glucuronidation of 1′-hydroxymethyleugenol by UGT 1A9 or 2B7.

Evaluation of interindividual human variability in formation of 1′-sulfooxymethyleugenol on population level

A Monte Carlo simulation was performed to evaluate the extent of variation in formation of 1′-sulfooxymethyleugenol in the liver that could occur in the population as a whole. In Table 5, the parameters that were varied and the distributions assigned to these parameters are given. Figure 7 presents the predicted frequency distribution of the formation of 1′-sulfooxymethyleugenol in individual human livers at a dose of 0.217 mg/(kg bw). The difference between the highest and the lowest predicted formation of 1′-sulfooxymethyleugenol in the liver is 912-fold. The highest value amounts to 1.55 nmol/(g liver), which was predominantly due to a low level of detoxification of methyleugenol via P450 2B6 catalyzed epoxidation. This situation occurred once in the 10,000 simulations. The lowest value amounts to 0.0017 nmol/(g liver) and was due to a high level of oxidation of 1′-hydroxymethyleugenol in combination with a low level of sulfonation of 1′-hydroxymethyleugenol. This situation occurred once in the 10,000 simulations. The 50th, 95th, and 99th percentiles of the distribution of the formation of 1′-sulfooxymethyleugenol correspond to 0.09, 0.33, and 0.52 nmol/(g liver), respectively.

With the results obtained with the Monte Carlo simulation on the variability in formation of 1′-sulfooxymethyleugenol, a so-called chemical-specific adjustment factor (CSAF) can be derived, which can be used as replacement of the default uncertainty factor for interindividual percentile to represent a sensitive individual and the 50th percentile to represent the average human difference in kinetics. Based on the guidelines of the International Program on Chemical Safety (IPCS, 2005), CSAFs can be calculated as the ratio between given percentiles (such as 95th, 97.5th, or 99th) and the central tendency for the whole population. Using the 95th individual,

the CSAF amounts to 3.7. Using the 99th percentile to represent a sensitive individual the CSAF amounts to 5.8.

Discussion

The present study aimed at evaluating interindividual differences in formation of the ultimate carcinogenic metabolite 1′-sulfooxymethyleugenol in the human population. Insights in the level of variation of key metabolic routes could be obtained by determining kinetic constants for the metabolic reactions by specific isoenzymes and taking the level of variation in activity of these enzymes in the population into account or, when specific isoenzymes were not commercially available, by measuring the kinetic constants in incubations with a range of individual human liver fractions.

Table 5. Distributions assigned to the parameters that were varied in the Monte Carlo simulation.

Parameter	Mean	CV (%)	Min-max value in the simulation	Fold variation
V_{max}, 1′HME_1A2	1427[a]	67	137-13027	95
V_{max}, 1′HME_2C9*1	2007[a]	54	267-13173	49
V_{max}, 1′HME_2C19	347[a]	105	12-7260	629
V_{max}, 1′HME_2D6*1	92[a]	61	9-596	67
V_{max}, 1′HME_3A4	3466[a]	114	42-65229	1551
V_{max}, MEO_2B6	1115[a]	39	4-30988	8068
V_{max}, MEO_2E1	538[a]	61	67-4797	72
V_{max}, 1EU_1A2	268[a]	67	21-2198	105
V_{max}, 1′HMEG_1A9	171[a]	49	22-885	41
V_{max}, 1′HMEG_2B7	479[a]	64	45-4091	90
V_{max}, 1′OME	73727[a]	27	25140-180466	7
K_m, 1′OME	1567[b]	46	247-6618	27
V_{max}, 1′HMES	299[a]	38	47-894	17
K_m, 1′HMES	109[b]	36	24-398	19

[a] V_{max} expressed at μmol/hr
[b] K_m expressed as μmol/L

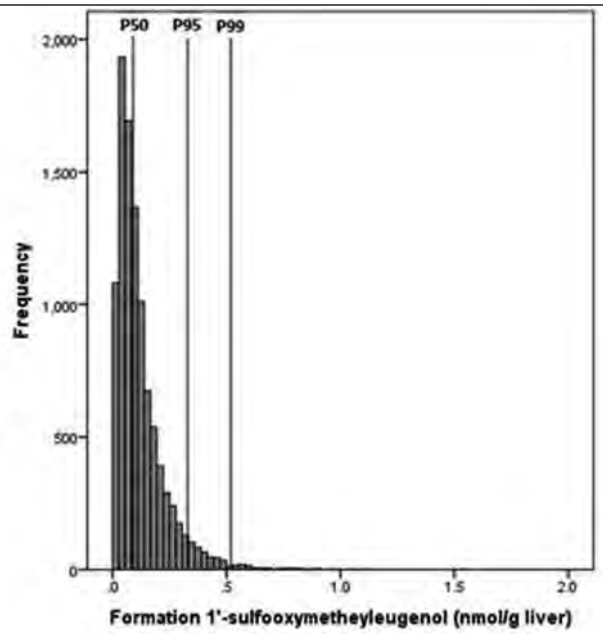

Figure 7. Predicted frequency distribution of the formation of 1′-sulfooxymethyleugenol human livers. P50, P95, and P99 represent the 50th, 95th, and 99th percentiles of the distribution.

The present study revealed that the first step in bioactivation of methyleugenol to the carcinogenic metabolite 1′-hydroxymethyleugenol is predominantly catalysed by cytochrome P450 1A2, contributing to 85% of the catalytic efficiency of this reaction when taking the activity level of P450 1A2 in pooled human liver microsomes into account. This is in line with what was previous observed by Jeurissen *et al.* (2006) who revealed that P450 1A2 contributes to 94% of the total catalytic efficiency based on incubations with Gentest microsomes expressing the individual cytochrome P450 enzymes to roughly average liver levels. The involvement of P450 1A2 indicates that life-style factors such as smoking can increase the susceptibility to the adverse effects of methyleugenol (Jeurissen *et al.*, 2006). The isoenzymes involved in detoxification via epoxidation of methyleugenol or *O*-demethylation to eugenol

have not been identified before and were shown in the present study to be P450 2B6 and P450 1A2 respectively. The activity level of P450 2B6 can be affected by genetic polymorphisms with the Japanese population having lower activity levels of this enzyme than Caucasians which may affect the susceptibility to the adverse effects of methyleugenol in these populations (Shimada *et al.*, 1994).

Isoenzymes involved in other metabolic reactions of methyleugenol, were not identified since the previously developed physiologically based kinetic (PBK) model for methyleugenol in human and a sensitivity analysis of this model, revealed that formation of 1′-sulfooxyestragole is not affected by these metabolic parameters. This indicates that interindividual human variation in these reactions will not significantly affect bioactivation of methyleugenol.

In case of the metabolic reactions of 1′-hydroxymethyleugenol, the present study revealed that glucuronidation of 1′-hydroxymethyleugenol was catalysed by both UGT 1A9 and 2B7. This is in line with what has been previously observed for glucuronidation of the 1′-hydroxy-metabolite of the related alkenylbenzene estragole (Iyer *et al.*, 2008). The *in vivo* catalytic efficiency for glucuronidation that was predicted based on the kinetic constants for glucuronidation by these enzymes, was observed to be 42-fold lower than the predicted *in vivo* catalytic activity for oxidation of 1′-hydroxymethyleugenol. This indicates that glucuronidation is only a minor detoxification route in humans and that formation of the ultimate carcinogenic metabolite 1′-sulfooxymethyleugenol will not be affected by lifestyle factors and polymorphism in UGT1A9 and 2B7. In case of oxidation and sulfonation of 1′-hydroxymethyleugenol, the kinetic constants for these reactions by specific isoenzymes could not be determined in the present study due to limited availability of the recombinant enzymes that are likely to be involved in these reactions. Therefore, the variation in sulfonation and oxidation of 1′-hydroxymethyleugenol as observed with individual human liver S9 fractions was assumed to represent the level of variation in the population as a whole.

Based on the state-of-the-art knowledge on the probable enzymes involved in sulfonation and oxidation of 1′-hydroxymethyleugenol an indication can be obtained whether the observed levels of variation in these reactions are indeed relevant for the population as a whole. Recently,

Herrmann *et al.* (2012) revealed that SULT1A1 and SULT1E1 are the main liver sulfotransferease enzymes involved in sulfonation of 1′-hydromethyleugenol by measuring mutagenicity of 1′-hydroxymethyleugenol in *Salmonella typhimurium* strains expressing human sulfotransferease enzymes. The reported coefficient of variation for SULT1A1 and SULT1E1, as determined with enzyme-selective probe substrates in human liver tissue fractions, amounts to 34% and 47% respectively (Riches *et al.*, 2009). The level of variation in sulfonation of 1′-hydroxymethyleugenol observed in the present study indicates a CV of 37.6 % for the apparent maximum sulfonation rate of 1′-hydroxymethyleugenol and a CV of 35% for the apparent K_m, values that are comparable with the levels of variation in SULT1A1 and SULT1E1 reported in the literature (Riches *et al.*, 2009). The isoenzymes involved in oxidation of 1′-hydroxymethyleugenol have not been identified so far. We previously suggested that oxidation of the related alkenylbenzene estragole may be catalyzed by 17β-hydroxysteroid dehydrogenase type 2 (17β-HSD2) based on the subcellular localization of the reaction, which occurred mainly in incubations with microsomes, and the enzyme specificity, with NAD+ being the preferred cofactor. Current knowledge about 17 β -HSD2 does not give a complete insight in the level of variation in enzyme activity that could occur in the human population. Recently, Audet-Walsh *et al.* (2012) reported that genetic polymorphisms occur in the gene encoding 17β-HSD2, which could lead to reduced 17β-HSD2 expression or function. The impact of such polymorphisms in 17β-HSD2 for its activity remains to be elucidated. The coefficients of variation in the V_{max} for oxidation of 1′-hydroxymethyleugenol, amounting to 27.1 %, and in the K_m, amounting to 46 %, as observed in the present study are considered to represent an average level of variation (Covington *et al.*, 2007).

With the results obtained with the Monte Carlo simulation on the variability in formation of 1′-sulfooxymethyleugenol, a so-called chemical-specific adjustment factor (CSAF) could be derived, which can be used to evaluate the appropriateness of the default factor of 3.16 generally assumed to reflect interindividual variation in kinetics within the human population (Gentry *et al.*, 2002; IPCS, 2005). Using the 95th percentile to represent a sensitive individual and the 50th percentile to represent the average individual, the CSAF amounts to 3.7. This

predicted CSAF is comparable to the default factor of 3.16 for kinetic variability and suggests that the default uncertainty factor adequately protects 95% of the population. Using the 99th percentile to represent a sensitive individual the CSAF amounts to 5.8 indicating that protecting 99% of the population would require a higher uncertainty factor than the default value of 3.16. Obviously, definite conclusions on the value of the CSAF have to await further data on the actual variation in the 17b-HSD2 and sulfotransferase activity to be expected within the human population.

Acknowledgement

The authors would like to thank the Nestlé Research Centre for providing the LC-MS/MS API 3000 instrument. Also, this work was supported by a grant from sandwich PhD fellowship program / Wageningen University, the Netherlands.

References

Al-Subeihi, A.A.A., Spenkelink, B., Boersma, M.G., Punt, A.,van Bladeren, P.J., and Rietjens, I.M.C.M. (2012). Physiologically based kinetic modeling of bioactivation and detoxification of the alkenylbenzene methyleugenol in human as compared with rat. Toxicol Appl Pharm 260, 271-284.

Al-Subeihi, A.A.A., Spenkelink, B., Rachmawati, N., Boersma, M.G., Punt, A., Vervoort, J.,van Bladeren, P.J., and Rietjens, I.M.C.M. (2011). Physiologically based biokinetic model of bioactivation and detoxification of the alkenylbenzene methyleugenol in rat. Toxicol In Vitro 25, 267-285.

Audet-Walsh, É., Bellemare, J., Lacombe, L., Fradet, Y., Fradet, V., Douville, P., Guillemette, C., and Lévesque, É. (2012). The impact of germline genetic variations in hydroxysteroid (17-beta) dehydrogenases on prostate cancer outcomes after prostatectomy. Eur Urol 62, 88-

96.

Barter, Z.E., Bayliss, M.K., Beaune, P.H., Boobis, A. R., Carlile, D. J., Edwards, R.J., Brian H.,J., Lake, B.G., Lipscomb, J.C., Pelkonen, O.R., Tucke, G.T., and Rostami-Hodjegan, A.W., (2007). Scaling factors for the extrapolation of in vivo metabolic drug clearance from in vitro data: Reaching a consensus on values of human microsomal protein and hepatocellularity per gram of Liver. Curr Drug Metab 8, 33-45.

Covington T.R., Robinan G.P.,van Landingham C.B., Andersen M.E., Kester J.E., and Clewell H.J. (2007). The use of Markov chain Monte Carlo uncertainty analysis to support a public health goal for perchloroethylene. Regul Toxicol Pharm 47, 1–18.

Drinkwater, N.R., Miller, E.C., Miller, J.A., and Pitot, H.C. (1976). Hepatocarcinogenicity of estragole (1-allyl-4-methoxybenzene) and 1'-hydroxyestragole in the mouse and mutagenicity of 1'-acetoxyestragole in bacteria. J Natl Cancer Inst 57, 1323-1331.

Evans, M.V. and Anderson, M.E. (2000). Sensitivity analysis of a physiological model for 2,3,7,8-tetrachlorodibrnzo-p-dioxin (TCDDD): Assessing the impact of specific model parameters on sequestration in liver and fat in rat. Toxicol Sci 54, 71-80.

Fisher, M.B., Campanale, K., Ackermann, B.L., Van Den Branden, M., and Wrighton, S.A. (2000). In vitro glucuronidation using human liver microsomes and the pore-forming peptide alamethicin. Drug Metab Dispos 28, 560-566.

Gardner, I., Wakazono, H., Bergin, P., Waziers, I., Beaune, P., Kenna, J.G., and Caldwell, J. (1997). Cytochrome P450 mediated bioactivation of methyleugenol to 1′-hydroxymethyleugenol in Fischer 344 rat and human liver microsomes. Carcinogenesis 18, 1775-1783.

Gentry P.R., Hack C.E., Haber L., Maier A., and Clewell, III, H.J. (2002). An approach for the quantitative consideration of genetic polymorphism data in chemical risk assessment: Examples with warfarin and parathion. Toxicol Sci 70, 120-139.

Girard, H., Court, M.H., Bernard, O., Fortier, L.C., Villeneuve, L., Hao, Q., Greenblatt, D.J., von Moltkeb, L.L., Perussed, L., and Guillemette, C. (2004). Identification of common polymorphisms in the promoter of the UGT1A9 gene: Evidence that UGT1A9 protein and

activity levels are strongly genetically controlled in the liver. Pharmacogenetics 14, 501–515.

Hall, R.L. and Oser, B.L. (1965). Recent progress in the consideration of flavoring ingredients under the food additives amendment III. GRAS substances. Food Technol 253, 151–197.

Herrmann, K., Engst, W., Appel, K.A., Monien, B.H., and Glatt, H. (2012). Identification of human and murine sulfotransferases able to activate hydroxylated metabolites of methyleugenol to mutagens in Salmonella typhimurium and detection of associated DNA adducts using UPLC–MS/MS methods. Mutagenesis 15, 1–10.

Holthe, M., Rakva°g, T.N., Klepstad, P., Idle, J.R., S Kaasa, S., Krokan, H.E., and Skorpen, F. (2003). Sequence variations in the UDP glucuronosyltransferase 2B7 (UGT2B7) gene: identification of 10 novel single nucleotide polymorphisms (SNPs) and analysis of their relevance to morphine glucuronidation in cancer patients. Pharmacogenomics J 3, 17–26.

IPCS (2005). International Programme on Chemical Safety. Chemical-specific adjustment factors for interspecies difference and human variability: Guidance document for use of data in dose/concentration-response assessment. Harmonization Project Document No. 2. World Health Organization, Geneva (Switzerland). http://whqlibdoc.who.int/publications/2005 /9241546786_eng.pdf

Iyer, L.V., Ho, M.N., Shinn, W.M., Bradford, W.W., Tanga, M.J., Nath, S.S., and Green, C.E. (2003). Glucuronidation of 1′-Hydroxyestragole (1′-HE) by human UDP-Glucuronosyl-transferases UGT2B7 and UGT1A9. Toxicol Sci 73, 36-43.

Lin, J.H., and Wong, B.K. (2002). Complexities of glucuronidation affecting in vitro in vivo extrapolation. Curr Drug Metab 3, 623-646.

Luo, G., and Guenthner, T.M. (1995). Metabolism of allylbenzene 2′,3′-oxide and estragole 2′,3′-oxide in the isolated perfused rat liver. J Pharmacol Exp Ther 272, 588-596.

Jeurissen, S.M.F., Bogaards, J.J.P., Boersma, M.G., ter Horst J.P.F., Awad, H.M., Fiamegos, Y.C., van Beek T.A., Alink, G.M., Sudhölter E.J.R., Cnubben N.H.P., and Rietjens, I.M.C.M. (2006). Human cytochrome P450 enzyme specificity for bioactivation of methyleugenol to the proximate carcinogen 1′-hydroxymethyleugenol. Chem Res Toxicol

19, 111-116.

Miele, M., Dondero, R., Ciarallo, G., and Mazzei, M.J. (2001). Methyleugenol in Ocimum basilicum L.cv. Genovese Gigante. J Agr Food Chem 49, 517-521.

Miller, E.C., Swanson, A.B., Phillips, D.H., Fletcher, T.L., Liem, A., and Miller, J.A. (1983). Structure-activity studies of the carcinogenicities in the mouse and rat of some naturally occurring and synthetic alkenylbenzene derivatives related to safrole and estragole. Cancer Res 43, 1124-1134.

NTP (2000). Toxicology and carcinogenesis studies of methyleugenol (CAS No. 93-15-12) in F344/N rats and B6C3F1 mice (Gavage studies). Natl Toxicol Program Tech Rep Ser, 491, 1-412.

Paini, A., Punt, A., Scholz, G., Gremaud, E., Spenkelink, B., Alink, G., Schilter, B., van Bladeren, P.J., and Rietjens, I.M.C.M. (2012). In vivo validation of DNA adduct formation by estragole in rats predicted by physiologically based biodynamic modeling. Mutagenesis 27, 653-663.

Patten C.J. (2009). Strategies for in vitro metabolic stability testing. http://www.bdbiosciences.com /documents/webinar_2009_12_metabolic_stability.pdf

Punt, A., Paini, A., Boersma, M.G., Freidig, A.P., Delatour, T., Scholz, G., Schilter, B., van Bladeren, P.J., and Rietjens I.M.C.M. (2009). Use of physiologically based biokinetic (PBBK) modeling to study estragole bioactivation and detoxification in humans as compared with male rats. Toxicol Sci 110, 255–269.

Riches, Z., Stanley, E.L., Bloomer, J.C., and Coughtrie, M.W. (2009). Quantitative evaluation of the expression and activity of five major sulfotransferases (SULTs) in human tissues: The SULT "pie". Drug Metab Dispos 37, 2255-2261.

Rietjens, I.M.C.M., Louisse, J., and Pun, A. (2011). Tutorial on physiologically based kinetic modeling in molecular nutrition and food research. Mol Nutr Food Res 55, 941–956.

Robison S.H., and Barr D.B. (2006). Use of biomonitoring data to evaluate methyleugenol exposure. Environ Health Perspect 114, 1797–1801.

Rostami-Hodjegan, A. and Tucker, G.T. (2007). Simulation and prediction of in vivo drug

metabolism in human populations from in vitro data. Nat Rev Drug Discov 6, 140-148.

SCF (2001). Opinion of the scientific committee on food on methyleugenol (4-allyl-1,2 dimethyxybenzene). European Commission, Scientific Committee on Food. Brussels, BE. http://ec.europa.eu/food/fs/sc/scf/out104_en.pdf

Shimada, T., Yamazaki, H., Mimura, M., Inui, Y. and Guengerich, F.P. (1994). Interindividual variations in human liver cytochrome P-450 enzymes involved in the oxidation of drugs, carcinogens and toxic chemicals: Studies with liver microsomes of 30 Japanese and 30 Caucasians. J Pharmacol Exp Ther 270, 414-423.

Smith, R.L., Adams, T.B., Doull, J., Feron, V.J., Goodman, J.I., Marnett, L.J., Portoghese,P.S., Waddell, W.J., Wagner, B.M., Rogers, A.E., Caldwell, J., and Sipes, I.G. (2002). Safety assessment of allylalkoxybenzene derivatives used as flavoring substances – methyl eugenol and estragole. Food Chem Toxicol 40, 851-870.

Solheim, E., and Scheline, R.R. (1976). Metabolism of alkenebenzene derivatives in the rat. II. Eugenol and isoeugenol methyl ethers. Xenobiotica 6, 137-150.

Stresser D.M., Crespi C.L., and Patten P.J. (2009). Cytochrome P450 enzyme mapping in drug discovery using BD Supersomes enzymes. http://www.bdbiosciences.com/external _files/dl/doc/tech_bulletin/live/web_enabled/467.pdf

Zhang, X., Tsang, A.M., Okino, M.S., Power, F.W., Knaak, J.B., Harrison, L.S., and Dary, C.C. (2007). A physiologically based pharmacokinetic/pharmacodynamic model for carbofuran in Sprague-Dawley rats using the exposure-related dose estimating model. Toxicol Sci 100, 345–359.

6

General discussion

General discussion

The alkenylbenzene methyleugenol is a natural constituent of the essential oils of various herbs such as tarragon, basil, nutmeg, lemon grass, pay leaf, and allspices (Environmental Canada, 2010; Smith *et al.*, 2002). Methyleugenol is also found in edible fruits such as for instance grapefruit, bananas as well as in some forest fruits at a level of less than 0.1 mg/kg (TNO, 2010). Moreover, methyleugenol was recognized as a volatile flavor compound in the juice of Kogyoku apples (Yagima *et al.*, 1984). Dietary human exposure to methyleugenol may occur through: (i) the consumption of fruits and vegetables containing methyleugenol or food products derived from them, (ii) the consumption of foods and beverages flavored with these aromatic herbs or their essential oil fractions which are added to food intentionally as flavors, (iii) the consumption of foods and beverages which are flavored with pure methyleugenol (Burdock, 2005; Smith *et al.*, 2010; Smith *et al.*, 2002), and/or iv) the use of methyleugenol containing plant food supplements (van den Berg *et al.*, 2011). It has been reported for example that some brands of cookies available in the USA can contain approximately 3.3 mg/kg methyleugenol which was added as flavor (Schecter *et al.*, 2004), and some plant based food supplements may contain up to 1 mg methyleugenol/g supplement (van den Berg *et al.*, 2011). The interest in the risk assessment of methyleugenol as a food constituent came from its widespread use in a variety of foods and beverages as well as from its structural resemblance to the known carcinogen safrole (Johnson *et al.*, 2000). In addition, methyleugenol has been reported to be carcinogenic and genotoxic, inducing malignant tumors in multiple tissues of rats and mice as well as inducing unscheduled DNA synthesis in rat liver (Ding *et al.*, 2011; NTP, 2000; Smith *et al.*, 2002).

In 1965, the Expert Panel of the Flavor and Extract Manufacturers Association (FEMA) considered that methyleugenol was GRAS (Generally Recognized As Safe) when used intentionally at low levels as a flavoring substance in food (Hall and Oser, 1965). This consideration of using methyleugenol as a food flavor was confirmed by the US Food and Drug

Administration (FDA, 2004) and consequently methyleugenol is allowable for direct addition for human consumption as a synthetic flavoring substance in the USA (FDA, 2010). The FEMA assessment took into account: i) the various experimental data that suggest a non-linear relationship between dose and profiles of metabolism and metabolic activation and ii) the fact that the exposure due to use as a flavoring is relatively low (Smith *et al.*, 2002). In another evaluation of methyleugenol and specifically in 2000, the National Toxicology Program (NTP) reported that methyleugenol is carcinogenic in both rats and mice (NTP, 2000). In 2001, the FEMA Expert Panel reassessed the available data for methyleugenol and confirmed that there is no considerable cancer risk resulting from consumption of methyleugenol as flavoring substance and affirmed the GRAS status of methyleugenol at the low levels of use as a flavoring substance (Smith *et al.*, 2002). In 2001, the Scientific Committee on Food (SCF) of the European Union published a scientific opinion on methyleugenol in which it was concluded that methyleugenol is genotoxic and carcinogenic and that reductions in exposure and restrictions in use levels are indicated (SCF, 2001). A more recent evaluation performed by the Joint FAO/WHO Expert Committee on Food Additives (JECFA) in 2008, has indicated that although evidence of carcinogenicity to rodents given high doses of methyleugenol exists, further research is needed to assess the potential risk to human health at relevant dietary exposure to methyleugenol present in foods and essential oils and used as flavoring agent (JECFA, 2008). In the EC Regulation 1334/2008 of the EU, which became effective in January 2011, addition of methyleugenol to foods was prohibited and restrictions were made on the concentration of methyleugenol in foods that have been prepared with flavorings or food ingredients with flavoring properties (European Commission, 2008).

The occurrence of these different risk assessments to some extent reflects the absence of scientific agreement on the unequivocal translation of carcinogenicity data from rodent animal experiments obtained at high levels of exposure to the risks for humans at relevant low levels of dietary intake. Predicting the cancer risk in humans at relevant dietary intake levels requires extrapolation of the animal carcinogenicity data taking in consideration species, dose and interindividual variation. The present PhD project aimed at obtaining quantitative insight into

the consequences of dose- and species- dependent effects (chapter 2 and chapter 3), matrix effects (chapter 4) and interindividual differences (chapter 5) for the bioactivation and detoxification of methyleugenol by using physiologically based kinetic (PBK) modeling. In chapter 2 a physiologically based kinetic (PBK) model for methyleugenol was developed in rat based on *in vitro* metabolic parameters determined using relevant tissue fractions, *in silico* derived partition coefficients, and physiological parameters derived from the literature. The model was based on the model previously developed for the related alkenylbenzene estragole and consists of eight compartments including liver, lung, and kidney as metabolizing compartments, and separate compartments for fat, arterial blood, venous blood, richly perfused and slowly perfused tissues. Evaluation of the model was performed by comparing the PBK predicted concentration of methyleugenol in the venous compartment to methyleugenol plasma levels reported in the literature, by comparing the PBK predicted dose-dependent percentage of the dose converted to 2-hydroxy-4,5-dimethoxyallylbenzene, 3-hydroxy-4-methoxyallylbenzene, and 1′-hydroxymethyleugenol glucuronide to the corresponding percentage of these metabolites excreted in urine reported in the literature, which were demonstrated to be in the same order of magnitude. With the model obtained the relative extent of bioactivation and detoxification of methyleugenol at different oral doses was examined. At low doses, formation of 3-(3,4-dimethoxyphenyl)-2-propen-1-ol and methyleugenol-2′,3′-oxide leading to detoxification appeared to be the major metabolic pathways, occurring in the liver. At high doses, the model revealed a relative increase in the formation of the proximate carcinogenic metabolite 1′-hydroxymethyleugenol, occurring in the liver. This relative increase in formation of 1′-hydroxymethyleugenol leads to a relative increase in formation of 1′-hydroxymethyleugenol glucuronide, 1′-oxomethyleugenol, and 1′-sulfooxymethyleugenol with increasing dose levels, the latter metabolite being the ultimate carcinogenic metabolite of methyleugenol. These results indicate that the relative importance of different metabolic pathways of methyleugenol may vary in a dose-dependent way, leading to a relative increase in bioactiviation of methyleugenol at higher doses. Close analysis of these data reveal that the percentage of the dose converted to the ultimate carcinogenic metabolite 1′-sulfooxymethyleugenol increases from 0.05% of the

dose at 0.217 mg/(kg bw)/day, a dose level relevant for human dietary intake, to 0.07% of the dose at a dose level of 15.3 mg/kg bw/day, the $BMDL_{10}$ for tumor formation (van den Berg *et al.*, 2011). This reflects a change of only 1.4-fold over the dose range of interest, which is a change that would be expected to only marginally influence the cancer risk estimate. Furthermore this increase is so limited that a plot of the absolute amount of 1′-sulfooxymethyleugenol formed against the dose is apparently linear over the dose range as high as the BMD_{10} down to dose levels relevant for human intake (Figure 1). Thus the results of the PBK modeling reflect that there are no relevant kinetic arguments, such as saturation of metabolic pathways, that argue against linear extrapolation of the tumor data from high doses used in animal experiments to low doses relevant for human dietary intake. In addition the kinetic data also do not reveal a threshold for bioactivation. Obviously it remains to be established whether dynamic processes following metabolic activation, would be non-linear or leading to an apparent threshold for the ultimate tumor formation.

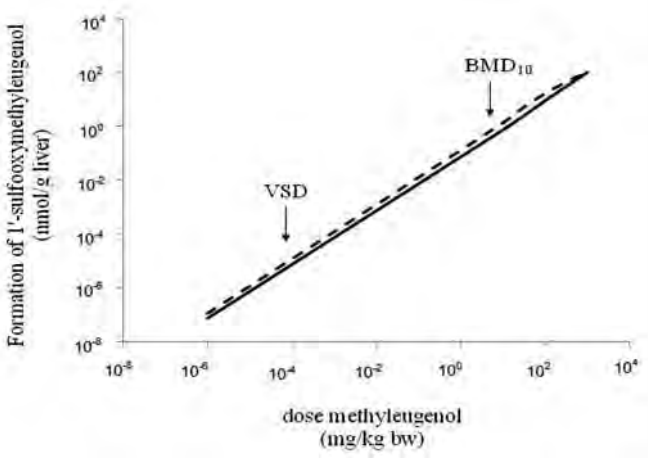

Figure 1. PBK model predicted dose-dependent formation of 1'-sulfooxymethyleugenol in the liver of rat (solid line) and human (dotted line). The VSD represents the so-called virtual safe dose at which the additional cancer risk upon life time exposure would be one in a million and is considered negligible. The BMD_{10} (benchmark dose 10%) represents the dose resulting in 10% tumor incidence above background levels.

Another argument often used against the linear extrapolation and calculation of a virtual safe dose (VSD) based on animal tumor data is that species effects are not taken into account since tumor data are extrapolated directly from the animal bioassay to the human situation (EFSA, 2005). The results obtained in the present thesis also provided insight into the species dependent effects on bioactivation of methyleugenol. In order to obtain this insight into the species-dependent differences in kinetics of methyleugenol a PBK model for methyleugenol in human, based on *in vitro* and *in silico* derived parameters, was developed in chapter 3. With the model obtained bioactivation and detoxification of methyleugenol at different dose levels could be investigated in human and compared to the results obtained with the PBK model for methyleugenol in male rat. This comparison reveals that formation of 1′-hydroxymethyleugenol glucuronide, a major metabolic pathway in male rat liver, appears to represent a minor metabolic pathway in human liver whereas in human liver a significantly higher formation of 1′-oxomethyleugenol compared with male rat liver is observed. In spite of this species dependent difference in the detoxification pathways for 1′-hydroxymethyleugenol, formation of 1′-sulfooxymethyleugenol was predicted to be similar in the liver of both human and male rat at oral doses as low as 0.0034 up to dose levels of 300 mg/kg bw (Figure 1). Thus, despite a significant difference in especially the metabolic pathways of the proximate carcinogenic metabolite 1′-hydroxymethyleugenol between human and male rat, the influence of species differences on the ultimate overall bioactivation of methyleugenol to 1′-sulfooxymethyleugenol appeared to be limited (i.e. less than 1.06 fold). Moreover, the PBK model predicted the formation of 1′-sulfooxymethyleugenol in the liver of human and rat to be linear from doses as high as the benchmark dose (BMD_{10}) down to as low as the virtual safe dose (VSD) (Figure 1). This corroborates that kinetic data do not provide a reason to argue against linear extrapolation from the rat tumor data to the human situation.

A third aspect that should be taken into account when extrapolating data from a rodent bioassay to the human situation is the fact that for adequate risk estimation of food-borne carcinogens, matrix and combination effects may have to be taken into account. Whereas animal carcinogenicity experiments are conducted with a pure compound, human dietary

exposure to methyleugenol will occur in a complex food matrix containing other ingredients. In a complex food matrix, interactions can occur that can affect the bioavailability of food components (Schilter *et al.*, 2003). For example, a slow or incomplete release of methyleugenol from the matrix could result in a lower bioavailability than when dosed as a pure compound by oral gavage. The results described in chapter 3 pointed at such a possible matrix effect for the bioavailability of methyleugenol as reported from gingersnaps served as a breakfast together with orange juice provided as a beverage (Schecter *et al.*, 2004). PBK modeling revealed the predicted values would match that the experimental values when the bioavailability of methyleugenol from the gingersnaps and orange juice food matrix would be 13.8%. The occurrence of such a difference in the bioavailability of a compound when ingested within a food matrix or as a pure compound has been reported for other compounds as well. Manach *et al.* (2004) for example reported that the level of ferulic acid metabolites recovered in the urine of rats amounts to only 3% of the ingested dose when ferulic acid is provided as wheat bran, whereas recovery of the metabolites is 50% of the dose when ferulic acid is dosed as a pure compound. Also the bioavailability of ß-carotene has been observed to be one order of magnitude higher when provided as a pure compound added to foods than when present in foods (van het Hofs *et al.*, 2000).

In addition to the effect of the food matrix on the bioavailability, interactions with other herbal ingredients might occur at the level of metabolic activation and/or detoxification. It was for instance observed by Jeurissen *et al.* (2008) that a methanolic basil extract was able to efficiently inhibit the sulfotransferase-mediated DNA adduct formation in HepG2 human hepatoma cells exposed to 1′-hydroxyestragole. In later work the basil ingredient responsible for this effect on estragole bioactivation was identified as the flavonoid nevadensin (Alhusainy *et al.*, 2010).

To investigate whether also for methyleugenol such a matrix effect can be expected the influence of nevadensin on the bioactivation of methyleugenol was investigated in chapter 4 of this thesis. In this study, the effects of nevadensin on the sulfonation and the subsequent DNA adduct formation of the proximate carcinogen 1′-hydroxymethyleugenol were studied using the

human hepatoma cell line HepG2. Nevadensin was shown to be able to inhibit DNA adduct formation in HepG2 cells exposed to the proximate carcinogen 1′-hydroxymethyleugenol in the presence of this flavonoid. This inhibition was shown to occur at the level of sulfotransferase (SULT)-mediated bioactivation of 1′-hydroxymethyleugenol. In order to investigate possible *in vivo* implications the SULT inhibition by nevadensin was integrated into the male rat and human PBK models for bioactivation and detoxification of methyleugenol. The results thus obtained revealed that co-administration of methyleugenol with nevadensin may reduce the levels of bioactivation of 1′-hydroxymethyleugenol to the DNA reactive metabolite, without reducing its detoxification via glucuronidation or oxidation. This effect may be significant even at realistic low dose human exposure levels. The results obtained point at a potential reduction of the cancer risk when methyleugenol exposure occurs by oral intake within a relevant food matrix containing SULT inhibitors compared to what is observed in rodent bioassays upon exposure to pure methyleugenol dosed by gavage. Important to note is that the regular human diet is rich in other SULT inhibitors ranging from a number of natural dietary chemicals, such as polyphenols (Eaton *et al.*, 1996; Morimitsu *et al.*, 2004) to a number of food additives such as (±)-catechin, (+)-catechin, 4-chlorobenzoic acid, aspartame, benzoic acid, erythrosine, gallic acid, octyl gallate, *p*-hydroxybenzoic acid, propyl gallate, protocatechuic acid, saccharin, tannic acid, tartrazine and vanillin which have all been shown capable of inhibiting the sulfonation of a number of xenobiotics and endobiotics in human liver cytosol to varying extents (Bamforth *et al.*, 1993). These other SULT inhibitors may add to the effect since the combined effect of several flavonoid SULT inhibitors on SULT mediated reactions has recently been shown to be additive (Alhusainy *et al.*, 2012).

It is also important to note that the efficiency of nevadensin in inhibiting the sulfonation of 1′-hydroxymethyleugenol and thus its potential protective effect against bioactivation of methyleugenol to the proximate DNA reactive metabolite still needs to be established in *in vivo* experiments where factors such as its bioavailability and metabolic stability will play a crucial role. Of interest in this respect is that methylated flavones such as nevadensin have been demonstrated to be much more metabolically stable than their non-methylated analogues which

is reflected by their resistance to hepatic metabolism and stability in the intestinal epithelial cell layer (Walle, 2007; Wen and Walle, 2006). Furthermore, they also have higher intestinal absorption through Caco-2 cell monolayers (Walle, 2007; Wen and Walle, 2006). Both factors should increase their oral bioavailability as compared to the bioavailability of non-methylated flavones. Furthermore, recent studies in which estragole was dosed to rats in either the absence or presence of nevadensin revealed significant reduction in the amount of estragole derived DNA adducts formed in the liver upon co-administration of estragole with the flavonoid SULT inhibitor nevadensin (Alhusainy *et al.*, unpublished results), suggesting that the effects observed in the present thesis for methyleugenol may in future also appear relevant for the *in vivo* situation. In these studies nevadensin was able to significantly reduce the formation of estragole DNA adduct (E-3'-N^2-dGuo**)** in the liver of Sprague Dawley rats exposed to the alkenylbenzene estragole and nevadensin simultaneously by 40%. Whether such about two-fold reduction in DNA adduct formation would have a significant impact on the ultimate risk assessment remains to be seen, especially given the other uncertainties in the low dose extrapolation of cancer risks from animal data to the human situation.

A final factor of uncertainty in the risk assessment of methyleugenol that was studied in more detail in the present thesis was the identification of the interindividual differences in its bioactivation and detoxification. In chapter 5 of this thesis these interindividual differences were studied in more detail by predicting the level of formation of the ultimate carcinogenic metabolite 1′-sulfooxymethyleugenol in the human population taking the variability in key bioactivation and detoxification reactions into account using Monte Carlo simulations. Insight in the interindividual variation in relevant metabolic routes was obtained by determining kinetic constants for the metabolic reactions by specific isoenzymes or by measuring the kinetic constants in incubations with a range of individual human liver fractions. The results of the study indicated that formation of 1′-sulfooxymethyleugenol is predominantly affected by i) P450 1A2 catalyzed bioactivation of methyleugenol to 1′-hydroxymethyleugenol, ii) P450 2B6 catalyzed epoxidation of methyleugenol, iii) the apparent kinetic constants for detoxification of 1′-hydroxymethyleugenol via oxidation and iv) the apparent kinetic constants for bioactivation

of 1′-hydroxymethyleugenol to 1′-sulfooxymethyleugenol. Based on the interindividual variation in these key biotransformation steps and Monte Carlo simulations a distribution of the interindividual variation in the level of formation of 1′-sulfooxymethyleugenol in the human liver could be obtained. From this distribution a chemical-specific adjustment factor (CSAF) could be derived which is defined as the 95th or 99th percentile divided by the 50th percentile of the predicted distribution of the formation of 1′-sulfooxymethyleugenol in the liver (IPCS, 2005). The obtained CSAF value at the 95th percentile of 3.7 indicates that the default uncertainty factor of 3.16 for human variability in kinetics may adequately protect 95% of the population. Protecting 99% of the population requires a larger uncertainty factor of 5.8. This uncertainty factor is part of the margin of 10,000 suggested by EFSA to be a value for the Margin of Exposure (MOE) for a compound that is both genotoxic and carcinogenic to be of low priority for risk management (EFSA, 2005). The CSAF value obtained for methyleugenol in the present thesis obviously does not present an argument to modify this value of 10,000 in the case of methyleugenol.

Furthermore, it is of importance to note that in the present thesis especially dose-, species-matrix- and interindividual-dependent effects on the kinetics of methyleugenol were characterized and quantified. The carcinogenic effects of methyleugenol will ultimately also depend on toxicodynamic processes including processes such as the formation of DNA adducts, DNA repair, induction of mutations and the ultimate formation and development of the tumors. Although kinetics were shown not to provide an argument against linear extrapolation from high doses to low doses, non-linear dose-dependent effects may still occur at one of these other steps in the pathway leading to tumor formation. Non-linear dose response behavior could for example occur when DNA repair becomes saturated at relatively high doses, resulting in a relative increase in DNA adduct formation with increasing dose. Saturation of DNA repair at increasing dose levels may be a reason why dose dependent increases in cancer incidences should be described by non-linear rather than linear models. This could be investigated in further detail by extending the PBK models of the present thesis into so-called physiologically based dynamic (PBD) models in which dose levels and 1'-sulfooxymethyleugenol formation

should be coupled to DNA adduct formation, and, ultimately, cancer incidence. With these PBD models the level of DNA adduct formation can be predicted at different oral doses, including doses relevant for dietary human intake. This approach allows taking into account possible effects of DNA repair in the extrapolation from high to low dose methyleugenol for rat and human. Since DNA adduct formation is presently considered a marker of exposure rather than a biomarker for tumor incidence (Phillips, 2005; Sander *et al.*, 2005), a full PBD model should ultimately also find a way to link the predicted DNA adduct formation to tumor incidences.

Moreover, the PBK models developed in the current thesis can be used to facilitate the prediction of carcinogenic potency of other structurally related alkenylbenzenes, for which the toxicological database is far more limited or unavailable (van den Berg *et al.*, 2012). Read-across from data on methyleugenol, for which *in vivo* data are available, might be an efficient approach for risk assessment of related alkenylbenzenes. Building a PBK model for the related alkenylbenzene to predict and thus compare its bioactivation to that of methyleugenol may provide insight in the relative potency of this related alkenylbenzene. As a first approximation the $BMDL_{10}$ for methyleugenol may then be corrected by this factor to estimate the $BMDL_{10}$ for the related alkenylbenzene for which tumor data are unavailable. On the basis of such considerations, the specific $BMDL_{10}$ value of methyleugenol (15.3-34.0 mg/(kg bw)/day) was used to estimate a possible $BMDL_{10}$ value for elemicin, using the outcomes of their PBK models to estimate their differences in bioactivation to the corresponding 1′-sulfooxymetabolite. PBK modeling revealed that the formation of the 1′-sulfoxymetabolite of elemicin would be 2-fold lower, and thus the $BMDL_{10}$ of elemicin was estimated by multiplying the $BMDL_{10}$ values of methyleugenol by that factor. Using the estimated $BMDL_{10}$ value thus obtained, MOE values for elemicin could be calculated based on the estimated daily intake (van den Berg *et al.*, 2012). The results obtained indicated that the daily exposure to elemicin resulting from the use of spices, food, and essential oils would be of lower priority for risk management than the exposure to the related alkenylbenzene methyleugenol resulting from these sources (van den Berg *et al.*, 2012). Given that the PBK models developed and used for this approach are based especially on parameters obtained in *in vitro* studies, and that such a read-across would help to

set priorities for *in vivo* carcinogenicity testing, this PBK model-based read-across may contribute to the 3Rs (replacement, reduction, refinement) of animals studies.

In summary, it has been shown that integrating *in vitro* metabolic, physiological, and biochemical parameters in PBK models forms a good tool to give insight into the possible dose-dependent effects, species difference effects, matrix effects, and human variation effects on the bioactivation of methyleugenol. The results obtained were also able to reveal the mechanisms underlying the dose dependent effects and to show the species difference in bioactivation and detoxification of methyleugenol. Furthermore, the outcomes of the current studies showed that food matrix and combination effects may play a role in the ultimate bioactivation of methyleugenol by reducing formation of the ultimate carcinogenic metabolite 1′-sulfooxymethyleugenol. Moreover, PBK modeling gave more insights in the possible occurrence of human variation concerning the bioactivation of methyleugenol to its ultimate carcinogenic metabolite 1′-sulfooxymethyleugenol. Also the results obtained strengthen the method of extrapolation of animal carcinogenicity data obtained at high doses to predict the possible carcinogenic outcomes at low doses which are relevant to the human situation. Additionally, the PBK models can facilitate a read-across in risk assessment from compounds for which *in vivo* toxicity studies are available to a compound for which only limited toxicity data have been described, thus contributing to development of alternatives for animal testing.

References

Alhusainy, W., Paini, A., Punt, A., Louisse, J., Spenkelink, B., Vervoort, J., Delatour, T., Scholz, G., Schilter, B., Adams, A., van Bladeren, P.J., and Rietjens, I.M.C.M. (2010). Identification of nevadensin as an important herb-based constituent inhibiting estragole bioactivation and physiology-based biokinetic modeling of its possible in vivo effect. Toxicol and Appl Pharm 245, 179-190.

Alhusainy, W., Paini, A., van den Berg, J.H.J., Punt, A., Scholz, G., Schilter, B., van Bladeren,

P.J., Taylor, S., Adams, T.B., and Rietjens, I.M.C.M. The basil ingredient nevadensin, a novel natural SULT inhibitor able to inhibit SULT-mediated formation of estragole E-3'-N^2-dGuo DNA adduct in male Sprague-Dawley rats and a physiologically based biokinetic (PBBK) modeling of estragole and nevadensin interaction in rat and human (unpublished results).

Alhusainy, W., van den Berg, S.J.P.L., Paini, A., Campana, A., Asselman, M., Spenkelink, A., Punt, A., Scholz, G., Schilter, B., Adams, T.B., van Bladeren, P.J., and Rietjens, I.M.C.M. (2012). Matrix modulation of the bioactivation of estragole by constituents of different alkenylbenzene-containing herbs and spices and physiologically based biokinetic modeling of possible in vivo Effects. Toxicol Sic 129, 174-187.

Bamforth, K.J., Jones, A.L., Roberts, R.C., and Coughtrie, M.W. (1993). Common food additives are potent inhibitors of human liver 17α-ethinyloestradiol and dopamine sulphotransferases. Biochem Pharmacol 46, 1713-1720.

Burdock G.A. (2005). Fenaroli′s Handbook of Flavor Ingredients, 5th ed. Boca Raton, FL: CRC Press, pp. 672–673.

Ding, W., Levy, D.D., Bishop, M.E., Lyn-Cook Lascelles, E., Kulkarni, R., Chang, C.W., Aidoo, A., and Manjanatha, M.G. (2011). Methyleugenol genotoxicity in the Fischer 344 rat using the comet assay and pathway-focused gene expression profiling. Toxicol Sci 123,103-112.

Eaton, E.A., Walle, U.K., Lewis, A.J., Hudson, T., Wilson, A.A., and Walle, T. (1996). Flavonoids, potent inhibitors of the human P-form phenolsulfotransferase: Potential role in drug metabolism and chemoprevention. Drug Metab Dispos 24, 232-237.

EFSA (2005). Opinion of the Scientific Committee on a request from EFSA related to a harmonised approach for risk assessment of Substances Which are both Genotoxic and Carcinogenic. EFSA J. 282, 1-31. http://www.efsa.europa.eu/en/efsajournal/doc/282.pdf

Environment Canada (2010). Screening Assessment for the Challenge Benzene, 1,2-dimethoxy-4-(2-propenyl)-(Methyl eugenol). Chemical Abstracts Service Registry Number 93-15-2.

Environment Canada – Health Canada. http://www.ec.gc.ca/ese-ees/0129FD3C-B0FF-41C8-8BF5-7B2CD016AD36/batch9_93-15-2_en.pdf

European Commission (2008). Regulation (EC) No 1334/2008 of the European Parliament and of the Council of 16 December 2008 on flavourings and certain food ingredients with flavouring properties for use in and on foods and amending Council Regulation (EEC) No 1601/91, Regulations (EC) No 2232/96 and (EC) No 110/2008 and Directive 2000/13/EC. Off J Eur Union, L354/34: http://eur-lex.europa.eu/LexUriServ/LexUriServ.do?uri =OJ:L:2008:354:0034:0050:en:pdf

FDA (2010). Flavoring Agents and Related Substances. In: Food additives permitted for direct addition to food for human consumption. Subpart F, Sec. 172.515 Synthetic flavoring substances and adjuvants. U.S. Departmentof Health and Human Services, Food and Drug Administration. Title 21, volume 3. Revised as of April 1 2012. http://www.accessdata. fda.gov/scripts/cdrh/cfdocs/cfcfr/CFRSearch.cfm?fr=172.515.

FDA (2004). Synthetic flavoring substances and adjuvants. Washington D.C.: US Food and Drug Administration, Code of Federal Regulations, 21 CFR §172.515. http://edocket. access.gpo. gov/cfr_2004/aprqtr/pdf/21cfr172.515.pdf

Hall, R.L. and Oser, B.L. (1965). Recent progress in the consideration of flavoring ingredients under the food additives amendment III. GRAS substances. Food Technol 253, 151-197.

(IPCS) (2005). International Programme on Chemical Safety. Chemical specific adjustment factors for interspecies differences and human variability: Guidance document for use of data in dose/concentration-response assessment. Harmonization Project Document No. 2. World Health Organization, Geneva, Switzerland. http://whqlibdoc.who.int/ publications/ 2005/9241546786_eng.pdf

JECFA (2008). Sixty-ninth meeting Rome, Italy, 17-26 June 2008. http://www.who.int/entity /ipcs /food/jecfa/summaries/summary69.pdf

Jeurissen S.M.F, Punt A., Delatour T., and Rietjens I.M.C.M. (2008). Basil extract inhibits the sulfotransferase mediated formation of DNA adducts of the procarcinogen 1'-hydroxy-estragole by rat and human liver S9 homogenates and in HepG2 Human Hepatoma Cells.

Food Chem Toxicol, 46, 2296-2302.

Johnson, J.D., Ryan, M. J., Toft II, J.D., Graves, S.W., Hejtmancik, M.R., Cunningham, M.L., Herbert, R., and Abdo, K.M. (2000). Two-year toxicity and carcinogenicity study of methyleugenol in F344/N rats and B6C3F1 mice. J Agr Food Chem 48, 3620-3632.

Manach, C., Scalbert, A., Morand, C., Remesy, C., and Jimenez, L. (2004). Polyphenols: food sources and bioavailability. Am J Clin Nut 79, 727-747.

Morimitsu, Y., Sugihara, N., and Furuno, K. (2004). Inhibitory effect of flavonoids on sulfo- and glucurono-conjugation of acetaminophen in rat cultured hepatocytes and liver subcellular preparations. Biol Pharm Bull 27, 714-717.

Nijssen L.M., Ingen-Visscher C.A., van Donders J.J. (2010). Volatile Compounds in Food (VCF) database. TNO Nutrition and Food Research, Zeist, the Netherlands. http://www.vcf-online.nl/VcfHome.cfm

NTP (2000). Toxicology and carcinogenesis studies of methyleugenol (CAS No. 93-15-12) in F344/N rats and B6C3F1 mice (Gavage studies). Natl Toxicol Program Tech Rep Ser, 491, 1-412.

Phillips, D.H. (2005). DNA adducts as markers of exposure and risk. Mutat Res 577, 284-292.

Sander, M., Cadet, J., Casciano, D.A., Galloway, S.M., Marnett, L.J., Novak, R.F., Pettit, S.D., Preston, R.J., Skare, J.A., Williams, G.M., van Houten, B. and Gollapudi, B.B. (2005). Proceedings of a workshop on DNA adducts: biological significance and applications to risk assessment Washington, DC, April 13-14, 2004. Toxicol Appl Pharmacol 208, 1-20.

SCF (2001). Opinion of the scientific committee on food on methyleugenol (4-allyl-1,2-dimethyxybenzene). European Commission, Scientific Committee on Food. Brussels, BE. http://ec.europa.eu/food/fs/sc/scf/out104_en.pdf

Schecter, A., Lucier, G.W., Cunningham, M.L., Abdo, K.M, Blumenthal, G., Silver, A.G., Melnick, R., Portier, C., Barr, D.B., Barr, J.R., Stanfill, S.P., Patterson Jr., D.G., Needham, L.L., Stopford, W., Masten, S., Mignogna, J., and Tung, K.C. (2004). Human consumption of methyleugenol and its elimination from serum. Environ Health Persp 112, 678-680.

Schilter, B., Andersson, C., Anton, R., Constable, A., Kleiner, J., O'Brien, J., Renwick, A.G.,

Korver, O., Smit, F., and Walker, R. (2003). Guidance for the safety assessment of botanicals and botanical preparation for use in food and food supplements. Food Chem Toxicol 41, 1625-1649.

Smith, B., Cadby, P., Leblanc, J., and Setzer, R. (2010). Application of the margin of exposure (MoE) approach to substances in food that are genotoxic and carcinogenic. Example: Methyleugenol, CASRN: 93-15-2. Food Chem Toxicol 48, S89-S97.

Smith, R.L., Adams, T.B., Doull, J., Feron, V., Goodman, J.I., Marnett, L.J., Portoghese, P.S., Waddell, W.J., Wagner, B.M., Rogers, A.E., Caldwell, J., and Sipes, I.G. (2002). Safety assessment of allylalkoxybenzene derivatives used as flavoring substances methyl eugenol and estragole. Food Chem Toxicol 40, 851-870.

van den Berg, S.J.P.L., Punt, A., Soffers, A.E.M.F., Vervoort, J., Ngeleja, S., Spenkelink, B., and Rietjens, I.M.C.M. (2012). Physiologically based kinetic models for the alkenylbenzene elemicin in rat and human and possible implications for risk assessment. Chem Res Toxicol 25, 2352-2367.

van den Berg, S.J.P.L., Restani, P., Boersma, M.G., Delmulle L., and Rietjens, I.M.C.M. (2011). Levels of genotoxic and carcinogenic ingredients in plant food supplements and associated risk assessment. Food Nutr Sci 2, 989-1010.

van het Hof, K.H., West, C.W., Weststrate, J.A., and Hautvast, J.G. (2000). Dietary factors that affect the bioavailability of carotenoids. J Nutr 130, 503–506.

Walle, T. (2007). Methylation of dietary flavones greatly improves their hepatic metabolic stability and intestinal absorption. Mol Pharm 4, 826–832.

Wen, X., and Walle, T. (2006). Methylated flavonoids have greatly improved intestinal absorption and metabolic stability. Drug Metab Dispos 34, 1786–1792.

Yagima I., Yanai T., Nakamura M., Hidemasa, S., and Kazuo, H. (1984). Volatile flavor components of Kogyoku Apples. Agric Biol Chem 48, 849–855.

7

Summary

Summary of the results

Methyleugenol, which occurs naturally in various herbs such as tarragon, basil, nutmeg and allspice, is added to food either directly as a flavoring substance or as a constituent of added essential oils (Smith *et al.*, 2002). The interest in the risk of methyleugenol as a food constituent came from its widespread use in a variety of foods and beverages as well as its structural resemblance to the known carcinogen safrole (Johnson *et al.*, 2000). In addition, methyleugenol has been reported to be DNA reactive and carcinogenic, inducing malignant tumors in multiple tissues of rats and mice as well as inducing unscheduled DNA synthesis in rat liver (Ding *et al.*, 2011; NTP, 2000; Smith *et al.*, 2002). The safety of human exposure to methyleugenol at low dietary intake levels has been assessed several times (Hall and Oser, 1965; NTP, 2000; SCF, 2001; Smith *et al.*, 2002) without reaching a scientific agreement on how to translate the carcinogenicity data of rodent animal experiments obtained at high levels of exposure to the relevant human situation. A recent evaluation, performed by the Joint FAO/WHO Expert Committee on Food Additives (JECFA) in 2008, has indicated that although evidence of carcinogenicity to rodents given high doses of methyleugenol exists, further research is needed to assess the potential risk to human health at relevant dietary exposure resulting from the presence of methyleugenol in foods and essential oils and its use as flavoring agent (JECFA, 2008).

Predicting the cancer risk in humans at relevant dietary intake levels requires extrapolation of the animal carcinogenicity data taking in consideration dose, species, and interindividual variation. Furthermore, it implies extrapolation from rat or mouse studies with high dose levels of the pure compound to the human situation in which exposure at low dose levels occurs within the context of a complex food matrix. The aim of the present PhD project was to obtain quantitative insight into the consequences of dose- and species-dependent effects and of interindividual differences and matrix effects for the bioactivation and detoxification of methyleugenol by using physiologically based kinetic (PBK) modeling.

The first chapter of this thesis presents background information to the topic. In chapter 2, a physiologically based kinetic (PBK) model for the alkenylbenzene methyleugenol in rat was defined based on *in vitro* metabolic parameters determined using relevant tissue fractions, *in silico* derived partition coefficients (Payne and Kenny, 2002 and reference therin), and physiological parameters (Brown *et al.*, 1997) derived from the literature. The model was based on the model previously developed for the related alkenylbenzene estragole and consists of eight compartments including liver, lung, and kidney as metabolizing compartments, and separate compartments for fat, arterial blood, venous blood, richly perfused and slowly perfused tissues (Punt *et al.*, 2008). Evaluation of the model was performed by comparing the PBK predicted concentration of methyleugenol in the venous compartment to methyleugenol plasma levels reported in the literature, by comparing the PBK predicted dose-dependent % of formation of 2-hydroxy-4,5-dimethoxyallylbenzene, 3-hydroxy-4-methoxyallylbenzene, and 1′-hydroxymethyleugenol glucuronide to the corresponding % of metabolites excreted in urine reported in the literature, which were demonstrated to be in the same order of magnitude (Solheim and Scheline, 1976). With the model obtained the relative extent of bioactivation and detoxification of methyleugenol at different oral doses was examined. At low doses, formation of 3-(3,4-dimethoxyphenyl)-2-propen-1-ol and methyleugenol-2′,3′-oxide leading to detoxification appear to be the major metabolic pathways, occurring in the liver. At high doses, the model reveals a relative increase in the formation of the proximate carcinogenic metabolite 1′-hydroxymethyleugenol, occurring in the liver. This relative increase in formation of 1′-hydroxymethyleugenol leads to a relative increase in formation of 1′-hydroxymethyleugenol glucuronide, 1′-oxomethyleugenol, and 1′-sulfooxymethyleugenol the latter being the ultimate carcinogenic metabolite of methyleugenol. These results indicate that the relative importance of different metabolic pathways of methyleugenol may vary in a dose-dependent way, leading to a relative increase in bioactiviation of methyleugenol at higher doses.

In subsequent studies described in chapter 3 a physiologically based kinetic (PBK) model for methyleugenol in human based on *in vitro* and *in silico* derived parameters was identified based on the model previously developed for the related alkenylbenzene estragole. The model

consists of six compartments including liver as metabolizing compartment, and separate compartments for fat, arterial blood, venous blood, richly perfused and slowly perfused tissues (Punt et al., 2009). With the model obtained, bioactivation and detoxification of methyleugenol at different dose levels could be investigated. The outcomes of this human model were compared with those of the PBK model for methyleugenol in male rat. The results obtained reveal that formation of 1′-hydroxymethyleugenol glucuronide, a major metabolic pathway in male rat liver, appears to represent a minor metabolic pathway in human liver whereas in human liver a significantly higher formation of 1′-oxomethyleugenol compared with male rat liver is observed. Furthermore, formation of 1′-sulfooxymethyleugenol, which readily undergoes desulfonation to a reactive carbo-cation that can form DNA or protein adducts, is predicted to be the same in the liver of both human and male rat at oral doses of 0.0034 up to 300 mg/(kg bw). Altogether it was concluded that despite a significant difference in especially the metabolic pathways of the proximate carcinogenic metabolite 1′-hydroxymethyleugenol between human and male rat, the influence of species differences on the ultimate overall bioactivation of methyleugenol to 1′-sulfooxymethyleugenol appears to be negligible. Moreover, the PBK model predicted the formation of 1′-sulfooxymethyleugenol in the liver of human and rat to be linear from doses as high as the benchmark dose (BMD_{10}) down to as low as the virtual safe dose (VSD). This shows that kinetic data do not provide a reason to argue against linear extrapolation from the rat tumor data to the human situation.

Another aim of the present PhD study was to study the effect of the basil constituent nevadensin on the bioactivation and genotoxicity of herb based methyleugenol. The results presented in chapter 4 show that nevadensin is able to inhibit DNA adduct formation in HepG2 cells exposed to the proximate carcinogen 1′-hydroxymethyleugenol in the presence of this flavonoid. This inhibition occurs at the level of sulfotransferase (SULT)-mediated bioactivation of 1′-hydroxymethyleugenol. In order to investigate possible *in vivo* implications the SULT inhibition by nevadensin was integrated into the male rat and human PBK models for bioactivation and detoxification of methyleugenol. The results thus obtained reveal that co-administration of methyleugenol with nevadensin may reduce the levels of bioactivation of 1′-

hydroxymethyleugenol to the DNA reactive metabolite, without reducing its detoxification via glucuronidation or oxidation. This effect may be significant even at realistic low dose human exposure levels. The results obtained point at a potential reduction of the cancer risk when methyleugenol exposure occurs by oral intake within a relevant food matrix containing SULT inhibitors compared to what is observed in rodent bioassays upon exposure to pure methyleugenol dosed by gavage.

Besides dose-dependent effects, species differences effects, and matrix effects on the bioactivation of methyleugenol the effect of interindividual variation on methyleugenol detoxification and bioactivation was investigated in chapter 5. To this end we predicted the level of formation of the ultimate carcinogenic metabolite 1′-sulfooxymethyleugenol in the human population by taking the variability in key bioactivation and detoxification reactions into account using Monte Carlo simulations. Insight in the variation in relevant metabolic routes was obtained by determining kinetic constants for the metabolic reactions by specific isoenzymes or by measuring the kinetic constants in incubations with a range of individual human liver fractions. The results of the study indicate that formation of 1′-sulfooxymethyleugenol is predominantly affected by i) P450 1A2 catalyzed bioactivation of methyleugenol to 1′-hydroxymethyleugenol ii) P450 2B6 catalyzed epoxidation of methyleugenol and iii) the apparent kinetic constants for detoxification of 1′-hydroxymethyleugenol via oxidation and iv) the apparent kinetic constants for bioactivation of 1′-hydroxymethyleugenol to 1′-sulfooxymethyleugenol. Based on the Monte Carlo simulation a chemical-specific adjustment factor (CSAF) for intraspecies variation could be derived which is defined as the 95th or 99th percentile divided by the 50th percentile of the predicted distribution of the formation of 1′-sulfooxymethyleugenol in the liver. The obtained CSAF value at the 95th percentile was 3.7 indicating that the default uncertainty factor of 3.16 for human variability in kinetics (WHO, 1999) may adequately protect 95% of the population. While protecting 99% of the population requires a larger uncertainty factor of 5.8.

Altogether, the results shown in this thesis reveal that integrating *in vitro* metabolic parameters within a framework of a PBK model provides a good method to evaluate the

occurrence of dose-dependent effects, species differences, and human variability in detoxification and bioactivation of a genotoxic carcinogen. Moreover, the results presented in this thesis show the possible protective effect of the basil constituent nevadensin on SULT catalysed bioactivation and DNA adduct formation of methyleugenol *in vitro*. Upon validation of these effects *in vivo*, it may turn out that rodent carcinogenicity data on methyleugenol substantially overestimate the risks posed when humans are exposed to methyleugenol within a nevadensin containing food matrix.

References

Brown, R.P., Delp, M.D., Lindstedt, S.L., Rhomberg, L.R., and Beliles, R.P. (1997). Physiological parameter values for physiologically based pharmacokinetic models. Toxicol Ind Health 13, 407-484.

Ding, W., Levy, D.D., Bishop, M.E., Lyn-Cook Lascelles, E., Kulkarni, R., Chang, C.W., Aidoo, A., and Manjanatha, M.G. (2011). Methyleugenol genotoxicity in the Fischer 344 rat using the comet assay and pathway-focused gene expression profiling. Toxicol Sci 123,103-112.

Hall, R.L. and Oser, B.L. (1965). Recent progress in the consideration of flavoring ingredients under the food additives amendment III. GRAS substances. Food Technol 253, 151–197.

JECFA (2008). Sixty-ninth meeting Rome, Italy, 17-26 June 2008. http://www.who.int/entity /ipcs /food/jecfa/summaries/summary69.pdf

Johnson, J.D., Ryan, M.J., Toft II, J.D., Graves, S.W., Hejtmancik, M.R., Cunningham, M.L., Herbert, R., and Abdo, K.M. (2000). Two-year toxicity and carcinogenicity study of methyleugenol in F344/N Rats and B6C3F1 Mice. J Agr Food Chem 48, 3620-3632.

NTP (2000). Toxicology and carcinogenesis studies of methyleugenol (CAS No. 93-15-12) in F344/N rats and B6C3F1 mice (Gavage studies). Natl Toxicol Program Tech Rep Ser, 491, 1-412.

Payne, M.P., and Kenny, L.C. (2002). Comparison of models for the estimation of biological partition coefficients. J Toxicol Environ Health A 65, 897–931.

Punt, A, Freidig, A.P., Delatour, T., Scholz, G., Boersma, M.G., Schilter, B., van Bladeren, P.J., and Rietjens, I.M.C.M. (2008). A physiologically based biokinetic (PBBK) model for estragole bioactivation and detoxification in rat. Toxicol Appl Pharm 231,248-259.

Punt, A., Paini, A., Boersma, M.G., Freidig, A.P., Delatour,T., Scholz, G., Schilter, B., van Bladeren, P.J., and Rietjens I.M.C.M. (2009). Use of physiologically based biokinetic (PBBK) modeling to study estragole bioactivation and detoxification in humans as compared with male rats. Toxicol Sci 110, 255–269**.**

SCF (2001). Opinion of the scientific committee on food on methyleugenol (4-allyl-1,2-dimethyxybenzene). European Commission, Scientific Committee on Food. Brussels, BE. http://ec.europa.eu/food/fs/sc/scf/out104_en.pdf

Smith, R.L., Adams, T.B., Doull, J., Feron, V., Goodman, J.I., Marnett, L.J., Portoghese, P.S., Waddell, W.J., Wagner, B.M., Rogers, A.E., Caldwell, J., and Sipes, I.G. (2002). Safety assessment of allylalkoxybenzene derivatives used as flavoring substances - methyl eugenol and estragole. Food Chem Toxicol 40, 851-870.

Solheim, E., and Scheline, R. (1976). Metabolism of alkenebenzene derivatives in the rat. II. Eugenol and isoeugenol methyl ethers. Xenobiotica 6, 137-150.

WHO (1999). International Programme on Chemical Safety (IPCS): Assessing human health risks of chemicals: Principles for the assessment of risk to human health from exposure to chemicals. Environmental Health Criteria 210, World Health Organisation, Geneva, Switzerland. http://www.inchem.org/documents/ehc/ehc/ehc210.htm

8

Samenvatting

Methyleugenol, dat van nature voorkomt in verschillende kruiden zoals dragon, basilicum, nootmuskaat en piment, wordt aan voedsel toegevoegd, hetzij als een smaakstof of als bestanddeel van toegevoegde essentiële oliën (Smith *et al.*, 2002). De belangstelling voor het risico van methyleugenol als levensmiddelbestanddeel ontstond door het wijdverbreide gebruik in een verscheidenheid van voedingsmiddelen en dranken en door de structurele gelijkenis ervan met het bekende carcinogeen safrole (Johnson *et al.*, 2000). Bovendien is van methyleugenol bekend dat het DNA-reactief en carcinogeen is en zowel kwaadaardige tumoren in verschillende weefsels van ratten en muizen veroorzaakt als DNA-adducten in rattenlever (Ding *et al.*. , 2011; NTP, 2000; Smith et al., 2002). De veiligheid van menselijke blootstelling aan methyleugenol bij lage innameniveaus is meerdere malen onderzocht (Hall en Oser, 1965; NTP, 2000; SCF, 2001; Smith *et al.*, 2002) zonder dat er een wetenschappelijke consensus bereikt is over de wijze waarop de carcinogeniteitsdata van dierproeven die verkregen zijn bij hoge blootstelling, vertaald kunnen worden naar de menselijke situatie. Een recente evaluatie, uitgevoerd door de "Joint FAO / WHO Expert Committee on Food Additives" (JECFA) in 2008, heeft geconcludeerd dat, hoewel het bewijs bestaat van carcinogeniteit bij knaagdieren die hoge doseringen van methyleugenol toegediend kregen, verder onderzoek nodig is om het potentiële risico te beoordelen voor de gezondheid van de mens bij relevante blootstelling via de voeding als gevolg van de aanwezigheid van methyleugenol in voedingsmiddelen en essentiële oliën en het gebruik ervan als smaakstof (JECFA, 2008). Het voorspellen van het risico op kanker bij de mens bij de relevante innameniveaus vereist extrapolatie van de diercarcinogeniteitgegevens, daarbij rekening houdend met dosis-, soort-, en interindividuele variatie. Bovendien houdt dit extrapolatie in van rat- of muisstudies met hoge doseringen van de zuivere stof naar de menselijke situatie waarin blootstelling aan lage doses plaatsvindt binnen de context van een complexe voedselmatrix. Het doel van dit PhD project was om kwantitatief inzicht te krijgen in de gevolgen van dosis-en species-afhankelijke effecten en van interindividuele verschillen en matrixeffecten voor de bioactivering en detoxificering van methyleugenol op basis van het gebruik van op de fysiologie gebaseerde kinetische (PBK) modellering.

Het eerste hoofdstuk van dit proefschrift presenteert achtergrondinformatie bij het onderwerp. In hoofdstuk 2 wordt een op de fysiologie gebaseerd kinetisch (PBK) model voor methyleugenol in rat gedefinieerd op basis van *in vitro* metabole parameters bepaald met behulp van incubaties met relevante weefselpreparaten, *in silico* verkregen verdelingscoëfficiënten (Payne en Kenny, 2002 en de verwijzing daarnaar), en fysiologische parameters ontleend aan de literatuur (Brown *et al.*, 1997). Het model is gebaseerd op het eerder ontwikkelde model voor de qua structuur vergelijkbare alkenylbenzeen estragole en bestaat uit acht compartimenten waaronder lever, longen en nieren waarin omzetting van methyleugenol plaatsvindt, en gescheiden compartimenten voor vet, arterieel bloed, veneus bloed, rijk doorbloed en langzaam doorbloed weefsel (Punt *et al.*, 2008). Evaluatie van het model werd uitgevoerd door vergelijking van de met het PBK model voorspelde concentratie van methyleugenol in het veneuze bloed met methyleugenol plasmaspiegels zoals vermeld in de literatuur, en door vergelijking van het met het PBK model voorspelde percentage van de dosis omgezet naar 2-hydroxy-4,5-dimethoxyallylbenzene, 3-hydroxy-4-methoxyallylbenzene en 1'-glucuronide hydroxymethyleugenol met de overeenkomstige percentages van metabolieten in urine zoals vermeld in de literatuur (Solheim en Scheline, 1976), die dezelfde orde van grootte hadden. Met het verkregen model werd vervolgens de relatieve omvang van bioactivering en detoxificering van methyleugenol bij verschillende orale doses onderzocht. Vorming van 3-(3,4-dimethoxyfenyl)-2-propen-1-ol en methyleugenol-2',3'-oxide bij lage doses, leidt tot detoxifcering en blijken belangrijke metabolische routes, die zich in de lever voordoen. Bij hoge doses laat het model in de lever een relatieve toename zien van de vorming van de proximale carcinogene metaboliet 1'-hydroxymethyleugenol Deze relatieve toename in de vorming van 1'-hydroxymethyleugenol leidt tot een relatieve toename in de vorming van 1'-hydroxymethyleugenol glucuronide, 1'-oxomethyleugenol en 1'-sulfooxymethyleugenol, waarbij de laatstgenoemde de uiteindelijke carcinogene metaboliet van methyleugenol blijkt te zijn. Deze resultaten geven aan dat het relatieve belang van verschillende metabole routes van methyleugenol kan variëren op een dosisafhankelijke manier, wat leidt tot een relatieve toename in bioactivering van methyleugenol bij hogere doses.

In de daaropvolgende studies, beschreven in hoofdstuk 3, werd een op de fysiologie gebaseerd kinetisch (PBK) model voor methyleugenol in de mens ontwikkeld gebaseerd op *in vitro* en *in silico* bepaalde parameters en het eerder ontwikkelde model voor de gerelateerde alkenylbenzeen estragole. Het model bestaat uit zes compartimenten waaronder lever als metaboliserend compartiment en aparte compartimenten voor vet, arterieel bloed, veneus bloed, rijk doorbloed en langzaam doorbloed weefsel (Punt *et al.*, 2009). Met het verkregen model konden bioactivering en detoxificering van methyleugenol in verschillende dosesniveaus worden onderzocht. De resultaten van dit menselijk model werden vergeleken met die van het PBK model voor methyleugenol in de mannelijke rat. De verkregen resultaten tonen aan dat de vorming van 1'-hydroxymethyleugenol glucuronide een belangrijke metabole route is in de mannelijke rat maar een relatief onbelangrijke metabole route in de menselijke lever, terwijl in de menselijke lever een significant hogere vorming van 1'-oxomethyleugenol is gevonden, vergeleken met de mannelijke rattenlever. Ondanks dit verschil bleek de vorming van 1'-sulfooxymethyleugenol, dat een reactief carbo-kation en DNA- of eiwitadducten kan vormen, hetzelfde te zijn in de lever van de mens en de mannelijke rat bij orale doses van 0.0034 tot 300 mg/(kg lichaamsgewicht). Ten slotte werd geconcludeerd dat, ondanks een significant verschil in vooral de metabole routes van de proximale carcinogene metaboliet 1'-hydroxymethyleugenol tussen de mens en de mannelijke rat, de invloed van soortverschillen op de uiteindelijke totale bioactivering van methyleugenol naar 1'-sulfooxymethyleugenol te verwaarlozen lijkt. Bovendien voorspelde het PBK-model dat de vorming van 1'-sulfooxymethyleugenol in de lever van mens en rat lineair zou zijn bij doses zo hoog als de zogenoemde Benchmarck Dose 10 (BMD10), die 10% extra tumor incidentie geef, tot een dosis zo laag als de virtuele veilige dosis (VSD), de dosis die leidt tot 1 extra geval van kanker op 1 miljoen bij levenslange blootstelling. Dit toont aan dat de kinetische gegevens geen argument zijn tegen lineaire extrapolatie van de rattumorgegevens naar de menselijke situatie.

Een ander doel van het huidige promotieonderzoek was het bestuderen van het effect van het basilicumbestanddeel nevadensin op de bioactivering en genotoxiciteit van methyleugenol. De resultaten in hoofdstuk 4 tonen aan dat nevadensin DNA-adductvorming kan onderdrukken

in HepG2 cellen die zijn blootgesteld aan het proximale carcinogeen 1'-hydroxymethyleugenol en deze flavonoïde. Deze remming treedt op op het niveau van sulfotransferase (SULT) gemedieerde bioactivering van 1'-hydroxymethyleugenol. Om mogelijke *in vivo* implicaties te onderzoeken werd de SULT remming door nevadensin geïntegreerd in de mannelijke rat en menselijke PBK modellen voor bioactivering en detoxificering van methyleugenol. De aldus verkregen resultaten tonen aan dat gelijktijdige toediening van methyleugenol met nevadensin de niveaus van bioactivering van 1'-hydroxymethyleugenol naar de DNA reactieve metaboliet kunnen verminderen, zonder verminderde detoxificering via glucuronidering of oxidatie. Dit effect kan aanzienlijk zijn, zelfs bij realistische lage dosisblootstelling bij de mens. De resultaten wijzen op een potentiële vermindering van het risico op kanker wanneer methyleugenol blootstelling plaatsvindt door orale inname binnen een relevante voedingsmatrix die SULT remmers bevat in vergelijking met wat wordt gevonden in knaagdier bioassays bij blootstelling aan pure methyleugenol toegediend door gavage.

Naast dosis-afhankelijke effecten, effecten door soortverschillen en matrixeffecten op de bioactivering van methyleugenol, werd in hoofdstuk 5 de invloed onderzocht van inter-individuele variatie in methyleugenol detoxificering en bioactivering. Om dat te onderzoeken voorspelden we het niveau van vorming van de uiteindelijke kankerverwekkende metaboliet 1'-sulfooxymethyleugenol in de menselijke populatie rekening houdend met de variabiliteit in de belangrijkste bioactivering- en detoxificeringreacties met behulp van Monte Carlo simulaties. Inzicht in de variatie in relevante metabole routes werd verkregen door de kinetische constanten te bepalen voor de metabole reacties door specifieke isoenzymen of door meting van de kinetische constanten in incubaties met een reeks individuele menselijke leverpreparaten. De resultaten van de studie geven aan dat vorming van 1'-sulfooxymethyleugenol hoofdzakelijk beïnvloed wordt door i) P450 1A2 gekatalyseerde bioactivering van methyleugenol naar 1'-hydroxymethyleugenol, ii) P450 2B6 gekatalyseerde epoxidatie van methyleugenol en iii) de schijnbare kinetische constanten voor detoxificering van 1 '-hydroxymethyleugenol via oxidatie en iv) de schijnbare kinetische constanten voor bioactivering van 1'-hydroxymethyleugenol naar 1'-sulfooxymethyleugenol. Uit de Monte Carlo-simulatie kon een stof-specifieke correctiefactor

(CSAF) voor intraspecies variatie worden afgeleid die wordt gedefinieerd als het 95^{e} of 99^{e} percentiel gedeeld door het 50^{e} percentiel van de voorspelde verdeling van de vorming van 1'-sulfooxymethyleugenol in de lever. De verkregen CSAF-waarde op het 95^{e} percentiel was 3.7, wat aangeeft dat de standaard onzekerheidsfactor van 3.16 voor menselijke variabiliteit in kinetiek (WHO, 1999) 95% van de bevolking afdoende kan beschermen. Voor bescherming van 99% van de bevolking is een grotere onzekerheidsfactor van 5.8 vereist.

Al met al laten de resultaten, beschreven in dit proefschrift, zien dat de integratie van *in-vitro* metabole parameters binnen een kader van een PBK-model een goede methode biedt om het optreden van dosis-afhankelijke effecten, soortverschillen, en menselijke variabiliteit in detoxicifiering en bioactivering van een genotoxisch carcinogeen te evalueren . Bovendien laten de resultaten, gepresenteerd in dit proefschrift, de mogelijkheid zien van de beschermende effecten van het basilicumbestanddeel nevadensin op SULT gekatalyseerde bioactivering en DNA-adductvorming van methyleugenol *in vitro*. Bij het valideren van deze effecten *in vivo*, zou kunnen blijken dat carcinogeniteitgegevens van methyleugenol verkregen in knaagdierstudies met pure methyleugenol, de risico's bij de mens die wordt blootgesteld aan methyleugenol binnen een voedsel matrix met nevadensin aanzienlijk overschatten.

Referenties

Brown, R.P., Delp, M.D., Lindstedt, S.L., Rhomberg, L.R., and Beliles, R.P. (1997). Physiological parameter values for physiologically based pharmacokinetic models. Toxicol Ind Health 13, 407-484.

Ding, W., Levy, D.D., Bishop, M.E., Lyn-Cook Lascelles, E., Kulkarni, R., Chang, C.W., Aidoo, A., and Manjanatha, M.G. (2011). Methyleugenol genotoxicity in the Fischer 344 rat using the comet assay and pathway-focused gene expression profiling. Toxicol Sci 123,103-112.

Hall, R.L. and Oser, B.L. (1965). Recent progress in the consideration of flavoring ingredients

under the food additives amendment III. GRAS substances. Food Technol 253, 151–197.

JECFA (2008). Sixty-ninth meeting Rome, Italy, 17-26 June 2008. http://www.who.int/ entity /ipcs /food/jecfa/summaries/summary69.pdf

Johnson, J.D., Ryan, M.J., Toft II, J.D., Graves, S.W., Hejtmancik, M.R., Cunningham, M.L., Herbert, R., and Abdo, K.M. (2000). Two-year toxicity and carcinogenicity study of methyleugenol in F344/N Rats and B6C3F1 Mice. J Agr Food Chem 48, 3620-3632.

NTP (2000). Toxicology and carcinogenesis studies of methyleugenol (CAS No. 93-15-12) in F344/N rats and B6C3F1 mice (Gavage studies). Natl Toxicol Program Tech Rep Ser, 491, 1-412.

Payne, M.P., and Kenny, L.C. (2002). Comparison of models for the estimation of biological partition coefficients. J Toxicol Environ Health A 65, 897–931.

Punt, A, Freidig, A.P., Delatour, T., Scholz, G., Boersma, M.G., Schilter, B., van Bladeren, P.J., and Rietjens, I.M.C.M. (2008). A physiologically based biokinetic (PBBK) model for estragole bioactivation and detoxification in rat. Toxicol Appl Pharm 231,248-259.

Punt, A., Paini, A., Boersma, M.G., Freidig, A.P., Delatour,T., Scholz, G., Schilter, B., van Bladeren, P.J., and Rietjens I.M.C.M. (2009). Use of physiologically based biokinetic (PBBK) modeling to study estragole bioactivation and detoxification in humans as compared with male rats. Toxicol Sci 110, 255–269**.**

SCF (2001). Opinion of the scientific committee on food on methyleugenol (4-allyl-1,2-dimethoxybenzene). European Commission, Scientific Committee on Food. Brussels, BE. http://ec.europa.eu/food/fs/sc/scf/out104_en.pdf

Smith, R.L., Adams, T.B., Doull, J., Feron, V., Goodman, J.I., Marnett, L.J., Portoghese, P.S., Waddell, W.J., Wagner, B.M., Rogers, A.E., Caldwell, J., and Sipes, I.G. (2002). Safety assessment of allylalkoxybenzene derivatives used as flavoring substances - methyl eugenol and estragole. Food Chem Toxicol 40, 851-870.

Solheim, E., and Scheline, R. (1976). Metabolism of alkenebenzene derivatives in the rat. II. Eugenol and isoeugenol methyl ethers. Xenobiotica 6, 137-150.

WHO (1999). International Programme on Chemical Safety (IPCS): Assessing human health risks of chemicals: Principles for the assessment of risk to human health from exposure to chemicals. Environmental Health Criteria 210, World Health Organisation, Geneva, Switzerland. http://www.inchem.org/documents/ehc/ehc/ehc210.htm

Abbreviations, acknowledgement, curriculum vitae and publications

Abbreviations

SCF, Scientific Committee on Food

FEMA, Flavor and Extract Manufacturers Association

NTP, National Toxicology Program

PBK, physiologically based kinetic

ME, methyleugenol

1′HME, 1′-hydroxymethyleugenol

3DMPOH, 3-(3,4-dimethoxyphenyl)-2-propen-1-ol

2HDME, 2-hydroxy-4,5-dimethoxyallylbenzene

MEO, methyleugenol-2′,3′-oxide

1EU, eugenol

3HMA, 3-hydroxy-4-methoxyallylbenzene

1′HMEG, 1′-hydroxymethyleugenol glucuronide

1′HMES, 1′-sulfooxymethyleugenol

1′OME, 1′-oxomethyleugenol

1′OME_mic, 1′-oxomethyleugenol formed by microsomal enzymes

1′OME_cyt, 1′-oxomethyleugenol formed by cytosolic enzymes

GSH, glutathione

GS-1′-oxomethyleugenol, 3′-(glutathione-S-yl)-1′-oxo-2′-3′-dihydromethyleugenol

NEV, Nevadensin

1′ACME, 1′-acetoxymethyleugenol

ES, estragole

7HC, 7-hydroxycoumarin

7HCS, 7-hydroxycoumarin sulphate

2′dG, 2′-deoxyguanosine

***$^{15}N_5$*-2′dG**, $^{15}N_5$-2′-deoxyguanosine

ME-3'-N^2-dG, N^2-*(trans*-isomethyleugenol-3′-yl)-2′-deoxyguanosine

(*$^{15}N_5$*) **ME-3'-N^2-dG**, $^{15}N_5$- labelled N^2-*(trans*-isomethyleugenol-3′-yl)-2′-deoxyguanosine

E-3′-N^2-dG, N^2-(*trans*-isoestragole-3′-yl)-2′-deoxyguanosine

NADPH, reduced β-nicotinamide adenine dinucleotide phosphate

NADP, β-nicotinamide adenine dinucleotide phosphate

NADH, reduced β-nicotinamide adenine dinucleotide

NAD, β-nicotinamide adenine dinucleotide

UDPGA, uridine 5′-diphosphoglucuronic acid

PAPS, 3′-phosphoadenosine-5′-phosphosulfate

DMSO, dimethylsulfoxide

BMD, benchmark dose;

BMDL, lower confidence bound of the benchmark dose

VSD, virtual safe dose

PCP, pentachlorophenol

SULT, sulfotransferase

NMWL, nominal molecular weight limit

L, liver

Lu, lung

K, kidney

GC, gas chromatography

LC, liquid chromatography

MS, mass spectrometry

RT, retention time

hr, hour

min, minute

bw, body weight

K_i, inhibition constant

Acknowledgement

I owe a lot to Ivonne Rietjens and unable to thank her for the unlimited support and motivation I received from her during my PhD study. To Peter van Bladeren for the valuable meetings we had during his visits to Wageningen.

I am appreciative to Ans from whom I have learned so much during my PhD project. Special thanks to Wasma for her support in introducing to me the protocols of experiments in the laboratories at Toxicology in Wageningen. Many thanks to Bert, Noval, Alicia, Reiko, Marelle, Laura, Ans Soffar, and Hans who have contributed directly or indirectly to this thesis.

Also I am indebted to Jacques for offering the LC-MS/MS instrument. Special thanks to the powerful administrative assistant, Irene (at TOX) and her colleague, Gre′.

I would like also to thank Arif, Erryana, and Suzanne. Thanks to all the PhD students and staff at the department of Toxicology for the time spent together.

I would like to acknowledge my friends: Hassan, Samai, Mohammad, Jia, Hamada, Jamal, Mostafa, Saleh, Wesam, Abdel Azeez, Abo Ramzi, Husian, Ahmad, Abdel Rahman, Kashif, Akmal, Abed, and Layakat for the wonderful time spent in the Netherlands.

Thanks from the bottom of my heart to my family who encouraged me during my PhD study: Father, mother, brothers and sisters. Off course I will not forget to thank my wife Ghofran who did her utmost to support me during my study and especially taking care of our children Shaima′a and Abdel Rahman.

Thank you all for your support and encouragement during this long but interesting journey!

Ala′

Curriculum Vitae

Ala′ Al-Subeihi was born on the 26th of August 1976, in Amman, Jordan. In 1995, he finished his secondary school in Amman. In 1995, he joined a 4 year study program in Chemistry at the University of Jordan. In 1999, he obtained his BSc and enrolled for the master degree in Analytical Toxicology at the Department of Pathology and Microbiology and Forensic Medicine at the University of Jordan. After completing his master in 2002, he started to work in marketing. In 2005, he became a Chemical Analyst at the Environment Health Directorate at the Ministry of Health in Amman. In 2006 he changed his job to become an Organic Chemistry analyst at Aqaba International Laboratories (Ben Hayyan) at Aqaba Special Economic Zone Authority (ASEZA) in Aqaba, Jordan. From February 2008 to February 2012 he was appointed in the PhD position at the Toxicology Department under supervision of Prof. Ivonne M.C.M. Rietjens, on the project discussed in the present thesis. During his PhD he followed several postgraduate courses in Toxicology forming the basis for his registration as a European Toxicologist. Moreover, he attended several conferences during his PhD study. From June 2012 to October 2015 he is participating in a project implemented under the ENPI CBC Mediterranean Sea Basin Programme funded by the European Union through the European Neighborhood and Partnership Instrument entitled: “Botanical Risk Assessment training in the Mediterranean Area (BRAMA)”, in collaboration with partners from Egypt, Greece, Italy, and the Netherlands.

List of Publications

Al-Subeihi, A.A., Spenkelink, B., Rachmawati, N., Boersma, M.G., Punt, A., Vervoort, J., van Bladeren, P.J., and Rietjens, I.M.C.M. (2011). Physiologically based biokinetic model of bioactivation and detoxification of the alkenylbenzene methyleugenol in rat. Toxicol In Vitro 25, 267-285.

Al-Subeihi, A.A., Spenkelink, B., Boersma, M.G., Punt, A.,van Bladeren, P.J., and Rietjens, I.M.C.M. (2012). Physiologically based kinetic modeling of bioactivation and detoxification of the alkenylbenzene methyleugenol in human as compared with rat. Toxicol Appl Pharm 260, 271-284.

Al-Subeihi, A.A., Paini A., Punt A., Vervoort J., van Bladeren P.J., and Rietjens I.M.C.M. Inhibition of methyleugenol bioactivation by the herb-based constituent nevadensin and prediction of possible in vivo consequences using physiologically based kinetic modeling (Submitted).

Al-Subeihi, A.A., Kiwamoto, R., Spenkelink, B., van Bladeren, P.J., Rietjens, I.M.C.M., and Punt, A. Evaluation of the interindividual human variation in bioactivation of methyleugenol using physiologically based kinetic modeling and Monte Carlo simulation (In preparation).

Overview of completed training activity

Courses

General Toxicology, WUR, Wageningen,	2010
Pathobiology, PET, Utrecht,	2010
Organ toxicology, PET, Utrecht,	2011
Physiologically Based kinetic (PBK) Modeling, Wageningen,	2009
Laboratory Animal Science (LAS), PET, Utrecht,	2010
Immunotoxicology, PET, Utrecht,	2011
Risk Assessment, PET, Wageningen,	2008
Ecotoxicology, PET, Utrecht/Wageningen,	2009
Molecular Toxicology, PET, Amsterdam,	2011
Reproductive Toxicology, PET, Utrecht,	2011
Quality Control in Chemical Analysis, Ben Hayyan, Aqaba-Jordan.	2011

Optional

Preparation of Research Proposal,	2008
Attending research discussions at Toxicology.	2008-2011

Meetings

Biological Reactive Intermediates VIII, Bercelona,	2010
47th Congress of the European Society of Toxicology, Paris.	2011

Approved by Graduate School VLAG